Report No. WMCS-001

NASA CR-160731

FINAL REPORT

for the

WIRELESS MICROPHONE COMMUNICATION SYSTEM

TELEPHONICS P/N 484D000-1

for the

SPACE SHUTTLE ORBITER VEHICLE

Contract No. NAS-9-14824

(NASA-CR-160731) WIRELESS MICROPHONE COMMUNICATION SYSTEM TELEPHONICS P/N 484D000-1 (Telephonics, Huntington, N.Y.) 281 p HC A13/MF A01 CSCL 17B G3/32

N80-26573

Unclas 23569

Approved John R. Klymenko

114379

Telephonics

ABSTRACT

The Wireless Microphone designed and developed by Telephonics Corporation is a lightweight, portable and wireless voice communications device for use by the crew of the Space Shuttle Orbiter. The Wireless Microphone allows the crew to have normal hands-free voice communication while they are performing various mission activities. The unit is designed to transmit at 455 or 500 kilohertz and employs narrow band FM modulation. Two orthogonally placed antennas are used to insure good reception at the receiver.

SUMMARY

OBJECTIVES

Voice communications between crew members of the Space Shuttle Orbiter play a vital role in the successful mission of the space craft and therefore necessitated a need for reliable communication systems and equipment. Since it is highly probable that crew members will be away from their assigned stations, and, at these times have the need for verbal communication, the requirement for development of the Wireless Microphone Communication System became obvious.

SCOPE

This Final Report provides information pertaining to the development of the Wireless Microphone Communication System. The report provides in depth coverage of the investigation, tests, and evaluation of the following:

- Propagation methods leading to the selection of a 455 KHz carrier frequency as described in Appendix A.
- Equipment design and modification which is described in Appendix B.
- Tests performed on the equipment as described in Appendix C.
- Schematics are provided in Appendix D.
- In addition, separate investigations were made on various headsets best suited for use with the Wireless Microphone Communication System. Final reports have been published on these items and are included in this report (see Appendix E).
- Test results are provided in Appendix F.

TECHNICAL CONSIDERATIONS

A major effort involving the development of a multi-channel two-way communication system was pursued, but, due to subsequent financial limitations, the resulting end product design became a two-channel one-way communication system of which four transmitters and two receivers were delivered. As a final modification made prior to delivery, a limited multi-channel option was included to enable the transmitters to broadcast on either ICOM or PTT basis. This last minute addition, coupled with limited funding remaining, could not result in completely foolproof implementations.

RESULTS

Of the four methods of wave propagation (magnetic, RF, optical, and acoustic) investigated for use in the Wireless Microphone Communication System, it has been determined that magnetic coupling best matched the operating and propagation environment of the metallic spacecraft environment.

Magnetic field strength did not exhibit the deep nulls that could be experienced at RF frequencies or be as sensitive to path or transducers blockage as the optical or ultrasonic links. While the RF links were more efficient for a given transmitted power, the advantage was of small consequence within the short propagation distances of the cabin. Optical and RF links could provide larger bandwidths that the magnetic or ultrasonic but for the voice band that was needed, the advantge was of little value. The receiver at the magnetic frequency of 450 KHz did not require the superheterodyning of the RF receiver at VHF. The optical system required multiple radiation diodes to overcome possible path interference and even with the best of diode layout could not assure complete freedom from diode blockage.

The interference of the wireless communicator with other spacecraft equipment required great care with the RF system. However, based upon the NASA supplied data on spacecraft frequencies an RF frequency at 400 MHz would have been satisfactory; the 450 KHz magnetic frequency caused no interference.

CONCLUSIONS

Conclusions derived from the investigations conducted during the development of the Wireless Microphone Communication System are as follows:

- Magnetic coupling proved to be the best method of wave propagation which was selected for this purpose.
- The equipment, as built, has the necessary characteristics to meet requirements as demonstrated by the performance tests but has not yet been refined to a final configuration suitable for direct inclusion in the wireless microphone or in the receiver/SMU portion of the Audio Distribution System.

RECOMMENDATIONS

Recommendations offered by this Final Report are as follows:

- Work should be continued to build a wireless microphone communication system that uses fully militarized and NASA components leading to a system with improved reliability and reproducibility.

- Build a receiver unit with equivalent characteristics to that of the transmitter and package the receiver to fit into the SMU of the Audio Distribution System.

- Expand the Wireless Microphone Communication System to enable two-way communications.

- Adequate funding be provided to enable the development and subsequent delivery of a multi-channel system with two-way communication possibilities.

MAIN BODY OF REPORT

INTRODUCTION

This section of the final report reviews the design considerations of the Wireless Microphone System delivered to NASA under this contract. First, a review of Telephonics' study of the prior art and available equipment is presented which reveals several basic shortcomings of such available equipment when used in a space vehicle environment. Secondly, the synthesis of a suitable system is discussed in detail. Finally, reasons for the particular circuit design are discussed in relation to the technical specifications of the contract.

The purpose of the Wireless Microphone is to provide crew members of the Space Shuttle Orbiter with a communications capability while away from their normal station positions. The wireless microphone eliminates the need for connecting umbilical cables which would be inconvenient, interfere with free movement, and possibly even be hazardous. In the "VOX" mode, it permits hands-free automatic operation so that the crew member can concentrate on various mission activities.

DISCUSSION

A review of prior state-of-the-art and available equipment was made in which three sources of information were researched: (1) final reports of military study contracts, (2) technical journals of various engineering societies and (3) catalogs and data sheets of commercially available equipment. Briefly, in making this review, it became quickly obvious that none of these references and equipment designs dealt adequately with signal fade-out due to nulls caused by strong reflected waves when operated inside a metallic enclosure such as the space shuttle. In order to reduce the probability of a drop-out, standard practice was to use more than one receiver either in frequency or space diversity. Still, the drop-out probability was nowhere near the zero percent value which Telephonics felt was mandatory for a space application. In addition, there was the problem of avoiding antenna directional characteristics which would also produce nulls or signal drop-outs. This is the characteristic of wire or whip antennas. Furthermore, such antennas can be easily detuned by touching them, they take up space and interference with crew movements, they are a hazard to eyes and can easily be broken off. All of this rules out the whip antennas that are used in wireless microphone equipment.

All of the commercial systems we know of use frequencies above 20 megahertz. At these frequencies, narrow band voice frequency channels require precise crystal-controlled superheterodyne or double superheterodyne receivers. Transmitters also require crystal control and, in the case of FM modulation preferred over other forms of modulation, the portable package carried by the crew man becomes too complex, bulky, and power-hungry. All of this tends to degrade reliability and materially raise costs. It was clear that the communications industry had never addressed itself to the unique requirements of NASA.

Lastly, a choice of frequency had to be made. Certainly, the whole of the radio frequency spectrum is, for all practical purposes, saturated world-wide. While the system is to operate within the craft, it is not shielded against high frequency signals due to the relatively large window openings. While NASA's contract does not specify a secure system free of jamming, Telephonics has taken this into full consideration.

NASA requires the wireless microphone to operate within the space shuttle in the upper flight deck and in the lower living quarters deck. The two decks are connected by a passage way opening about 30" in diameter. The wireless microphone transmitters are to have a choice of two operating frequencies, one for the upper deck and one for the lower deck. This avoids the interference that would be caused when crew members are near the opening between decks and only one frequency is used for both decks. Each deck is provided with a receiver so positioned as to limit the maximum operating range from the transmitter to 11 feet. NASA has located the receivers on the rear bulkhead in the best position to keep the operating range to a minimum.

It is our understanding from discussions with Rockwell that the receiver locations are just below fluorescent lights located less than one foot from the receiver antenna. At this time we do not know if these lights are shielded or what the noise level at the antennas will be. Since we lack definite data on noise level to be expected within the craft, it was decided to design the transmitter for one watt input to its antennas. Should this power not be needed, this level can be easily lowered by changing the value of one resistor.

One watt appeared to be close to the maximum power that could be drawn from the new Mallory Lithium Organic batteries and have them last the expected 90 hour mission time. The lithium organic cells, unlike other types of lithium cells, have a proven record against explosion, even with unrealistic extremes of tests. This, coupled with a built-in fuse to limit the maximum possible short-circuit current, further guarantees protection against its explosion. It is to be remembered that all batteries can rupture or explode under short-circuit conditions. Full information submitted by the lithium battery division of Mallory has been presented to NASA for evaluation. This type of cell is remarkable in that it has several times the watt-hour capability of any other kind of battery for a given weight or size. During the course of this contract, no preference could be determined from NASA or Rockwell with respect to a choice of small cells, to be replaced during the mission, or larger cells to last the duration of the mission. The latter was Telephonics' choice and the design was implemented accordingly. VOX or PTT transmitter operation is required by NASA, and such operation conserves battery power. No firm figure could be determined, however, either from NASA or Rockwell, as to the probable ratio of ON to OFF time. This ratio and the power required to override noise are certainly difficult matters to determine and Telephonics appreciates this. Hence, it was planned to make the battery pack separate from the transmitter so that it is simple to redesign the pack without distrubing the transmitter design. This type of cell has a nominal voltage of 2.92 volts which, under light loads, remains almost as constant as a mercury battery to the end of its life. This considered, it was decided to design the transmitter circuits to operate on a 6V supply.

In order to avoid nulls produced by strong reflections, the wavelength of the signal must be much larger than the spacecraft dimensions. For this reason, low frequencies of 455 and 500 kilohertz were chosen, corresponding to wavelengths of 660 and 600 meters, respectively. Since the maximum dimension in either the upper or lower deck compartments is about seven meters, reflections from the walls will be in phase for all practical purposes. With the direct and reflected waves in phase, the two will add and noticeably improve the signal level. With the receiving antennas less than one inch from an aluminum reflecting surface, there will be about a 6 dB improvement in signal level due to the first reflection.

At these low frequencies, very compact ferrite antennas are practical for covering the small range (11 feet) inside the craft. For this short range, use is made of the near magnetic field. In effect, the transmitter and receiver antennas constitute loosely coupled transformer windings. Strength of this coupling decreases as the inverse cube of distance, hence the system is inherently a short range one which insures security and freedom from jamming. Furthermore, the craft's relatively small window openings, compared to wavelength, will substantially attenuate signals entering and leaving the craft. The rapid attenuation of the signal with distance also guarantees that multiple reflections will not cause nulls due to increasing phase differences.

In order to make an omnidirectional system with ferrite antennas, the transmitter requires two bar antennas mounted orthogonally and excited by two signals in time quadrature. Also, two independent receivers with ferrite antennas mounted orthogonally are required to avoid nulls due to the directional characteristics of the antennas. The orthogonal relationship of each set of antennas is in the form of an "X", rather than an "L", in order to avoid objectionable mutual coupling between antennas.

The transmitter antennas are 2.5" long with a cross-section of 0.48" x 0.12". The receiver antennas are 3.75" long with the same cross-section. We find these antennas can be mounted as close as 0.5" from an aluminum surface with the 0.48" dimension parallel to the surface without any significant degradation in performance. This applies to both the receiver ana the transmitter. Tests show that detuning due to hand capacity, 0.5" from the antennas, does not degrade performance to any noticeable extent. Since the efficiency of a ferrite antenna is extremely low for the power input used in this system, the radiated power density 10 meters from the antenna will be less than one micro-microwatt. Each time the antenna length is cut in half, the range is cut in half for a given power. Through a series of experiments, Telephonics has reduced the length of the transmitter and receiver antennas until transmitter battery power reached one watt for a range of 22 feet. At this range, FM reception was clear, quiet and solid for all relative positions of transmitter and receiver antennas. The noise environment of the Telephonics Lab is judged to be a very high one due to many large fluorescent lights that are closely spaced and about eight feet above the floor. Here the characteristics of an FM system, which suppresses noise and holds signal level constant with large signal strength variations, proved highly useful. (A full study of this system's RFI immunity was made and was discussed in Test No. 8 of the report made to NASA on September 15, 1976 (see Appendix D).

From the above, it is seen that battery size vs. antenna size must be a trade off. This also involved the decision to have a separate battery pack last the duration of the mission which is at most seven days. A study of the Mallory Lithium Organic Cells shows the LO-30 size capable of meeting these requirements for an ON/OFF duty time of 15%. This cell is slightly smaller than a D size cell, 1.16" diameter and 2.35" long, with electrical ratings of 7.5 A/Hr., 160 mA rated drain, and an open circuit voltage of 2.92V. The cell must be operated about 12 minutes to bring the voltage up to its rated value. Under load, the cell voltage will be 2.85V until about 90% of its life is reached, thereafter it begins to roll off rapidly. For 160 mA and 90% life cell will last 42 hours. For 15% ON/OFF duty, the cell will last 280 hours. Two cells are required for the 5.70V transmitter supply design. Cells smaller than the LO-30 drop rapidly in efficiency for their size. Also, efficiency drops about 30% for temperture extremes of -20^{o} and 125^{o}F.

This study formed the basis of the system recommended by Telephonics, which considers many special requirements. In the future, Telephonics believes this system can easily be extended in range by the use of more than one set of receivers. The simplicity of the receivers (two mount on a plug board 3" x 5") makes this practical. This simplicity also could make a two-way system practical.

TRANSMITTER DESIGN

The system proposed uses narrow band FM moudulation where the modulation index is unity. The audio frequency range is 300 - 3000 Hertz. The system is capable of being modulated down to dc. This is necessary because a momentary dc controlled shift in transmitter frequency is used to generate a signal which activates the receiver ICOM mode.

With an index of one, the bandwidth will be 6 kilohertz. A bridge T type oscillator is modulated by means of back-to-back varicap capacitors. Oscillation amplitude is held constant and in class A operation by diode limiters. The supply voltage is held constant by a zener diode. Overmodulation is prevented by back-to-back diodes which limit the modulation voltage to 1.0V pp. The microphone amplifier low power IC is capable of sufficient gain to work with any low level, low impedance microphone. It is recommended that the gain be set for 12 dB clipping by the modulation limiter diodes to improve the signal/noise of the system. This type of FM modulated oscillator is sufficiently stable to stay well within the wider passband of the receiver over the required temperature range. Associated with the microphone amplifier are the VOX circuits. Attack and hold time constants are separate. In VOX operation, the standby power consumption is kept as low as possible (12 mw).

The oscillator provides two output signals phased 90° apart. This is accomplished by an R-C network connected to the collector and emitter. This network requires the signals at the collector and emitter. This network requires the signals at the collector and emitter to be equal in amplitude, hence R1-5 and R1-6 are made equal. In order to avoid loading this network and the oscillator, two buffer FET amplifiers are used between the oscillator and the final power amplfiers. The power amplifiers are Class C type, using 2N3467 transistors. These are conservatively rated for the 0.5 watt output to each ferrite antenna. They are also able to take the extra load prior to tuning the antenna in production.

The final amplifiers have sufficient drive to cause the collector to saturate and essentailly produce a square wave output, thereby keeping efficiency as high as possible. The 7.5. ohm resistor in the collector is small compared to the antenna input impedance and limits current before the antenna is tuned in production.

The transmitter is designed to operate at 455 and 500 kilohertz. This requires the frequency of the oscillator tuning and the tuning of two ferrite antennas to be changed. The simplest way to change oscillator tuning is to switch between two pretuned slug-tuned inductors. The simplest way to change antenna tuning is to switch between pretuned capacitors. The most practical way to do this is to use miniature TO-5 latching relays, one located close to the oscillator and another in the subassembly containing the antennas, final power amplifiers and associated tuning capacitors. This plastic protected subassembly measures 2.25" x 2.25" x 1.25" and is carefully designed with a PC board assembly to insure short rigid leads between various associated components. This package has to be plastic to permit radiation from the antenna.

The remainder of the circuits, consisting of the low level audio amplifier, VOX, modulation components, oscillator and buffers, are enclosed in a shielded package of the same size as above. These circuits must be highly shielded against the magnetic field radiated by the antennas for proper and stable operation. All control switches and the microphones and battery connectors are mounted on this subassembly. The two subassemblies are then combined to form the complete wireless microphone package measuring 4.5" x 2.25" x 1.25".

The transmitter is provided with three switch controls. The selection of either 455 or 500 kilohertz is made by a three-position switch. Moving this switch momentarily to one side or the other of the normally-off center position sets latching relays for one frequency or the other. Another three position switch has a center position for transmitter idle, one momentary position for PTT ICOM and the other momentary position for PTT XMIT. The third switch has two steady positions, one for VOX, the other for VOX. The transmitter is completely off with no power drain in the VOX position only. The VOX mode operates only in conjunction with the XMIT mode.

RECEIVER DESIGN

The receiver design is just as important as the transmitter design in order to obtain a smoothly operating, reliable overall system. Prior existing receiver equipment far from meets the special requirements of this application.

Even though the transmitter radiates an onmidirectional signal, two receiving antennas are required, orthogonally placed to insure reception for all positions relative to the transmitter antennas. Furthermore, it is not possible to combine signals from these receiving antennas into one receiver, because some position may be found where the signals in each antenna are equal but opposite in phase, thereby giving zero output. It is therefore necessary to use two receivers and to select the best signal automatically for 100% reliability in all positions of the antennas. This sounds complicated and appears to require much equipment. As will soon be seen, however, this is not the case. Actually, both receivers (less their antennas) could be mounted on a 3" x 3" PC board with a maximum parts height of 0.75". This compactness enables the receivers to be mounted in the SMU at the cost of a small increase in the height of its housing. The two antennas, in the form of an "X", are mounted in front of the SMU speaker. They will be encased in a tough plastic housing which makes them mechanically reliable. Tests show that the sound pattern is not noticeably affected by this antenna arrangement in front of the speaker. (Test results for this arrangement are given an an attachment to this report.)

At the low frequencies of 455 and 500 kilohertz, it is not necessary to use a superheterodyne frequency conversion receiver. This factor alone constitutes a substantial step in reducing complexity and space requirements. Furthermore, a local oscillator with its radiation problems is avoided. Two receivers are to be furnished NASA under this contract (each is actually two receivers as described above), one operating at 455 and the other at 500 kilohertz. As discussed earlier, each deck of the craft will use a different frequency. The two receivers have the same design and differ only in the tuning of the antenna, the frequency of a ceramic bandpass filter, the tuning of the discriminator and the tuning of a third harmonic circuit to be discussed later.

Thus, these FM receivers are supplied fixed-tuned to one frequency. Due to the nature of an FM receiver, the output signal level will remain constant regardless of signal input level so long as limiting exists. A unique means is provided in each receiver to gate off the output audio before any noticeable degradation of quality or any noticeable reduction in signal/noise occurs due to a drop of input signal level. No objectionable noise bursts are allowed before gate-off occurs when the transmitter is cut off. Should a fade-out occur for one receiver, a selector circuit will switch to the other receiver if it is providing a good signal. The selector will hold this signal so long as it is good, even though the other receiver may have returned to good operation with a stronger signal input. This switching between receivers is free of transients and is fast enough not to be noticeable. Since the audio signal output is fed to the SMU, which has an automatic gain control, neither the transmitter nor the receiver needs AGC. The receiver audio output is over one volt rms with a driving impedance of 200 ohms. Receiver sensitivity is sufficient to operate properly at a 22 foot range, which is twice the maximum range encountered in the space shuttle. Since the transmitted signal attenuates 18 dB each time distance is doubled, it is believed this design has a conservative safety factor.

The receiver antennas use the same type of ferrite that is used in the transmitter: Ferroxcube Q-1 material with an initial permeability of 125, a cross section of 0.48" x 0.12" and a length of 3.75". The winding uses 160 turns of No. 28 copper wire. The Q of the tuned antenna is 20, giving a bandwidth of 25 kilohertz at 500 kilohertz and 22.5 kilohertz at 455 kilohertz. (The bandwidth is much greater than the 6.0 kilohertz bandwidth of the transmitted signal and is therefore not critical.) The impedance of the antenna is about 60K ohms. This high impedance requires the first amplifier to have a high input impedance. The SD-304, made by Signetics, is a dual gate FET capable of very low intermodulation at high signal levels. Other strong signals or noise components that may be present in the craft therefore have less chance of causing intermodulation with the desired signal. The antenna is capable of generating several thousand microvolts when the transmitter is very close to the receiver. In the future, more than one transmitter might be used in the same chamber, so it is desirable to avoid a serious intermodulation problem.

The output of the first amplifier couples to a bandpass filter where practically all the selectivity of the receiver is obtained. This filter is a very compact one that will meet the MIL and NASA specs.

It uses ceramic discs to produce a bandwidth of 16 kilohertz at the 6 dB points and an attenuation of 50 dB at twice this bandwidth. This filter, made by Vernitron, is about .327" in diameter and 1.17" long. The filter output is coupled to a TV-FM chip by means of a matching transformer which provides a voltage gain of 12 dB. The minimum limiting level of this chip (3065, made by several firms and meeting MIL/NASA specs when packaged in a ceramic case) is 200 uv. This chip limits the signal at the 1.6V p-p level, detects the signal with a quadrature detector requiring a single tuned circuit, amplifies the audio signal to 1.0V rms and also provides an electronic attenuator which is used to mute the output when transmission ceases or drops below the limiting level as described above.

The circuit that selects the signal from only one of the receivers is a form of flip-flop circuit with some hysteresis to prevent jitter when the two control signals are equal. Each control signal is derived from the output of the last limiter. The selector circuit operates on the principle that as long as limiting occurs, a square wave output will be present and this will contain a third harmonic component signal. This signal is detected in each receiver and is used to control the flip-flop in such a way as to obtain the audio switching and muting described earlier. The two receivers use a total of one watt power from a single-ended supply of 12 VDC.

The overall total harmonic distortion of the transmitter and receiver is less than 5%.

Telephonics CORPORATION

WIRELESS MICROPHONE COMMUNICATION SYSTEM

REPORT NO. WMCS–001

APPENDIX A

SPACE SHUTTLE
WIRELESS COMMUNICATOR

COMPARISON OF PROPAGATION TECHNIQUES
WITHIN CABIN ENCLOSURES

TABLE OF CONTENTS

4.4 Transmission efficiency
- Bandwidth
- Power

4.5 EM compatability

5.0 OPTICAL

5.1 Optical link

5.2 Optical propagation

5.3 Electronic-optical transducer

5.4 Transmission efficiency

5.5 Optical compatability

6.0 ACOUSTIC

6.1 Sonics

6.2 Acoustic propagation

6.3 Electronic-acoustic transducers

6.4 Acoustic transmission efficiency

6.5 Sonic compatability

7.0 CONCLUSIONS

SPACE SHUTTLE TRANSCEIVER

1.0 WIRELSSS COMMUNICATION WITH CABIN ENCLOSURES

Wireless coupling within the cabin enclosures is possible by using sonic or electromagnetic propagation phenomena. Electromagnetic propagation covers the frequency spectrum from the low end of magnetic linkage, through the radiation frequencies of RF, to the near-visual light frequencies of optical techniques. The best technique depends upon the quality and reliability of transmission for a given power and equipment complexity that can be obtained within the equipment compatability requirements for the shuttle environment.

Magnetic coupling at a frequency of 450KHz proved to be the technique which provided the most uniform field structure within a shuttle enclosure and best met the requirements over the relatively short interior propagation distances with the least complex of mobile and static equipments.

In this report the propagation techniques are evaluated and the advantages of magnetic coupling delineated. The cabin enclosure model that was used will first be described followed by sections on field structures, coupling and propagation efficiency within this model for the magnetic, RF, optical and acoustic techniques.

2.0 SHUTTLE CABIN ENCLOSURE MODEL

Efficiency of signal propagation, one factor in the relative evaluation of techniques, depends upon the quality of the signal received for a given level of radiated power at the transmitter. A measure of this reception quality is the signal-to-noise ratio at the receiver input. The free-space loss of field strength with distance is well known; a distance-squared loss for radiation fields and a distance-cubed loss for the reactive fields of magnetic linkages. Fields within enclosures, however, are complicated by multiple boundary reflections of the propagated energy and by the intervention of obstacles between the transmitter and receptor.

Cabin geometry determines the nature of these reflected field structures. Cabin dimensions and wall materials determine attenuation rates, mode structure and null depths of the field. Port openings and damping materials within the "container" further influence the field structure. Shuttle cabin geometries and interior structures are complex, consequently for analytic simplicity, they are reduced to simple shapes which adequately model the enclosure affects upon internal field structure.

Sketches of the two shuttle cabin enclosures within which the ATE will be used are shown in Figure 2.1. Overlays of the simplifying geometric shapes - a half parabolic cylinder for the flight deck and rectangular volume for the lower deck - are shown with the approximating dimensions. For EM waves, the lowest order mode for the upper deck is the TM_{111} mode with a cutoff of 80MHz and the TE_{101} mode with a cutoff frequency of 87MHz. These cutoff frequencies clearly separate the bands anticipated for RF propagation and magnetic linkage into modes that are attenuated only by the lossy materials of the container and those that are attenuated primarily by the below cutoff condition. This will be expanded upon further in the sections on magnetics and RF that follow.

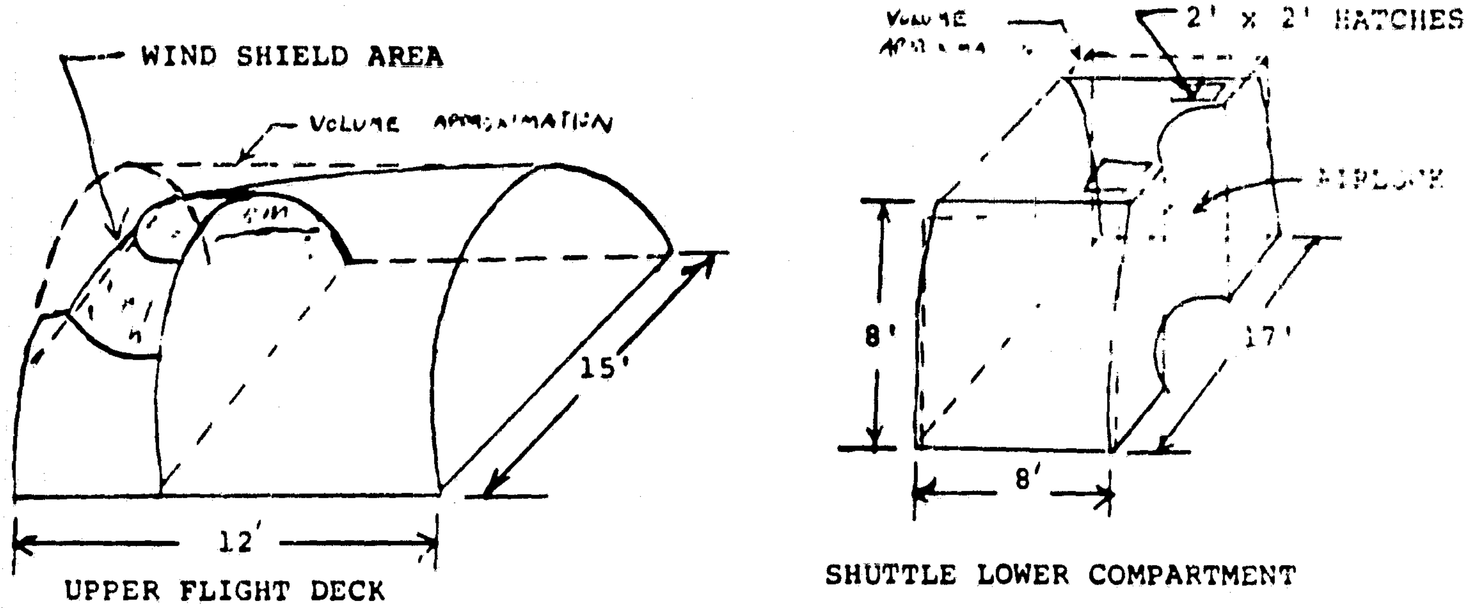

SHUTTLE ATE COMPARTMENTS

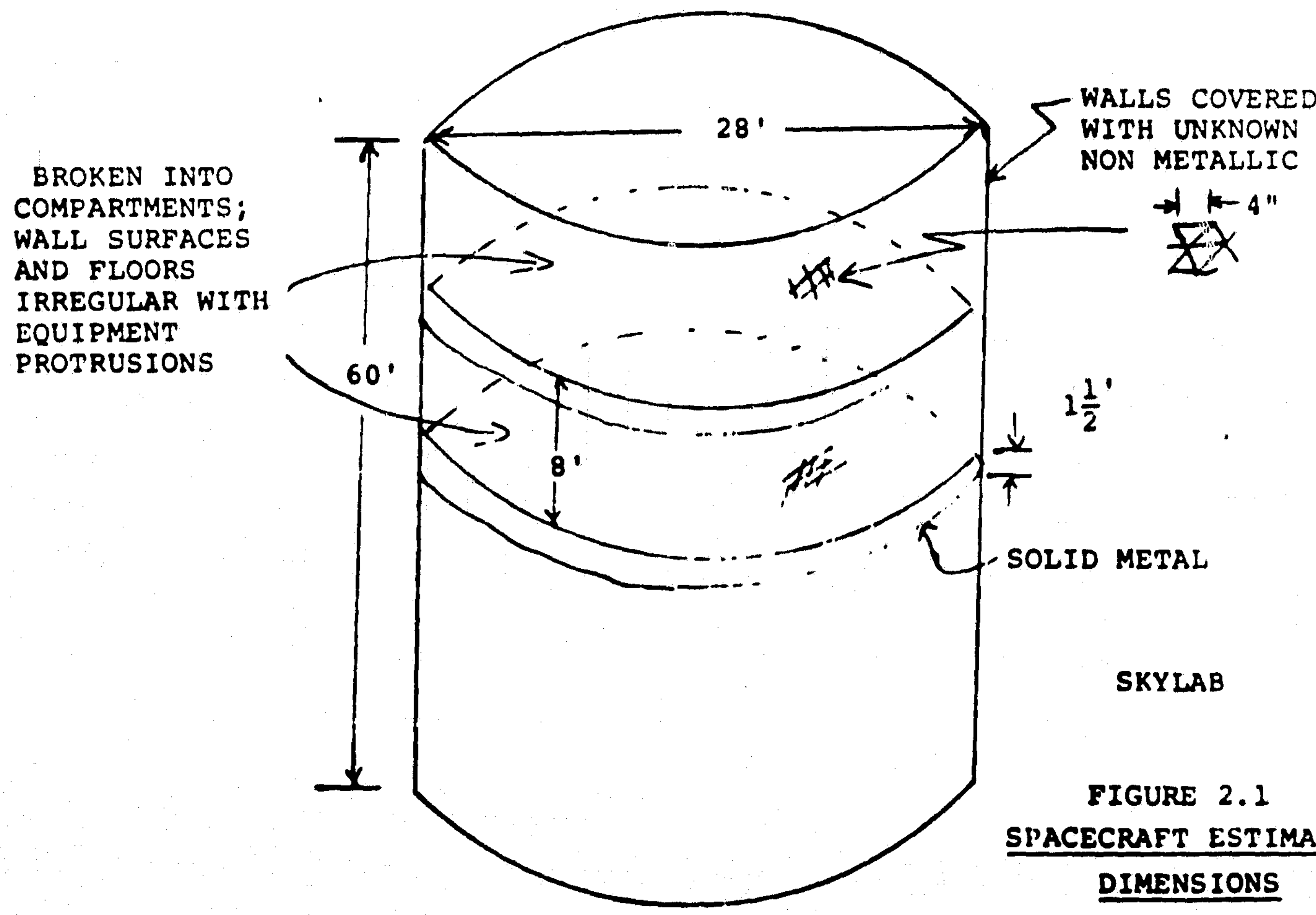

FIGURE 2.1
SPACECRAFT ESTIMATED DIMENSIONS

RF propagation above the cutoff frequency causes nulls in the interior field structure whose depth depends upon the damping of the interior. Three basic factors influence this damping: the windows, ports, and hatches allow EM leakage from the interior; the interior of the enclosures contain non-metallic lossy material; surface losses are introduced by the metal ohmic losses, high resistance junctures, and the high irregularity of the surface itself.

The RF model, for these reasons, considered an upper deck leakage window (windscreen area) of 10% as the major damping factor, while below, where leakage ports are improbable, the major damping factor would be the bodies of the astronauts which were assumed to occupy 10% of the volume. Wall losses were assumed to be those of sheet aluminum; the damping of any of the polystyrene covering (or other, if any) was considered negligible.

The field intensity of sonic and optical carriers is uniform within the enclosure, provided the sources are not impeded by obstacles. Wavelengths are small so nulls are of little concern. Shadowing by obstructions, however, are; these shadow areas must be irradiated by enclosure reflections and by diffraction about the blockage. For purpose of optical propagation it was pessimistically assumed that the direct path between the light source and detector was blocked and that all energy received was reflected off walls with a Lambert scatter of 0.5. Similarly for the sonic transmission, an obstacle was postulated and the diffraction field calculated. The field was negligibly small so that good reflection off boundary surfaces is required. Sonic reflection coefficients for the shuttle were not available; consequently for transmission efficiency evaluation an unimpeded path was used.

Evaluation of competing techniques must include the possible susceptibility of the chosen ATE link to extraneous fields falling within the ATE frequency band and must chose a band which would preclude interference in the bands of other spacecraft systems.

The EM susceptibility model for the shuttle cabin environment uses the interference level maximums specified by the MIL-STD-461A as amended for the space shuttle. In addition the radiation bands of shuttle equipment as defined by NASA and the bands assigned to high powered terrestrial transmission were delineated in the model as bands to be avoided for ATE operation.

The optical interference model assumes cabin lighting producing 4 watts/micron in the optical transmission band and standard solar and earth scatter spectrums that are used to determine the attenuation required of these natural sources at openings in the shuttle enclosure to exterior space.

The sonic noise environment for the shuttle structure at blast off and other operating conditions could not be determined at this time.

3.0 MAGNETIC COUPLING

Antenna field patterns are the sum of reactive magnetic and electric fields in the near vicinity and the radiation field which dominates as distance increases. In contrast to free space propagation where reactive fields attenuate as the cube and radiation fields directly with distance, fields within an enclosed space are the sum of multiple reflections whose strength must be dermined by mode analysis.

At frequencies above the cutoff frequency of the container, energy propagates primarily in a radiation waveguide mode, is reflected by "end caps" of the container and causes deep nulls within the container field pattern. This mode is discussed more fully in the next section on RF propagation. At frequencies below cutoff, however, the field regions fall in the near field of the antenna where the fields are primarily reactive. Antennas are coupled by the alternating magnetic flux linkages. Containment of the field increases the intensity above free space intensities. The choice of frequency is a compromise between pattern uniformity and the driving force needed to overcome the interaction between the antenna and container.

This section derives the field relations for an enclosed half cylinder model of the shuttle upper deck with transmitting and receiving antennas that are crossed ferrite solenoids; evaluates the effect of enclosure loading; determines the propagation transfer function for these fields; and transmission efficiency.

3.1 Magnetic Enclosure Fields

Magnetic field strength is derived for the half cylinder enclosure model that corresponds to the command deck of the shuttle. For the large wavelength to enclosure dimension ratio, retardation effects are negligible, consequently the field structures are solved statically and then varied at the carrier frequency to dermine the transmission function; i.e., the quasi-static solution for enclosed magnetic fields.

The derived field function, Figure 3.1, shows that the field at a static receiver antenna for a transmit antenna that is moved along the axis of the cabin falls off at the free space rate up to one meter from the antenna and at a lower rate at greater spacing. The received field strength from a distance of 0.3 meters spacing to the end of the enclosure is less than 50dB. When the axis of either of the orthogonal antennas approaches within some 6 centimeters of the enclosure surface the interaction between the surface and antenna rapidly drives that antenna's field to zero as the spacing closes. The orthogonal antenna is not affected (except in corners) and is, under these conditions, the primary link.

The plot of field strength, Figure 3.1, is based upon the field relationships summarized in Figure 3.2 and derived in Appendix 3.1 for the illustrated enclosure model. The magnetic components β_ρ and β_θ are considered since the receiver antenna is mounted on the end walls of the cabin and responds to these components only. The solutions are separatable into functions of the three cylindrical coordinates in which z variation is expressed through hyperbolic, θ variations by sinusoidal, and ρ variations by Bessel functions. The relationships apply for two orthogonal solenoidal antennas located anywhere within the enclosure. The field components are the sum of cylindrical harmonics each with attenuation rates determined by the enclosure dimensions. For simplicity field plots are separated into three regions; (1) close to the antenna where, since the cylindrical harmonics attenuate slowly, the free space relationship is more economically used; (2) far from the antenna where only one or two nodes predominate; and (3) the intermediate region where for simplicity the function was faired in between the first two.

The free space function for a solenoidal coil, as given in Appendix 3.1, relates field strength near the antenna. This relation is successively approximated by simpler reduced functions; first, as the distance becomes greater than the axial length, then as the distance becomes greater than the effective radius. The final reduction gives the well known distance-cubed magnetic dipole equation.

The half cylinder flux density is derived in Appendix 3.2. through the magnetic vector potential functions for cylindrical coordinates. Boundary conditions for the half-cylinder specified the mode attenuation functions and these modes that can be supported. Image analysis with the summation of multiple reflections determines the constants for the z function.

The magnitude of the cylindrical constants (C_{nk}) are determined by the boundary conditions at the antenna coil. The coil shape was deliberately distorted to simplify the derivation to correspond to differential area shapes. For the relative dimensions of enclosure and coil the approximation is valid.

The loss coefficients for sixteen modes for the chosen half cylinder model are tabulated in the Appendix 3.2. Intensities of the dominant modes at the receiver as a function of transmitter spacing along the cylinder axis are plotted in Figure 3.3. These plots are used to dermine the transition point between the far zone where the single low order mode predominates alone and the intermediate zone of multiple harmonics.

The cabin intensity, based on these derived relationships, is shown as a function of z spacing for a transmitter located midway between the cylinder wall and floor. The receiver coil is located at the end wall at a radius of 1.2 meters at an angle of maximum reception. The intensity for a coil with its axis coaxial with the cabin axis is stronger than the coil whose axis is orthogonal to the cabin axis except when the antenna approaches the end walls. The lowest order mode of each orientation predominates at a distance roughly one half the cabin length. The free space relation predominates within spacings of a meter or less down to about 6 cm where enclosure interaction affects the coaxial oriented antenna. The received field strength varies less than 50dB from a spacing of 0.3 meter to the cabin extreme of 3.66 meters.

The enclosure of an antenna by a metal surface reacts on the antenna input impedance. With a magnetic coil antenna the impedance is primarily inductive; this inductance is reduced as the enclosure becomes smaller and consequently the current to obtain a given field strength increases. Position changes of the transmitter within the enclosure causes variable loading and detuning. As the following analysis showed, this loading only became critical when the antenna approached within 6 centimeters of a container boundary.

The analysis examined two extremes of position: (1) when the antenna was in a position where only the dominant mode of the container interacted with the antenna; and, (2) when the antenna approached the container surface.

For the dominant mode analysis of Appendix 3.4 energy considerations provided an expression for inductance:

$$L = \frac{\pi a^2 \mu_c N^2}{\ell}\left[1 - \left(\frac{\mu_c}{\mu_c}\right)\left(\frac{1}{\ell \mu_1}\right)\left(\frac{\pi a^2}{\pi b^2}\right)\frac{1}{J_c(\mu_1 b)}\right]$$

where
- N = antenna turns
- a = antenna coil radius
- ℓ = antenna length
- μ_c = antenna core permeability
- b = cabin radius
- μ_1 = primary mode attenuation factor

For the design parameters of the antenna

$N = 128$

$a = 3.72\times10^{-5}$

$\mu_c = 100$

and the cabin mode b = 2.3m. The inductance change from free space was .05%.

As the antenna approaches the container surface free space image analysis is more appropriate. The relations used to derive the change in inductance with distance, Figure 3.4, is derived in Appendix 3.3. Serious reduction of inductance begins at spacing of 0.1 meters.

These results show that cabin boundary loading on the transmitter is negligible except when extremely close to the walls, a condition not expected to be encountered too frequently.

3.3 Electronics-Magnetic Field Coupling

The transducer between transmitter electronics and the magnetic field and between field and receiver electronics are solenoidal coil antennas. In this section the transduction ratios input impedances, transmitter drive power, and receiver sensitivity are determined.

The inductance of a solenoid of length l and radius R is given by

$$L_c = (\pi \mu R^2 N^2)/(l + 0.7R) \text{ henrys}$$

The magnetic field in the core of the solenoid is

$$B = \frac{LI}{AN}$$

$$\simeq \frac{NI}{l}$$

where $A = \pi R^2$

The transmitter transduction ratio is therefore $\mu N/l$.

The losses in the solenoid, since there is no radiated power, determines the transmitter power requirements. The losses are primarily core, wiring and the coupled losses of the container. The parameters of the solenoidal antenna used in the design are:

Ferrite core

12.2mm x 3mm x 95mm

Q = 40

N = 128

μ_c = 100

The inductance Lo is 370 microhenries. In a tuned circuit, the resonant input impedance is resistive and 275K ohms.

The receiver transduction gain between input magnetic intensity B and the antenna output current is given through the energy equality

$$\frac{1}{2} i_L^2 L = \frac{1}{2} \int_V \mu H^2 dV$$

For a receiving antenna volume of $V = \pi a^2 (\mu_c/\mu_0) \ell$ the transduction ratio

$$\frac{i_L}{B} = \left[\frac{\pi a^2 \ell}{\mu L}\right]^{1/2} = \frac{\ell}{\mu_c N}$$

for receiver antenna parameters the same as the transmitter antenna is 5.9 amperes/weber.

The sensitivity of the receiver is determined by the noise current of

$$i_n^2 = \frac{4KT_eB}{Req.}$$

where T_e = effective temperature of the circuit
B = bandwidth
Req = equivalent circuit resistance

3.4 Transmission Efficiency

One measure of comparison between wireless communication propagation links is the ratio of received signal power to noise for a given input power for a fixed receiver/transmitter position. This measure is defined as the efficiency of transmission.

The margin of the signal power above noise indicates how well the unit performs within regions of low field strength within the cabin. Figure 3.5 schematically shows the link for a receiver and transmitter at opposite ends of the half-cylinder cabin model. The antenna parameters are those previously defined in Section 3.3. The field intensity loss at the receiver from Figure 3.3 is -104dB. The received signal is 94dB above noise. This gain margin is sufficient to provide good transmission even under conditions of field strength loss that are not accounted for in the simple half cylinder enclosure mode.

Electromagnetic Compatability

The specification "Electromagnetic Interference Characteristics, Requirements for the Space Shuttle Program" SL - E - 0002 dated June 9, 1973 specifies that continuous or repetitive broadband E-field emissions shall not be generated and radiated in excess of values shown in Figure 22A.

The limit at 450KHz from Figure 22A is 94dBμV/m/MHz. This radiation level coverts to -28dB amps turn/m for a 4KHz band. The flux level is -146dB weber/m^2 and is 14dB below the flux density of -131.4dB weber/m^2 for the wireless communicator transmission level at the antenna.

Assuming equal attenuation of the signal and this interference would provide only marginal received signal-to-noise ratio. Care would need to be exercised in choosing a transmission band that does not fall in an interference region just meeting the above specification.

FIGURE 3.1

SUMMARY

HALF - CYLINDER CABIN MAGNETIC FIELD STRENGTH RELATIONS

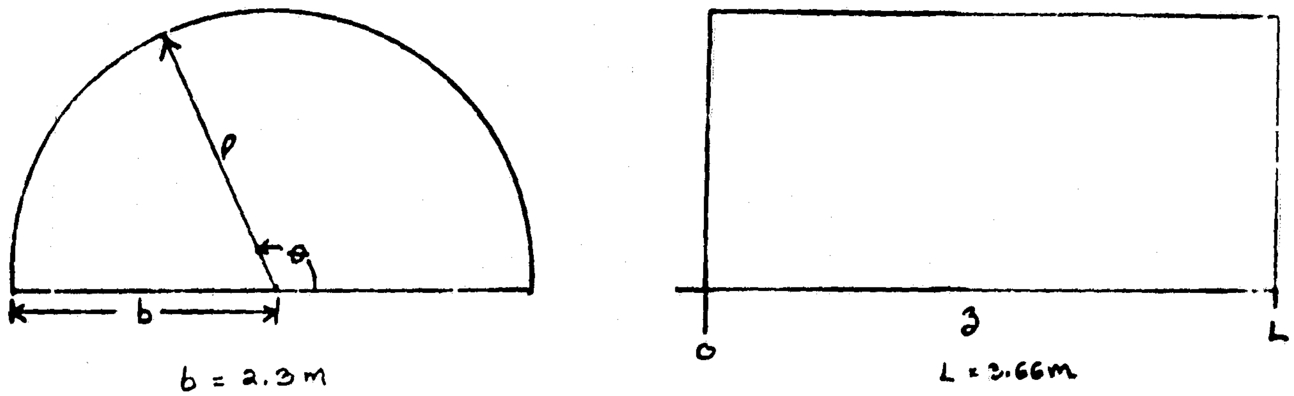

TRANSMITTER COIL AXIS COAXIAL WITH CABIN AXIS:

$$B_\rho = \sum_r \sum_m (\mu_r C_{rm}) \frac{\sinh[\mu_r(L - z_r)]}{\sinh \mu_r L} \cosh \mu_r z \cos m\theta \left[-J_m'(\mu_r \rho)\right]$$

m must be even

$$\mu_r C_{rm} = \frac{\mu N I}{l} \left(\frac{\pi a^2}{\pi b^2}\right)(-1)^{m/2} \left\{ \frac{8m^2 \left(J_m'(\mu_r x_0)/(\mu_r x_0)\right)}{\pi \varepsilon \, J_{m+1}^2(\mu_r b)} \right\}$$

$\varepsilon = 2$ for $m = 0$ $\qquad \varepsilon = 1$ for $m \neq 0$

TRANSMITTER COIL AXIS CROSS-AXIAL WITH CABIN AXIS.

$$B_\theta = \sum_r \sum_m (\mu_r C_{rm}) \frac{\cosh[\mu_r(L - z_r)]}{\sinh \mu_r L} \cosh \mu_r z \sin m\theta \left(\frac{m}{\mu_r \rho}\right) J_m(\mu_r \rho)$$

m must be odd

$$\mu_r C_{rm} = \frac{\mu N I}{l} \left(\frac{\pi a^2}{\pi b^2}\right)\left(\frac{l}{a}\right)(-1)^{\frac{m-1}{2}} \left\{ \frac{2m \left(J_m(\mu_r x_0)/\mu_r x_0\right)}{\pi \, J_{m+1}^2(\mu_r b)} \right\}$$

μ_r = CABIN MODE ATTENUATION COEFFICIENT

L = CABIN LENGTH

b = CABIN RADIUS

z_r = XMTR z LOCATION

x_0 = " ρ LOCATION

$J_m(y)$ = Bessel Function order m.

l = XMTR COIL LENGTH

a = XMTR COIL EFFECTIVE RADIUS

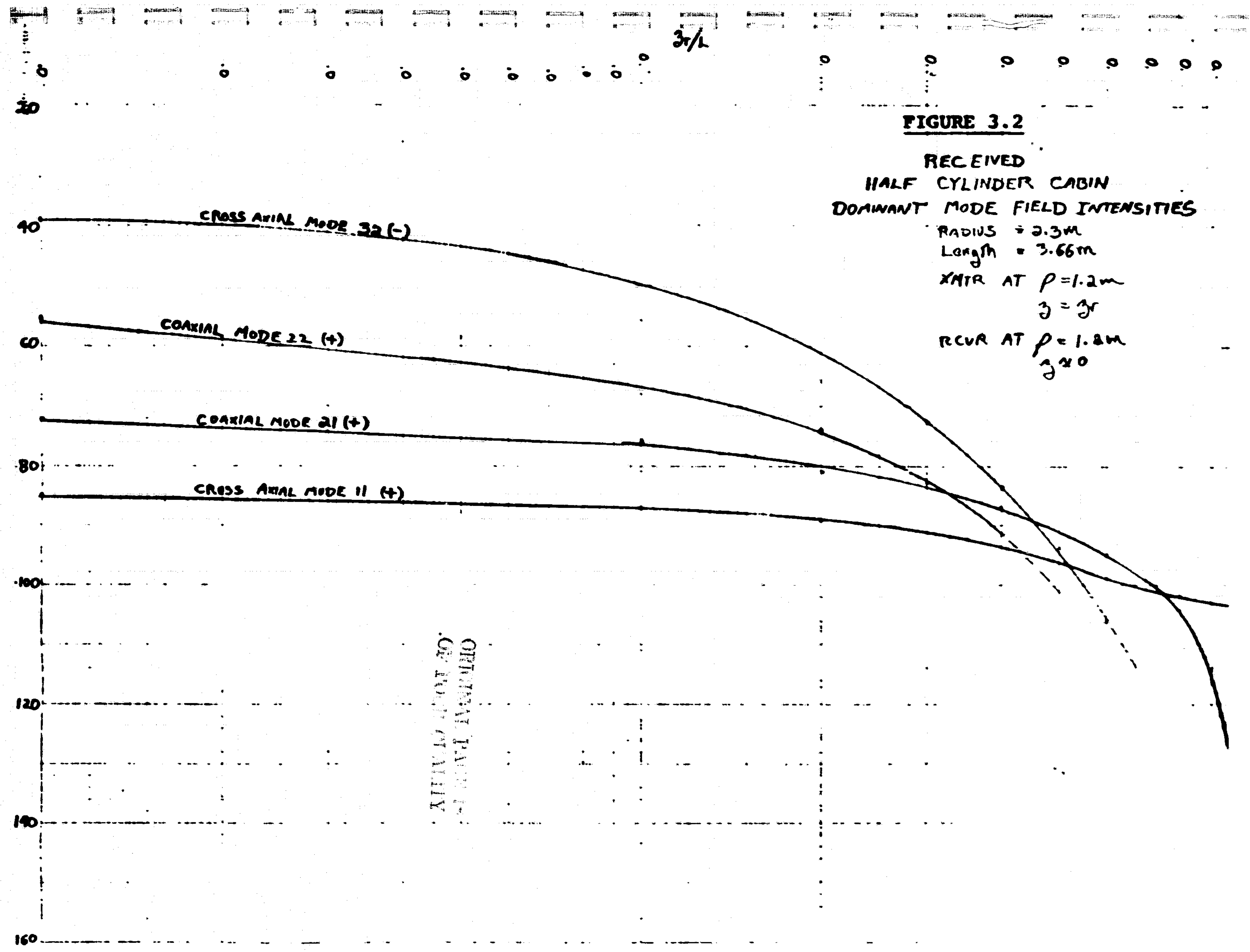

FIGURE 3.2

RECEIVED
HALF CYLINDER CABIN
DOMINANT MODE FIELD INTENSITIES

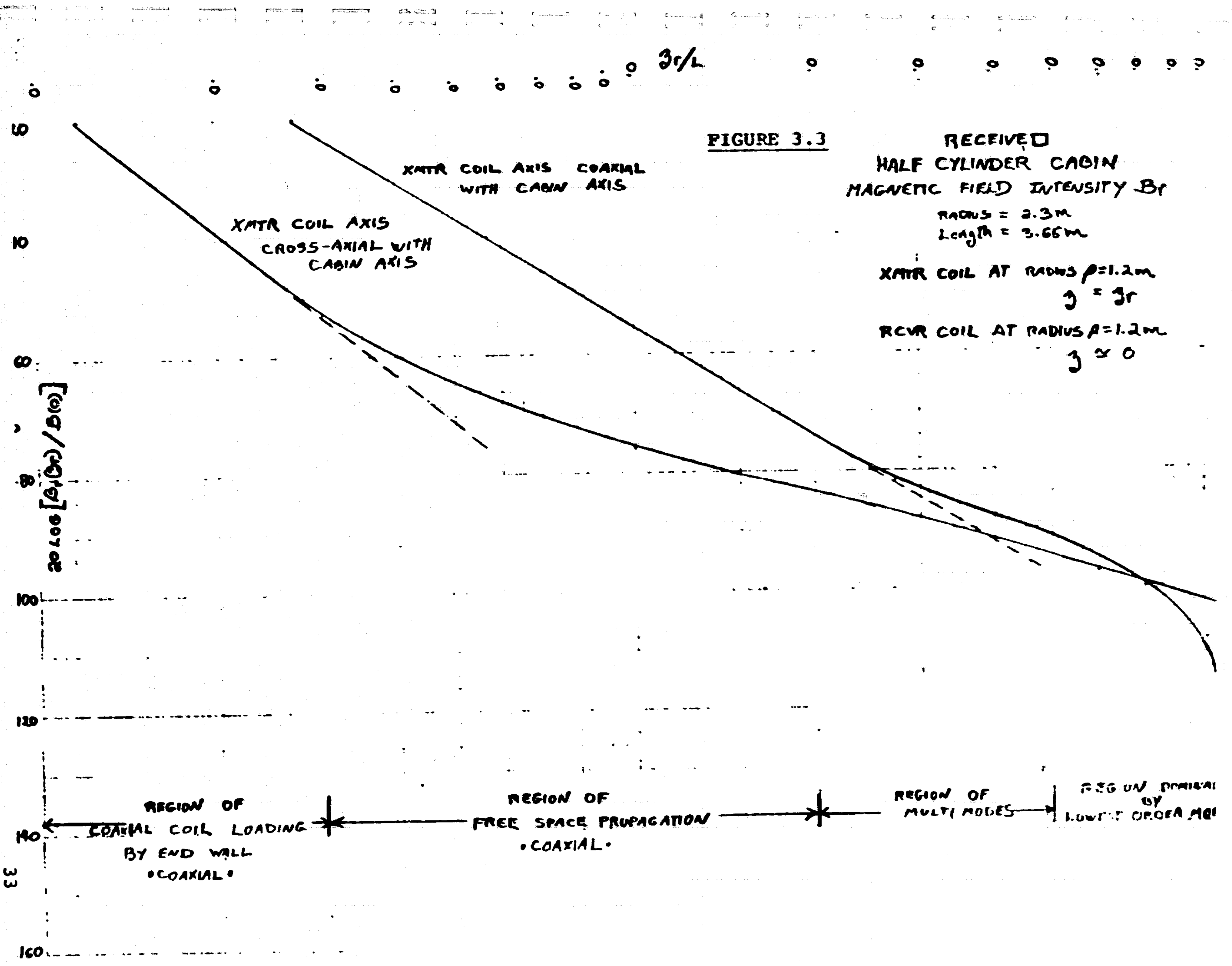
3r/L
RECEIVED
HALF CYLINDER CABIN
MAGNETIC FIELD INTENSITY Br
RADIUS = 2.3m
Length = 3.66m
XMTR COIL AT RADIUS ρ=1.2m
z = 3r
RCVR COIL AT RADIUS ρ=1.2m
z ≈ 0
XMTR COIL AXIS COAXIAL
WITH CABIN AXIS
XMTR COIL AXIS
CROSS-AXIAL WITH
CABIN AXIS
20 LOG [Br(3r)/B(0)]
10
60
80
100
120
140
160
REGION OF
COAXIAL COIL LOADING
BY END WALL
•COAXIAL•
REGION OF
FREE SPACE PROPAGATION
•COAXIAL•
REGION OF
MULTI MODES
FIGURE 3.3

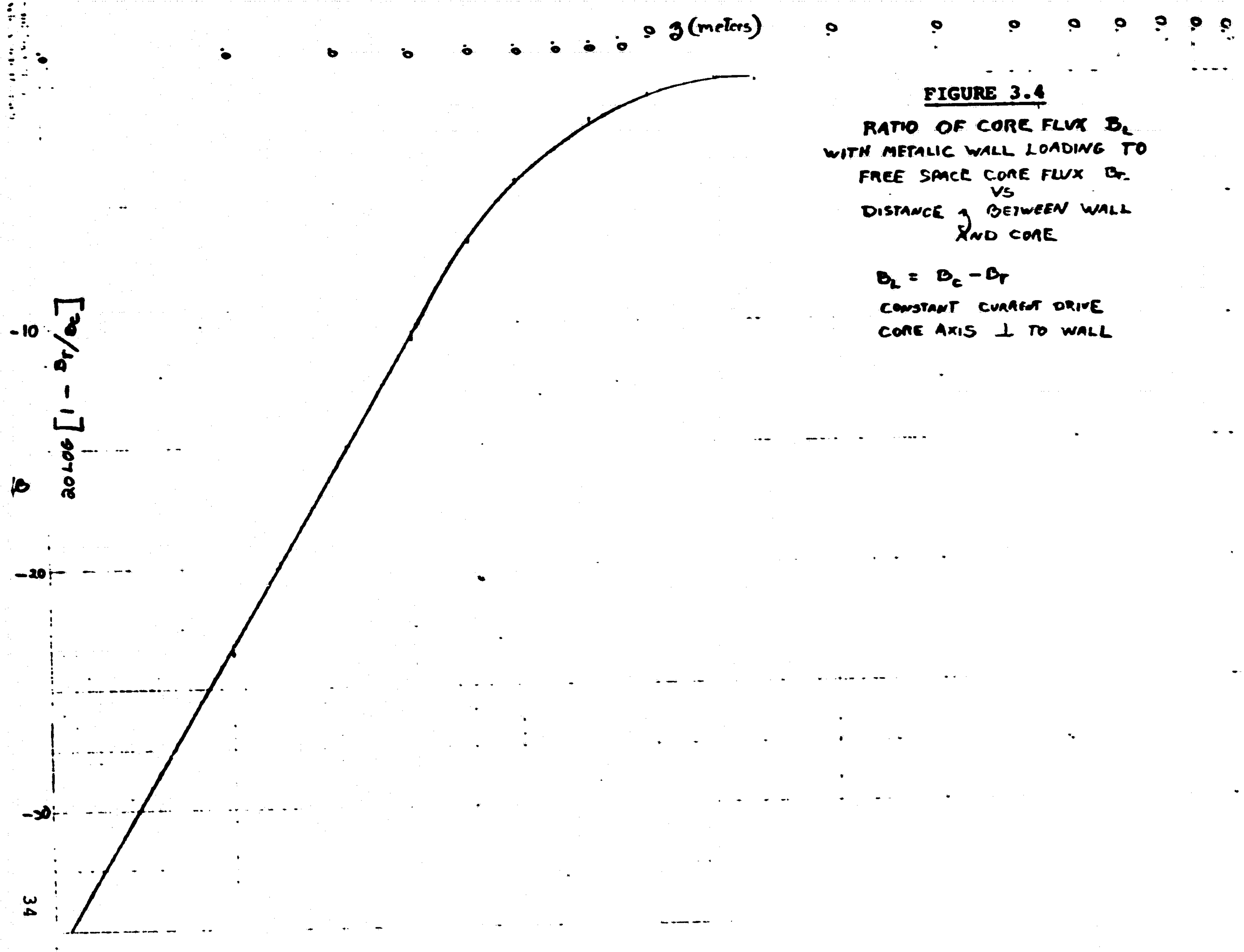

FIGURE 3.4

RATIO OF CORE FLUX B_L WITH METALIC WALL LOADING TO FREE SPACE CORE FLUX B_T VS DISTANCE z BETWEEN WALL AND CORE

$B_L = B_C - B_T$

CONSTANT CURRENT DRIVE

CORE AXIS ⊥ TO WALL

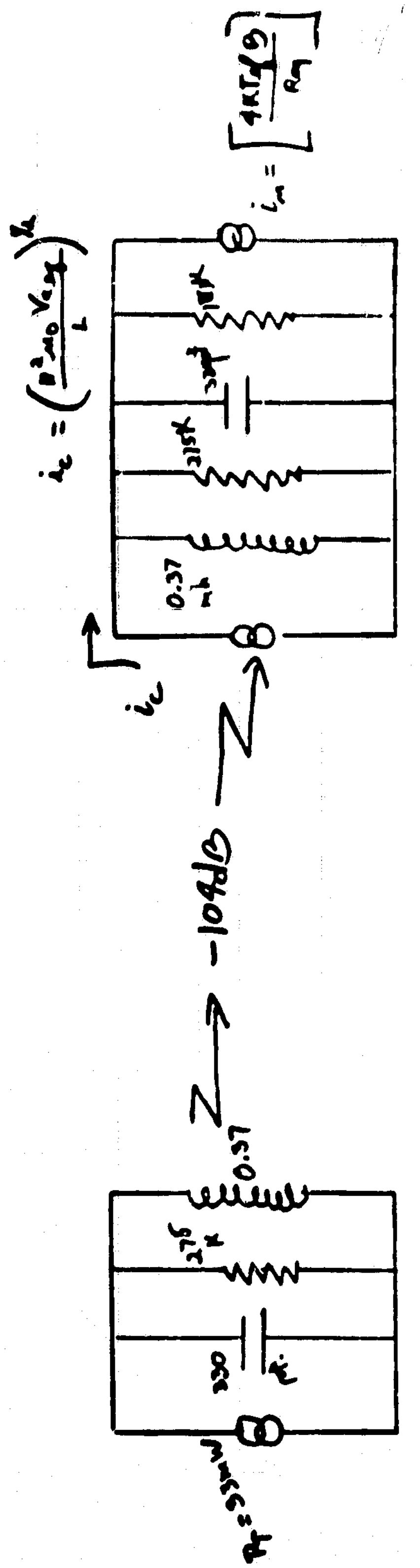

FIG 3.5

APPENDIX 3.1

FREE SPACE FIELD SOLENOIDAL COIL

AXIAL MAGNETIC FLUX DENSITY B_z:

$$B_z = \frac{\mu I}{4\pi a \tan\alpha}\left\{\frac{N\pi a\tan\alpha + z}{\left[a^2 + (N\pi a\tan\alpha + z)^2\right]^{1/2}} + \frac{N\pi a\tan\alpha - z}{\left[a^2 + (N\pi a\tan\alpha - z)^2\right]^{1/2}}\right\}$$

α = winding pitch

L = coil length = $2\pi N a \tan\alpha$

a = radius of solenoid

N = number of turns

$$B_z = \frac{\mu_0 N I}{2L}\left\{\frac{L/2 + z}{\left[a_\varepsilon^2 + (L/2 + z)^2\right]^{1/2}} + \frac{L/2 - z}{\left[a_\varepsilon^2 + (L/2 - z)^2\right]^{1/2}}\right\}$$

where $a_\varepsilon = \left(\frac{\mu_c}{\mu_0}\right)^{1/2} a_{actual}$

$$B_z \Rightarrow \frac{\mu_0 N I a_\varepsilon^2}{2(a_\varepsilon^2 + z^2)^{3/2}} \qquad z \gg l$$

$$\Rightarrow \frac{\mu_0 N I \pi a_\varepsilon^2}{2\pi z^3} \qquad z \gg a_\varepsilon$$

CORE FLUX

$$B_z(0) = \frac{\mu N I}{L}\left[1 + \left(\frac{2a_\varepsilon}{L}\right)^2\right]^{1/2}$$

APPENDIX 3.2

HALF CYLINDER FLUX DENSITY

VECTOR MAGNETIC POTENTIAL; CYLINDRICAL COORDINATES

$$A_\rho = \left(-Ae^{hz} + Be^{-hz}\right)\left[cJ_{m+1}(h\rho)\right]\cos(m\theta+\delta)$$

$$A_\theta = \left(-Ae^{hz} + Be^{-hz}\right)\left[cJ_{m+1}(h\rho)\right]\sin(m\theta+\delta)$$

$$A_z = \left(Ae^{hz} + Be^{-hz}\right)\left[cJ_m(h\rho)\right]\cos(m\theta+\delta)$$

FLUX DENSITY

$$\bar{B} = \nabla \times \bar{A}$$

$$= \hat{\rho}B_\rho + \hat{\theta}B_\theta + \hat{k}B_z$$

$$= \hat{\rho}\left[\frac{\partial A_z}{\rho\partial\theta} - \frac{\partial A_\theta}{\partial z}\right] + \hat{\theta}\left[\frac{\partial A_\rho}{\partial z} - \frac{\partial A_z}{\partial \rho}\right] + \hat{k}\left[\frac{\partial \rho A_\theta}{\rho\partial\rho} - \frac{\partial A_\rho}{\rho\partial\theta}\right]$$

$\delta = \pi/2$

$$B_\rho = (hc)\left(Ae^{hz} + Be^{-hz}\right)\left[\cos m\theta\right]\left[-J_m'(h\rho)\right]$$

$$B_z = (hc)\left(-Ae^{hz} + Be^{-hz}\right)\left[\cos m\theta\right]\left[J_m(h\rho)\right]$$

$$B_\theta = (hc)\left(Ae^{hz} + Be^{-hz}\right)\left[\sin m\theta\right]\left(\frac{m}{h\rho}\right)\left[J_m(h\rho)\right]$$

BOUNDARY CONDITIONS: HALF CYLINDER

$B_\rho = 0$ when $\rho = b$ i.e., $J_m'(hb) = 0$

$B_\theta = 0$ when $\theta = 0, \pi$

$B_z = 0$ when $z = 0, L$

Z FUNCTION CONSTANTS

Images of loop reflected off ends of half-cylinder. Image located at $z = 2mL + z_r$ and $z = 2mL - z_r$

For $z < z_r$

ANTENNA AXIS PARALLEL TO CYLINDER AXIS:

$$F_z(z) = \sum_{m=0}^{\infty} e^{-\mu_r(2mL + z_r - z)} + \sum_{m=1}^{\infty} e^{-\mu_r(2mL - z_r + z} - \sum_{m=1}^{\infty} e^{-\mu_r(2mL - z_r - z} - \sum_{m=0}^{\infty} e^{-\mu_r(2mL + z_r + z)}$$

$$= 2\left(e^{-\mu_r z_r} \sum_{0}^{\infty} e^{-2m\mu_r L} - e^{+\mu_r z_r} \sum_{m=1}^{\infty} e^{-2m\mu_r L}\right) \sinh \mu_r z$$

$$= 2\left[\left(e^{-\mu_r z_r} - e^{+\mu_r z_r}\right) \sum_{m=0}^{\infty} e^{-2m\mu_r L} + e^{\mu_r z_r}\right] \sinh \mu_r z.$$

$$F_z(z) = 2 \frac{\sinh \mu_r(L - z_r)}{\sinh \mu_r L} \sinh \mu_r z$$

$$F_\rho(z) = + \sum_{m=0}^{\infty} e^{-\mu_r(2mL + z_r - z)} + \sum_{m=} e^{-\mu_r(2mL}$$

CONSTANTS C_{mk}: ANTENNA COAXIAL WITH HALF-CYLINDER

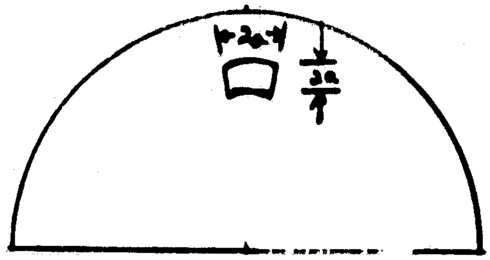

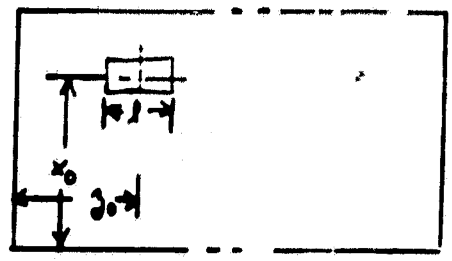

$$\mu i = \nabla \times B$$

$$\mu i_\phi = \frac{\partial B_\rho}{\partial z} - \frac{\partial B_z}{\partial \rho}$$

$= 0$ in space.

$$\mu i_\phi = -\frac{\partial B_z}{\partial \rho} \; ; \quad \text{since } \frac{\partial B_\rho}{\partial z} = 0 \text{ at current sheet.}$$

$$= \sum\sum C_{mk} \cosh kz \cos m\phi \, k^2 J_m'(k\rho)$$

$$= \mu \frac{IN}{l} \operatorname{rect}\left(\frac{z-z_0}{l}\right) \operatorname{rect} \frac{x_0\theta}{2a} \left\{\delta(\rho = x_0 + a) - \delta(\rho = x_0 - a)\right\}$$

Multiply both sides of equality by $\cos m\phi \, J_m(k\rho) \, d\rho \, d\phi \, dz$ and integrate over half-cylinder space:

$$\frac{\mu IN}{l}(l) \int_{\frac{\pi}{2} - \frac{a}{x_0}}^{\frac{\pi}{2} + \frac{a}{x_0}} \cos m\phi \, d\phi \int_0^b J_m(k\rho)\left[\delta(\rho = x_0 + a) - \delta(\rho = x_0 - a)\right] d\rho$$

$$= kC_{mk} \int_{z_0 - l/2}^{z_0 + l/2} \cosh kz \, dz \int_0^\pi \cos m\phi \cos m\phi \, d\phi \left(\frac{1}{4m}\right) \int_0^b (k\rho)\left[J_{m-1}^2(k\rho) - J_{m+1}^2(k\rho)\right] d(k\rho)$$

$m = \text{even}$

$$\mu I N (-1)^{m/2} \left(\frac{2a}{x_0}\right) \left\{ J_m[h(x_0+a)] - J_m[h(x_0-a)] \right\} = h C_{mh} (l) \left(\frac{\pi}{2} \epsilon\right) \frac{1}{2} J_m^2(hb)$$

$$\epsilon = 2 \text{ when } m = 0$$
$$= 1 \quad m \neq 0$$

$$(h C_{mh}) = \frac{(-1)^{m/2} 2 \mu I N a \left\{ J_m[h(x_0+a)] - J_m[h(x_0-a)] \right\}}{\pi l x_0 \, \epsilon \left[\frac{(hb)^2 J_{m+1}^2(hb)}{m^2} \right]}$$

$m = 0$

$$h C_{0h} = (-1)^{m/2} \frac{\mu I N (\pi a^2)}{l} \frac{4 J_m'(h x_0) h^2}{(h x_0) \pi^2}$$

CONSTANTS C_{mh}: ANTENNA CROSSAXIAL WITH HALF-CYLINDER

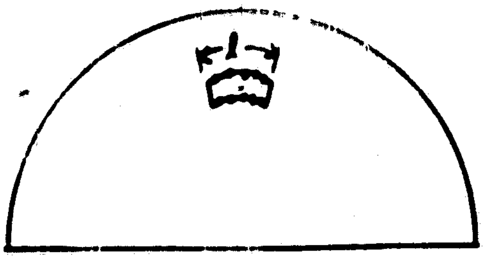

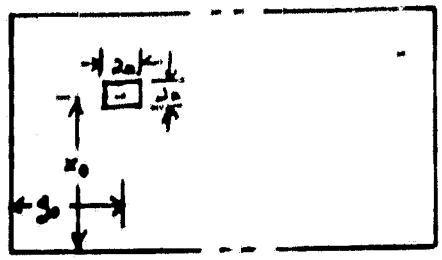

$$\mu i = \nabla \times B$$

$$\mu i_z = \frac{\partial \rho B_\phi}{\rho \partial \rho} - \frac{\partial B_\rho}{\rho \partial \phi}$$

$= 0$ in space

$$= -\frac{\partial \rho B_\phi}{\rho \partial \rho} \quad \text{since} \quad \frac{\partial B_\rho}{\rho \partial \phi} = 0 \quad \text{at current sheet}$$

$$= 2 \sum\sum h C_{mh} \cosh hz \sin m\phi \frac{m}{\rho} J_m'(h\rho)$$

$$= \frac{\mu N I}{l} \operatorname{rect} \frac{z - z_0}{2a} \operatorname{rect} \frac{x_0 \phi}{l} \left[\delta(\rho = x_0 - a) - \delta(\rho = x_0 + a)\right]$$

Multiply both sides of equality by:

$$[J_{m-1}(h\rho) + J_{m+1}(h\rho)] \sin m\phi \, \rho^2 \, d\rho \, d\phi \, dz$$

$$= m \frac{J_m(h\rho)}{h} \sin m\phi \, \rho \, d\rho \, d\phi \, dz.$$

Integrate over half-cylinder space:

$$(hC_{mh}) m \int_{z_0-a}^{z_0+a} \cosh hz \, dz \int_0^\pi \sin(m\phi) \sin(m\phi) \, d\phi \; 2\int_0^b \rho \, J_m'(h\rho)[J_{m-1}(h\rho) + J_{m+1}(h\rho)] \, d\rho$$

$= 0$ if $m \neq m$

$= 0$ if $l \neq h$ since $J'(hb) = 0$

$$m = m \quad = (hC_{mh}) \, m \, (2a) \left(\frac{\pi}{2}\right) \int_0^b \rho \left[J_{m-1}^2(h\rho) - J_{m+1}^2(h\rho)\right] d\rho.$$

$$= (hC_{mh})(2a)\left(\frac{m\pi}{2}\right) \frac{2m}{h^2} J_m^2(hb)$$

$$= \frac{\mu N I}{\ell} (2a) \left[\int_{\pi/2 - a/2x_0}^{\pi/2 + a/2x_0} \sin m\theta \, d\theta \right] \left(\frac{\alpha}{h^2}\right) \int \rho \, J_m(h\rho) \left[\delta(\rho = x_0 - a) - \delta(\rho = x_0 + a) \right] d\rho$$

$= 0$; For "m" even

$$= \frac{2 \mu N I}{\ell} (-1)^{\frac{m-1}{2}} \left(\frac{\ell}{x_0}\right) \left\{ (x_0 - a) J_m[h(x_0 - a)] - (x_0 + a) J_m[h(x_0 + a)] \right\}$$

For "m" odd

$$= (-1)^{\frac{m-1}{2}} \mu N I \left\{ \frac{h(x_0 - a)}{x_0} J_m[h(x_0 - a)] - \frac{h(x_0 + a)}{x_0} J_m[h(x_0 + a)] \right\}$$

$$h C_{mh} = \frac{(-1)^{\frac{m-1}{2}} \mu N I \left\{ h(x_0 - a) J_m[h(x_0 - a)] - h(x_0 + a) J_m[h(x_0 + a)] \right\}}{\pi m \, J_m^2(hb) \, x_0}$$

$a \ll x_0$

$$h C_{mh} = \frac{(-1)^{\frac{m-1}{2}} \mu N I \left[2 h^2 a \, J_m(h x_0) \right]}{(h x_0) \pi m \, J_m^2(hb)}$$

HALF-CYLINDER LOSS COEFFICIENTS

RADIUS = 2.3 meters

TABLE OF LOSS COEFFICIENTS μ_r
FOR THE HALF CYLINDER MODES mr

m \ r	1	2	3	4
0	—	1.67	3.05	4.42
1	0.8	2.32	3.71	5.09
2	1.33	2.92	4.35	5.73
3	1.83	3.48	4.93	6.34
4	2.31	4.03	5.51	6.94

$$F(d) = e^{-\mu_r d}$$

$$20 \log F(d) = -8.69 \mu_r \ dB/m.$$

APPENDIX 3.3

ENCLOSURE LOADING ON CORE FIELD STRENGTH

A: COIL CURRENT LOSS WITH INDUCTANCE DETUNING

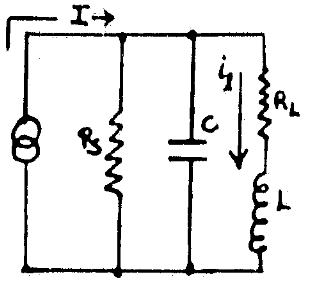

TUNED ANTENNA CIRCUIT

$$\frac{i_l}{I} = \frac{R_S}{R_S(1-\omega^2 LC) + R_L + j\omega\left[L + R_L R_S C\right]}$$

$R_S \to \infty$

$$\frac{i_l}{I} = \frac{1}{(1-\omega^2 LC) + j\omega C R_L}$$

$$= \frac{1}{1-\left(\frac{\omega}{\omega_0}\right)^2\left(\frac{L}{L_0}\right) + j\left(\frac{\omega}{\omega_0}\right)Q^{-1}}$$

$\omega = \omega_0$

$$\frac{i_l}{I} = \frac{1}{1-(L/L_0) + jQ^{-1}} \simeq \frac{1}{1-L/L_0}$$

B: COIL FLUX REDUCTION BY METAL WALL FOR CONSTANT CURRENT

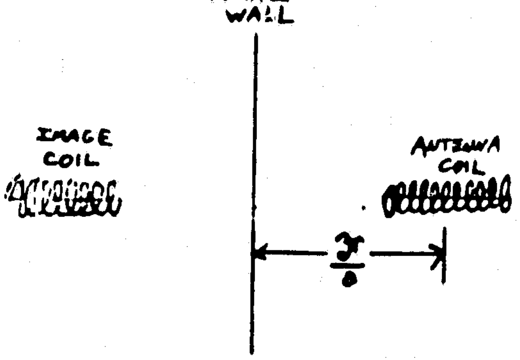

Image coil axial flux $B_z(z_r)$:

$$\frac{B_z(z)}{B_z(0)} = \frac{1}{2}\left[1+\left(\frac{2a_c}{l}\right)^2\right]^{1/2}\left\{\frac{1+(2z/l)}{\left[\left(\frac{2a_c}{l}\right)^2+\left(1+\frac{2z}{l}\right)^2\right]^{1/2}} + \frac{1-\left(\frac{2z}{l}\right)}{\left[\left(\frac{2a_c}{l}\right)^2+\left(1-\frac{2z}{l}\right)^2\right]^{1/2}}\right\}$$

$$\frac{B_z(0) - B_z(z_r)}{B_z(0)} = 1 - \frac{B_z(z_r)}{B_z(0)}$$

TRANSMIT ANTENNA INPUT IMPEDANCE

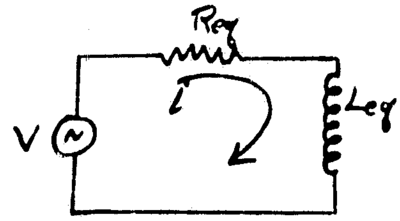

$$V = i\left(R_{eq} + j\omega L_{eq}\right)$$

From energy considerations

$$\frac{1}{2} L i^2 = \frac{1}{2\mu}\int_V B^2 dV$$ integrated over enclosure volume.

where $B^2 = B_\rho^2 + B_z^2$

$$\therefore \quad L_\alpha = \frac{1}{\mu i^2}\int_0^L\int_0^{2\pi}\int_0^b \left[B_\rho^2(\rho,z) + B_z^2(\rho,z)\right]\rho\, d\rho\, d\theta\, dz.$$

$$B_z \simeq I\sum K_r e^{-\mu_r(z-z_r)} J_0(\mu_r\rho) \qquad z > z_r$$

$$B_\rho \simeq I\sum K_r e^{-\mu_r(z-z_r)} J_1(\mu_r\rho)$$

$$K_r = \frac{\mu N a^2}{l\left[J_0(\mu_r b)\right]^2 b^2}$$

$$L = -\frac{K_1^2\, 2\pi}{\mu_0}\left[\int_0^b \rho J_0^2(\mu_1\rho)\, d\rho + \int_0^b \rho J_1^2(\mu_1\rho)\, d\rho\right]\left[\int_0^L e^{-2\mu_1(z-z_r)}\, dz\right] + \left[\frac{\pi a^2 \mu_c N^2}{l}\right]_{coil}$$

$$= -\frac{K_1^2\, 2\pi}{\mu_0}\left[b^2 J_0^2(\mu_1 b)\right]\left[\frac{1}{2\mu_1}\left(1 - e^{-2\mu_1(L-z_r)}\right)\right] + \frac{\pi a^2 \mu_c N^2}{l}$$

$$\simeq \frac{\pi a^2 \mu_c N^2}{l}\left[1 - \left(\frac{\mu_c}{\mu_0}\right)\left(\frac{1}{l\mu_1}\right)\left(\frac{\pi a^2}{\pi b^2}\right)\frac{1}{J_0^2(\mu_1 b)}\right]$$

4.0 RF

4.1 RF EM Links

RF propagation within metalic enclosures such as spacecraft requires consideration of effects which are unique to volume field coupling of sources and detectors. The metalic boundaries enclosing the source reflect the RF wave hundreds of times back and forth before it is dissipated by losses within the propagation space.

Multiple reflections affect information propagation in two major ways. First, interference of the multipath reflections causes signal reinforcement and cancellation, the amplitude range of which is a function of the losses within the volume. Cancellation could cause signal levels to approach or fall below the EM noise level or receiver sensitivity levels and reduce the possible information rate. Second, the reflections restrict the information bandwidth. This effect can be visualized by considering a signal sampled at the Nyquist rate: if a given sample once propagated does not attenuate fast enough, it interferes with subsequent samples that are transmitted.

Received RF noise levels are determined by the EMI levels allowed through specification and the receiver noise level is reflected in its sensitivity figure.

The range of signal level within the enclosure, the EMI level, and receiver sensitivity are functions of the RF frequency.

Consequently, the objective of the study was to find that range or bands of frequencies that would give signal/noise margins and bandwidths adequate for the required voice quality and desired control reliability. Further, those bands within which other spacecraft subsystems operate as well as those that could result in destructive intermodulation products have been delineated. The final choice of RF frequency within these recommended bands would depend upon RF and antenna design considerations.

4.2 RF Enclosure Fields

The field equations for these simple geometries are separable in the appropriate coordinate systems. The lowest order mode for the upper flight deck would correspond to a TM_{111} mode with a cutoff frequency of 80 MHz. The lowest order mode for the lower deck correspond to a TE_{101} mode with a cutoff frequency of 87 MHz. The irregularity of interior metallic surfaces and the protusions of spacecraft equipment increase the surface current attenuation within the surrounding conducting surfaces and consequently increase the signal dissipation rate. However, in order to establish a reference level corresponding to the most pessimistic case the Q of these simple enclosures with electrically smooth walls was computed as a function of frequency in Appendix 4.1.

The resulting null depth at a reference frequency of 300MHz was 76dB below the allowable maximum of 2 volts per meter. The damping factor is proportional to the square root of frequency. The plot of this function is included in the curves of Figure 4.1 and shows that the minimum signal level would fall below that required for the desired audio quality. The transmission bandwidth corresponding to these enclosures is shown in Figure 4.2 and is sufficient for intended ATE operation.

Three basic phenomena associated with the actual spacecraft interiors increase the damping of the enclosure. First, these shuttle closures have windows, ports, and hatches between compartments that allow the RF signal to leak from the interiors. Second, the highly irregular surfaces of the interior increase the linear path of the EMP surface penetration and, in all probability, the current would encounter high resistances within these path traverses. Third, the interior of enclosures contain non-metalic lossy material, the largest of which would be the bodies of the astronauts themselves.

The effect of losses upon enclosure damping is conventionally treated through the relationship

$$\frac{1}{Q_e} = \frac{1}{Q_o} + \frac{1}{Q_u} \tag{1}$$

where Q_o is that of the resonant cavity and Q_u that of the loading introduced by coupling ports and interior lossy materials. The Q_u of lossy materials is the inverse of the material loss tangent. Each of the above loss mechanisms will now be treated in terms of these dissipation parameters.

Leakage port attentuation for the upper deck was calculated for a simple model consisting of an opening in one wall of the half-right parabolic cylinder corresponding to the windscreen area of 10% of the wall surface in Appendix 4.2. The null depth for this type of escape port would be 46dB at the reference frequency of 300MHz. A plot of this null depth in Figure 4.1 is well above that of the desired audio quality level.

The enclosure below the flight deck has few escape ports (only a few ceiling hatches apparently). Consequently the damping of the non-metalic materials are considered. This damping is introduced primarily by the astronaut bodies and in the major source considered at this time. Figure 4.3 is a plot of the power loss tangents of human fat and muscle as derived from measured body conductivities and dielectric constants.

For purposes of calculation, it was assumed that an astronauts body would occupy 10% of the enclosure volume and consists of 60% fat and 40% muscle. It was further assumed that the position of this body was located in a region of maximum electric field strength so that the following approximation would suffice.

$$\frac{1}{Q_e} = \frac{0.9}{Q_o} + .06 \tan\phi_{FAT} + .04 \tan\phi_{MUS} \tag{2}$$

The effective Q of the enclosure at the reference frequency of 433MHz dropped to 14.29 and indicates the body is a highly effective damping source. The effect of the body on radiation patterns will be considered subsequently. Null depth from body damping is shown in Figure 4.1.

Damping caused by irregularities of the metalic inner surface is reflected by three parameters which express the ratio of actual surface path lengths to that of the approximating cavity and the height of protusion to the depth of penetration. Estimates based upon visual observation of spacecraft interiors indicate that this mechanism alone would increase the damping 10 to 20dB above that of the resonant simplification.

Interior walls of the spacecraft that were seen at JSC were bare metal surfaces except for the Skylab interior which was covered with some kind of insulating material. The depth and type of material will be identified in a subsequent document to be supplied by NASA describing all non-metalic material on-board spacecrafts. The thickness of these wall materials would generally be less than the depth of penetration of the RF energy; consequently, the wave is reflected off the metalic undersurface with a phase shift but small attenuation. As an example, a one centimeter layer of polystyrene was assumed and the added attenuation reduced the null depth by 6dB.

4.3 RF Electronic Coupling

The electronic contribution of the audio noise level is produced primarily by the receiver noise and the EM leakage of other spacecraft electronics. The limit of radiated EMI as specified for narrowband emissions by ISC - SL - E - 0002 (June 4,1973) is plotted in Figure 4.1.

The receiver noise level, as reflected to the radiation space at the antenna input, is plotted as a function of frequency in Figure 4.1. The following noise figures of commercially available RF transistors for the frequency bands were used:

FREQUENCY	NOISE FIGURE (dB)
10-200MHz	2.5
200-1000MHz	3.5
1000-4000MHz	4.5

Other assumptions made pertaining to system design:

Bandwidth	3MHz
Other gain losses	15dB

Antenna gain corresponds to that of an omnidirectional short dipole whose length is 0.1 wavelength with an arbitrary limit of 15 centimeters in length.

The gain function of an antenna

$$Pr = \frac{E_s^2}{\eta} A_{eq}, \tag{3}$$

where E_s = the electric field strength

η = free space impedance

A_{eq} = equivalent antenna area

when equated to the noise power

$$P_n = KT\ W\ \overline{NF}L, \tag{4}$$

where

K = Boltzmans constant

T = temperature

W = bandwidth

$\overline{NF}$ = rcvr noise figure

L = additional losses

provides the inverse gain factor for noise reflected to the antenna input

$$E_n = \left[\frac{KT\ W\ \overline{NF}\ N\ L}{A_{eq}}\right]^{1/2} \qquad (5)$$

The equivalent area A_{eq} for a short dipole

$$A_{eq} = \left(\frac{1.5\lambda_0^2}{4\pi}\right)\left(\frac{\lambda}{\lambda_0}\right)^2 \qquad (6)$$

when substituted in (5) completes the relationship plotted in Fig. 4.1 for receiver noise vs frequency.

$$E_n = \left(\frac{4\pi\ KT\ W\ \overline{NF}\ \eta\ L}{1.5\lambda_0^2}\right)^{1/2}\left(\frac{\lambda_0}{\lambda}\right) \qquad (7)$$

The increase in noise level with frequency is caused by the shortening of the dipole length in order to retain the broad beam characteristics of the dipole. The dipole has been used for evaluating propagation and is not meant to suggest a final antenna design.

The noise composite shows that the allowable EMI levels predominate over receiver noise up to 350MHz. Also, it may be noted that the receivers will have a much narrower bandwidth than 3MHz; consequently receiver senitivity should fall well under allowable EMI levels.

An audio quality contour 20dB above the composite electronic noise level, plotted in Fig. 4.1, shows that with the slightest interval damping the system will meet specifications over a wide frequency range.

ORIGINAL PAGE IS OF POOR QUALITY

4.4 Transmission Efficiency

The S/N ratio, as set forth in Fig. 4.4 for the RF system depends upon the radiation power (antenna losses considered negligiby small), a field dispersion loss that varies inversely with range, and the receiver antenna transduction ratio.

A quarter wave antenna (20cm) with a radiation resistance of 73 ohms, a gain of 1.64, and an equivalent antenna area of .07 $(\text{meters})^2$ is used for the comparison. For 100 milliwatts transmitter power the signal/noise at 25 meters is 100dB.

This power margin is sufficient to overcome the effects of interior nulls and shadow zones.

4.5 EM Compatability

Choice of RF frequency depends strongly on the RF bands of other spacecraft electronics. A frequency for the ATE system should not interfere directly or interact with other radiation to form destructive cross products frequencies in any of the other equipment. Conversely, in spite of EMI specifications it would be wise to avoid frequencies of not only the radiated signals but also the frequencies of any other frequency source used for local oscillator references in these equipments. At this time the chart of orbiter radio frequencies shown in Figure 4.1 has been supplied by NASA. More detailed information is needed to analyze intermodulation products that could be generated in conjunction with all signals in the spacecraft environment and determine those additional bands which the ATE equipment must avoid.

High power terrestrial transmission bands associated with TV and other communication links must also be avoided. Stations transmitting 10KW of power and 20dB antenna gains could produce radiation levels external to the shuttle of 15 millivolts at altitudes of 200 miles. Spacecraft shielding would reduce this level internally at the lower decks; however, the upper flight deck has large window areas that would attenuate the level very little.

NASA has a report which they are in the process of preparingwhich lists all high power terrestrial bands to be avoided. Prior to the receipt of this report, one can only say that the FM bands between 88MHz and 108MHz, TV bands 174 and 216MHz, earth-space bands between 136MHz and 138MHz and coastal telephony bands between 156 and 162MHz are to be avoided.

The results of the RF propagation study are in summary:

. The RF enclosure damping produced by windows and leakage ports, the irregularity and roughness of the interior equipment, and the body attenuation of the astronaut is enough to keep null depths greater than -30dB over the band of RF frequencies between 100MHz and 10,000MHz.

. This level of null depth and damping assures more than adequate signal to noise and bandwidth for the specified audio and control signal quality.

. The heavy high power terrestrial RF activity between 90MHz and 300MHz precludes this band for ATE operation.

. Similarly TACAN, shuttle communication bands between 960MHz and 2300MHz as well as the altimeter band at 4400MHz are bands to be avoided.

. The specified EMI levels are low enough and the projected receiver sensitivities high enough that no EM noise problem is expected with the allowed 2V/meter transmission level.

Therefore, based upon the above, it is recommended that the RF ATE frequency be chosen in the bands between 350MHz and 900MHz and between 2500MHz and 3500MHz. Certain regions within these recommended bands may be further restricted by information contained in the NASA reports that are being transmitted. The final choice of frequency will depend upon tradeoffs in the design of the antenna and RF sections of the system.

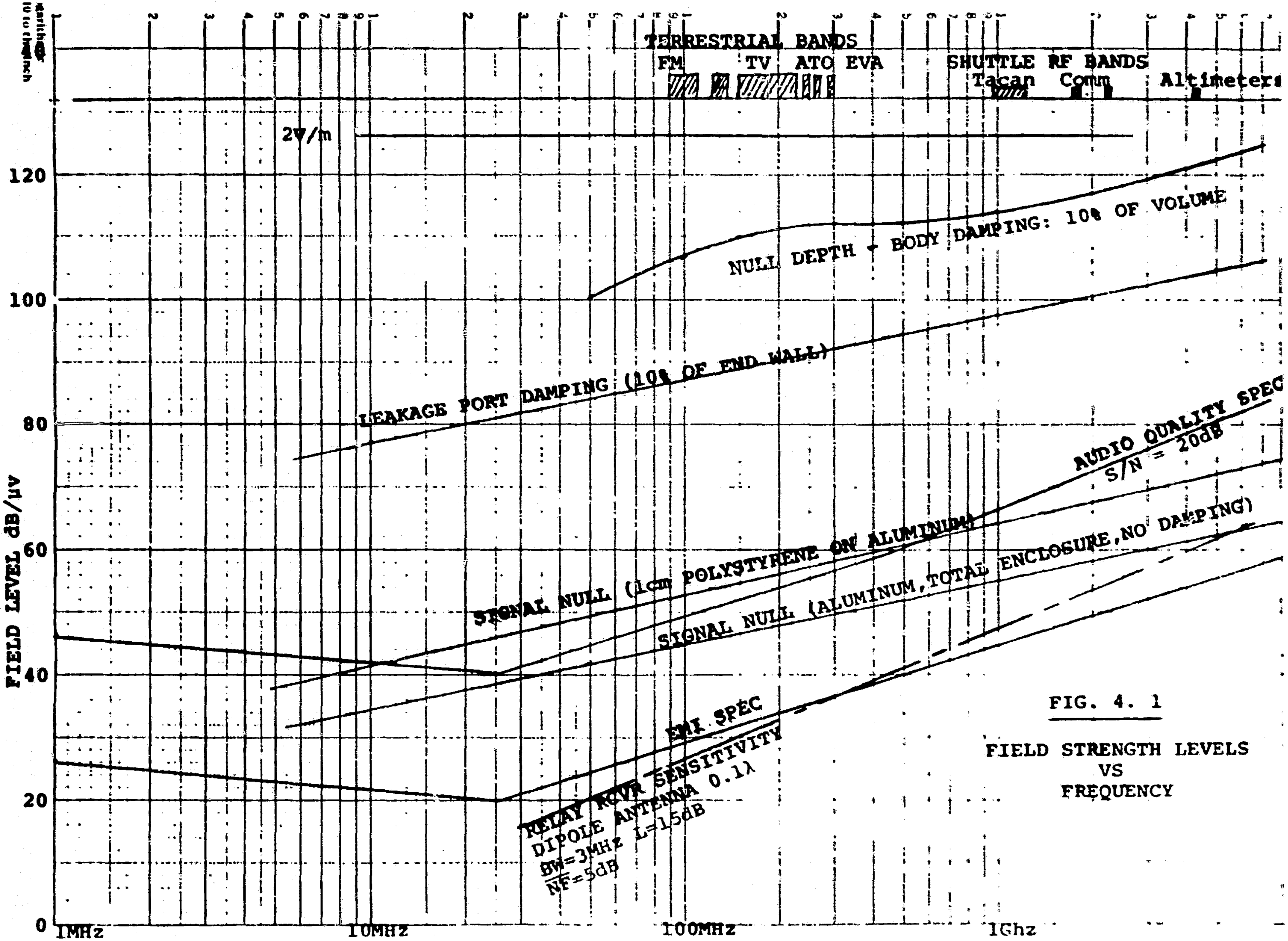

FIG. 4. 1

FIELD STRENGTH LEVELS
VS
FREQUENCY

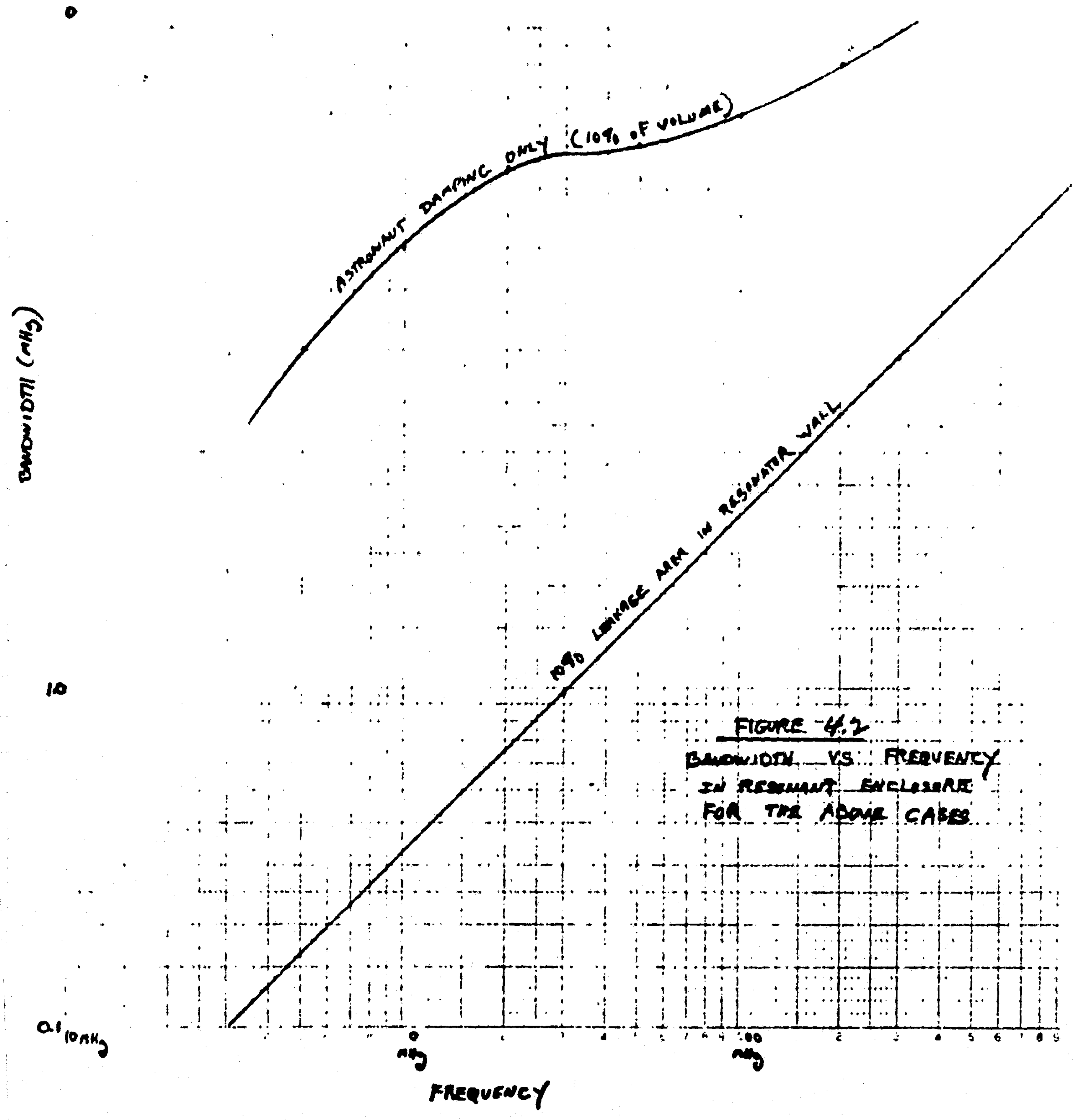

FIGURE 4.2
BANDWIDTH VS FREQUENCY
IN RESONANT ENCLOSURE
FOR THE ABOVE CASES

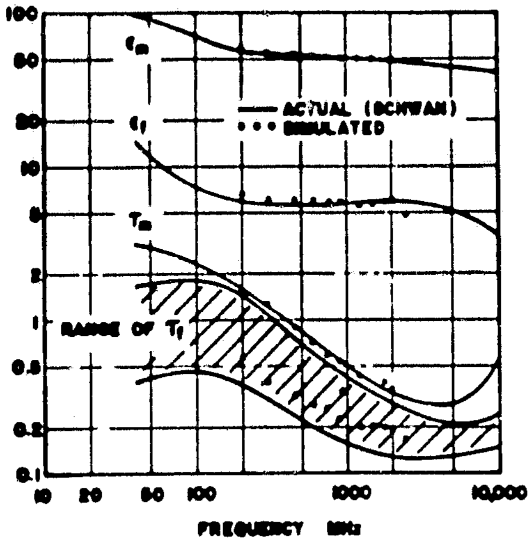

Comparison between dielectric properties of actual and simulated human fat and muscle. ($\epsilon_{f,m}$ are dielectric constants; $\tau_{f,m}$ are loss tangents of fat and muscle, respectively.)

FIGURE 4.3

FIG 4.4 GAIN MARGIN

RADIATION COUPLED TRANCEIVER LINK

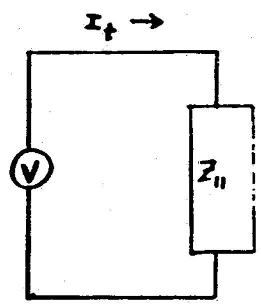

$$|Z_{21}|^2 = \frac{R_{r_1} R_{r_2} g_1 A_{e_2}}{\pi r^2}$$

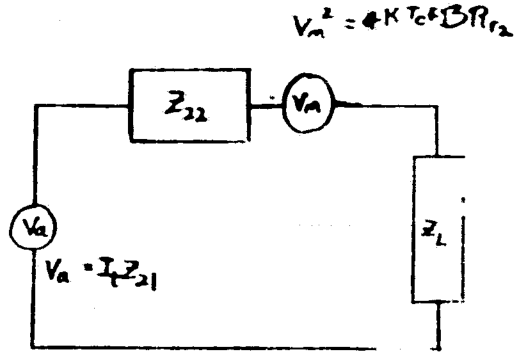

R_{r_1} = XMTR Antenna Radiation Resistance = 73 Ω

R_{r_1} = RCVR Antenna Radiation Resistance = 73 Ω

g_1 = XMTR Antenna Gain = 1.64

$A_{e_2} = \frac{g\lambda^2}{4\pi}$ = RCVR Antenna Effective Area = .07 m^2

r = Transmission range = 25 m

$$\frac{S}{N} = \frac{(Z_{21} I_t)^2}{4KT_{ef}BR_{r_2}^2} = \frac{(I_t^2 R_{r_1})\, g_1 A_{e_2}}{4\pi r^2\, KT_{ef}B}$$

	+	−
r^2		28
KT_{ef}	200	
B		41
g_1	2.1	
A_{e_2}		11.5
P_t		10.0
4π		11.0
	[illegible]	[illegible]

GAIN MARGIN . 100.6 dB

APPENDIX 4.1

ENCLOSURE NULL DEPTH VS WALL ATTENUATION

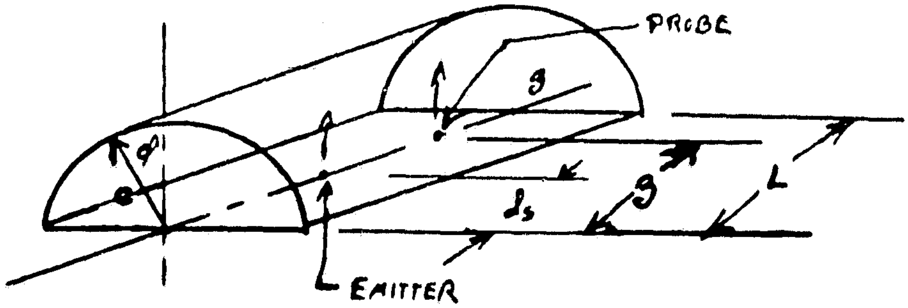

HALF CIRCULAR CYLINDRICAL RESONATOR : TM_{11p} MODE

FIELD AMPLITUDE E_z

$$E_z = E(z, \alpha, \Gamma, l_s)\, J_1(k_c r) \cos\phi \qquad ; \; k_c = \frac{3.83}{c}$$

α = attenuation of walls ; $a = e^{-\alpha_a}$ for ends.

l_s = z position of emitter

z = z position of probe

Γ = propagation constant. $= \alpha_1 + j\beta$

E is the summation of an infinite number of reflections off end walls; each reflection attenuated by a.

$$E = \sum_0^{\infty} a^{2m} e^{-\Gamma[2mL + (z - l_s)]} + \sum_1^{\infty} a^{2m} e^{-\Gamma[2mL - (z - l_s)]}$$
$$- \sum_0^{\infty} a^{2m+1} e^{-\Gamma[2mL + (z + l_s)]} - \sum_1^{\infty} a^{2m-1} e^{-\Gamma[2mL - (z + l_s)]}$$

$$= \left[e^{-\Gamma(z - l_s)} - a e^{-\Gamma(z + l_s)} + e^{+\Gamma(z - l_s)} - \frac{1}{a} e^{+\Gamma(z + l_s)} \right] \sum_0^{\infty} \left(a e^{-\Gamma L} \right)^{2m}$$
$$- e^{+\Gamma(z - l_s)} + \frac{1}{a} e^{+\Gamma(z + l_s)}$$

SINCE

$$\sum_0^{\infty}\left(a e^{-\Gamma L}\right)^{2m} = \frac{1}{1-(ae^{-\Gamma L})^2} \; ; \; 0 < a e^{-\Gamma L} < 1$$

$$= \frac{1}{1-e^{-2(\alpha_2+\Gamma L)}}$$

$$= \frac{e^{\alpha_2+\Gamma L}}{2\sinh(\alpha_2+\Gamma L)}$$

THEN

$$E = e^{-\Gamma z}\left(e^{+\Gamma l_s}-a e^{-\Gamma l_s}\right)+e^{+\Gamma z}\left(e^{-\Gamma l_s}-\frac{1}{a}e^{+\Gamma l_s}\right)\frac{e^{\alpha_2+\Gamma L}}{2\sinh(\alpha_2+\Gamma L)}$$

$$- e^{+\Gamma z}\left(e^{-\Gamma l_s}-\frac{1}{a}e^{+\Gamma l_s}\right)$$

LETTING $a = e^{-\alpha_2}$

$$E = -2\sinh\left(\frac{\alpha_2}{2}+\Gamma l_s\right)\left\{\frac{e^{\alpha_2+\Gamma L}\sinh\left(\frac{\alpha_2}{2}+\Gamma z\right)}{\sinh(\alpha_2+\Gamma L)}-e^{\frac{\alpha_2}{2}+\Gamma z}\right\}$$

NULL DEPTH $|E_{min}/E_{max}|$ LET $\beta L \cong \pi$, $\alpha = \alpha_2+\alpha_1 L$

$$|E_{max}| = -2\sinh\left(\frac{\alpha_2}{2}+\Gamma l_s\right)\left\{\frac{j e^{\alpha}\cosh\alpha/2}{\sinh\alpha}-je^{\alpha/2}\right\}$$

$$|E_{min}| = -2\sinh\left(\frac{\alpha_2}{2}+\Gamma l_s\right)\left\{\frac{-e^{\alpha}\sinh\alpha/2}{\sinh\alpha}+e^{\alpha/2}\right\}$$

$$\mathcal{R} = \left|\frac{E_{min}}{E_{max}}\right| \approx -j\tanh\alpha/2$$

APPENDIX 4.2

ENCLOSURE Q: RECTANGULAR RESONATOR; SLIT APERTURE

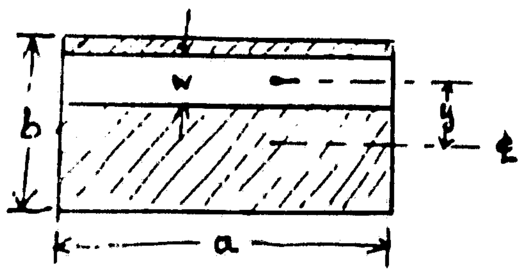

RESONATOR END WALL - SLIT APERTURE

Rectangular Resonator Q_ℓ with slit in End wall

$$\frac{1}{Q_\ell} = \frac{2}{\pi}\left(\frac{\lambda}{\lambda_g}\right)^2\left[\left(\frac{Y_0}{B}\right)^2 + \alpha\,\ell_c\right]$$

$$\frac{B}{Y_0} = \frac{4b}{\lambda_g}\ln\left\{\operatorname{cosec}\frac{\pi w}{2b}\,\sec\frac{\pi y}{b}\right\}$$

$$\lambda_g = \lambda\left\{1-\left(\frac{\lambda}{\lambda_c}\right)^2\right\}^{-1/2} \qquad \lambda_c = 2\left[\left(\frac{m}{b}\right)^2+\left(\frac{n}{a}\right)^2\right]^{-1/2}$$

$$\alpha = \frac{R_s}{b\eta}\left[1-\left(\frac{f_c}{f}\right)^2\right]^{-1/2}\left[1+\frac{2b}{a}\left(\frac{f_c}{f}\right)^2\right]$$

$$R_s = \frac{1}{\sigma\delta}$$

Assume aluminum shell: $\sigma = 3.72\times10^7$, $\delta = .0826 f^{-1/2}$

Then for $f = 300$ MHz

$R_s = 5.6\times10^{-3}$ ohms

$\alpha = .00021$

If $a = 3$ m, $b = 4$ m, $w = 1/2$ m, $\ell_c = 3$ m.

$B/Y_0 = 16.55$

Then

$$Q_\ell = 310$$

$$BW = 0.96\,MHz$$

$$\frac{\alpha}{2} = \frac{\pi}{2\lambda Q}$$

$$= .005 \quad (-46\,dB)$$

5.0 OPTICAL

5.1 Optical Link

Modulated light beams have desirable features for intracabin communication. The intensity levels of the light within the cabin do not exhibit interference nulls and consequently, when not occluded, presents a uniform field for detection. While optical links have the potential for wideband transmission, the advantage is not needed for this audio application.

Shadowing of the direct path radiated light at the detector by equipment and astronauts on the move is the major disadvantage to be overcome, since transmission must depend upon reflection of light off cabin surfaces for communication. Background illumination, such as lighting, sun, earth and sky scatter must be attenuated in the optical band to maintain good detection sensitivity.

5.2 Optical Propagation

The cabin model has been simplified to that of a cylindrical box in order to determine the path loss between the luminescent source and detector diode with reflection. An opaque obstacle is assumed which completely shadows the detector but for mathematical tractability does not shadow the reflective inner surface of the cylinder. The transfer function for single reflections is derived in Appendix 5.1 and plotted in Figure A.1. as a normalized function of the length to radius ratio of the cylinder.

The loss by blockage of the direct luminance in a cabin 2.24 meters in radius and 3.32 meters long - the approximate dimensions of the flight deck - with respect to the direct plus reflected is 5dB.

Optical Transducers

The communication link was modeled using transducers typical of the commercially available units. The Siemens LD 241 gallium arsenide diode radiating 15 milliwatts defocused over a solid angle of 2π radians was assumed for the transmitter. The photodiode detector characteristics typical of its class are listed in Table I.

TABLE I

Photo-diode Characteristics

Sensitivity	5 microamps/watt/m^2
Dark current	0.2 microamps
R_L	2.4K
C_d	7 pf.
A_d	$9x10^{-2} cm^2$

5.4 Transmission Efficiency

Figure 5.1.1 of Appendix 5.2 illustrates an optical link using a single gallium arsenide diode emitter and a single photo detector located on the axis of a cylindrical cabin with dimensions approaching those of the shuttle upper deck. The emitter power (typically falling within an 18° beam) has been defocused for good coverage over 2π steradians. An obstruction of the direct path light and reception of boundary scattered light is assumed.

The signal current from the detector for 100% modulation of the light and the given detector sensitivity is 488 pico amps.

The noise consists of diode shot noise and receiver thermal noise and a background radiation level of 5×10^{-3} watts-m^{2}-μm^{-1}. This corresponds to a light source with 4 watts/micron at the optical wavelength of 9350A° located 6 meters from the detector with a detector window of 0.5 microns. Presumably the choice of cabin lighting would be better than this. In any case the shot noise current was small with respect to the receiver noise; the noise level is not sensitive to cabin background illumination.

The signal-to-noise ratio for the single diode is 4.34dB for a bandwidth of 3KHz. To achieve a signal/noise of 20dB at least 37 emitter diodes would be needed.

The conclusion is that the optical link is not practical.

5.5 Optical Compatibility

The natural and manmade illumination within the gallium arsenide optical band at 9350A° must be attenuated below the noise level of the photodiode or the number of emitters must be increased to overcome this interference.

The attenuation for suppression of external direct sun light and earth scatter are calculated in Appendix 5.3. Attenuations fall within reasonable optical filtering capability. The practicality of using optical filtering of cabin viewing ports needs investigation.

APPENDIX 5.1

OPTICAL REFLECTED FIELD: CYLINDRICAL ENCLOSURE

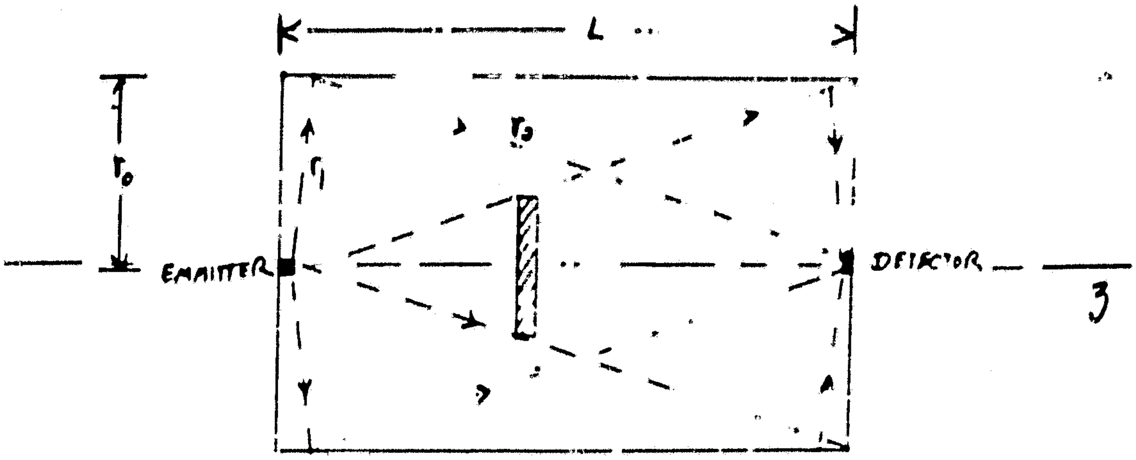

FIGURE 5.1.1 DIRECT RAY BLOCKAGE. SINGLE REFLECTIONS ONLY

A.1 Ray off element surface dA of cylinder.

$$dI_r = \frac{P\alpha A_d \; dA}{(2\pi)^2 r_1^2 r_2^2}$$

where

dA = ring increment on cylinder $= 2\pi r_0 \, dy$

A_d = rcv diode area

α = Lambert scatter constant of surface

P = radiated power

dI_r = incremental received radiation

Power defocused over 2π steradians, scatter over 2π steradians

A.2 $$I_r = \frac{P\alpha A_d}{4\pi^2} \int \frac{dA}{r_1^2 r_2^2}$$ where $r_1 = (r_0^2 + y^2)^{1/2}$, $r_2 = [r_0^2 + (L-y)^2]^{1/2}$

$$dA = 2\pi r_0 \, dy$$

$$I_r = K \int_0^L \frac{dy}{(r_0^2+y^2)[r_0^2+(L-y)^2]} \qquad K = \frac{P\alpha A_d r_0}{2\pi}$$

RECEIVED RADIATED POWER
WITH DIRECT PATH BLOCKAGE

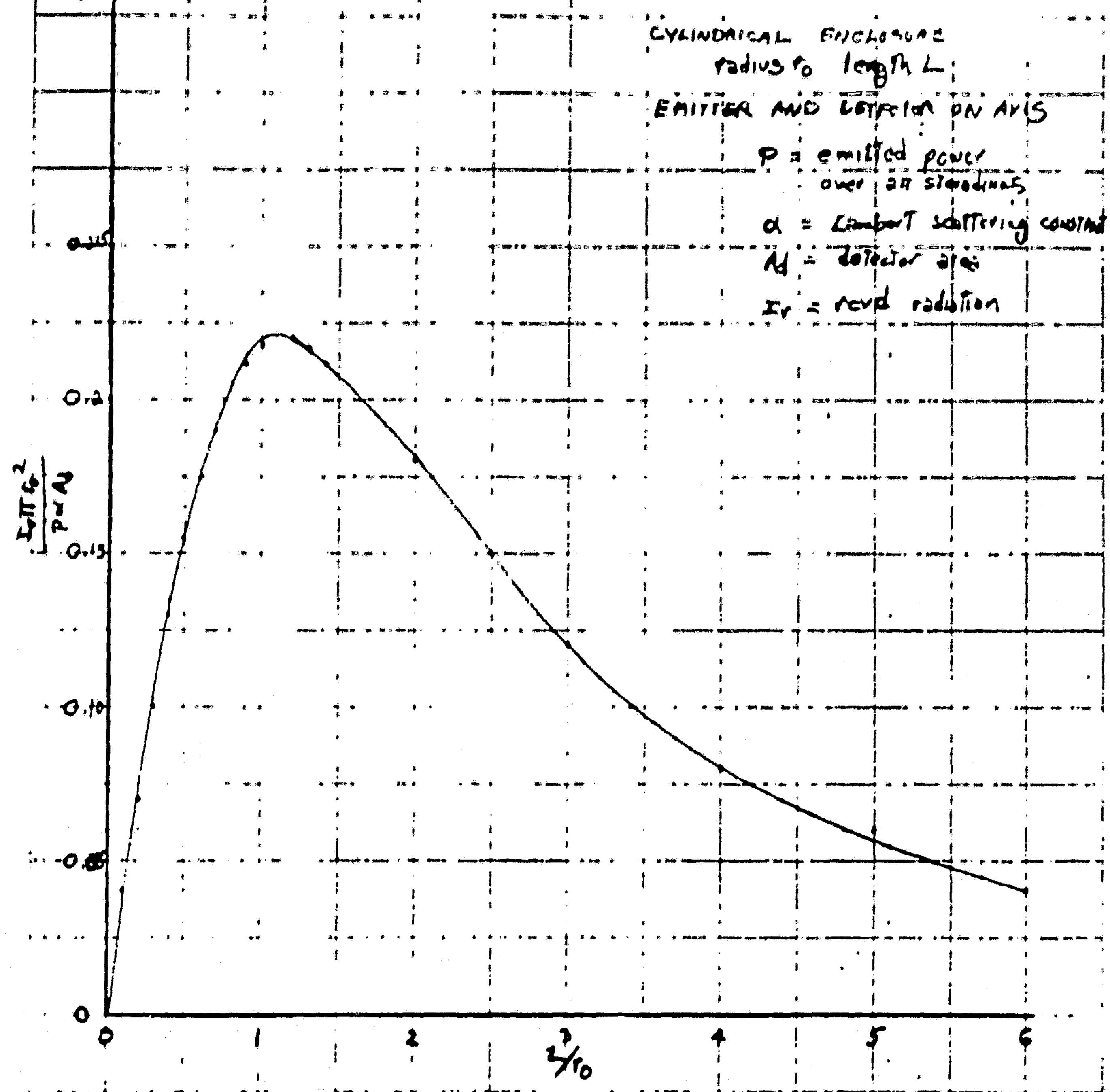

$$\frac{1}{r_1^2 r_2^2} = \frac{1}{L(L^2+4r_0^2)}\left[\frac{L+2z}{z^2+r_0^2} + \frac{3L-2z}{(L-z)^2+r_0^2}\right]$$

therefore

$$I_r = \frac{K}{L(L^2+4r_0^2)}\left\{\int_0^L \frac{L+2z}{z^2+r_0^2}\,dz + \int_0^L \frac{L+2x}{x^2+r_0^2}\,dx\right\}$$

where $x = L - z$

$$= \frac{2K}{L(L^2+4r_0^2)}\left\{\frac{L}{r_0}\tan^{-1}\frac{z}{r_0} + \log\left(z^2+r_0^2\right)\right\}_0^L$$

$$= \frac{P\alpha A_d r_0}{\pi L(L^2+4r_0^2)}\left[\frac{L}{r_0}\tan^{-1}\frac{L}{r_0} + \log\left[\frac{L^2+r_0^2}{r_0^2}\right]\right]$$

$$= \frac{P\alpha A_d}{\pi r_0^2\left[4+\left(\frac{L}{r_0}\right)^2\right]}\left\{\tan^{-1}\frac{L}{r_0} + \frac{r_0}{L}\log\left[1+\left(\frac{L}{r_0}\right)^2\right]\right\}$$

A.3 LOSS OVER DIRECT PLUS SURFACE SCATTERED.

Direct path Power = $\frac{PA_d}{2\pi L^2}$

$$L = \frac{P_{scattered}}{P_{direct} + P_{scattered}} = \frac{\alpha K\left(\frac{1}{r_0}\right)}{\alpha K\left(\frac{1}{r_0}\right) + \frac{1}{2}\left(\frac{r_0}{L}\right)^2}$$

Let $\alpha = 0.5$, $\frac{L}{r_0} = 1.5$

Then

$$L = \frac{(0.5)(.265)}{(0.5)(.265) + (0.5)(1.5)^{-2}} = 0.3157$$

$$= -5\,dB$$

APPENDIX 5.2

A SYSTEM DESIGN EXAMPLE

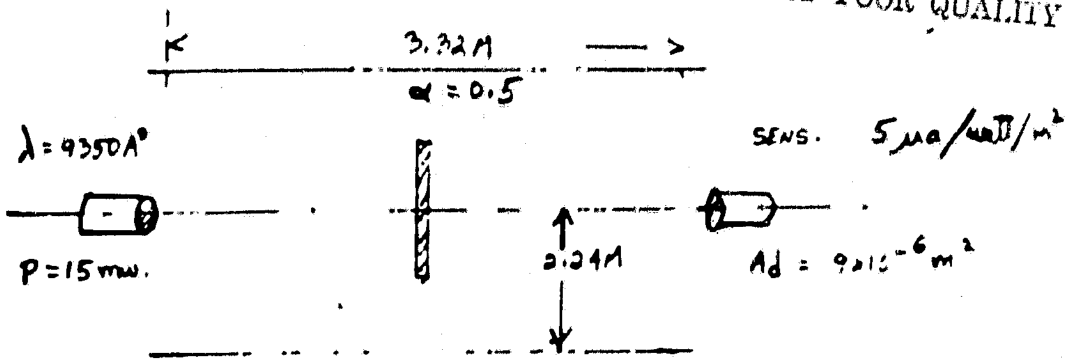

FIGURE 5.2.1

RECEIVED POWER:

$$\frac{L}{r_o} = 1.5$$

$$K\left(\frac{L}{r_0}\right) = 0.015 \quad \text{From Fig A.1}$$

$$P_r = \frac{P\alpha}{\pi r_o^2} K\left(L/r_o\right) = \frac{(15\times10^{-3})(0.5)(.205)}{\pi\,(2.24)^2}$$

$$= 9.75\times10^{-5}\ \text{watts}/m^2$$

$$i_s = 4.88\times10^{-10}\ \text{amps}$$

SIGNAL/NOISE

$$\frac{S}{N} = \frac{0.5\, i_s^2}{\left[2 i_q + 4\frac{kT_E}{R_{eq}}\right]B}$$

where

$i_s = g\, I_r$ = signal current

i_q = shot noise $= 2q(i_s + i_d + i_b)$

i_d = dark current

i_b = background induced current

T_E = rcvr effective temperature

R_{eq} = detector equivalent load resistance

B = rcvr bandwidth

k = Boltzmann constant

q = electronic charge

Assume :

Background radiation = 5×10^{-3} watts $-m^{-1}$-μm^{-1}

Req = 2.5K

T_E = 410°

Detector :

Sensitivity : 5 μamps $-w^{-1}-m^2$

i_d = 0.2 μamp.

$$i_q = 2(1.6\times10^{-19})\{0.2\times10^{-6} + 5\times10^{-6}[9.75\times10^{-5} + 5\times10^{-3}]\}$$

$$= 7.2\times10^{-26}$$

$$\frac{4\,KT_E}{Req} = \frac{4(1.38\times10^{-23})(410)}{2500} = 9\times10^{-24}$$

$$\frac{S}{N} = \frac{0.5\times(9.88\times10^{-10})^2}{[2\times7.2\times10^{-26} + 9\times10^{-24}](3000)}$$

$$= 4.34$$

Number of diodes to achieve $\frac{S}{N}$ = 20dB

$$10 \log N = 20 - 4.34$$

$$N = 37$$

ORIGINAL PAGE IS OF POOR QUALITY

APPENDIX 5.3

BACKGROUND RADIATION

ORIGINAL PAGE IS
OF POOR QUALITY

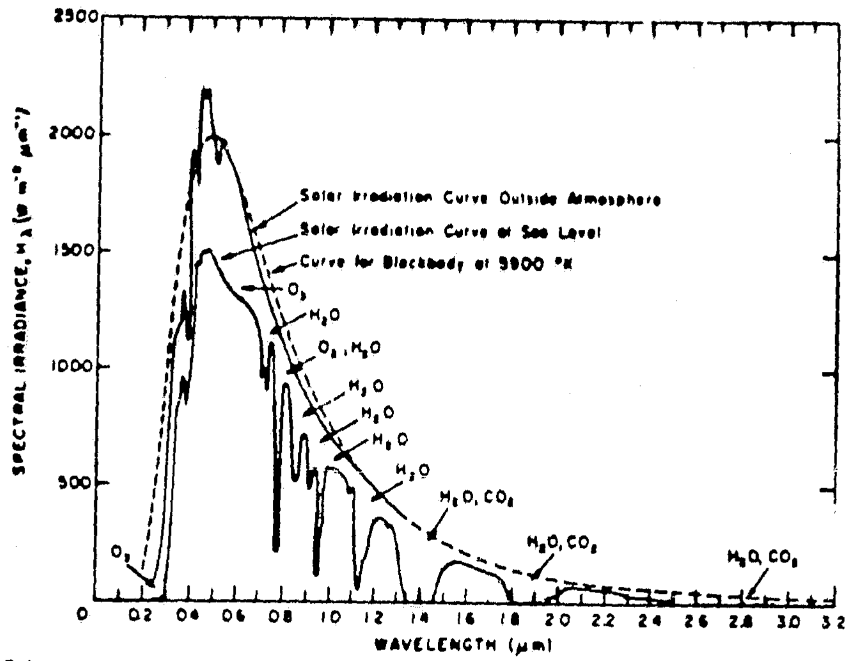

Solar spectral irradiance with Sun at zenith. Absorption bands are shown shaded (after Gast

C.1 Assume a Tolerable Background Level = 5×10^{-3} W·m^{-2}·μm^{-1}

C.2 Sun Radiation (9350 A°) = 700 W·m^{-2}·μm^{-1}

Attenuation required $= \dfrac{700}{5\times10^{-3}} = 1.4\times10^{5}$

= 52dB

C.3 Earth scatter (9350 A°) = 0.8 W - m^{-2} - μ.

Attenuation required $= \dfrac{0.8}{5\times10^{-3}} = 160$

= 22dB.

6.0 ACOUSTIC

6.1 Sonics

Audio transmission via ultrasonic carriers is limited by the signal bandwidth available for propagation. The lower frequency must not fall within the aural sensitivity region of the human ear and the upper frequency must be within the capability of state-of-the-art sonic transducers. These requirements limit the ultrasonic band to between 25 Kilohertz and 75 to 100 Kilohertz. This band could support five or six voice channels.

6.2 Acoustic Propagation

Field intensities of ultrasonic sound within an enclosure depends upon the sonic reflectivity characteristic of the boundary surfaces, shadowing by obstacles within the space, and upon the attenuation of the signal by the propagating medium.

The wavelength of the ultrasonic signals (25KHz to 100KHz) falls in the range between 1 and 0.25 centimeters. Consequently the field structure within the volume would not experience deep interference nulls.

The reflectivity of the boundary surface is a function of frequency. This function is difficult to predict theoretically and can only be determined accurately by measurements on the completed shuttle structures. Broad variations of reflectivity coefficient versus frequency change only the relative reception intensity between channels and is not serious. Sharp resonances whose response is narrower than the audio band would distort the audio. High damping at the boundary surfaces would mitigate the distortion. However, good reflectivity at the boundaries is necessary to fill-in zones within the volume that are shadowed from the direct waves of the source by intervening obstacles.

Sonic intensities of the direct ultrasonic wave in the shadow zone are plotted in Figure 6.1.

While the plot can be generalized to any obstacle dimension, and source and observation points distances, a particular case was chosen for illustration where D, the obstacle size is 1/2 meter with an ultrasonic source located 1/2 meter behind. For a point located 1/2 meter from the obstacle, the sonic attenuation varies between -27dB and -32dB over the expected transmission band. At two meters from the obstacle, the attenuation varies between -24.8dB and -30dB. The degree of possible shadowing attenuation requires good reflectivity of the enclosing surfaces in order to assure good reception over the entire volume.

The shadowing function indicates that the ultrasonic transducers must have a clear field of view since the reduction of the source distance below 1/2 meter would further attenuate the signal in the shadow zone. Accidental muffling of the transducers must be avoided.

Figure 6.2 is a curve of the absorption of sound in air as a function of frequency. The oxygen space craft environment should not differ substantially from dry air. The attenuation between 55KHz and 100KHz varies between 0.1 and 0.36dB/ft. For a propagation path of 10 feet the attenuation of 1 to 3.6dB is small.

6.3 Electronic-Acoustic Transducers

The bandwidth of ultrasonic transducers limit the application of ultrasonics in the baseline concept. Figures 6.4 to 6.7 contain curves typical of commercially available transducers. The bandwidths are wide enough to carry audio amplitude modulated on ultrasonic carriers between 30KHz and 75KHz with good transmitting gain and receiving response. The response, Figure 6.3

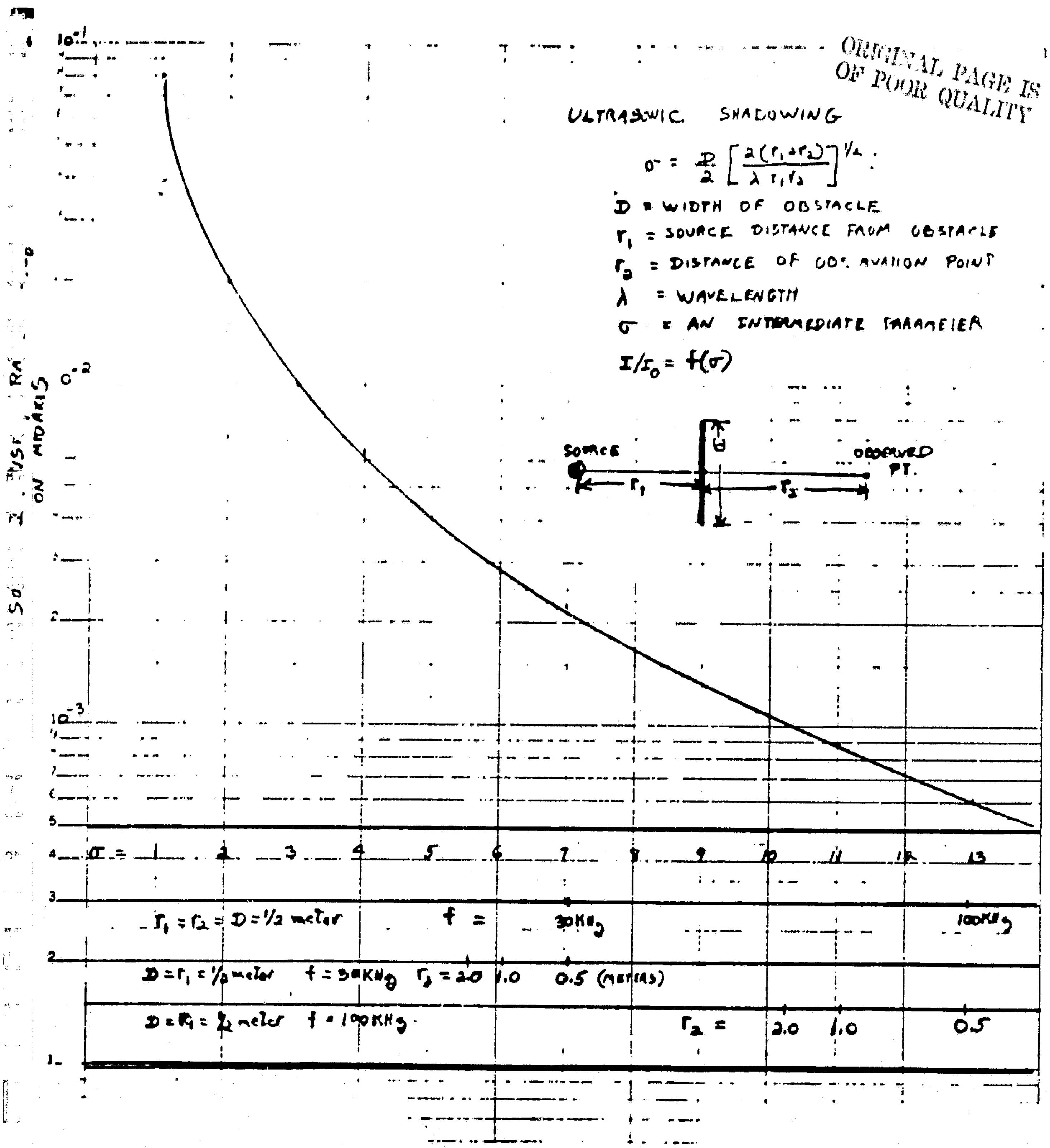
ULTRASONIC SHADOWING
D = WIDTH OF OBSTACLE
r1 = SOURCE DISTANCE FROM OBSTACLE
λ = WAVELENGTH
σ = AN INTERMEDIATE PARAMETER
I/I0 = f(σ)
SOURCE
OBSERVED PT.
σ = 1 2 3 4 5 6 7 8 9 10 11 12 13
r1 = r2 = D = 1/2 meter f = 30KHz 100KHz
D = r1 = 1/2 meter f = 30KHz r2 = 2.0 1.0 0.5 (METERS)
D = r1 = 1/2 meter f = 100KHz r2 = 2.0 1.0 0.5

FIGURE 6.2

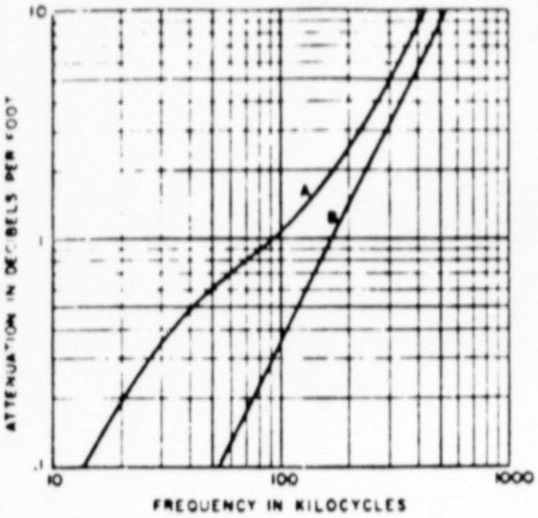

Absorption of sound in air as a function of frequency. Curve *A* is the average of experimental data for average atmospheric conditions 75°F and 37 percent relative humidity. Curve *B* is the theoretical attenuation for dry air from classical theory.

FIGURE 6.3

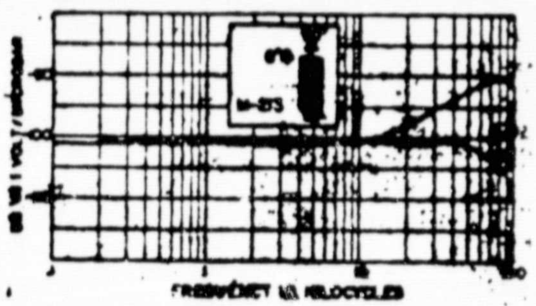

Photograph and frequency response of commercially available reference standard ADP microphone for making accurate measurements of sound pressure over very large dynamic ranges.

of a reference standard ADP microphone shows that wider band-widths can be obtained with a resulting sacrifice in sensitivity.

6.4 Acoustic Transmission Efficiency

Signal levels for a 10 foot ultrasonic link using the TR-89B transducers are given in Figure 6.8. 10 milliwatts drive power produces 10 millivolts output for the direct transmission path. The directivity of the transducer compensates for the rather poor efficiency of air transducers. The directivity pattern, as given in the data, has a beamwidth of 16 degrees and would not satisfactory for the intended application. Extrapolating the data to omni directional patterns, the signal link gain would drop about 40dB producing an output signal level of 100 microvolts. This level is 40dB above the electronics input noise level.

6.5 Sonic Compatability

The ultrasonics noise level within the shuttle enclosures will be the major factor in determining the signal to noise ratio. NASA noise level estimates of the shuttle operational environments have not been provided.

In conclusion, since no measurements on ultrasonic noise levels exist for all phases of shuttle operations, this mode of propagation is a risky option. In addition assuring unimpeded transmission paths and preventing accidental transducer muffling are potential problem areas.

FIGURE 6.4

The Model TR-89B/Type 40 is a rugged electroacoustic transducer designed for the efficient generation of ultrasonic energy in air for a wide variety of applications. The one piece housing with integral diaphragm provides a moisture-proof unit, suitable for both indoor and outdoor use when mounted, so that the rear terminals are protected from exposure to the outdoor atmosphere.

Several hundred thousand TR-89B transducers are presently in widespread use in ultrasonic intrusion alarms and other remote control and proximity detection applications.

Performance Characteristics

DIRECTIONAL RADIATION PATTERN AT 40 kHz

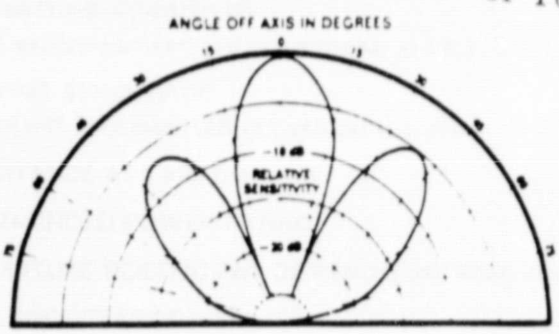

TRANSMITTING RESPONSE

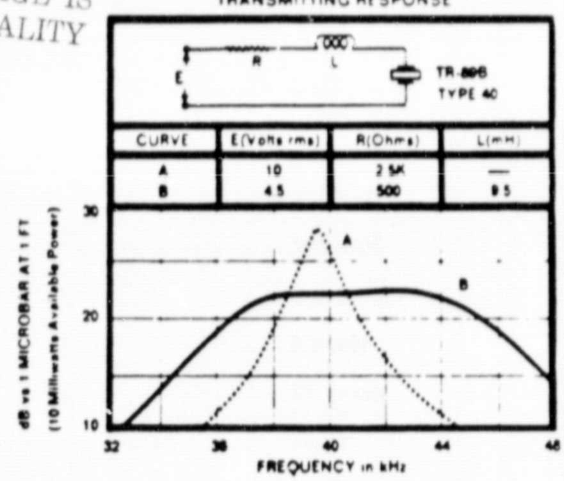

IMPEDANCE

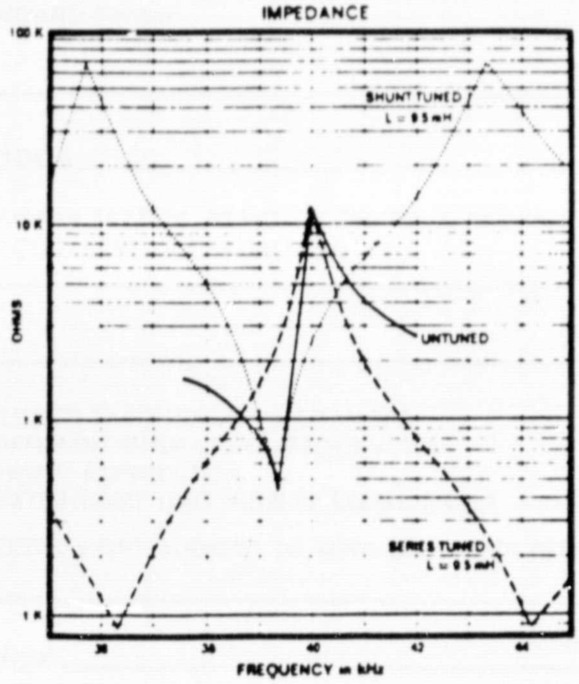

RECEIVING RESPONSE

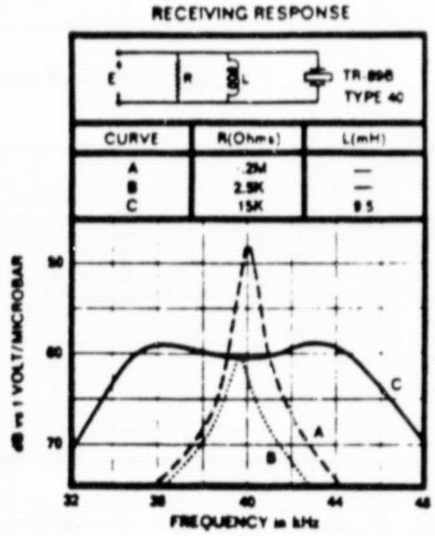

Outline Dimensions

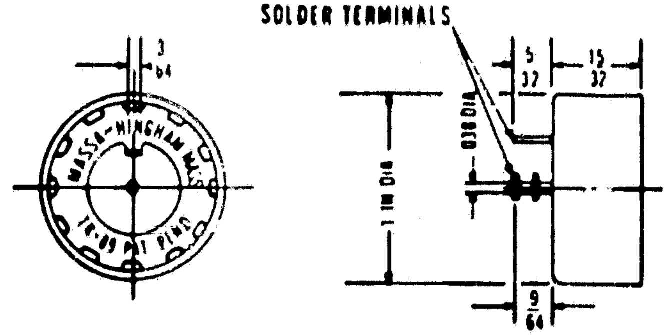

Specifications

FREQUENCY AT MAXIMUM IMPEDANCE (with no load)	40 kHz ± 2 kHz
BANDWIDTH (matched load)	1.0 kHz
TRANSMITTING SENSITIVITY (10 mW available power) (dB vs 1 microbar at 1 ft.)	+27
RECEIVING SENSITIVITY (untuned with 2MΩ load) (dB vs 1 volt per microbar)	−48
CAPACITANCE AT 1 kHz (nominal)	2300 pF
RECOMMENDED POWER RATING	200 mW
TEMPERATURE COEFFICIENT OF RESONANT FREQUENCY	3 x 10^{-4}/°F
TUNING INDUCTANCE (nominal)	8.5 mH
WEIGHT	11 grams
STANDARD FINISH	black

Applications

INTRUSION ALARMS, REMOTE CONTROLS, PROXIMITY DETECTION, ECHO RANGING, SOLID OR LIQUID LEVEL MEASUREMENT

Options

1. CLOSER FREQUENCY TOLERANCES
2. DIFFERENT OPERATING FREQUENCIES
3. PHONO CONNECTOR
4. WATER-TIGHT UNIT WITH INTEGRAL CABLE

(AT EXTRA COST SUBJECT TO MINIMUM ORDER REQUIREMENTS)

Patent Notice

MASSA Ultrasonic Transducers are protected by the following U.S. Patents: 2,967,957; 3,128,532; 3,510,698; 3,578,995; 3,638,052; 3,707,131; 3,716,681; 3,752,941; 3,736,632; 3,777,192, and other Patents Pending.

MASSA CORPORATION ■ 280 LINCOLN STREET, HINGHAM, MASSACHUSETTS 02043 ■ TEL: 617/749-4800

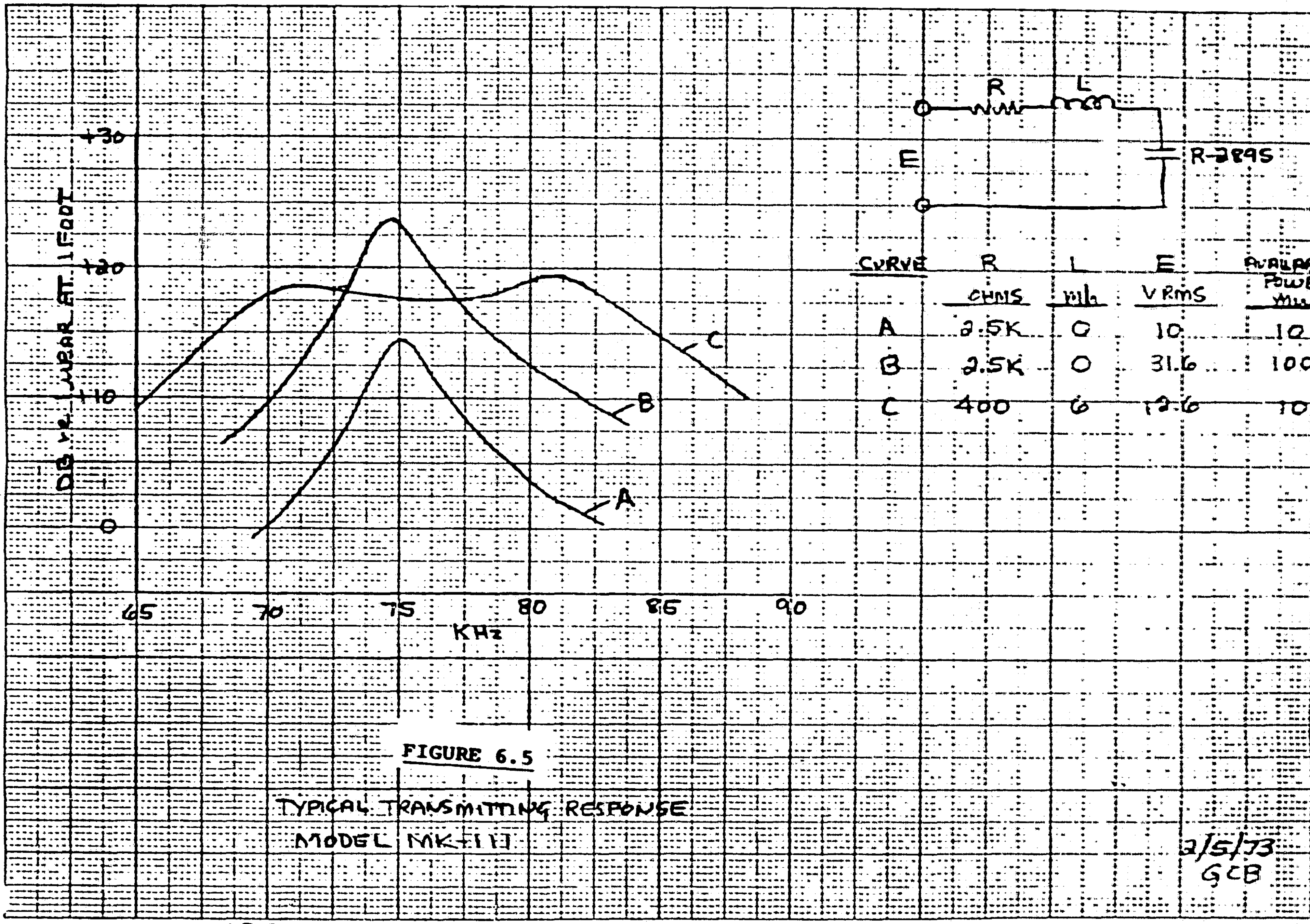

CURVE	R (OHMS)	L (mh)	E (V RMS)	AVAILABLE POWER (mw)
A	2.5K	0	10	10
B	2.5K	0	31.6	100
C	400	6	12.6	10

FIGURE 6.5

TYPICAL TRANSMITTING RESPONSE
MODEL MK-113

WAS R-289S

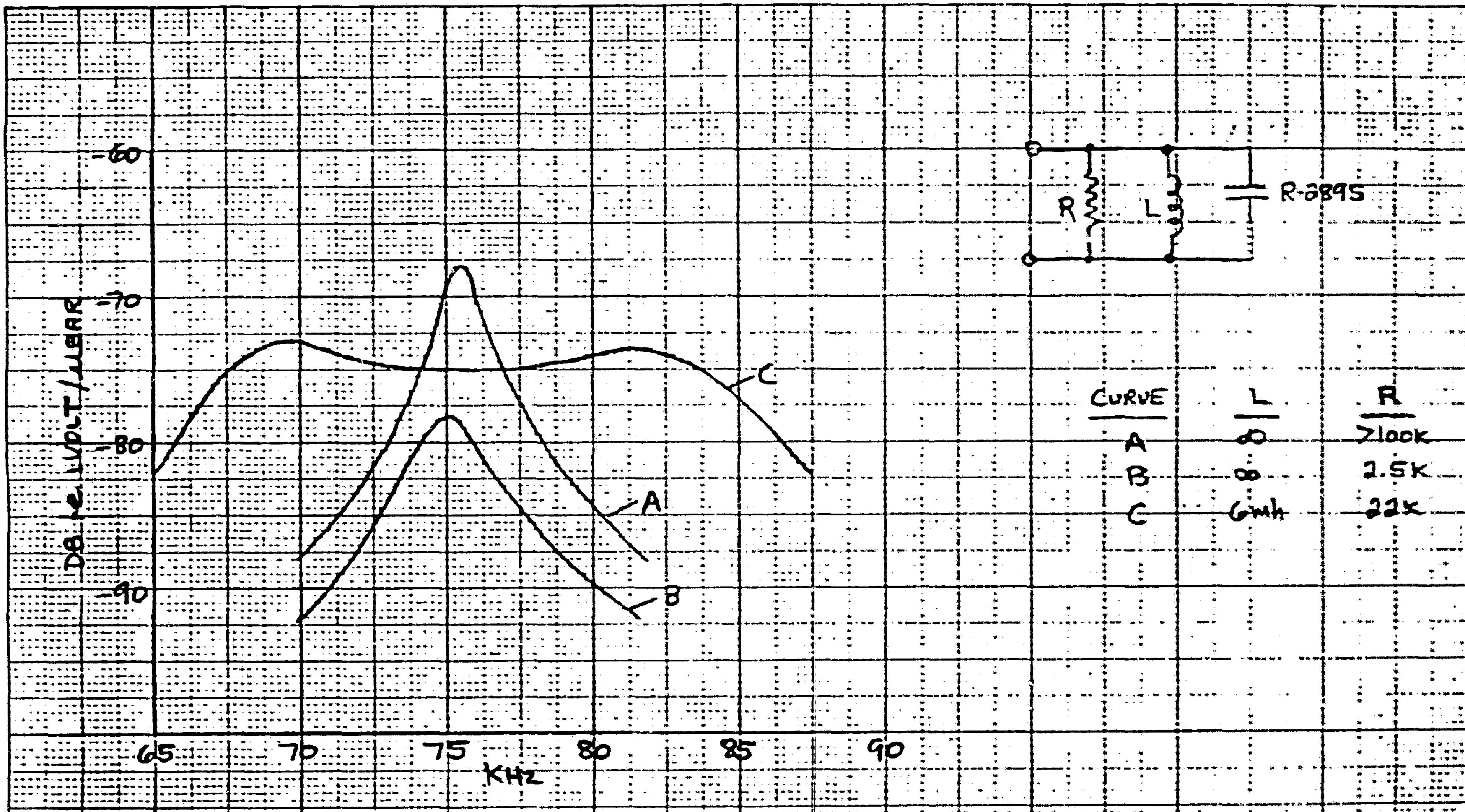

FIGURE 6.6

TYPICAL RECEIVING RESPONSE
MODEL MK-111

2/5/73
GCB

ED-10394-3

66

WAS R-2895

67

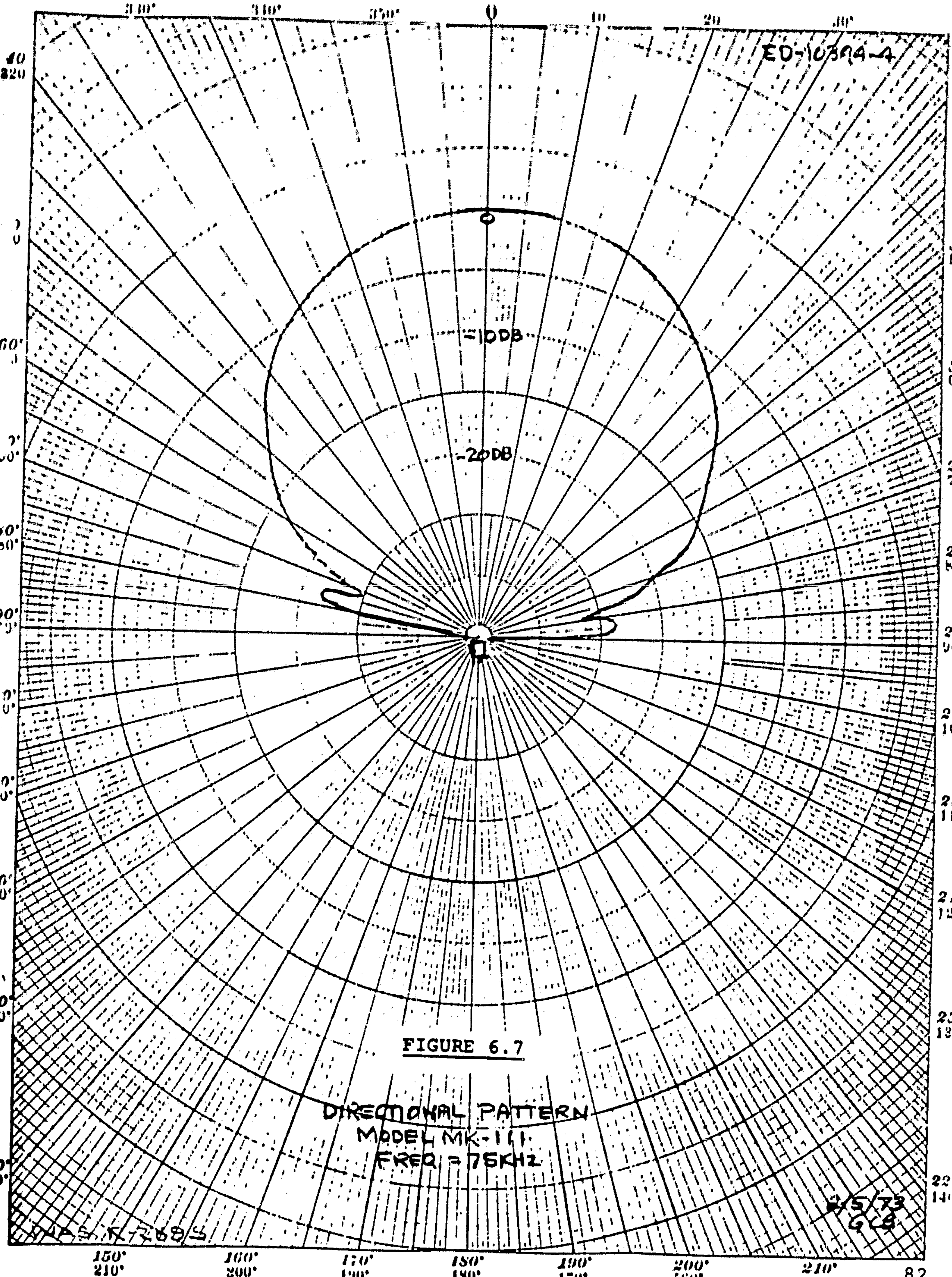
ED-10304-4
-10DB
-20DB
DIRECTIONAL PATTERN
MODEL MK-111
FREQ = 75KHz
2/5/73
GCB
K-268S

FIGURE 6.7

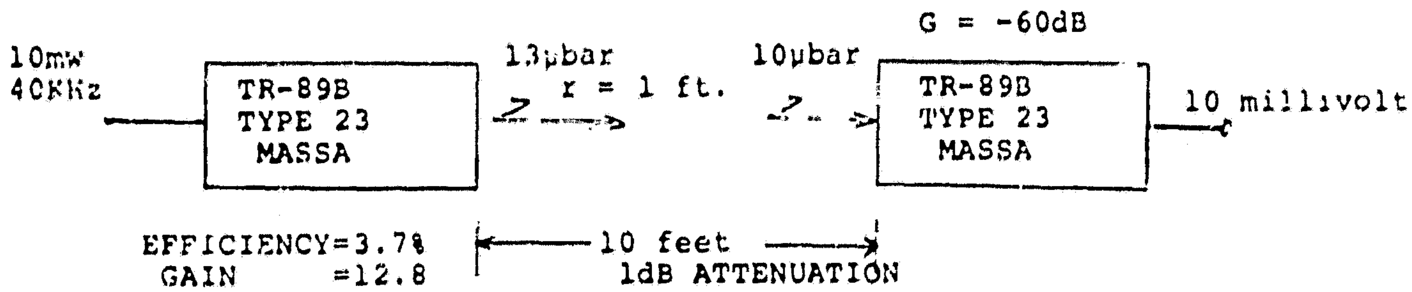

TYPICAL PARAMETERS OF AN ULTRASONIC AUDIO LINK

FIGURE 6.8

7.0 SUMMARY

Potential methods of wireless communication within the shuttle cabin enclosures included the options of magnetic coupling between loop antennas, radiation at RF frequencies, optical or ultrasonic propagation links.

The particular propagation method had to provide the specified transmission fidelity over a one-way voice link from any position within the cabin enclosures to wall mounted receivers. Consequently internal field patterns had to be free of resonant nulls and rapid signal attenuation with antenna spacing; the signal strength could not be radically affected by shadowing of objects in the propagation path or by incidental blockage of the propagation transducers. The systems had to be relatively free of detuning effects of the metallic cabin enclosure.

In addition the choice of signal parameters had to be assure that other sensitive spacecraft equipment would not be affected by the communicator and that the wireless communicator would in turn not be affected by other radiation or noise interference.

The summary comparison chart, Figure 7.1, lists those factors that are evaluated in this report. Those factors underlined were key considerations. This study concludes that the characteristics of magnetic coupling best matched the operating and propagation environment of the metallic spacecraft enclosures.

Magnetic field strength did not exhibit the deep nulls that could be experienced at RF frequencies or be as sensitive to path or transducers blockage as the optical or ultrasonic links. While the RF links were more efficient for a given transmitted power, the advantage was of small consequence within the short propagation distances of the cabin. Optical and RF links could provide larger bandwidths than the magnetic or ultrasonic but for the voice band that was needed, the advantage was of little value. The receiver at the magnetic frequency of 450KHz did not require the superheterodyning of the RF receiver at VHF. The optical system required multiple radiation diodes to overcome possible path interference and even with the best of diode layout could not assure complete freedom from diode blockage.

The interference of the wireless communicator with other spacecraft equipment required great care with an RF system. However, based upon the NASA supplied data on spacecraft frequencies an RF frequency at 400MHz would have been satisfactory; the 450KHz magnetic frequency caused no interference.

The specifications on EMI within the cabin assured that with the chosen transmission power levels that the specified transmission fidelity would be met. The uncertainty of the level of interference in the optical and ultrasonic bands under all shuttle operations made these choices too risky for any of the possible advantages to be gained.

FIGURE 7.1 SUMMARY COMPARISON OF WIRELESS MICROPHONE METHODS OF SIGNAL PROPAGATION

(Primary Decision Factors Underlined)

INDUCTIVE COUPLING

- Enclosure field strengths without nulls
- Electronics less complex at lower frequency
- More transmit power required for given power margin
- Loading losses by enclosure higher at low frequency
- EM environment defined
- Transducers (antennas) not muffled by body or non-metallic accoutrements
- Detuning/loading right next to metallic enclosure wall

RF

- Greater transmission efficiency with distance
- Resonant field structure within enclosure
- Broad bandwidth
- Superhet design more complex
- RF signal environment requires careful consideration in defined RF environment
- Enclosure losses less at higher frequency
- Transducers (antennas) not muffled by body or non-metallic accoutrements

OPTICAL

- Susceptible to signal blockage and transducer blockage
- Free of RF interference
- Power margin requires multiple transmitter diodes
- Optical interference and noice environment not well defined

ULTRASONIC

- Narrow bandwith
- Ultrasonic noise environment not defined
- Free of RF interference
- Susceptible to transducer blockage
- Propagation losses higher than RF

Telephonics CORPORATION

WIRELESS MICROPHONE COMMUNICATION SYSTEM

REPORT NO. WMCS–001

APPENDIX B

APPENDIX B

WIRELESS MICROPHONE COMMUNICATION SYSTEM FOR THE SPACE SHUTTLE ORBITTER DEVELOPED FOR NASA AT TELEPHONICS, HUNTINGTON, N.Y. CONTRACT NO.: NAS-9-14824

1. INTRODUCTION

This section of the final report reviews the design considerations of the Wireless Microphone System delivered to NASA under this contract. First, a review of Telephonics' study of the prior art and available equipment is presented which reveals several basic short-comings of such available equipment when used in a space vehicle environment. Secondly, the synthesis of a suitable system is discussed in detail. Finally, reasons for the particular circuit design are discussed in relation to the technical specifications of the contract.

The purpose of the Wireless Microphone is to provide crew members of the Space Shuttle Orbiter with a communications capability while away from their normal station positions. The wireless microphone eliminates the need for connecting umbilical cables which would be inconvenient, interfere with free movement and possibly even be hazardous. In the "VOX" mode, it permits hands-free automatic operation so that the crew member can concentrate on various mission activities.

2. REVIEW OF PRIOR ART AND AVAILABLE EQUIPMENT

Three sources of information were researched: a) final reports of military study contracts, b) technical journals of various engineering societies and c) catalogs and data sheets of commercially available equipment. Briefly, in making this review, it became quickly obvious that none of these references and equipment designs dealt adequately with signal fade-out due to nulls caused by strong reflected waves when operated inside a metallic enclosure such as the space shuttle. In order to reduce the probability of a drop-out, standard practice was to use more than one receiver either in frequency or space diversity. Still, the drop-out probability was nowhere near the zero percent value which Telephonics felt was mandatory for a space application. In addition, there was the problem of avoiding antenna directional characteristics which would also produce nulls or signal drop-outs. This is the characteristic of wire or whip antennas. Furthermore, such antennas can be easily detuned by touching them, they take up space and interfere with crew movements, they are a hazard to eyes and can easily be broken off. All of this rules out the whip antennas that are used in wireless microphone equipment.

All of the commercial systems we know of use frequencies above 20 megahertz. At these frequencies, narrow band voice frequency channels require precise crystal-controlled superheterodyne or double superheterodyne receivers. Transmitters also require crystal control and in the case of fm modulations, preferred over other forms of modulation, the portable package carried by the crew man becomes too complex, bulky and power-hungry. All of this tends to degrade reliability and materailly raise costs. It was clear that the communications industry had never addressed itself to the unique requirements of NASA.

Lastly, a choice of frequency had to be made. Certainly, the whole of the radio frequency spectrum is, for all practical purposes, saturated world-wide. While the system is to operate within the craft, it is not shielded against high frequency signals due to the relatively large window openings. While NASA's contract does not specify a secure system free of jamming, Telephonics has taken this into full consideration.

3. SYNTHESIS OF A SYSTEM MEETING NASA'S REQUIREMENTS

NASA requires the wireless microphone to operate within the space shuttle in the upper flight deck and in the lower living quarters deck. The two decks are connected by a passage way opening about 30" in diameter. The wireless microphone transmitters are to have a choice of two operating frequencies, one for the upper deck and one for the lower deck. This avoids the interference that would be caused when crew members are near the opening between decks and only one frequency is used for both decks. Each deck is provided with a receiver so positioned as to limit the maximum operating range from the transmitter to 11 feet. NASA has located the receivers on the rear bulkhead in the best position to keep the operating range to a minimum.

It is our understanding from discussions with Rockwell that the receiver locations are just below fluorescent lights located less than one foot from the receiver antenna. At this time, we do not know if these lights are shielded or what the noise level at the antennas will be. Since we lack definite data on noise level to be expected within the craft, it was decided to design the transmitter for one watt input to its antennas. Should this power not be needed, this level can be easily lowered by changing the value of one resistor. One watt appeared to be close to the maximum power that could be drawn from the new Mallory Lithium Organic batteries and have them last the expected 90 hour mission time. The lithium organic cells, unlike other tyes of lithium cells, have a proven record against explosion, even with unrealistic extremes of tests. This, coupled with a built-in fuse to limit the maximum possible short-circuit current, further guarantees protection against its explosion. It is to be remembered that all batteries can rupture or explode under short-circuit conditions. Full information submitted by the lithium battery division of Mallory has been presented to NASA for evaluation. This type of cell is remarkable in that it has several times the watt-hour capability of any other kind of battery for a given weight or size. During the course of this contract, no preference could be determined from NASA or Rockwell with respect to a choice of small cells, to be replaced during the mission, or larger cells to last the duration of the mission. The latter was Telephonics' choice and the design was implemented accordingly. VOX or PTT transmitter operation is required by

NASA, and such operation conserves battery power. No firm figure could be determined, however, either from NASA or Rockwell as to the probable ratio of ON to OFF time. This ratio and the power required to override noise are certainly difficult matters to determine and Telephonics appreciates this. Hence, it was planned to make the battery pack separate from the transmitter so that it is simple to redesign the pack without disturbing the transmitter design. This type of cell has a nominal voltage of 2.92 volts which, under light loads, remains almost as constant as a mercury battery to the end of its life. This considered, it was decided to design the transmitter circuits to opertate on a 6V supply. In order to avoid nulls produced by strong reflections, the wavelength of the signal must be much larger than the spacecraft dimensions. For this reason, low frequencies of 455 and 500 kilohertz were chosen, corresponding to wavelengths of 660 and 600 meters, respectively. Since the maximum dimension in either the upper or lower deck compartments is about seven meters, reflections from the walls will be in phase for all practical purposes. With the direct and reflected waves in phase, the two will add and noticeably improve the signal level. With the receiving antennas less than one inch from an aluminum reflecting surface, there will be about a 6 dB improvement in signal level due to the first reflection.

At these low frequencies, very compact ferrite antennas are practical for covering the small range (11 feet) inside the craft. For this short range, use is made of the near magnetic field. In effect, the transmitter and receiver antennas constitute loosely coupled transformer windings. Strength of this coupling decreases as the inverse cube of distance, hence the system is inherently a short range one which insures security and freedom from jammings. Furthermore, the craft's relatively small window openings, compared to wavelength, will substantially attenuate signals entering and leaving the craft. The rapid attentuation of the signal with distance also guarantees that multiple reflections will not cause nulls due to increasing phase differences.

In order to make an omnidirectional system with ferrite antennas, the transmitter requires two bar antennas mounted orthogonally and excited by two signals in time quadrature. Also, two independent receivers with ferrite antennas mounted ortogonally are required to avoid nulls due to the directional characteristics of the antennas. The orthogonal relationship of each set of antennas is in the form of an "X" rather than an "L" in order to avoid objectionable mutual coupling between antennas.

The transmitter antennas are 2.5" long with a cross-section of 0.48" X 0.12". The receiver antennas are 3.75" long with the same cross-section. We find these antennas can be mounted as close as 0.5" from an aluminum surface with the 0.48" dimension parallel to the surface without any significant degradation in performance. This applies to both the receiver and the transmitter. Tests show that detuning due to hand capacity, 0.5" from the antennas, does not degrade performance to any noticeable extent. Since the efficiency of a ferrite antenna is extremely low for the power input used in this system, the radiated power density

10 meters from the antenna will be less than one micromicrowatt. Each time the antenna length is cut in half, the range is cut in half for a given power. Through a series of experiments, Telephonics has reduced the length of the transmitter and receiver antennas until transmitter battery power reached one watt for a range of 22 feet. At this range, fm reception was clear, quiet and solid for all relative positions of transmitter and receiver antennas. The noise environment of the Telephonics lab is judged to be a very high one due many large fluorescent lights that are closely spaced and about eight feet above the floor. Here the characteristics of an fm system , which suppresses noise and holds signal level constant with large signal strength variations proved highly useful. (A full study of this system's RFI immunity was made and was discussed in Test No. 6 of the report made to NASA on September 15, 1976.) From the above, it is seen that battery size vs. antenna size must be a trade off. This also involved the decision to have a separate battery pack last the duration of the mission which is at most seven days. A study of the Mallory Lithium Organic Cells shows the LO-30 size capable of meeting these requirements for an ON/OFF duty time of 15%. This cell is slightly smaller than 1 D size cell, 1.16" diameter and 2.35" long, with electrical rating of 7.5 A/hour, 160 ma rated drain and an open circuit voltage of 2.92V. The cell must be operated about 12 minutes to bring the voltage up to its rated value. Under load, the cell voltage will be 2.85V until about 90% of its life is reached, thereafter it begins to roll off rapidly. For 160 ma and 90% life this cell will last 42 hours. For 15% ON/OFF duty, the cell will last 280 hours. Two cells are required for the 5.70V transmitter supply design. Cells smaller than the LO-30 drop rapidly in efficiency for their size. Also, efficiency drops about 30% for temperature extremes of -20 and 125F.

This study formed the basis of the system recommended by Telephonics, which considers many special requirements. In the future, Telephonics believes this system can easily be extended in range by the use of more than one set of receivers. The simplicity of the receivers (two mount on a plug board 3" X 5") makes this practical. This simplicity also could make a two-way system practical.

4. THE WIRELESS MICROPHONE TRANSMITTER AND RECEIVER DESIGN

4.1 THE TRANSMITTER DESIGN

The system proposed uses narrow band fm modulation where the modulation index is unity. The audio frequency range is 300-3000 hertz. The system is capable of being modulated down to dc. This is necessary because of momentary dc controlled shift in transmitter frequency is used to generate a signal which activates the receiver ICOM mode. With an index of one, the bandwidth will be 6 kilohertz. A bridge T type oscillator is modulated by means of back-to-back varicap capacitors. Oscillation amplitude is held constant and in class A operation by diode limiters. The supply voltage is held constant by a zener diode. Overmodulation is prevented by back-to-back diodes which limit the modulation voltage to 1.0V pp. The microphone amplifier low power IC is capable of sufficient gain to work with any low level, low impedance microphone. It is recommended that the gain be set for 12 db clipping by the modulation limiter diodes to improve the signal/noise of the system. This type of fm modulated oscillator is sufficiently stable to stay well within the wider pass band of the receiver over the required temperature range. Associated with the microphone amplifier are the VOX circuits. Attack and hold time contants are separate. In VOX operation, the standby power consumption is kept as low as possible (12mw.).

The oscillator provides two output signals phased 90° apart. This is accomplished by an R-C network connected to the collector and emitter. This network requires the signals at the collector and emitter to be equal in amplitude, hence R-15 and R-16 are made equal. In order to avoid loading this network and the oscillator, two buffer FET amplifiers are used between the oscillator and the final power amplifiers. The power amplifiers are class C type, using 2N3467 transistors. These are conservatively rated for the 0.5 watt output to each ferrite antenna. They are also able to take the extra load prior to tuning the antenna in production.

The final amplifiers have sufficient drive to cause the collector to saturate and essentially poduce a square wave output, thereby keeping efficiency as high as possible. The 7.5 ohm resistor in the collector is small compared to the antenna input impedance and limits current before the antenna is tuned in production.

The transmitter is designed to operate at 455 and 500 kilohertz. This requires the frequency of the oscillator tuning and the tuning of two ferrite antennas to be changed. The simplest way to change oscillator tuniung is to switch between two pretuned slug-tuned inductors. The simplest way to change antenna tuning is to switch between pretuned capacitors. The most practical way to do this is to use miniature TO-5 latching relays - one located close to the oscillator and another in the subassembly containing the antennas, final power amplifiers and associated tuning capacitors. This platic protected subassembly measures 2.25" X 2.25" X 1.25" and is carefully designed with a PC board assembly to insure short rigid leads between various associated components. This package has to be plastic to permit radiation from the antenna. The remainder of the circuits, consisting of the low level audio amplifier, VOX, modulation components, oscillator and buffers, are enclosed in a shielded package of the same size as above. These circuits must be highly shielded against the magnetic field radiated by the antennas for proper and stable operation. All control switches and the microphone end battery connectors are mounted on this subassembly. The two subassemblies are then combined to form the complete wireless microphone package measureing 4.5" X 2.25" X 1.25". The transmitter is provided with three switch controls: the selection of either 455 or 500 kilohertz is made by a three-position switch. Moving this switch momentarily to one side or the other of the normally-off center position sets latching relays for one frequency or the other. Another three position switch has a center position for transmitter idle, one momentary position for PTT ICOM and the other momentary position for PTT XMT.

The third switch has two steady positions, one for VOX, the other for $\overline{\text{VOX}}$. The transmitter is completely off with no power drain in the $\overline{\text{VOX}}$ position only. The VOX mode operates only in conjunction with the XMT mode.

4.2 THE RECEIVER DESIGN

The receiver design is just as important as the transmitter design in order to obtain a smoothly operating, reliable overall system. Prior existing receiver equipment far from meets the special requirements of this application.

Eventhough the transmitter radiates an omnidirectional signal, two receiving antennas are required, orthogonally placed to insure reception for all positions relative to the transmitter antennas. Furthermore, it is not possible to combine signals from these receiving antennas into one receiver, because some position may be found where the signals in each antenna are equal but opposite in phase, thereby giving zero output. It is therefore necessary to use two receivers and to select the best signal automatically for 100% reliability in all positions of the antennas. This sounds complicated and appears to require much equipment. As will soon be seen, however, this is not the case. Actually, both receivers (less their antennas) could be mounted on a 3" x 3" PC board with a maximum parts height of 0.75". This compactness enables the receivers to be mounted in the SMU at the cost of a small increase in the height of its housing. The two antennas, in the form of an "X", are mounted in front of the SMU speaker. They will be encased in a tough plastic housing which makes them mechanically reliable. Tests show that the sound pattern is not noticeably effected by this antenna arrangement in front of the speaker. (Test results for this arrangement are given as an attachment to this report.)

At the low frequencies of 455 and 500 kilohertz, it is not necessary to use a superheterodyne frequency conversion receiver. This factor alone constitutes a substantial step in reducing complexity and space requirements. Furthermore, a local oscillator with its radiation problems is avoided. Two receivers are to be furnished NASA under this contract (each is actually two receivers as described above), one operating at 455 and the other at 500 kilohertz. As discussed earlier, each deck of the craft will use a different frequency. The two receivers have the same design and differ only in the tuning of the antenna, the frequency of a ceramic bandpass filter, the tuning of the discriminator and the tuning of a third harmonic circuit to be discussed later.

Thus, these FM receivers are supplied fixed-tuned to one frequency. Due to the natur of an FM receiver, the output signal level will remain constant regardless of signal input level so long as limiting exists. A unique means is provided in each receiver to gate off the output audio before any noticable degradation of quality or any noticable reduction in signal/noise occurs due to a drop of input signal

ORIGINAL PAGE IS
OF POOR QUALITY

level. No objectional noise bursts are allowed before gate-off occurs when the transmitter is cut off. Should a fade-out occur for one receiver, a selector circuit will switch to the other receiver if it is providing a good signal. The selector will hold this signal so long as it is good, even though the other receiver may have returned to good operation with a stronger signal input. This switching between receivers is free of transients and is fast enough not to be noticeable. Since the audio signal output is fed to the SMU, which has an automatic gain control, neither the transmitter nor the receiver needs AGC. The receiver audio output is over one volt rms with a driving impedance of 200 ohms. Receiver sensitivity is sufficient to operate properly at a 22 foot range, which is twice the maximum range encountered in the space shuttle. Since the transmitted signal attenuates 18 dB each time distance is double, it is believed this design has a conservative safety factor.

The receiver antennas use the same type of ferrite that is used in the transmitter: Ferroxcube Q-1 material with an initial permeability of 125, a cross section of 0.48" x 0.12" and a length of 3.75". The winding uses 160 turns of No. 28 copper wire. The Q of the tuned antenna is 20, giving a bandwidth of 25 kilohertz at 500 kilohertz and 22.5 kilohertz at 455 kilohertz. (The bandwidth is much greater than the 6.0 kilohertz bandwidth of the transmitted signal and is therefore not critical.) The impedance of the antenna is about 60k ohms. This high impedance requires the first amplifier to have a high input impedance. The SD-304, made by Signetics, is a dual gate FET capable of very low intermodulation at high signal levels. Other strong signals or noise components that may be present in the craft therefore have less chance of causing intermodulation with the desired signal. The antenna is capable of generating several thousand microvolts when the transmitter is very close to the receiver. In the future, more than one transmitter might be used in the same chamber, so it is desirable to avoid a serious intermodulation problem.

The output of the first amplifier couples to a bandpass filter where practically all the selectivity of the receiver is obtained. This filter is a very compact one that will meet the MIL-NASA SPECS. It uses ceramic discs to produce a bandwidth of 16 kilohertz at the 6 dB points and an attenuation of 50 dB at twice this bandwidth. This filter, made by Vernitron, is about .327" in diameter and 1.17" long. The filter output is coupled to a TV-FM chip by means of a matching transformer which provides a voltage gain of 12 dB. The minimum limiting level of this chip (3065, made by several firms and meeting MIL-NASA specs when packaged in a ceramic case) is 200 uV. This chip limits the signal at the 1.6V p-p level, detects the signal with a quadrature detector requiring a single tuned circuit, amplifies the audio signal to 1.0V rms and also provides an electronic attenuator which is used to mute the output when transmission ceases or drops below the limiting level as described above.

The circuit that selects the signal from only one of the receivers is a form of flip-flop circuit with some hysteresis to prevent jitter when the two control signals are equal. Each control signal is derived from the output of the last limiter. The selector circuit operates on the principle that as long as limiting occurs, a square wave output will be present and this will contain a third harmonic component signal. This signal is detected in each receiver and is used to control the flip-flop in such a way as to obtain the audio switching and muting described earlier.

The two receivers use a total of one watt power from a single-ended supply of 12 VDC.

The overall total harmonic distortion of the transmitter and receiver is less than 5%.

Telephonics CORPORATION

WIRELESS MICROPHONE COMMUNICATION SYSTEM

REPORT NO. WMCS–001

APPENDIX C

WIRELESS MICROPHONE COMMUNICATION SYSTEMS
FOR THE
SPACE SHUTTLE ORBITER VEHICLE

DEVELOPED FOR NASA

AT

TELEPHONICS, HUNTINGTON, N.Y.

CONTRACT NO: NAS-9-14824

SEPTEMBER 15, 1976

Telephonics

A DIVISION OF INSTRUMENT SYSTEMS CORPORATION

ORIGINAL PAGE IS
OF POOR QUALITY

WIRELESS MICROPHONE COMMUNICATION SYSTEM

INTRODUCTION

The wireless microphone system has been developed to provide crew members of the Space Shuttle Orbiter with a communication capability while away from their normal stations. The wireless microphone eliminates the need for trailing umbilical cables which would be inconvenient and possibly hazardous; it permits a hands-free operation which allows the crew member to concentrate on the instrument manipulations or repair activities that he is concerned with.

BACKGROUND

Both NBC and CBS in their recent coverage of both national conventions used wireless microphones and experienced fade-outs during several interviews. This occured even though more than one receiver was used. Today, communication engineers regard radio communication whthin an enclosure as unreliable, and it is the subject of many technical articles through the years. All of the commercial systems we know of use frequencies above 20 megahertz. Such systems invite multipath (reflections) problems which cause cancellation or null pickup problems. Furthermore, these systems are complex, large and power consumming. All of this, plus NASA's dislike for wire antennas that can easily be broken off or injure an eye pretty much ruled out the "usual" approach.

The demonstration system we bring with us today operates at 455 kHz. The transmitter is an omnidirectional radiator using the near magnetic field. The receiver (actually two receivers with ferrite antennas) also provides omnidirectional pickup. At this low frequency, reflections within the space craft will always be in phase (for all practical purposes) and will add to improve the signal level. Hence we have an overall omnidirectional system that will not experience null situations.

At these low frequencies, radiation in and out of the space craft will be highly attenuated due to the relatively small openings compared with the wavelength. This also applies between chambers of the space craft, so the same frequency can be used (FM system captures the strongest siganl) in different chambers. Although NASA did not make it a requirement, it is believed that a secure system, that is immune to spying or jamming from outside sources, would be desireable.

DESCRIPTION

Wireless Microphone Transmitter

The wireless microphone transmitter is a narrow band FM system which operates at 455 kHz carrier frequency (or 500 kHz), with a $\pm$ 3 kHz frequency deviation. The audio bandwidth is 300 Hz to 3.0 kHz, with less than 5% maximum distortion at 1.0 kHz.

C-2

ORIGINAL PAGE IS
OF POOR QUALITY

The low carrier frequency has been chosen to keep the wavelength large compared with any internal dimension of the vehicle, thereby eliminating any standing wave condition in the cabin volume, (λ = 600 meters). The long wavelength also assures that the radiated signal is vanishingly small; the receiver operates entirely in the near field of the transmitter antenna, and in effect the two antennas constitute loosely coupled transformer windings.

The transmitter uses a pair of ferrite bar antennas which are mounted orthogonally and driven by two signals which are in time quadrature. The resulting antenna magnetic field pattern is therefore rotating in space, and tends to prevent reception nulls which might arise for certain relative orientations of transmitter and receiver antennas.

Amplified microphone audio signals drive a pair of varactor diodes which form part of the tank circuit for the 455 kHz oscillator, modulating the oscillator frequency in proportion to the audio signal level. The output of the oscillator is fed through two MOSFET buffers to the two antenna coil drivers, with a 90^o phase shifter included at the input to one of the MOSFET's.

Both PTT and VOX modes of operation are provided. DC power to the main oscillator and antenna drivers is gated through the PTT switch, or via the VOX output switching transistor. In the VOX mode, an attack time of approximately 4 milliseconds is provided, with a release time of the order of 1.5 seconds.

The transmitter standing power drain is less than 12 milliwatts. When keyed, the transmitter drain is just under 3/4 watt. The transmitter dimensions are 3" x 3" x 1.5", less the battery pack, which is a separate package. It has been suggested by NASA, that a separate battery pack be used to enable flexibility in supply requirements for different mission requirements without upsetting the transmitter package.

We find that the ferrite antennas, whose dimensions are 0.48" x 0.120" x 3.75", can be located as close as 0.5" from an aluminum surface where the 0.48" dimensions is parallel with the aluminum surface, without any significant degradation in performance. This applies to both receiver and transmitter. This makes for a very compact antenna system which, when encapsulated in a suitable plastic, will offer high reliability. Also, tests show detuning due to hand capacity 0.5" from the antennas does not degrade performance to any noticable extent.

Battery Power for the Wireless Microphone

Telephonics recommends the use of the Mallory Lithium/Organic batteries as a power source for the Wireless Micorphone transmitter. This recommendation is based upon the superior energy density and voltage regulation attainable with L/O batteries as compared with Ni Cad, Mercury, Alkaline, or Carbon/Zinc cells. Manufacturer's data indicates that

ORIGINAL PAGE IS
OF POOR QUALITY

the Lithium cell can provide nearly three times the energy per pound achieved by the next best type, as well as 30% greater energy per unit volume.

A review of test data supplied by the Mallory Battery Company indicates that the LO-30 Lithium/Organic battery can be considered non-hazardous under the conditions of use anticipated for the wireless microphone. Extraordinarily severe abuse appears necessary to evoke either cell venting or explosion of the cell; appropriate fuse protection in the battery carrier should be sufficient to prevent the onset of any significantly abnormal condition.

In support of the viewpoint that the LO-30 type cells are non-hazardous, reference should be made to the following reports:

a) "Non-Hazardous Primary Lithium Organic Electrolyte Battery", by Mr. T. Watson, ECOM-73-0282-F, OSD-1366, Ocotber '74.

b) "Abuse Testing of Li/SO_2 Cells and Batteries", by H. Taylor and B. McDonald (of Mallory Co.), June '76. This pre-print includes a set of references to prior pages on the same subject.

c) LO-30 Data Sheet

d) Mallory Battery Company Correspondance

e) Mallory Battery System Characteristics

Wireless Microphone Receiver

At 455 kHz the receiver can be a straight tuned RF receiver that does not require a superhetrodyne frequency conversion, thus avoiding a local oscillator that would cause radiation problems. Our present design makes use of a TV-FM chip which takes the input signal at 455 kHz at the 200 uv level, limits the signal at 1.6v p-p, detects the signal with a quadrature detector requiring a simple tuned circuit, and amplifies the signal to earphone level. The chip (3065, made by several firms, meets MIL-NASA specs when packaged in a ceramic case) also provides an electronic attenuator circuit which we use to mute the output when transmission stops in either PTT or VOX operation. Actually two receivers and two antennas are used for 100% reception reliability. This is practical because each receiver requires only two chips, a small ceramic bandpass filter and a few associated discrete parts. It is practical to mount both receivers on a printed circuit board 3" x 3". The ferrite antennas are 3.75" long, arranged in a 90° "X" and protected by a plastic housing. Hence the receiver package will be not more than 3" x 3" x 1.5" including both electronics and antennas.

The receiver antennas provide circuit Q's of approximately 20; the input bandwidth is thus $\pm$ 11 kHz. The antenna signal is processed through a wideband op-amp with a 20 dB gain, then through a 9 hole lattice-filter having 10 kHz bandwidth at the 6 dB down points. The filtered FM signal is then fed into a 3065 "TV Sound System" integrated circuit which provides the FM limiting, detection, and audio pre-amplification functions on a single chip. A single LC tuned circuit is associated with the 3065 IC. Audio output level from the 3065 IC is over 1 volt rms at distortion levels below 5%.

The 3065 IC operates with a single ended supply of +12 VDC; this is also suitable for the dual wideband op-amp. Combined power dissipation with both receiver sections operating is of the order of one watt. Both receiver sections can be packaged on a printed circuit board 3" x 3" or less.

The receiver dimensions are such that the PC board can be mounted in the SMU at the cost of a small increase in the height of the housing. The receiving antenna can be mounted in front of the SMU speaker.

APPENDIX I - TEST PLAN

WIRELESS MICROPHONE TESTS

1) Determine minimum and maximum receiver audio outputs with the transmitter separated from the receiver by the following distances in feet: .5, 1, 2, 4, 8, 16, 32, and dropout.

2) Measure distortion through the system at transmitter/receiver spacings of 6 and 15 feet.

3) Measure the audio bandwidth of the system at the 3 and 6 dB points.

4) Measure the VOX attack and release times.

5) Measure the transmitter power while transmitting and not transmitting, and measure the receiver power.

6) Determine the transmitter field strength.

7) Determine the susceptibility of typical electronic equipment to the transmitter power at various distances.

8) With the transmitter/receiver spacing equal to 15 feet, determine the system susceptibility to a 455 kHz electronic current on a 3 foot length of wire spaced at various distances from the receiver. The wire/receiver orientation should be for maximum coupling and the transmitter/receiver orientation should be for minimum coupling. The data should show wire current as a function of wire/receiver spacing for loss of capture of transmitter signal.

9) Determine typical speech limiting in the transmitter.

APPENDIX II - TEST RESULTS

Test #1	Audio Output vs. Transmitter to Receiver Distance
Test #2	Audio Distortion
Test #3	Audio Frequency Response
Test #4	VOX Attack and Release Time
Test #5	Transmitter and Receiver Power Drain
Test #6	Field Strengths Previously Measured; See Appendix III
Test #7	Effect of Transmitter on Nearby Electronic Equipment
Test #8	Susceptibility of Wireless Microphone Receiver to Interference from Adjacent Shuttle Circuits
Test #9	Microphone Level

TEST #1

Determine minimum and maximum audio output vs. T/R spacing.

SPACING, FT.	AUDIO OUTPUT, mv. MIN.	MAX.
0.5	520	560
1.0	540	580
2.0	530	560
4.0	580	620
8.0	500	540
16.0	280	620
32.0*	280	680
22.0	280	620

* Careful orientation of receiver, one drop out position was found. At 22 feet solid reception was obtained.

ORIGINAL PAGE IS
OF POOR QUALITY

TEST #2

SYSTEM: TOTAL DISTORTION

A frequency selective HP Voltmeter #3591A was used to measure system distortion (transmitter and receiver). A 500 Hz tone at 60 uv level was used to modulate the transmitter to its full FM excursion $\pm$ 3 kHz, (without clipping, which protects against over modulation). Tests were made at 6 feet and 15 feet. (Bandwidth of voltmeter: 100 Hz)

	LEVELS, mv. 6 FT. SPACING	LEVELS, mv. 15 FT. SPACING
Fundamental (500 Hz)	540	560
2nd Harmonic (1000 Hz)	2.5	9.5
3rd Harmonic (1500 Hz)	23	22
4th Harmonic (2000 Hz)	6	4.3
5th Harmonic (2500 Hz)	3.9	4.7
6th Harmonic (3000 Hz)	1.2	1.4

$$\text{Total Distortion} = \frac{\sqrt{(2nd)^2 + (3rd)^2 + \ldots}}{\text{Fundamental}}$$

@ 6 FT. = 4.5% Distortion

@ 15 FT. = 4.4% Distortion

* Receiver output into 500 ohm load. The transmitter modulation level is set for a 60 uv microphone input for full modulation $\pm$ 3 kHz. Clipping is used above this level to limit FM excursion to 3.5 kHz. The demonstration receiver uses 500 Ohm earphones. Receiver bandwidth is 10 kHz @ the 6 dB points, this allows $\pm$ 2 kHz tolerance.

TEST #3

FREQUENCY RESPONSE OF SYSTEM: (TRANSMITTER AND RECEIVER)

FREQUENCY, Hz	LEVEL, mv. *
280	400
300	450 (-3 dB)
400	540
500	600
1000	660 (Max. 0-dB)
1500	620
2000	520
2200	470 (-3 dB)
2500	400
3000	330 (-6 dB)
3500	290
4000	260

* Receiver output into 500 Ohm laod for a transmitter input of 60 uv (just below limit level).

Transmitter - Receiver separation 15 Ft.

TEST #4

VOX ATTACK AND RELEASE TIME

Transmitter only using full modulation (70 uv 3000 Hz input), the VOX attack time is 0.6 ms.

Transmitter and receiver attack time (includes time for mute circuit to turn on) is 4 ms.

Transmitter release time is 1.6 seconds.

TEST #5

TRANSMITTER - RECEIVER POWER

Receiver: 12V @ 41 ma - 0.49 watts

Transmitter:	VOX (Stand By)	5.8V @ 2 ma 11.6 mw
	PTT (Transmit)	5.8V @ 122 ma 0.71 watts

TEST #7

EFFECT OF TRANSMITTER ON NEARBY ELECTRONIC EQUIPMENT

For this test, the wireless transmitter was placed a few inches from the microphone input circuit board of an open ATU. The transmitter was keyed repeatedly, while the operator listened to the ATU audio output. No perceptible interference was found, nor any keying clicks.

A similar test with the transmitter keyed adjacent to a high impedance oscilloscope probe did indicate some interference. This was not unexpected; significant electric fields do exist within a foot of the transmitter antenna.

TEST #8

EFFECT OF INTERFERING SIGNALS AT THE WIRELESS MIC RECEIVER

TEST #8A

Interfering Current: 200 microamps
Frequency: Approximately 455 KHz, vernier tuned for greatest degradation of received signal.
Distance From Transmitter to Receiver: 15 feet

Varied the distance between receiver and interfering wire. At 11 1/2 inches between antenna center and the wire, the signal is marginally intelligible. At 12 1/2 inches separation the received signal is very clear.

TEST #8B

Distance From Transmitter to Receiver: 15 Feet
Frequency: Approximately 455 KHz, vernier tuned for greatest degradation of received signal.
Distance From Antenna Center to Wire: 6"

Varied the interfering current. At 50 microamperes, the voice signal is marginally intelligible. At 40 ua or less the received voice signal is very clear. Calculations indicate that a long straight wire carrying 200 microamperes should induce approximately the same signal level at the receiver, located one foot from the wire, as the wireless transmitter would induce at a distance of 13 feet. This is a fairly good check on test 8A.

It was noted that a very minute de-tuning of the interfering signal, ie., a fraction of 1 KHz, would reduce the interference effect very drastically, leaving very clear reception. This was evident in both tests 8A and 8B. In other words, a concerted effort was required to achieve interference. At slightly greater detuning, the antenna could be brought within 1 1/2 inches of the interfering wire with no adverse effects.

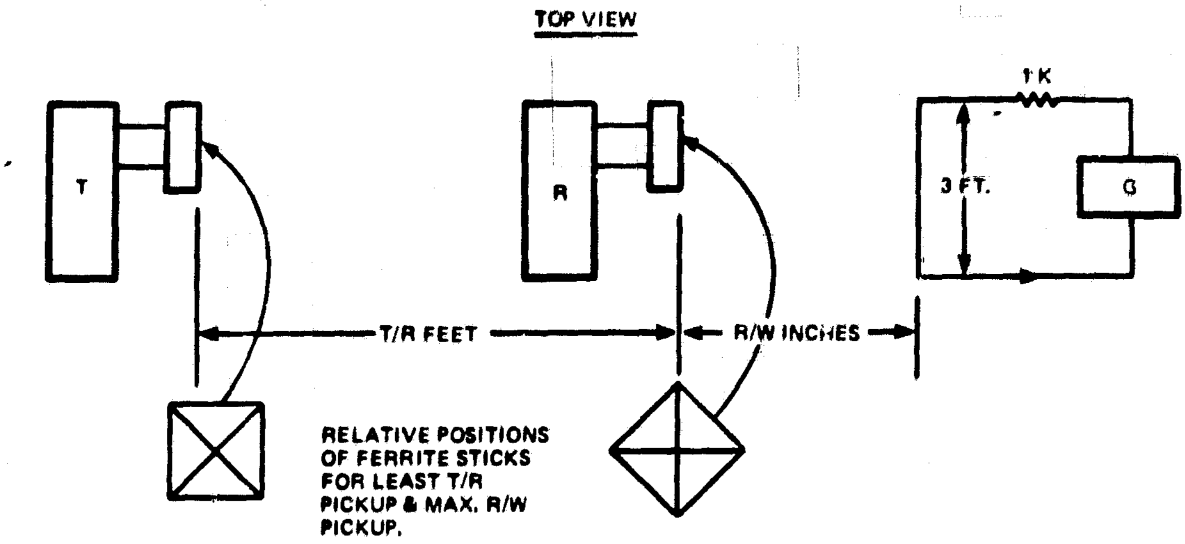

TEST #8C

For this test the wireless microphone transmitter was turned off. With no interfering current, the observed noise voltage across the headset resistance (500 ohms) was 0.6 millivolts.

The interfering current was adjusted to 455 KHz and set to various levels while the receiver separation from the wire was adjusted until a noise voltage increase to 1.5 millivolts was observed across the receiver headset resistance. This provided a check on the ability of interfering signals to release the noise muting. Typical results were:

1.2 ua	-	separation 12"
4.5 ua	-	separation 36"
7.6 ua	-	separation 72"
30.0 ua	-	separation 108"

This indicates that to avoid transmission of receiver noise to the rest of the ADS, circuits carrying 455 KHz signals in the spacecraft should be routed in metallic trays or otherwise shielded to avoid turning on the wireless microphone receiver noise.

An alternate would be to keep the wireless mic transmitter on, avoiding capture of the circuit by spurious signals.

TEST #9

MICROPHONE LEVEL

A Turner #35A dynamic microphone is used in the feasibility model.

When clipped on the chest 6" below the mouth, at normal speech level, full modulation occurs, with some limiting estimated at 6 dB.

APPENDIX III

ANTENNA CALCULATIONS

(1)

Wireless Mic Transmitter Antenna Parameters

Ferrite Core: 0.48" wide × 0.12" thick × 3.75" long
(±.02") (±.01")

Effective Q = 40 128 turns.
Coil Current = 90 ma, approx
Permeability 100

Core cross section = 0.48" × 0.12" = .0576 in^2
= .372 cm^2 = 3.72×10^{-5} $meter^2$

Effective cross section, with $\mu = 100$,
3.72×10^{-5} $meter^2$ × 100 = 3.72×10^{-3} m^2

Coil current: 90 ma

Coil amp turns: .09 amps × 128 turns = 11.5 ampturns

Antenna Dipole Moment: $m_0 = (NI) \times Area$
$m_0 = 11.5 \times 3.72 \times 10^{-3} m^2$
$m_0 = .043$ amp $meter^2$

$m_c = 0.043$ amp $meter^2$

②

<u>Magnetic Dipole Equations:</u>

a) $$E_\phi = -\frac{jk}{4\pi}\left(\frac{\mu_0}{\epsilon_0}\right)^{1/2}\left(\frac{1}{r^2}+\frac{jk}{r}\right) m_0 \sin\theta \, e^{j(\omega t - kr)}$$

b) $$H_\theta = \frac{1}{4\pi}\left(\frac{1}{r^3}+\frac{jk}{r^2}-\frac{k^2}{r}\right) m_0 \sin\theta \, e^{j(\omega t - kr)}$$

c) $$H_r = \frac{1}{2\pi}\left(\frac{1}{r^3}+\frac{jk}{r^2}\right) m_0 \cos\theta \, e^{j(\omega t - kr)}$$

where $k = \frac{2\pi}{\lambda}$ $\quad \mu_0 = 4\pi \times 10^{-7}$ $\quad m_0 = IA$

$\epsilon_0 = 8.85 \times 10^{-12}$ $\quad \left(\mu_0/\epsilon_0\right)^{1/2} = 120\pi$

$\mu_0\epsilon_0 = 1/c^2$

Reducing,

A) $$E_\phi = \left(-j\frac{60\pi}{\lambda r^2}+\frac{120\pi^2}{\lambda^2 r}\right) m_0 \sin\theta \, e^{j(\omega t - kr)}$$

B) $$H_\theta = \left(\frac{1}{4\pi r^3}+j\frac{1}{2\lambda r^2}-\frac{\pi}{\lambda^2 r}\right) m_0 \sin\theta \, e^{j(\omega t - kr)}$$

C) $$H_r = \left(\frac{1}{2\pi r^3}+j\frac{1}{\lambda r^2}\right) m_0 \cos\theta \, e^{j(\omega t - kr)}$$

At 455 KHz, $\lambda = \frac{3 \times 10^8 \text{ meters}}{4.55 \times 10^5} = 660$ meters

1 foot = .305 meters

(3)

(Near Field)

Field at a distance of 1 foot from antenna:

$$E_\phi = -j\frac{60\pi}{\lambda r^2} m_0 = \frac{60 \times 3.14}{660m \times (.305)^2} \times .043$$

$$H_\theta = \frac{1}{4\pi r^3} m_0 = \frac{1}{4 \times 3.14 \times (.305)^3} \times .043$$

$$H_r = \frac{1}{2\pi r^3} m_0 = \frac{1}{2 \times 3.14 \times (.305)^3} \times .043$$

E_ϕ at 1 foot = .132 volts/meter
H_θ at 1 foot = .119 amp turns/meter
H_r at 1 foot = .238 amp turns/meter

Near Field:

$$E_\phi = \frac{.0122}{r^2}$$

$$H_\theta = \frac{.0034}{r^3}$$

$$H_r = \frac{.0068}{r^3}$$

at 1 meter:
E_ϕ = .0122 volts/meter
H_θ = .0034 amp turns/meter
H_r = .0068 amp turns/meter

at 10 m:
1.22×10^{-4}
3.4×10^{-6}
6.8×10^{-6}

at 10 meters:
E_ϕ = .0000122 V/meter
H_θ = .0000034 AT/M
H_r = .0000068 AT/M

Note: the radiation (far) field at 10 meters is:

$$E_\phi = \frac{.043 \times 120\pi^2}{(660)^2 \times 10} = 1.16 \times 10^{-5} \text{ V/M}, \quad H_\theta = \frac{.043 \times \pi}{(660)^2 \times 10} = 3.1 \times 10^{-8} \text{ AT/M}$$

Telephonics

A DIVISION OF INSTRUMENT SYSTEMS CORPORATION

(4)

The radiated power density at 10 meters from the antenna would be $E_\phi \times H_\theta$

$$E_\phi \times H_\theta = 1.16 \times 10^{-5}\ V/M \times 3.1 \times 10^{-8}\ AT/M$$

$$= 3.6 \times 10^{-13}\ \text{watts/square meter}$$

If this were an isotropic radiator, the total radiated power would be:

$$\underbrace{4\pi \times 10^2}_{\text{area of sphere, 10 meter radius}} \times 3.6 \times 10^{-13}\ \text{watts/meter}^2 = 4.5 \times 10^{-10}\ \text{watts}$$

$$= 450\ \text{micro micro watts}$$

(5)

Lab measurement of antenna field strength.

Using a 10 turn coil, diameter = 3 inches,

measured 35 mv @ 1 foot, 1.1 mv at 3 ft

Induced Voltage: $e_{\text{induced (volts)}} = N \frac{d\phi}{dt} \times 10^{-8}$ (ϕ in maxwells)

but $\frac{d\phi}{dt} = \omega \Phi_{max} = 2\pi \times 4.55 \times 10^{5}\ \phi_{max}$

$\therefore$ at 1 foot, $e = .035 = N\omega\phi_{max} \times 10^{-8}$

$.035 = 10 \times 2\pi \times 4.55 \times 10^{5} \times 10^{-8}$

Solving for ϕ_{max}, $\Phi_{max} = \frac{.035}{10 \times 2\pi \times 4.55 \times 10^{5} \times 10^{-8}} = 0.123$ maxwells

Loop area $= \pi \times (1.5'' \times 2.54)^2 = 45.6\ cm^2$

then flux density in loop $= \frac{0.123 \text{ maxwells}}{45.6\ cm^2} = 0.0027$ gauss

$B = 2.7 \times 10^{-7} \frac{weber}{meter^2}$

Using magnetic dipole equations, H_r at 1 foot $= .238 \frac{amp turns}{meter}$

Using $B = \mu_0 H$, where $\mu_0 = 4\pi \times 10^{-7}$,

$B = 4\pi \times 10^{-7} \times .238 = 2.87\ 10^{-7} \frac{weber}{meter^2}$

which checks within 5%

Calculation of Antenna Coil Current (6)

Measured voltage across transmitter tank circuit

= 270 volts peak to peak

= 96 volts rms, approximately.

Tank capacitor is 330 pf, approximately.

$$i = \frac{e}{-j\,1/\omega C} = j\,\omega C e$$

$$i = 4.55 \times 10^5 \times 2\pi \times 330 \times 10^{-12} \times 96$$

$$i = 4.55 \times 6.28 \times 3.3 \times 9.6 \times 10^5 \times 10^{-10} \times 10$$

$$i = 910 \times 10^{-4} = .091 \text{ amp} = 91 \text{ ma}$$

APPENDIX IV

BATTERY DOCUMENTS

REPORTS CONTROL SYMBOL
OSD-1366

Research and Development Technical Report

Report ECOM-

NON-HAZARDOUS PRIMARY LITHIUM-ORGANIC ELECTROLYTE BATTERY BA-5598( )/U

Thomas Watson
P. R. Mallory & Co. Inc.
South Broadway
Tarrytown, NY 10591

October 1974

Final Report for Period July 1973 – September 1974

DISTRIBUTION STATEMENT

Approved for public release;
distribution unlimited.

Prepared for
P. M. REMBASS
Fort Monmouth, NJ 07703

ECOM

US ARMY ELECTRONICS COMMAND FORT MONMOUTH, NEW JERSEY 07703

NOTICES

Disclaimers

The findings in this report are not to be construed as an official Department of the Army position, unless so designated by other authorized documents.

The citation of trade names and names of manufacturers in this report is not to be construed as official Government indorsement or approval of commercial products or services referenced herein.

Disposition

Destroy this report when it is no longer needed. Do not return it to the originator.

ECOM-73-0282-F
OCTOBER 1974

REPORTS CONTROL SYMBOL
OSD-1366

NON-HAZARDOUS

PRIMARY LITHIUM ORGANIC ELECTROLYTE BATTERY

BA-5590 ( )/U

FINAL REPORT

JULY 1973 to SEPTEMBER 1974

CONTRACT NO. DAAB07-73-C-0282

DISTRIBUTION STATEMENT

Approved for Public Release; distribution unlimited.

Prepared by

Mr. Thomas Watson

MALLORY BATTERY COMPANY
DIVISION OF P. R. MALLORY & CO. INC.
60 ELM STREET
NORTH TARRYTOWN, NEW YORK 10591

FOR

U. S. ARMY ELECTRONICS COMMAND, FORT MONMOUTH, N. J,

TABLE OF CONTENTS

Page

PROGRAM SUMMARY

TECHNICAL GUIDELINES (OMITTED) *

TEST REPORT NO. 1 (OMITTED) **

* Section II has been omitted since it contains the test conditions (for the cell and battery) which have already been detailed in Section I.

** Section III has been omitted since it contains battery fabrication and discharge test requirements for only the particular battery - BA5590( )/U.

ORIGINAL PAGE IS
OF POOR QUALITY

I. PROGRAM SUMMARY

1. OBJECTIVE

The subject Final Technical Report concerns the development and fabrication of Battery No. BA-5590 ( )/U in accordance with the performance/safety requirements as defined in the Technical Guidelines for Non-Hazardous Primary Lithium-Organic Electrolyte Batteries dated 29 March 1973. Our primary concern has been the fabrication of the subject batteries in conformance with these guidelines and most important, the development of effective safety mechanisms to insure non-hazardous operation under all conditions of storage, use and operation. Basic considerations for such safety mechanisms were system reliability, effectiveness, economics and adaptability to eventual automated production.

2. REFERENCE DOCUMENTS

2.1 Contract No. DAAB07-73-C-0282, BA-5590 ( )/U dated 2 July 1973.

2.2 Technical Guidelines for Non-Hazardous Primary Lithium-Organic Electrolyte Batteries dated 29 March 1973.

2.3 Technical Report, DD Form 1423 Exhibit B, Battery BA-5590 ( )/U, Fabrication Test Phase dated 25 June 1974.

3. CELL CONFIGURATION

3.1 Cell Selection

The LO-26 "D" lithium cell was utilized to fabricate the required BA-5590 ( )/U battery.

3.2 Cell Construction

3.2.1 Cell Component Description

The anode consists of one continuous strip of lithium ribbon which serves as both the active electrode and current collector. Anode size as it interfaces with the cathode is nominally 20 x 1.75 inches yielding an active surface area of 35 square inches per cell.

The cathode consists of a carbonaceous mix deposited on a current collector of 5 A1 12-3/0 expanded aluminum grid. Cathode size is nominally 20 x 1.75 x .028 inches yielding an active surface area of 35 square inches per cell.

The separator is microporous polypropylene which is 48 inches long by 2 inches wide.

The electrolyte consists of 70% sulfur dioxide by weight. The remaining 30% contains lithium bromide and the organic solvents.

3.2.2 Cell Fabrication

The cell is constructed by winding rectangular strips of anode-separator-cathode-separator stacks of the aforementioned dimensions into a cylindrical roll which is then inserted in a nickel plated steel can as shown in Figure 1. This method of construction is employed to give the cell a high rate/low temperature capability by increasing the surface area of the electrodes The anode terminal is electrically connected to the steel can. The cathode terminal is electrically connected to the aluminum cover/vent assembly which is insulated by a glass filled polypropylene grommet. The cell is then hermetically sealed by mechanically crimping the cell can over the grommet. The cell is subsequently evacuated and filled by the introduction of electrolyte through the rubber septum. Epoxy is applied at the crimp interface to minimize low temperature electrolyte leakage. The vent disc fill port is then filled with solder to further minimize electrolyte leakage and permeation within the septum.

3.2.3 Cell Vent Mechanism

The cell employs a pressure sensitive venting mechanism which will safely deactivate a cell at an internal pressure of 350-450 psi (SO_2) which is equivalent to a temperature of 200-220°F. The vent design as shown in Figure 2 consists of an aluminum vent disc/copper ring tab which is ultrasonically ring welded to the cell top/septum assembly. Excessive internal pressure causes vertical displacement of the septum within the cell top. Cell venting is primarily accomplished by shearing of the vent disc by the septum. This results in complete venting of the pressurized electrolyte and cell deactivation.

3.3 Outline Dimensions

Cell Height: 2.345 inches maximum

Cell Diameter. 1.335 inches maximum

4. BATTERY CONFIGURATION

4.1 Packaging

Battery No. BA-5590 ( )/U consists of two identical 12 volt sections each containing five "D" lithium cells. The cells are packaged within a poly-laminated fiberboard case, painted lusterless olive drab per Federal Standard No. 595. Filler material is used as required to provide adequate structural strength to the battery and minimize internal movement. The battery utilizes a floating connector in accordance with requirements of the Technical Guidelines.

4.2 Electrical Protection

Each battery section is protected on its positive leg with a Littlefuse No. 313000 series fuse rated at 10 amps/32 volts. This fuse is of the "SLO-BLO" or time delay type designed to withstand momentary high current surges yet protect the battery against external short circuits. The electrical characteristics of this fuse are as follows:

FUSE RATING	RESPONSE TIME
110%	4 hours minimum
135%	1 hour minimum
200%	5-60 seconds

MALLORY BATTERY COMPANY

a division of P. R. MALLORY & CO. INC.

Broadway, Tarrytown, New York, 10591; Telephone: 914 591 7000

"D" CELL CROSS SECTION

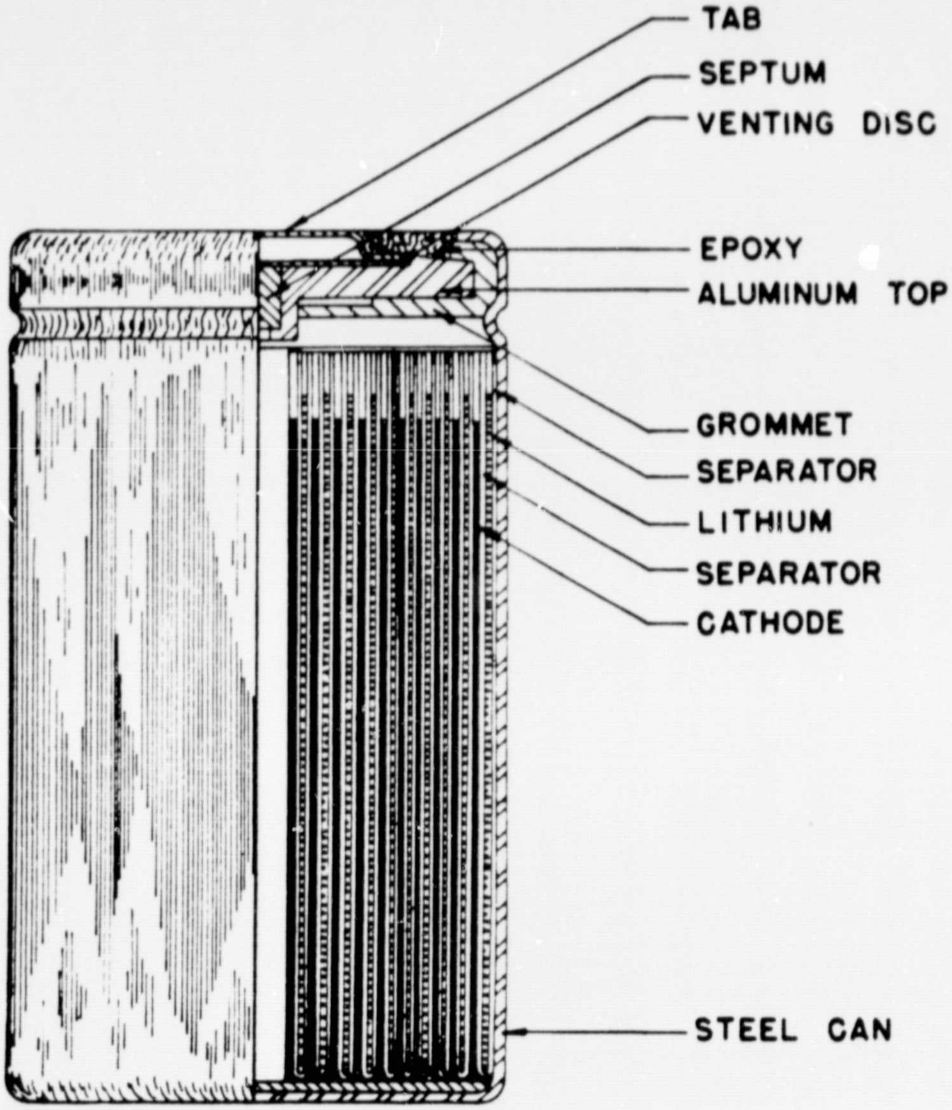

FIGURE 1

SCALE

MALLORY BATTERY COMPANY
a division of P R MALLORY & CO INC
[illegible] Broadway, Tarrytown, New York, [illegible] Telephone [illegible]

CELL VENT MECHANISM

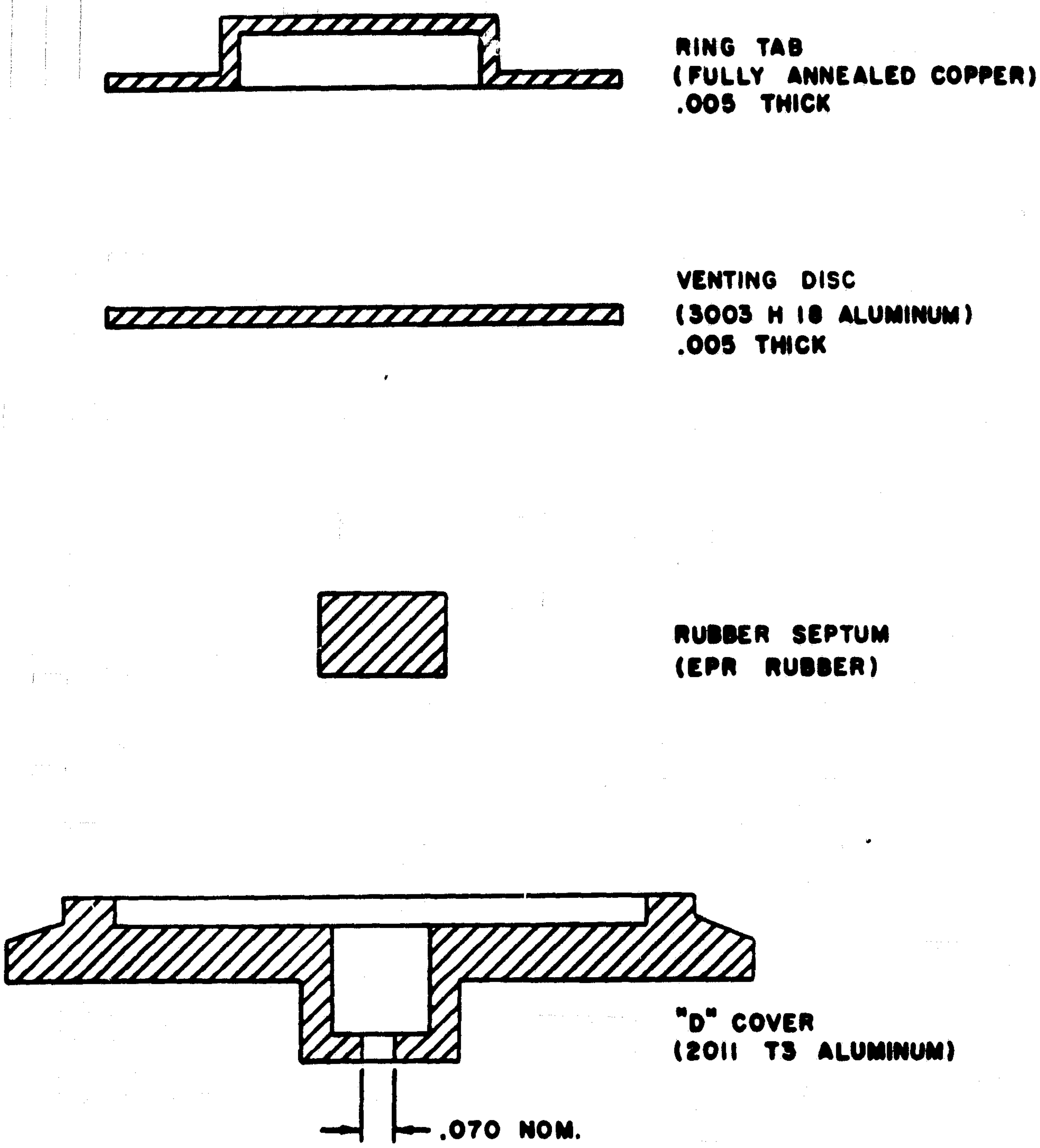

FIGURE 2

SCALE

5. ELECTRICAL REQUIREMENTS

5.1 Load Voltage

Voltage: 24.0 volts nominal

32.0 volts maximum

20.0 volts minimum

5.2 Discharge Characteristics

The battery was continuously discharged through load No. 1 resistance for 10 ms., then through load No. 2 resistance for one minute and finally through load No. 3 resistance for nine minutes.

LOAD No. 1 (ohms)	LOAD No. 2 (ohms)	LOAD No. 3 (ohms)
8 ± 1%	39 ± 1%	560 ± 1%

5.3 Service Requirements, End Voltage 20.0 Volts

a. 48 hours under immediate discharge at 75 ± 7°F.

b. 42 hours under immediate discharge at 125 ± 3°F following stabilization for a minimum of 8 hours at 125 ± 3°F.

c. 24 hours under immediate discharge at -20 ± 3°F following stabilization for a minimum of 8 hours at -20 ± 3°F.

5.4 Storage Requirements

The battery must deliver 90% of the above service requirements after 30 days storage at 160 ± 3°F.

6. SAFETY DESIGN INVESTIGATION

6.1 Temperature/Current Limiting Fuse

A fuse sensitive to both temperature and current was designed and fabricated in an effort to evaluate its merit as a safety mechanism. The basic design of the fuse is shown in Figure 3. This configuration permits insertion within the central winding cavity of each cell and connection in series with the anode tab. This tab was selected due to its metallurgical compatability with the fuse terminals thus minimizing electrochemical corrosion effects.

The fuse essentially consists of a non-resetable thermal cutoff in conjunction with an externally wound heater element. Incorporated in the design is a non-conductive solid pellet which maintains a spring loaded electrical contact under normal operating temperatures. When the predetermined rated temperature (185 ± 3°F) is exceeded in the cell the pellet will melt, allowing the electrical contact to open and break the circuit. The entire assembly, including the pellet and other components, is encased and epoxy sealed. The fuse assembly was encapsulated in Dow Corning QR-4-3110 silicone elastoplastic to minimize permeation of the electrolyte. The thermal/current fuse was found to electrically deactivate a cell under the following conditions:

FIGURE 3

NOTES:

1— ENCAPSULATE ASS'Y IN DOW CORNING QR-4-3110 SILICONE ELASTO-PLASTIC TO A MINIMUM THICKNESS OF .005 INCH

2— FUSE PARAMETERS
- FUSING CURRENT — 15 AMPS.
- FUSING TEMPERATURE — 185° F. ± 3° F.
- FUSE IMPEDANCE — 25 MILLIOHMS ± 10%
- RESPONSE TIME — 6—8 SECONDS (SO_2)

INTERNAL MULTIPROTECTOR

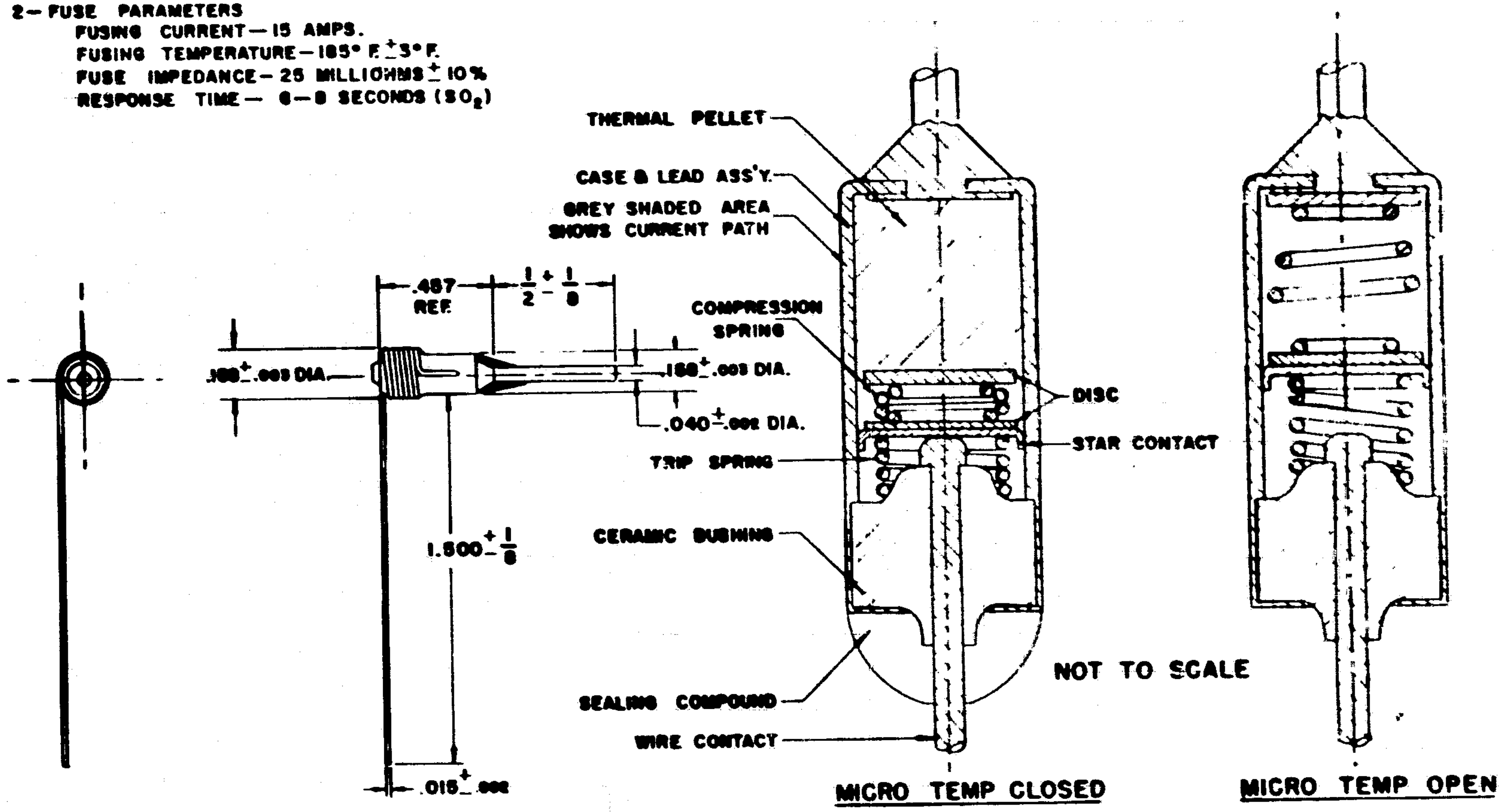

- External short circuit and/or high current discharge above the rated fusing current.

- High temperature/current discharge above the rated fusing temperature.

However, the thermal/current fuse will not protect against most internal winding shorts nor against severe high temperature storage environments. In addition, electrolyte permeation through the potted encapsulant resulted in corrosion of the internal fuse components. This corrosion was sufficient to form a variable resistive path which can cause cell self-discharge. In addition, there are several other disadvantages.

- The present thermal/current fuse represents a volume of approximately 0.98 cc. Use of this fuse will result in a corresponding reduction of electrolyte volume.

- Thermal/current fuse impedance will have an adverse effect on cell discharge performance and will degrade cell capacity during prolonged storage.

- Material and fabrication costs.

6.2 Current Limiting Fuse

An alternative internal fuse configuration for each cell was also evaluated in an effort to develop a more simplified and economical fusing mechanism. The fuse is shown in Figure 4a. It consists of a localized reduction in cross-sectional area of the anode tab material (nickel) which provides current limiting protection under most external short circuit conditions. Nickel was selected as the fuse material due to its compatability with the electrolyte and its overall metallurgical properties. In addition, a thermal shield (polyethylene) was installed around the fuse to minimize heat transfer to the electrolyte. This configuration permits insertion of the fuse along the external wall of the winding and connection in series with the anode tab as shown in Figure 4b. The current limiting fuse will electrically deactivate a cell only upon application of an external short circuit and/or high current discharge above the rated fusing current. The fuse will not protect against most internal winding shorts nor against severe high temperature storage environments. Again, some form of venting is required. In addition, there are several other disadvantages:

- The current limiting fuse is quite sensitive to low-level vibration and shock due to its small cross-sectional area.

- The fuses are quite difficult to fabricate and installation into the cell is quite operator sensitive. In addition, some form of thermal shielding may be required to obtain uniform fusing characteristics.

- Corrosion of the small cross-sectional area of the fuse during high temperature storage may alter the fuse parameters.

6.3 Recommendations

It is felt that the internal thermal/current fuse configuration is an unreliable safety mechanism due to electrolyte permeation within the fuse. The more economical current limiting fuse is not considered to be suitable due to its limited protection capabilities and its vulnerability to shock and vibration. A pressure sensitive vent mechanism is considered to be the most reliable, effective and economical means of cell deactivation.

6.4 Vapor Absorption

Cell venting of any nature results in the rapid emission of sulfur dioxide and electrolyte solvents within the battery. Should all ten cells vent under worst case conditions, internal battery case pressure can be as high as

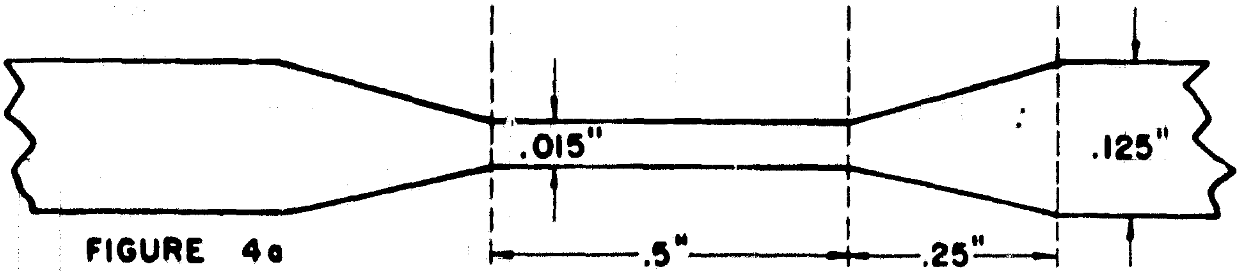

FIGURE 4a

DIMENSION OF THE INTERNAL FUSE

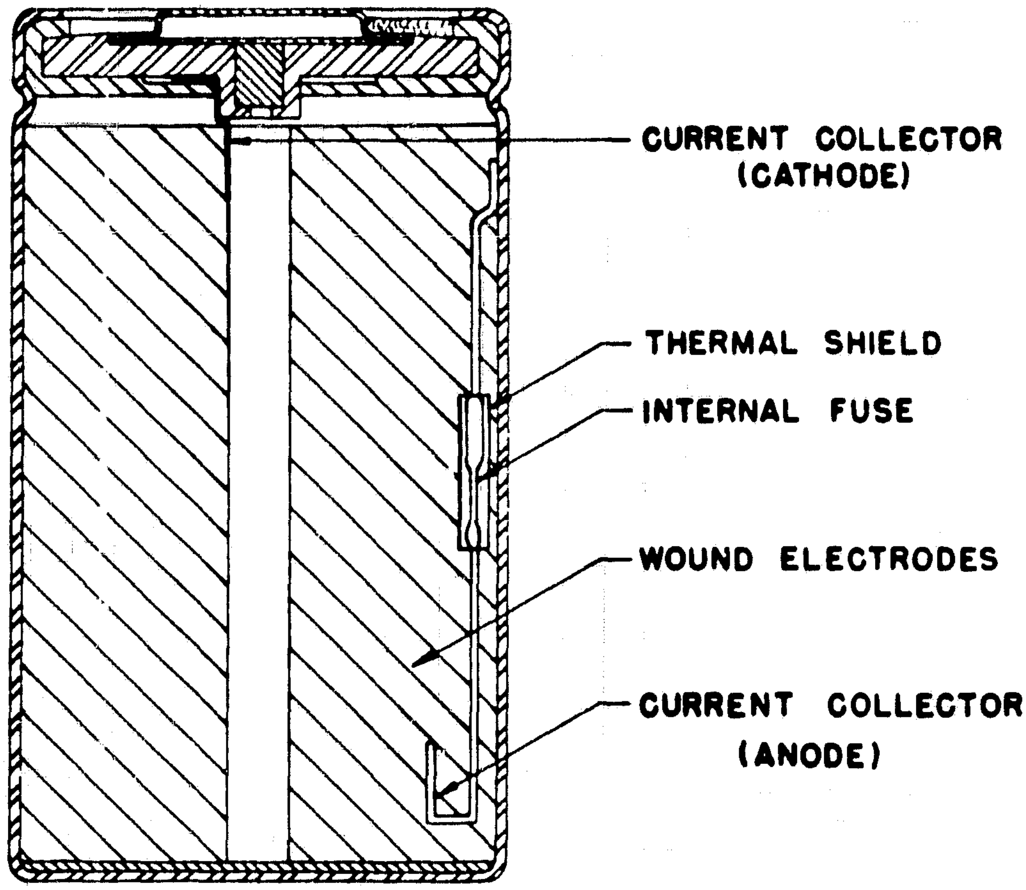

FIGURE 4b

THE CELL CONSTRUCTION OF THE FUSED CELLS

SCALE

210 psia. Control of such a condition may be accomplished in most applications by containment and subsequent absorption of the gaseous vapors. However, vapor containment requires hermetic sealing of the battery case and its connector assembly. Due to the materials and fabrication costs of such a battery package, it was recommended that vapor absorption not be utilized as a safety mechanism.

7. SAFETY EVALUATION

7.1 Cell Tests

Both fresh and partially discharged "D" cells were subjected to the following hazardous tests/environments in accordance with paragraph 3.2.1 of the Technical Guidelines:

a. Short Circuit Test

b. Increasing Load Test

c. Hot Plate Test

d. Cell Deformation Test

e. Dynamic Environmental Test

f. Case Rupture Test

g. Incineration Test

7.2 Battery Tests

BA-5590 (   )/U batteries were subjected to the following hazardous tests/environments in accordance with paragraph 3.2.2 of the Technical Guidelines:

a. Short Circuit Test

b. Increasing Load Test

c. Hot Plate Test

d. Immersion Test (Tap Water)

e. Immersion Test (Salt Water)

f. Reverse Discharge Test

7.3 Test Results – Cell Level

All tests were conducted within a fume hood under controlled environmental conditions.

7.3.1 Short Circuit Test

An external short circuit of less than 0.1 ohm was applied to the test cells until venting and/or stabilization occurred. All fresh cells were safely deactivated within 8 minutes when internal cell pressure was sufficient to activate the vent mechanism at approximately 370-470 psi. This is equivalent to an external temperature of 200-220°F. No explosive condition was observed during exposure of an open flame to fumes of the vented cells. Partially discharged cells were observed to thermally stabilize at a temperature below the venting level.

7.3.2 Increasing Load Test

Test cells were initially discharged at two amps (c/5) for one minute. The discharge rate was linearly increased at a rate of 1 amp/minute until venting and/or stabilization occurred. All fresh cells were safely deactivated when internal cell pressure was sufficient to activate the vent mechanism at a current level of 8-10 amps. External cell temperature was observed to be 200-230°F upon cell venting. Partially discharged cells were observed to thermally stabilize at a temperature below the venting level.

7.3.3 Hot Plate Test

Test cells were placed on a hot plate and heated at a rate of approximately 20°F per minute until venting occurred. Both fresh and partially discharged cells were safely deactivated within ten minutes when the internal pressure was sufficient to activate the vent mechanism at a cell temperature of 210-240°F. Maximum hot plate temperature was 350°F. However, this is not indicative of cell temperature due to substantial heat losses.

7.3.4 Cell Deformation Test

Test cells were placed between the insulated jaws of a vise in such a manner as to deform the lower half of the cell leaving the crimped seal section essentially intact. Pressure was slowly applied until a voltage drop indicated the presence of an internal short and/or until cell venting. All fresh cells safely vented due to condensation of sulfur dioxide gas into the liquid state and resulting hydraulic pressurization of the liquid. Internal winding short circuits were insufficient to substantially increase cell temperature and were not the cause of cell venting. The test was repeated on cells previously discharged to 50% of their nominal capacity with similar results.

7.3.5 Dynamic Environment Test

High "g" level sinusoidal vibration was applied along each axis of the test cells. Cell temperature and output voltage were continuously monitored to detect the presence of an internal short. The vibration profile was as follows:

50 g, 5-2000 cps for 15 minutes minimum along cell horizontal and vertical axes.

75 g, 100-2000 cps for 15 minutes minimum along cell horizontal and vertical axes.

No evidence of internal cell shorting was observed during the vibration test. Immediately following exposure to the above vibration levels, each cell was discharged under a 7 ohm load at room temperature. The results show an average cell capacity of 9 ampere hours.

7.3.6 Case Rupture Test

A 0.250 inch diameter hole was drilled completely through each rigidly mounted test cell along its horizontal axis using a high speed drill bit. Rapid escape of electrolyte through the drilled hole and a subsequent loss of OCV was observed. Some sparking was also observed during the drilling operation. Cell temperature in all cases decreased several degrees below room temperature due to the rapid loss of electrolyte pressure. No explosive conditions were observed during exposure of an open flame adjacent to the drilled hole. The test was repeated on partially discharged cells with similar results.

7.3.7 Incineration Test

The test cells were rigidly mounted in such a manner as to permit exposure of the cell base to the flame of a propane torch. An explosive condition was observed on two cells during exposure to the flame. It is our opinion that this explosive condition was due to combustion of organic solvents in the presence of lithium within the sealed cell. Venting of these cells did not prevent a simultaneous or subsequent explosion. Three additional test cells were observed to have safely vented upon exposure to the flame. Uniform heating of the cell was more likely to cause safe venting of the cell. Prolonged exposure of the cell to the flame after venting resulted in a lithium fire.

The design change was made to increase the fill port diameter from .070 to .125 inch. This will increase the initial force on the septum by a factor of 2.2 without altering the pre-established vent characteristics. In addition, it permits a more rapid venting of pressurized electrolyte thus minimizing the risk of a subsequent explosion.

7.4 Test Results – Battery Level

7.4.1 Short Circuit Test

An external short circuit of less than 0.1 ohm was applied to BA-5590 ( )/U batteries until fusing and/or venting occurred. Each battery section was electrically protected with a Littlefuse No. 313000 series "SLO-BLO" fuse rated at 10 amp/32 volts. All test batteries were safely deactivated by the electrical fuse and/or cell venting. The electrical fuse was not found to be adequate to deactivate some test batteries because it required a 200% current rating (20 amps) to affect electrical deactivation within 60 seconds. Test batteries did not always deliver this current level for the required time and, consequently the vent mechanism was activated. Battery deactivation was achieved by the venting of 1-2 cells.

7.4.2 Increasing Load Test

Test batteries were initially discharged at two amps (c/5) for one minute. The discharge rate was linearly increased at a rate of one amp/minute until venting and/or stabilization occurred. All batteries were safely deactivated when internal cell pressure was sufficient to activate the vent mechanism at a current level of 8-10 amps. Venting of one cell was sufficient to deactivate the entire battery. Battery fuses were rated at 10 amps/32 volts and were not activated.

7.4.3 Hot Plate Test

Test batteries were placed on a hot plate and heated at a rate of approximately 20°F per minute until venting occurred. All cells were observed to have safely vented when the internal pressure was sufficient to activate the vent mechanism at a maximum case temperature of 260°F. Maximum hot plate temperature was observed to be 420°F.

7.4.4 Immersion Test (Tap Water)

The test battery connectors were covered with waterproof tape. Each battery was fully immersed in tap water and subsequently discharged at the two amp rate to zero volts. All test batteries were safely discharged to zero volts within an average time of 12.5 hours. No significant voltage drop was observed during the tap water immersion.

7.4.5 Immersion Test (Salt Water)

The above test was repeated using water with a 3.5 ± 0.1% concentration of sodium chloride. A voltage drop of 0.3 volts was observed during the salt water immersion due to cell self-discharge. All test batteries were safely discharged to zero volts within an average time of 8.1 hours. This loss of capacity was attributed to partial cell self-discharge.

7.4.6 Reverse Discharge Test

Each test battery was discharged in series with an external power source at the two amp rate for a period of 15 hours. Two batteries were safely deactivated by the venting of 3-4 cells within each battery. One cell within the third battery exploded approximately 45 seconds after start of the reverse discharge. This cell was located adjacent to the battery connector. It is not known why this explosion occurred within such a short period of time. However, it is felt that localized combustion of the organic solvent in the presence of lithium may have initiated the explosion. Further combustion was most likely extinguished by the presence of sulfur dioxide within the cell. This condition was not observed on any other test samples, which safely vented during reverse discharge.

7.5 Conclusions

The cell vent mechanism and the battery fuse performed satisfactorily under most conditions of battery storage, use and operation. Vent activation occurred at a sufficiently high thermal level so as not to restrict high temperature cell/battery discharge performance. The ineffectiveness of the vent mechanism to preclude an explosive condition during the environments of the Incineration Test and Reverse Discharge Test was most likely due to the following:

a. Low internal pressure gradient due to the poor thermal conductivity of SO_2 (0.005 Btu/hr. ft. $^{\circ}F$).

b. Slow release of pressurized electrolyte through the vent due to the cell top configuration and/or blockage of the fill port with separator material.

7.6 Design Changes

7.6.1 Cell Vent Mechanism

A design change was made to increase the fill port diameter from .070 to .125 inch. This will increase the initial force on the septum by a factor of 2.2 without altering the pre-established vent characteristics. In addition, it permits a more rapid venting of pressurized electrolyte thus minimizing the risk of a subsequent explosion. The Incineration Test and the Reverse Discharge Test were subsequently repeated at Mallory Battery Company using cells with this design change. All cells and batteries were safely deactivated and no explosive conditions were observed. It was not felt necessary to conduct the other tests with this design modification.

7.6.2 Electrical Fuse

A design change was also made to decrease the battery fuse rating to 5 amps/125 volts to assure electrical deactivation under all external short circuit conditions yet permit proper battery operation under the required discharge profiles. The electrical characteristics of this fuse are as follows:

FUSE RATING	RESPONSE TIME
110%	4 hours minimum
135%	1 hour minimum
200%	5-60 seconds

The Battery Short Circuit Test was repeated on batteries with this design change. All test batteries were electrically deactivated and no cell venting was observed.

8. FABRICATION TEST PHASE

8.1 Test Requirements

Three (3) BA-5590 ( )/U batteries were fabricated and stored for 30 days at 160°F. They were subsequently discharged in accordance with paragraph 5.2 at -20°F, 75°F, and 125°F.

8.2 Test Results

The test results showed that the test batteries substantially exceeded all minimum electrical service requirements (See attached Test Report No. 1). A summary of this data is shown below:

SERIAL NO.	TEST TEMP.	HOURS REQUIRED TO 20.0 V	ACTUAL HOURS TO 20.0 V	START UP CYCLES TO REACH 20.0 V.
0136	+ 75°F	43.2	82.0	1
0149	+125°F	37.8	78.4	1
0129	-20°F	21.6	36.4	3

9. CONCLUSIONS/RECOMMENDATIONS

9.1 Electrical Performance

The electrical discharge capacity of battery BA-5590 ( )/U substantially exceeded the minimum specifications as required in the Technical Guidelines. In addition, the battery conformed to all dimensional and weight specifications. Therefore, the Mallory LO-26 "D" lithium cell is recommended as the cell component for the subject battery.

9.2 Safety Performance

The cell vent mechanism and electrical fuse performed satisfactorily under the prescribed conditions of battery use, storage and operation. The battery is therefore considered safe for use under all electrical discharge requirements as specified in the Technical Guidelines.

However, there are some extreme environmental conditions such as incineration and reverse discharge where the vent mechanism may not always be sufficient to prevent an explosive condition. Therefore, caution should be exercised during exposure of the battery to such extreme conditions. General battery usage precautions would include

Do not discard fresh or discharged cells/batteries in a fire.

Avoid direct short circuit of cells/batteries.

Do not attempt to charge or reverse discharge batteries.

Do not puncture or mutilate cells or batteries.

UNCLASSIFIED

SECURITY CLASSIFICATION OF THIS PAGE (When Data Entered)

REPORT DOCUMENTATION PAGE		READ INSTRUCTIONS BEFORE COMPLETING FORM
1. REPORT NUMBER ECOM-73-0282-F	2. GOVT ACCESSION NO.	3. RECIPIENT'S CATALOG NUMBER
4. TITLE (and Subtitle) Final Report Non-Hazardous Primary Lithium Organic Electrolyte Battery BA-5590 ( )/U		5. TYPE OF REPORT & PERIOD COVERED Final July 1973 - Sept. 1974
		6. PERFORMING ORG. REPORT NUMBER ECOM-0282F
7. AUTHOR(s) Mr. Thomas Watson		8. CONTRACT OR GRANT NUMBER(s) DAAB07-73-C-0282
9. PERFORMING ORGANIZATION NAME AND ADDRESS P. R. Mallory & Co., Inc. South Broadway, Tarrytown, NY 10591		10. PROGRAM ELEMENT, PROJECT, TASK AREA & WORK UNIT NUMBERS 673719.12.K73.05.11. VRZZZ-4
11. CONTROLLING OFFICE NAME AND ADDRESS P. M. Rembass Ft. Monmouth, NJ		12. REPORT DATE October 1974
		13. NUMBER OF PAGES 38
14. MONITORING AGENCY NAME & ADDRESS (if different from Controlling Office) US Army Electronics Command AMSEL-TL-PD Fort Monmouth, NJ 07703		15. SECURITY CLASS. (of this report) Unclassified
		15a. DECLASSIFICATION/DOWNGRADING SCHEDULE NA

16. DISTRIBUTION STATEMENT (of this Report)

Approved for public release; distribution unlimited.

17. DISTRIBUTION STATEMENT (of the abstract entered in Block 20, if different from Report)

18. SUPPLEMENTARY NOTES

NA

19. KEY WORDS (Continue on reverse side if necessary and identify by block number)

Pressure, venting, fusing, temperature, sulfur dioxide
Safety Lithium, Organic Electrolyte

20. ABSTRACT (Continue on reverse side if necessary and identify by block number)

The purpose of this program is to design, test, and fabricate a high performance, low cost primary lithium organic electrolyte battery designed for safe operation under any conditions of storage, use and disposal.

In order to demonstrate compliance with these goals, Mallory constructed and tested cells and batteries which incorporate a

DD FORM 1 JAN 73 1473 EDITION OF 1 NOV 65 IS OBSOLETE

UNCLASSIFIED

SECURITY CLASSIFICATION OF THIS PAGE (When Data Entered) unique fail-safe design developed by Mallory for commercial applications. This design was found to operate reliably, rendering cells and batteries safe under all test conditions covered under Technical Guidelines for Non-Hazardous Primary Lithium Organic Electrolyte Batteries dated 29 March 1973.

ABUSE TESTING OF Li/SO_2 CELLS AND BATTERIES

by

Harry Taylor and Bruce McDonald

P. R. MALLORY & CO., INC.
Northwest Industrial Park
Burlington, MA 01803

and

MALLORY BATTERY CO.
South Broadway
Tarrytown, NY 10591

INTRODUCTION

The Li/SO_2 system is amongst the most advanced, commercially and technically, of the new lithium systems developed over the last decade. Its forte as a primary power system for applications involving, particularly, high power and low temperatures is unsurpassed. Recent publications [1,2] illustrate these capabilities. The system moreover has excellent shelf life, voltage regulation and provides superior energy density, all over wide temperature extremes. With the advent of field use of Li/SO_2 cells and batteries, combined with recent adverse experience with the $Li/SOCl_2$ system [3,4,5] in some applications increased attention has been focused on the safe use and disposal of all lithium systems. It is the purpose of the present paper is to extend the information already provided [2,6,7] on the Li/SO_2 system in particular, based on experimental data generated on single cells and batteries.

EXPERIMENTAL METHODS

The basic preparation of materials and the construction of cells have been described previously.[1,2] 10Ahr size cells and batteries assembled from these were employed as test vehicles. All were of hermetic construction and had welded enclosures with a glass to metal feed through. A pressure activated vent (450 ± 40 psia) of novel design and reproducible operation was incorporated in each cell can using standard high volume production tooling.

Internally, each cell was designed for high power applications and employed approximately 500 cm^2 of cathode area. The electrolyte likewise was optimized for high power applications.

Cell voltages and current were recorded via Gould Model 220 Brush recorders. Temperature was similarly recorded using a pre-calibrated thermocouple affixed mechanically to the outside of the cell case. All the discharges and charges were controlled with Hewlett-Packard power supplies operated as high output voltage constant current sources. Cell impedances were measured at 1 Khz with a Wheatstone bridge using a Tektronix Type 555 Dual Beam Oscilloscope. The data were reproducible within ± 0.1Ω.

The internal pressure of selected cells was measured by means of a fine tubular pressure transducer and its associated amplifier controls (Standard Controls, Inc.) with a normal output of 5V at 750 psi and a ± 3 psi quoted accuracy. The transducer was pre-packed with an electrolyte resistant silicone grease and calibrated in the laboratory against a sensitive Bourdon gauge before and after each experimental run. In operation it was connected to each cell via a stainless steel needle inserted through a rubber septum in the cell top. The septum was normally encased hermetically within the cell top. Insignificant corrosion of components was noted and no change in transducer sensitivity from the beginning to the end of each run.

Cell incinerations were performed at 540°C by direct insertion of the system into an explosion proof furnace for a 20 min. period. In separate experiments the effects of direct application of a flame to individual cells were also examined.

In many tests no circuit protection was in built, vis-a-vis slow blow fuzes and diodes, and the cells or batteries were deliberately thermally insulated using fiber-frax. Such experiments constitute a deliberate mis-use of the system and were performed to establish any extremes or limits for its safe operation.

Cells were tested either in the fresh state, in that they were exposed to ambient temperature storage only, or after elevated temperature storage for as long as 102 days at 87°C. Moreover, the behavior of non-discharged and previously discharged cells and batteries was also characterized. Such prior discharge was conducted over the temperature range - 40°C to + 52°C.

RESULTS AND DISCUSSION

As a prelude to the ensuing discussion on the hazardous testing conducted here on the Li/SO_2 system it is instructive to note that all of the conventional primary alkaline systems now commercially available would constitute a hazard under one or more of the conditions selected. Nevertheless using proper controls cum safety measures the acceptance of such systems is widespread! It is equally important to recognize and appreciate the fact that the term lithium battery in the present market already encompasses quite a wide range of systems [8], each comprising different chemical constituents and materials of construction and design criteria.

It is quite clear then that the safe or hazardous nature of a particular chemical system within the family of lithium batteries is not necessarily a reflection on the characteristics of that entire family!

Note finally that in the present work specific attempts were made to evaluate only the hermetically sealed, ventable Mallory Li/SO_2 system, which was tested to its extreme limits. Indeed many of the tests conducted were carried beyond the limits which could be encountered in practice (with no severe hazards ensuing). Possible safety control devices (fuzes, diodes) were deliberately not employed in many tests.

THE TESTS

a. Incineration

Incineration tests were conducted at 540°C and were designed to investigate any hazards which might result from inadvertent exposure of the Li/SO_2 system to excessive temperatures as, for example, in a fire. Of additional interest was the question of deliberate exposure to such temperatures as a means of cell disposal. Data were generated on single cells and 15V battery packages. Cells in either case were in the relatively fresh state or stored for 1 month at 72°C. The state of discharge of the system prior to incineration ranged from non-discharged to fully discharged. Prior discharging of cells was conducted over a range of temperatures from - 40°C to 52°C.

In every case incineration for 20 min. resulted in quiet venting. Hermetic terminals remained unscathed; cell separators were destroyed; and lithium was apparently alloyed with materials of construction of the cells. The time to onset of venting could not be noted in the testing environment but presumably occurred within the first minute of cell incineration (when the internal cell temperature would result in an SO_2 vapour pressure sufficient to activate the vent).

Incineration thus appears to offer a possible means of disposal for the Li/SO_2 system when used in conjunction with a means for removal of SO_2 and other vapours released during the incineration period. The latter aspects require further consideration before any specific recommendation can be given.

b. Short Circuit

To investigate the behavior of the system on short-circuit a 0.001Ω load was applied across the terminals of single cells. No fuze protection was employed and in many cases cells were deliberately thermally insulated.

Cells were shorted at either ambient temperature or after prior equilibration to 72°C. Once again the state of discharge of the system prior to shorting ranged from non-discharged to fully discharged. Prior discharging of cells was conducted as before over a range of temperatures from - 40°C to + 52°C.

Figure 1 shows typical current, internal pressure and wall temperature profiles on a fresh (45 days ambient storage) non-discharged cell which was thermally insulated and pre-equilibrated at 77°C. The peak current was 70 amps, stabilizing in the region of 55 amps. Quiet venting of the cell occurred after 20 sec. at an internal pressure of 440 psia. Then the internal pressure fell to atmospheric within 3 minutes. The cell wall temperature remained relatively unchanged peaking at 83°C shortly after venting. The cell voltage then was zero. A very similar pattern was observed for cells shorted at ambient temperature while thermally insulated. The time to venting was somewhat increased but occurred generally in $\leq$ 1 minute.

Extension of these data was conducted on cells stored for up to 1 year at ambient temperature or 3 months at 72°C. With increase in storage time and/or temperature lower initial current output was realized. The latter tended to increase with increased time of application of the short. Using as test vehicles, cells stored for 1 month at 72°C then discharged in the temperature range - 40°C to + 52°C several facts emerged on subsequent shorting at ambient temperature or 72°C.

1. No hazardous reactions of explosive violence occurred.
2. On ambient temperature shorting only those cells pre-discharged at - 40°C and - 30°C vented. The latter occurred within 8 minutes at a wall temperature of 110°C.
3. On shorting at 160°F those cells pre-discharged at - 40°C, - 30°C and 24°C all vented quietly within 5 minutes. The cells pre-discharged at 52°C did not vent exhibiting a maximum wall temperature of $<$ 82°C.

Figure 1

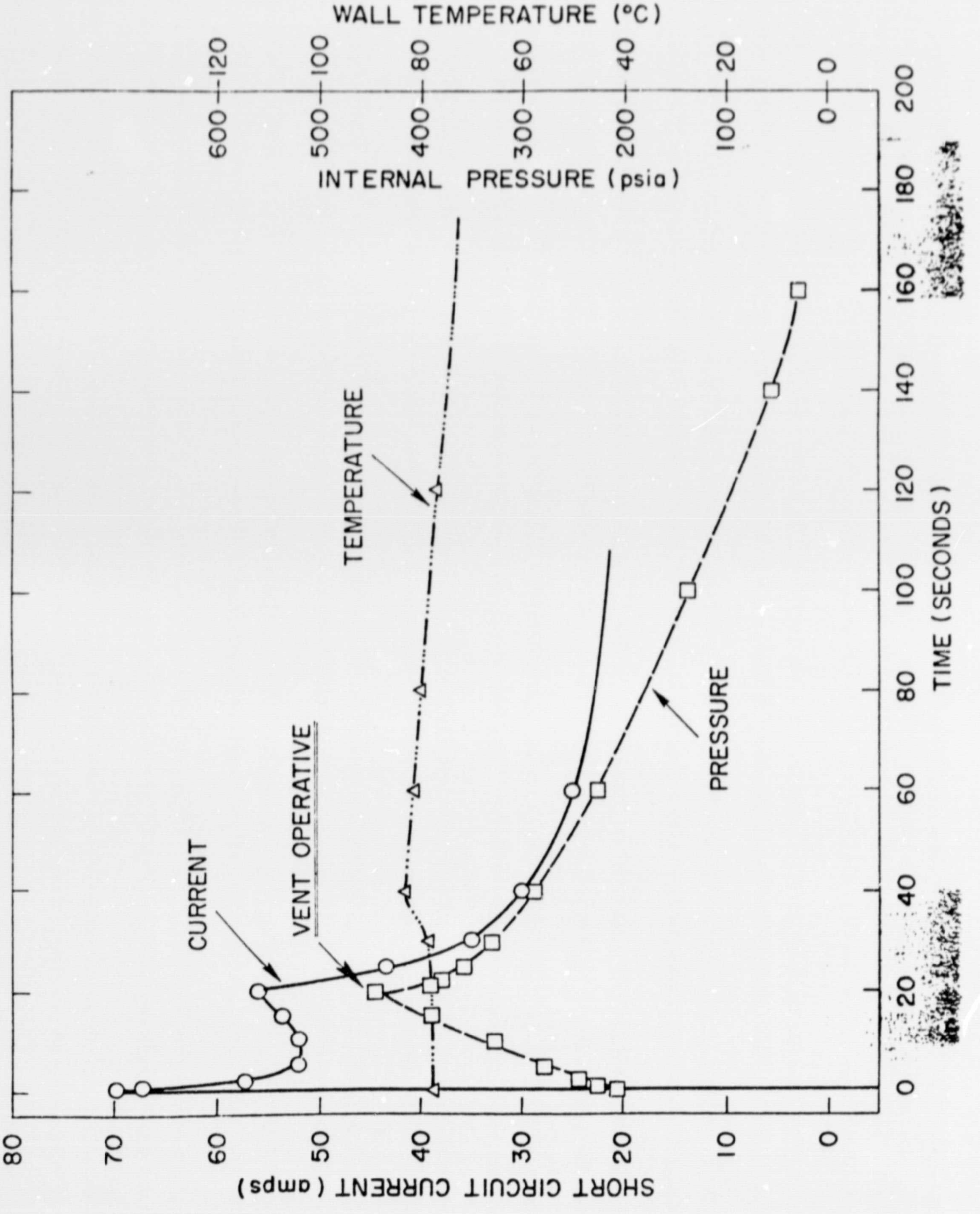

WALL TEMPERATURE (°C)
INTERNAL PRESSURE (psia)
TIME (SECONDS)
SHORT CIRCUIT CURRENT (amps)
TEMPERATURE
CURRENT
VENT OPERATIVE
PRESSURE

It is finally of interest to note that direct application of flame to vented cells using a bunsen burner did not cause any explosions. Relatively quiet burning of the lithium in the cells was noted here however.

It is concluded that the Li/SO_2 system will not explode or cause a fire when shorted externally or internally. Obviously it is recommended that both individual cells and batteries be fuzed to avoid SO_2 ejection from the cells. In production, exhaustive quality control procedures are rountinely applied to avoid internal shorts. Moreover, the stability of the system to adverse shock and vibration tests has been well documented.[7] Here again the ultimate safety device is a reproducible vent system combined with adequate SO_2 "getters". The former has already been developed at Mallory and the latter are presently under investigation.

c. Reverse Discharge

A condition may readily prevail in a series or series/parallel connected battery package with no diode protection wherein an inferior cell is driven by the series stack into voltage reversal. Tests to simulate this condition were conducted. Once again in selected tests, cells were thermally insulated to simulate operation in the middle of a battery package with inadequate cooling means. Cells (and battery packs) used as test vehicles had the same general background of storage, and state of discharge as those described in previous sections.

1. Non-discharged/Ambient Temperature Stored ($\leq$ 1 yr) Cells

Figure 2 shows typical results obtained on a 1 year old cell force discharged into voltage reversal at 1 amp. The power supply output voltage was in the range 15-20V. Voltage, internal pressure, wall temperature and cell impedance profiles are reported. The cell delivered 9.1 Ahr to 2V when rapid polarization was observed, which increased with continued application of the 1 amp constant current until the cell voltage had gone into reversal

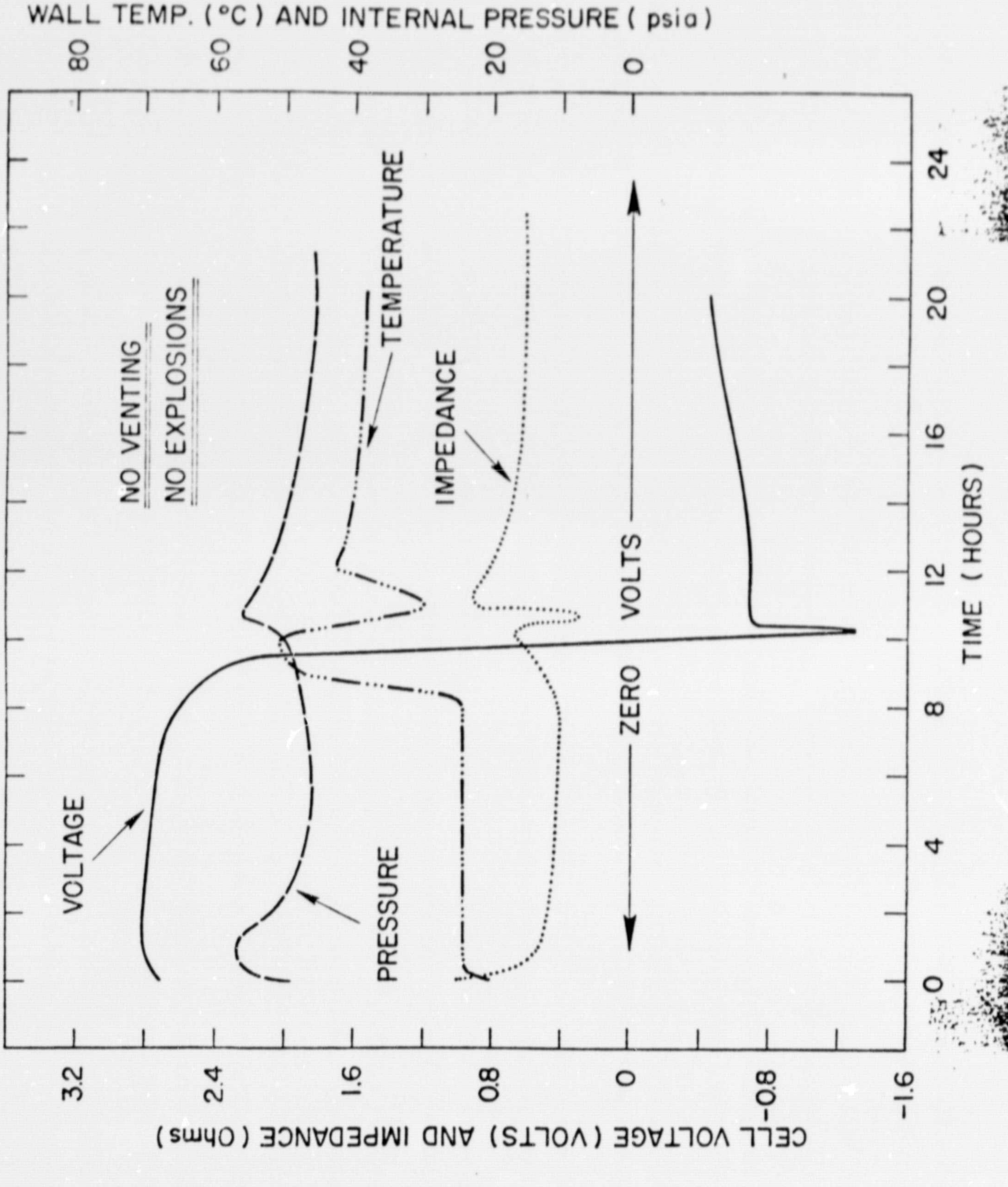
WALL TEMP. (°C) AND INTERNAL PRESSURE (psia)
80
60
40
20
0
NO VENTING
NO EXPLOSIONS
VOLTAGE
PRESSURE
TEMPERATURE
IMPEDANCE
ZERO
VOLTS
0
4
8
12
16
20
24
TIME (HOURS)
3.2
2.4
1.6
0.8
0
-0.8
-1.6
CELL VOLTAGE (VOLTS) AND IMPEDANCE (Ohms)

peaking at - 1.3V after 10.1 hr. At the start of discharge the cell wall temperature rose slightly to 24°C, this increase being reflected initially in a similar increase in internal pressure to 55 psia after 1 hr. The cell impedance concurrently fell from ∞ to 0.5 Ω over this time period. As the SO_2 was utilized in the course of discharge the pressure fell correspondingly while the temperature and impedance remained constant.

With the onset of rapid cell polarization the cell impedance increased, but by a factor of no more than 2. Likewise the wall temperature doubled and the cell pressure increased. None of these parameters however exhibited substantial excursion from the norm; all declined thereafter; and the cell did not even vent or change dimensionally. This latter condition prevailed even on application of the forced current for a total of 23 hr (or approximately 13 hr* after voltage reversal) when the cell voltage was - 0.4V.

The data in Figure 3 report the results of an exactly similar test, this time at 2 amps forced discharge on a cell which was 13 days old (room temperature). The cell delivered an excellent capacity of 9.1 Ahr to 2V before the onset of rapid polarization. An initial voltage reversal to - 0.32V at 5.05 hr was followed by a short pulse positive to 0.16V after 5.15 hr leading to a peaked reversal of -1.0V at 5.3 hr (the 2A current still being applied). Thereafter the voltage stabilized in the region of - 0.75V.

Whereas the cell pressure and wall temperature showed the trends reported in Figure 2 this time the excursions were severe enough to initiate cell venting after 5.15 hr at a wall temperature of 155°C and an internal pressure of 425 psia. Note that venting occurred quietly and that no fires

---

* Footnote: Note that this is a condition which could never be realized in practice since in a 10 Ahr series package a current of 1 amp could be forced through an initially dead cell for a maximum time of only 9.1 hr.

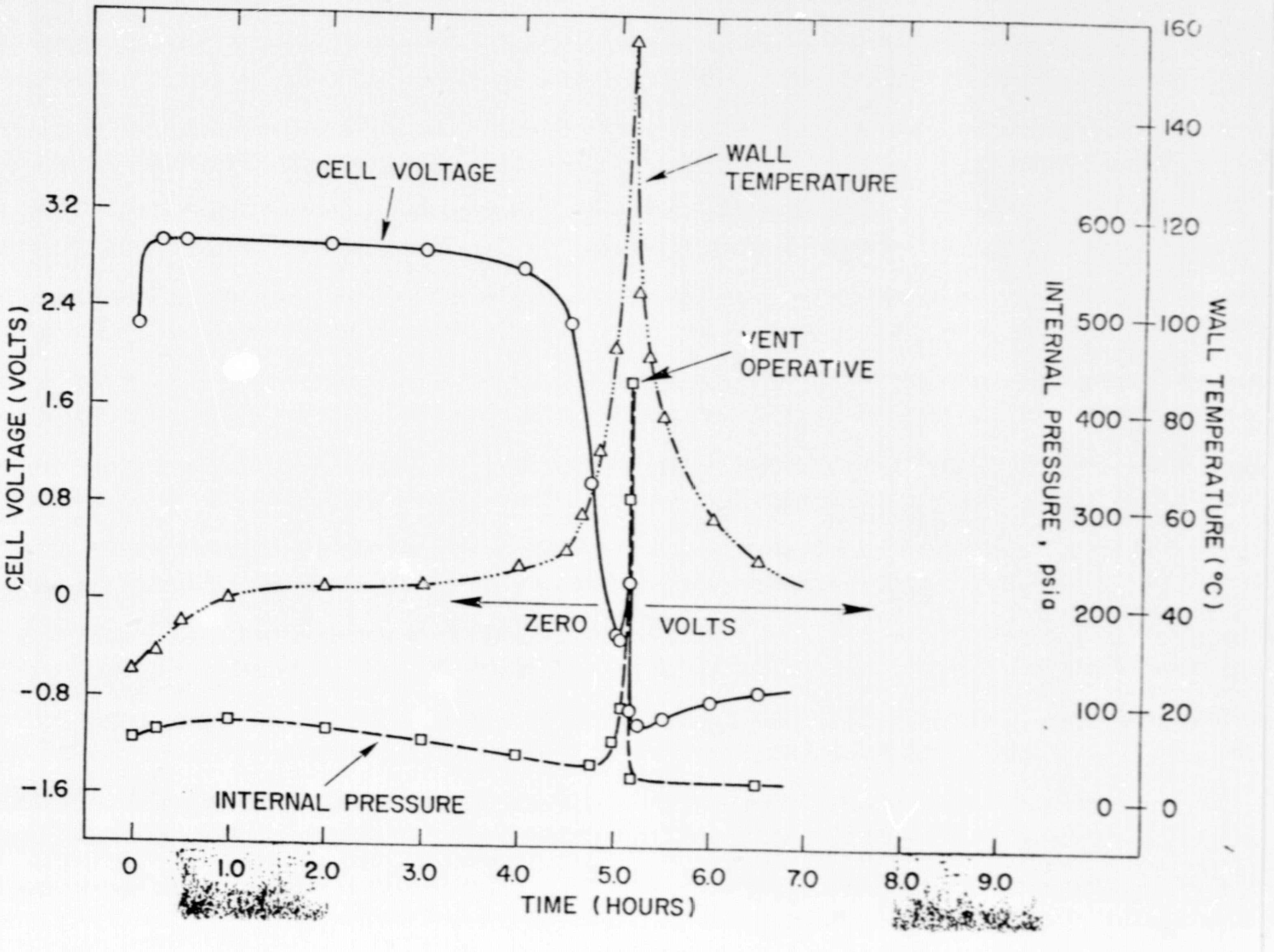
CELL VOLTAGE
WALL TEMPERATURE
VENT OPERATIVE
ZERO
VOLTS
INTERNAL PRESSURE
CELL VOLTAGE (VOLTS)
3.2
2.4
1.6
0.8
0
-0.8
-1.6
INTERNAL PRESSURE, psia
600
500
400
300
200
100
0
WALL TEMPERATURE (°C)
160
140
120
100
80
60
40
20
0
0
1.0
2.0
3.0
4.0
5.0
6.0
7.0
8.0
9.0
TIME (HOURS)

resulted. Moreover the vent was activated at the design limit and its operation has proven to be completely reliable throughout all our testing. Note further that the escape of SO_2 from a venting cell serves as a further safety device due to the cooling effect on the cell associated with such escape! Once again the driven discharge conducted for a total period of 6.75 hr did not result in any other hazardous effects.

It is interesting to note finally that even when forced discharged at 10 amps thermally insulated fresh cells delivered 4.5-5Ahrs before venting quietly at the point of precipitous voltage reversal. Subsequently the voltage stabilized at about - 1V (from a sharply peaked reversal of about - 6V). Again, no hazards were encountered over the course of a total discharge period of 68 min.

2. Non-discharged/High Temperature Stored Cells

Having demonstrated that the Li/SO_2 system was stable even when forced into voltage reversal for extended periods the question arose as to whether a similar stability would be encountered on cells stored beforehand at elevated temperatures. Figure 4 records typical data generated here on a cell stored at 87°C for 102 days and then discharged at ambient temperature and 1 amp into voltage reversal (while thermally insulating the cell).

The capacity output of 6.3 Ahr to 2V was excellent after such severe storage. Paralleling our ambient temperature data the cell did not even vent or change dimensionally notwithstanding the fact that the total discharge period was 42 hr (approximately 34 hr under a voltage reversal condition!)

We found again the same type (and indeed magnitude) of fluctuations in impedance and wall temperature encountered previously for the ambient temperature stored cells (cf Figure 2). These parameters both doubled on first polarization of the cell, the LATTER peaking at only 46°C. The internal pressure which first increased to 57 psia gradually fell during the course of discharge and remained relatively insensitive to changes in the impedance and wall temperature during initial cell polarization.

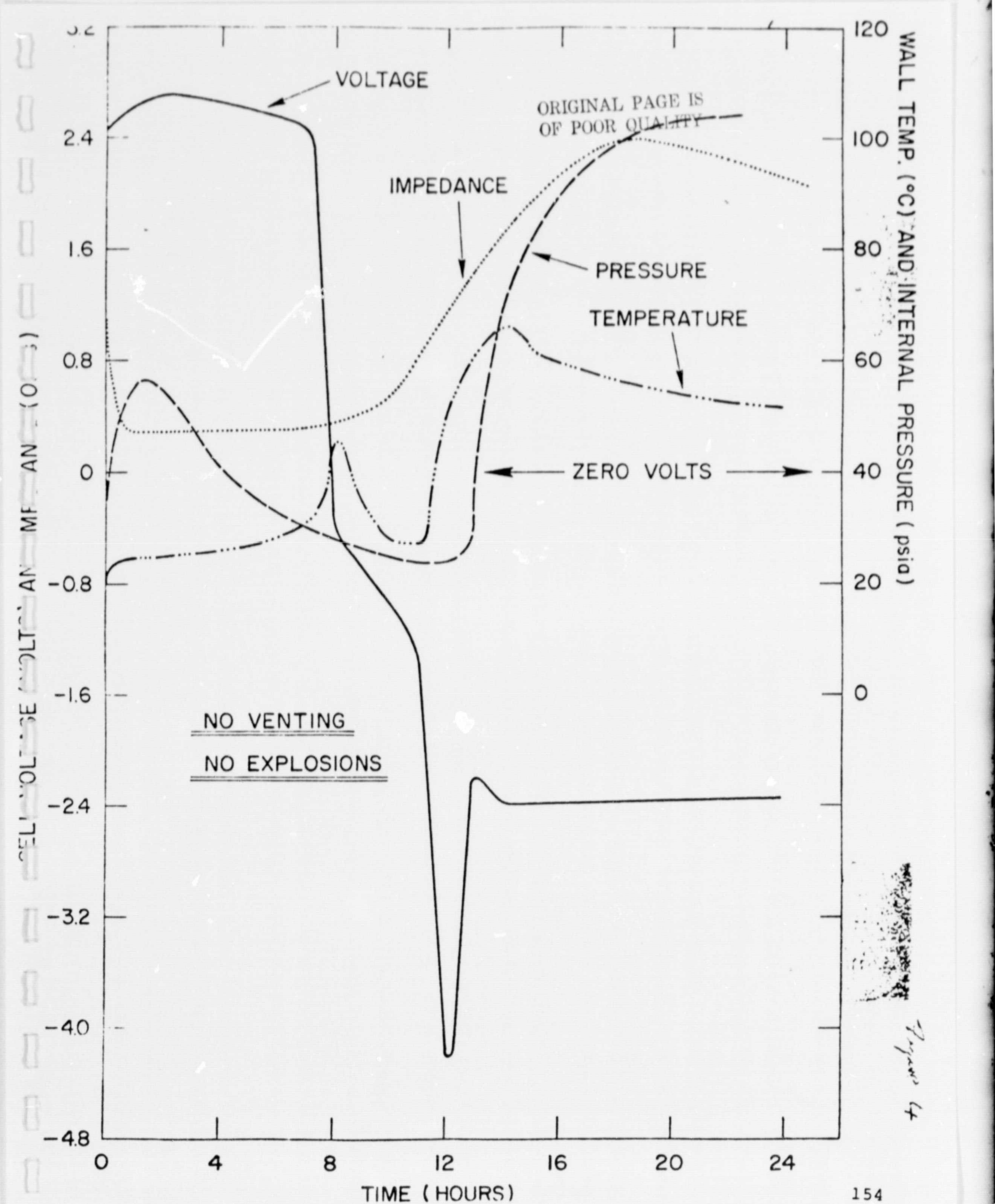

VOLTAGE
ORIGINAL PAGE IS OF POOR QUALITY
IMPEDANCE
PRESSURE
TEMPERATURE
ZERO VOLTS
NO VENTING
NO EXPLOSIONS
TIME (HOURS)
WALL TEMP. (°C) AND INTERNAL PRESSURE (psia)
2.4
1.6
0.8
0
-0.8
-1.6
-2.4
-3.2
-4.0
-4.8
120
100
80
60
40
20
0
4
8
12
16
20
24

In a manner typical of elevated temperature stored Li/SO_2 cells the rate of voltage decay after initial polarization now slowed down suggestive of residual capacity withdrawal at a lower voltage level than in fresh cells. This is reflected in the figure in a change of slope in the voltage time profile on voltage reversal of the cell after 7.4 hr. Only after 11 hr at 1 amp when the cell voltage was - 1.3V was much more rapid cell polarization again encountered this time peaking at - 4.2V. Within the period 7.4 hr to 11 hr the wall temperature declined to 28°C!

Substantial increases in internal pressure, wall temperature and impedance were now noted concurrent with the sharp peak reversal of the cell voltage. Moreover when the voltage shortly thereafter stabilized at - 2.4V a similar tendency towards stabilization of these three parameters was again encountered. It is interesting to note that the peak values in all these parameters occurred at a point in time equivalent approximately to 100% capacity utilization of originally added lithium and SO_2. It is emphasized that no venting occurred and no hazardous effects were noted at this or later stages of the voltage reversal of this or similarly tested cells.

The foregoing data indicated that any Mallory Li/SO_2 cells may be forced (by whatever means) into voltage reversal at $\lesssim$ 1 amp with impunity! In the range 1A to 2A (and of course above 2A) no fire or explosive hazards may be expected on voltage reversal but the cells will vent. In these, and indeed all applications diode protection is recommended and with such protection venting should not be encountered.

Our most recent data have confirmed these observations. For example, six Li/SO_2 cells which had previously been stored for 30 days at 72°C were connected in a series/parallel arrangement. The middle cell in one parallel leg (of 3 cells) had been previously discharged at 52°C. Under a forced discharge of 2 amps the latter cell vented as expected! Subsequently in an exactly similar experiment this time incorporating diodes in series with each string of 3, no venting of any cell was encountered.

d. Charging

Our experience with charging of Li/SO_2 cells has not been extensive and at the outset it is noted that we do not recommend such abuse of the system. It is therefore advisable to diode protect batteries or single cells against such an event. Moreover it is desirable that additional protection be built into each battery by judicious selection of terminal contacts. Setting aside these aspects the following has been our experience to date in this regard.

A non-discharged, ambient temperature stored cell was thermally insulated and charged for 10.5 hr at 0.5 amps. It was then discharged at the same current for 20 hr. The voltage reversed in the course of this discharge after 18.2 hr and was -1.6V at the 20 hr mark. No explosions or other hazardous reactions occurred as can be seen from Figure 5. There it is seen that during the charging period the cell voltage stabilized at 3.5V, presumably indicative of Br_2 evolution at the cathode viz

$$2\,Br^- \longrightarrow Br_2 + 2e$$

At the anode the corresponding reaction is

$$Li^+ + e \longrightarrow Li$$

It is further speculated that the released Br_2 which is soluble in the electrolyte[9] migrates to the Li anode with the resultant reaction

$$Br_2 + 2\,Li \longrightarrow 2\,Li\,Br$$

Our studies on the re-chargeability of Li anodes in SO_2 and other electrolytes indicate that re-plated Li loses a substantial portion of its electrochemical activity. Therefore a reduction in cell capacity (from 10 Ahr) would be expected as a result of the charging and this was indeed observed in the present experiment (7.6 Ahr output to 2V).

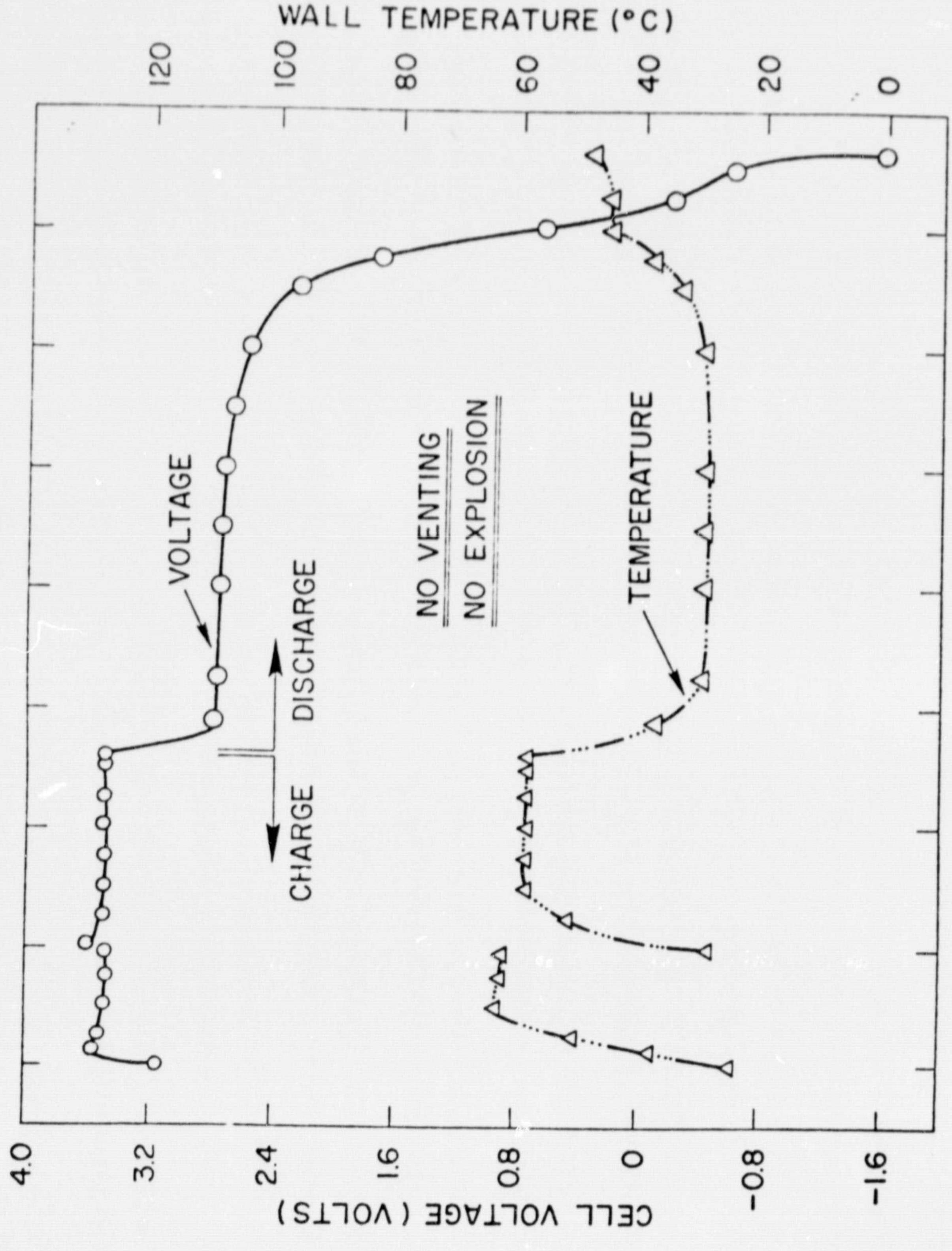
WALL TEMPERATURE (°C)
120
100
80
60
40
20
0
VOLTAGE
NO VENTING
NO EXPLOSION
TEMPERATURE
CHARGE
DISCHARGE
0
4
8
12
16
20
24
28
32
TIME (HOURS)
4.0
3.2
2.4
1.6
0.8
0
-0.8
-1.6
CELL VOLTAGE (VOLTS)

In a subsequent test a Li/SO_2 cell stored for 130 days at ambient temperature was thermally insulated and completely discharged (to - 0.8V) at 0.5A. The output was 9.1 Ahr to 2V. Cell internal pressure and wall temperature were recorded concurrently and trends observed are seen in Figure 6. The temperature was ostensibly constant at 27°C showing a slight peak to 37°C on sharp polarization of the cell. The pressure fell during discharge with a slight peak at 19 hr to 48 psia. The discharge was discontinued after 18.4 hr and charging at 0.5A commenced after 0.6 hr on open current stand. (19 hr from test initiation). The cell voltage rose sharply to 3.16V and climbed steadily over the next 20 hr to 3.4V. The internal pressure profile was a mirror image of that encountered during discharge illustrating the well known re-chargeable nature of the SO_2 cathode. The wall temperature also followed the profile noted during discharge. In the 21st hour of charging the cell voltage increased to 3.5 V and both internal pressure and wall temperature rose sharply after 21 hr. The cell vented with explosive violence at a wall temperature of $\gg$ 280°C.

The basic difference in these last two tests is that in the latter one a much greater quantity of (highly porous) freshly plated Li was generated on the anode. At the point of cell polarization to 3.5V it would not be surprising therefore to expect a violent exothermic reaction between Br_2 and this Li. In the absence of direct experimental evidence this is presumed to have caused the above explosion.

Somewhat surprisingly, in view of the above, two further tests involving charging at 0.5A of previously discharged cells resulted in no venting, no explosions or any other hazardous reactions. Both cells were stored before testing at 72°C for 30 days. One was discharged at - 40°C and the other at 24°C. Charging of the former was conducted for 20 hr (10 Ahr input) and for 32 hr (16 Ahr input) on the latter. A maximum wall temperature of 52°C was noted but no venting.

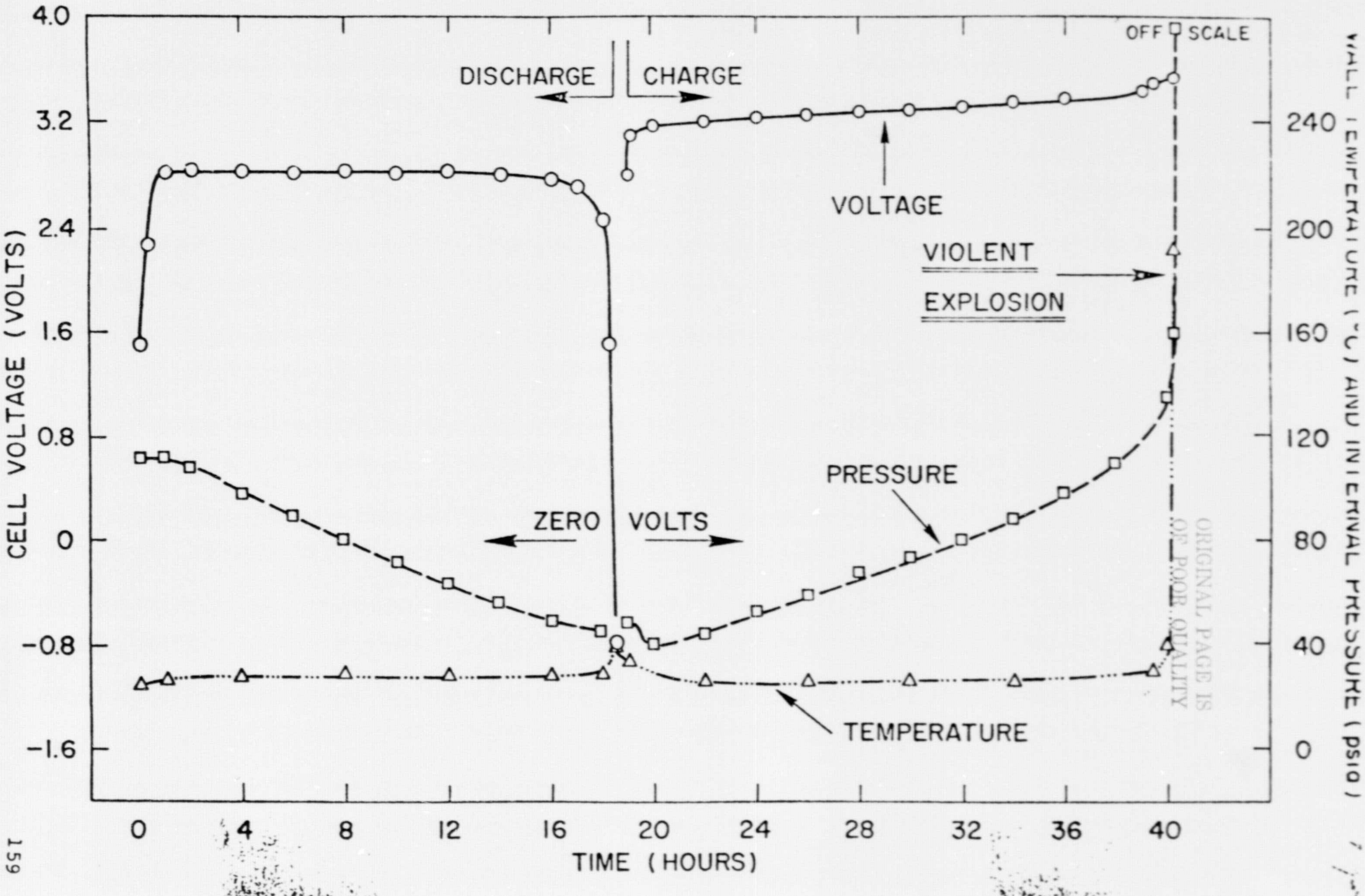
CELL VOLTAGE (VOLTS)
4.0
3.2
2.4
1.6
0.8
0
-0.8
-1.6
WALL TEMPERATURE (°C) AND INTERNAL PRESSURE (psia)
240
200
160
120
80
40
0
TIME (HOURS)
0
4
8
12
16
20
24
28
32
36
40
DISCHARGE
CHARGE
VOLTAGE
OFF SCALE
VIOLENT
EXPLOSION
PRESSURE
ZERO
VOLTS
TEMPERATURE
ORIGINAL PAGE IS OF POOR QUALITY

Setting aside the apparent dichotomy in these data it will immediately be appreciated that the circumstance wherein previously discharged cells are then charged would be most unlikely ever to occur in practice with a Li/SO_2 battery. Any improper connection of cells in a battery would result in charging of non-discharged cells and this is apparently not a hazard. Once again let us emphasize that in any event protection would be afforded by the diodes and terminal contact geometry built into the system.

CONCLUSIONS

Li/SO_2 cells and battery packages from the Mallory Co. were constructed from 10 Ahr units and comprised all hermetic seals (welds and glass/metal feed throughs) together with a reproducible vent mechanism. These units were subjected to a series of abuse tests many of which were conducted beyond the limits which would be encountered in field service. In most tests protective devices such as fuzes and diodes were deliberately omitted to further characterize any inherent hazards of the system. Data were generated on units stored at ambient temperature and elevated temperature for extended periods ($\geq$30 days at up to 87°C). The units ranged from fresh ones (non-discharged) to fully discharged ones. Prior discharges were conducted over the range of - 40°C to + 52°C. The system was shown to be safe (non-explosive) under all extremes of testing. A single exception to this was encountered on charging of an ambient temperature stored cell previously deep discharged. Such an event is not likely to occur in practice and can in any event readily be counteracted by diode and terminal contact protection. The following specific conclusions resulted from this work.

a. Incineration of the Li/SO_2 system at 540°C results in quiet venting and presumably quiet burning of any residual lithium. Direct application of flame to the system has the same effect.

b. Short circuit of the system through a 0.001 Ω load results in quiet venting which may be avoided by judicious fuzing.

c. The system, even when thermally insulated, may be driven into voltage reversal for extended periods with no explosion hazards resulting even at 10 amps/cell. Reversal at $\leq$ 1 amp forced current in a series stack is safe and results in no venting, dimensional changes or explosions. At 2 amps quiet venting may be expected shortly after voltage reversal but this may be circumvented by judicious diode protection.

ACKNOWLEDGEMENTS

The development by Dr. Wayne Lees of the reproducible vent mechanism used in the present system is gratefully acknowledged. The authors would also like to thank Dr. Per Bro for helpful discussions and Mr. Ed Curelop, Mr. Scott Simenas and Mr. David Joye for the generation of relevant experimental data.

REFERENCES

1. P. Bro, R. Holmes, N. Marincic and H. Taylor, in Power Sources 5, Ed. D. H. Collins, Oriel Press, Brighton, England, paper 45, (1974).

2. P. Bro, H. Y. Kang, C. Schlaikjer and H. Taylor, Tenth Intersociety Energy Conversion Engineering Conference, Newark, Delaware, p. 432 (1975).

3. J. F. McCartney, W. H. Shipman and C. R. Cundersen, "Development of Lithium Inorganic Electrolyte Batteries for Navy Applications", Fleet Engineering Department, NUC TN 1618, p. 48 (Oct., 1975).

4. A. N. Dey, "Sealed Primary Lithium Inorganic Electrolyte Cell", Research and Development Technical Reports, ECOM-74-0109-5 and 6, Mallory LPS, (August 1975 and November 1975).

5. N. Marincic and A, Lombardi, "Sealed Lithium Inorganic Battery", Research and Development Technical Report, ECOM-74-0108-6, GTE Laboratories, (December 1975).

6. H. F. Hunger and J. A. Christopulos, "Preliminary Safety Analysis of Lithium Batteries", Research and Development Technical Report, ECOM-4292, Electronics Technology and Devices Laboratory, (February, 1975).

7. E. S. Brooks, "Evaluation of Designs for Safe Operation of Lithium Batteries", 26th Power Sources Symposium, p. 42 (May 1974).

8. S. Gilman, "An Overview of the Primary Lithium Battery Program", 26th Power Sources Symposium, p. 28, (May 1974).

9. E. J. Woodhouse and J. H. Norris, Inorg. Chem. <u>10</u>, 614 (1971).

FIGURE CAPTIONS

Figure 1 Short circuit of a thermally insulated Li/SO_2 D-cell with vent through a 0.001 Ω load at 77°C.

Figure 2 Forced over-discharge at 1.0 amp of a thermally insulated Li/SO_2 D-cell with vent (1 year R.T. stored).

Figure 3 Forced over-discharge at 2.0 amps of a thermally insulated Li/SO_2 D-cell with vent (13 days R.T. stored).

Figure 4 Forced over-discharge at 1.0 amp of a thermally insulated Li/SO_2 D-cell with vent (102 days 87°C stored).

Figure 5 Charge-discharge cycle at 0.5 amp on a thermally insulated Li/SO_2 D-cell with vent (75 days R.T. stored).

Figure 6 Discharge-charge cycle at 0.5 amp on a thermally insulated Li/SO_2 D-cell with vent (130 days R.T. stored).

MALLORY BATTERY COMPANY
a division of P. R. MALLORY & CO. INC.
Broadway, Tarrytown, New York [illegible], Telephone [illegible]

LO-30

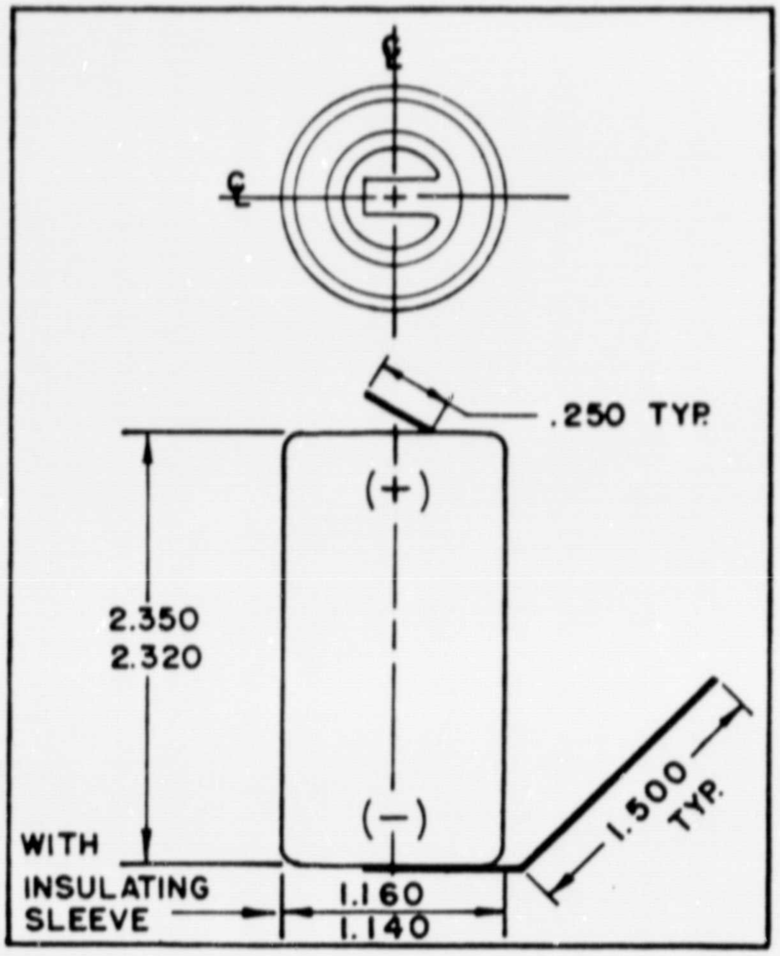

INCHES DEC.	M.M.
.250	6.35
1.140	28.96
1.160	29.46
1.500	38.10
2.320	58.93
2.350	59.69

SPECIFICATIONS

TYPE ______________ PRIMARY LITHIUM ORGANIC
NOMINAL VOLTAGE ______ 2.92 VOLTS ± .05
SERVICE CAPACITY (AT 70° F. TEMP. TO 2.0 VOLTS) 7.5 AMP. HRS.
(RATED CAPACITY AT 160 MILLIAMPERES
AVERAGE WEIGHT ______ 62 GMS. 2.19 OZ.
VOLUME ____________ 40 C.C. 2.44 CU. IN.

NOTE:

CELL SUPPLIED WITH INSULATING SLEEVE AND FLEXIBLE TAB TERMINALS AS SHOWN

SCALE: FULL

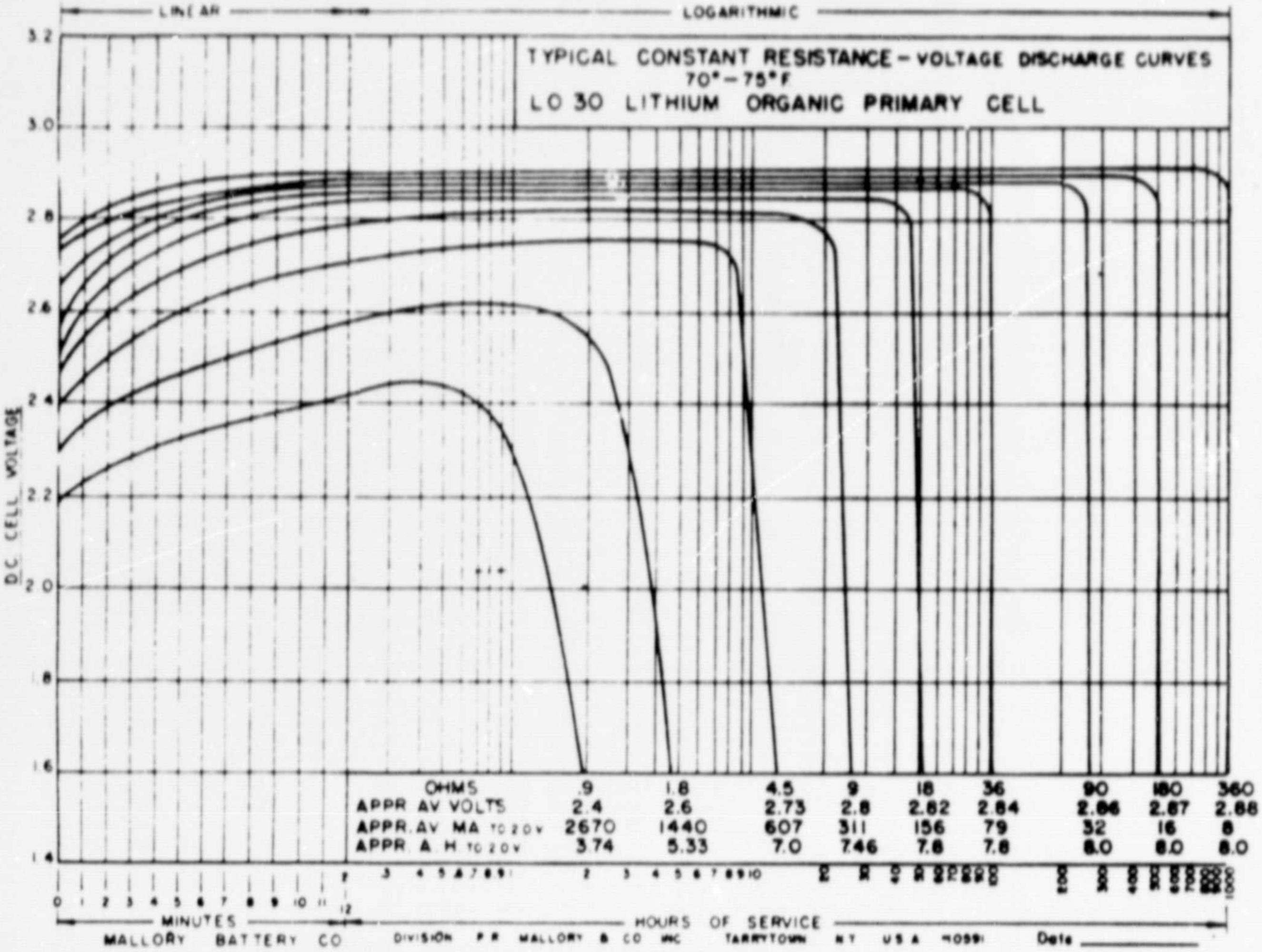

LO 30 LITHIUM ORGANIC PRIMARY CELL

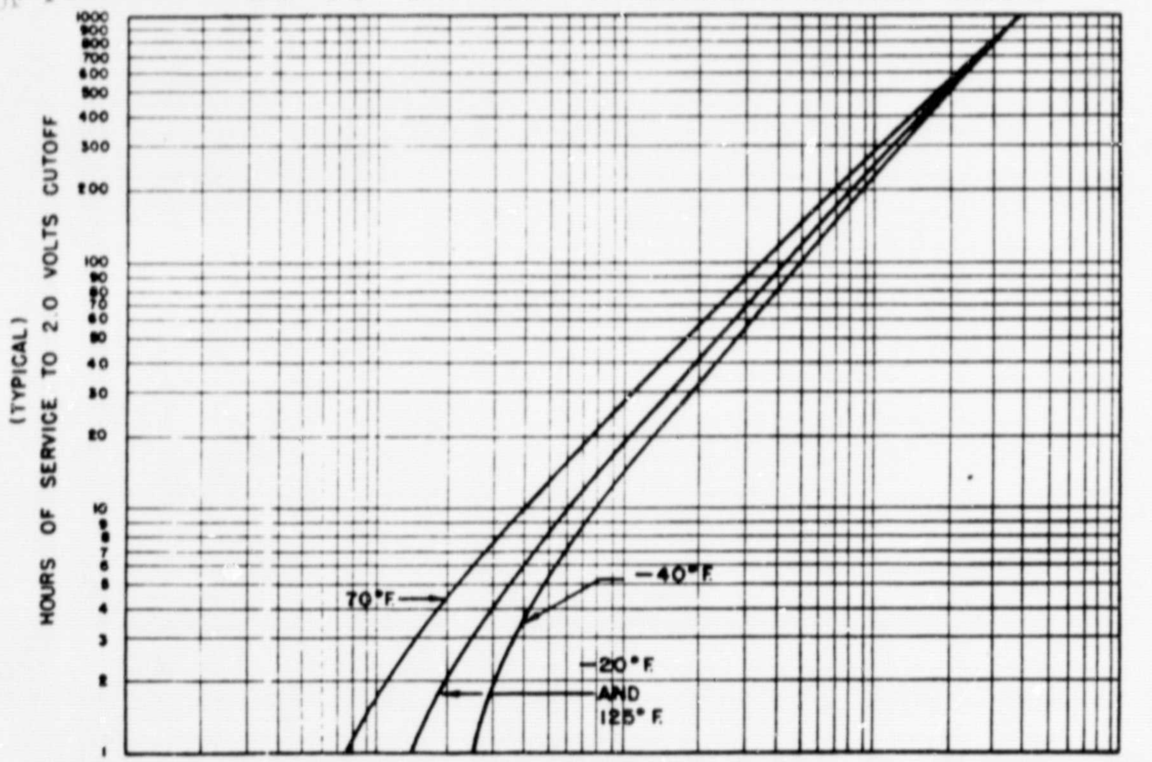

MALLORY BATTERY COMPANY
[illegible] MALLORY & CO. INC.
[illegible] Broadway, Tarrytown, New York [illegible] Telephone [illegible]

June 7, 1976

Mr. Hunter McShan
Telephonics
770 Park Avenue
Huntington, L.I., NY 11743

Dear Mr. McShan:

As a result of our phone conversation of June 7, 1976, I am sending you the following attached information.

(1) Product sheets describing the performance of the various available lithium cell sizes. Please be aware that these sheets describe the non-hermetic sealed cell, and are sent to you to describe the electrical characteristics of the various cell sizes which are the same as the hermetically sealed cells which we discussed.

(2) Contract report on work completed for the U.S. Army Signal Corps dealing with the hazardous properties of the system.

(3) A pre-print of a report to be presented later this month also dealing with abuse testing of lithium hermetically sealed cells.

After you have read the attached, please call if you have questions, or would like to discuss your particular application in more detail.

Sincerely,

MALLORY BATTERY COMPANY

Bruce McDonald
Manager, Lithium Systems

BMD/dmi
Enclosures - 3

MALLORY system characteristics –

	Alkaline Manganese	Mercury	Lithium	Zinc Carbon
Nominal O.C.V.	1.50 V	1.35-1.40 V	2.95 V	1.50 V
Load Voltage @ 25 Hrs.	1.20 V	1.15 V	2.82 V	1.20 V
End Volts @ 50 Hrs.	0.80 V	0.90 V	2.00 V	0.80 V
Capacity @ 50 Hrs. Rate	10 A–H	18 A–H	10 A–H	6 A–H
% of 50 Hr. Rate @ 0°C	80%	80%	95%	80%
% of 50 Hr. Rate @ −29°C	40%	40%	80%	20%
Watt-Hrs./Lb.	42	56	150	35
Watt-Hrs./Cu. In.	3.6	6.4	8.7	2.3

TYPICAL DISCHARGE ON "D" SIZE CELL AT 200 ma AVERAGE DRAIN

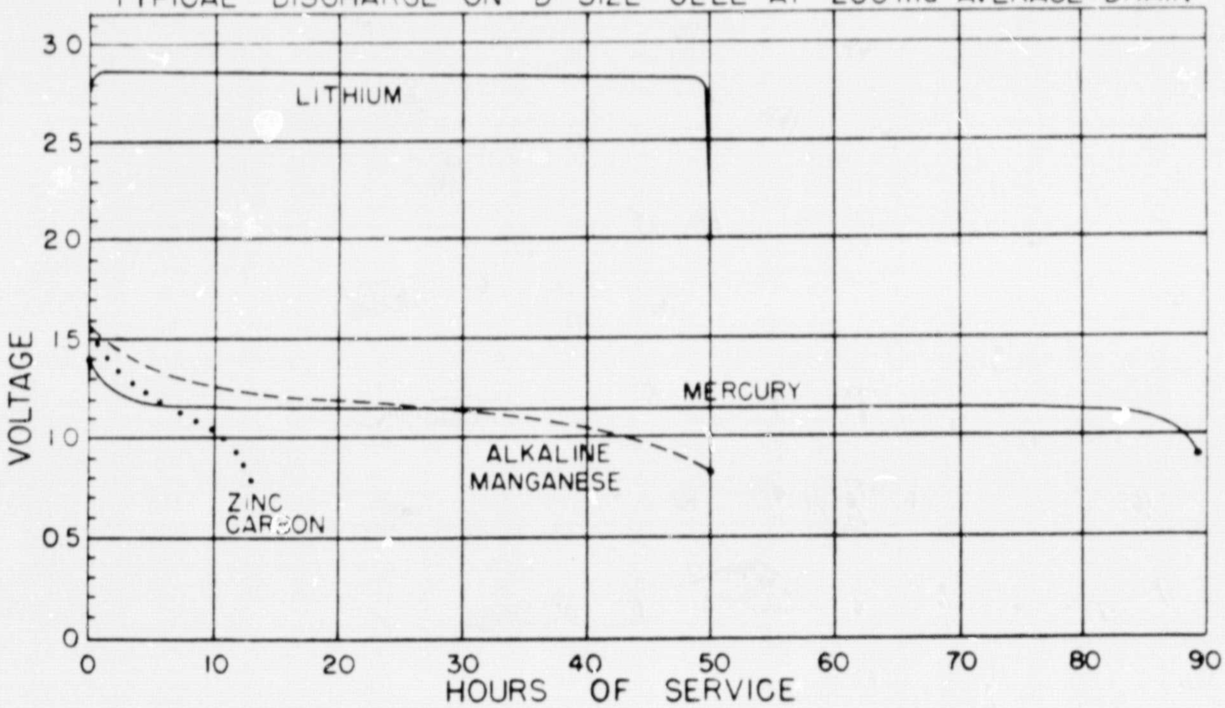

APPENDIX V

SCHEMATICS

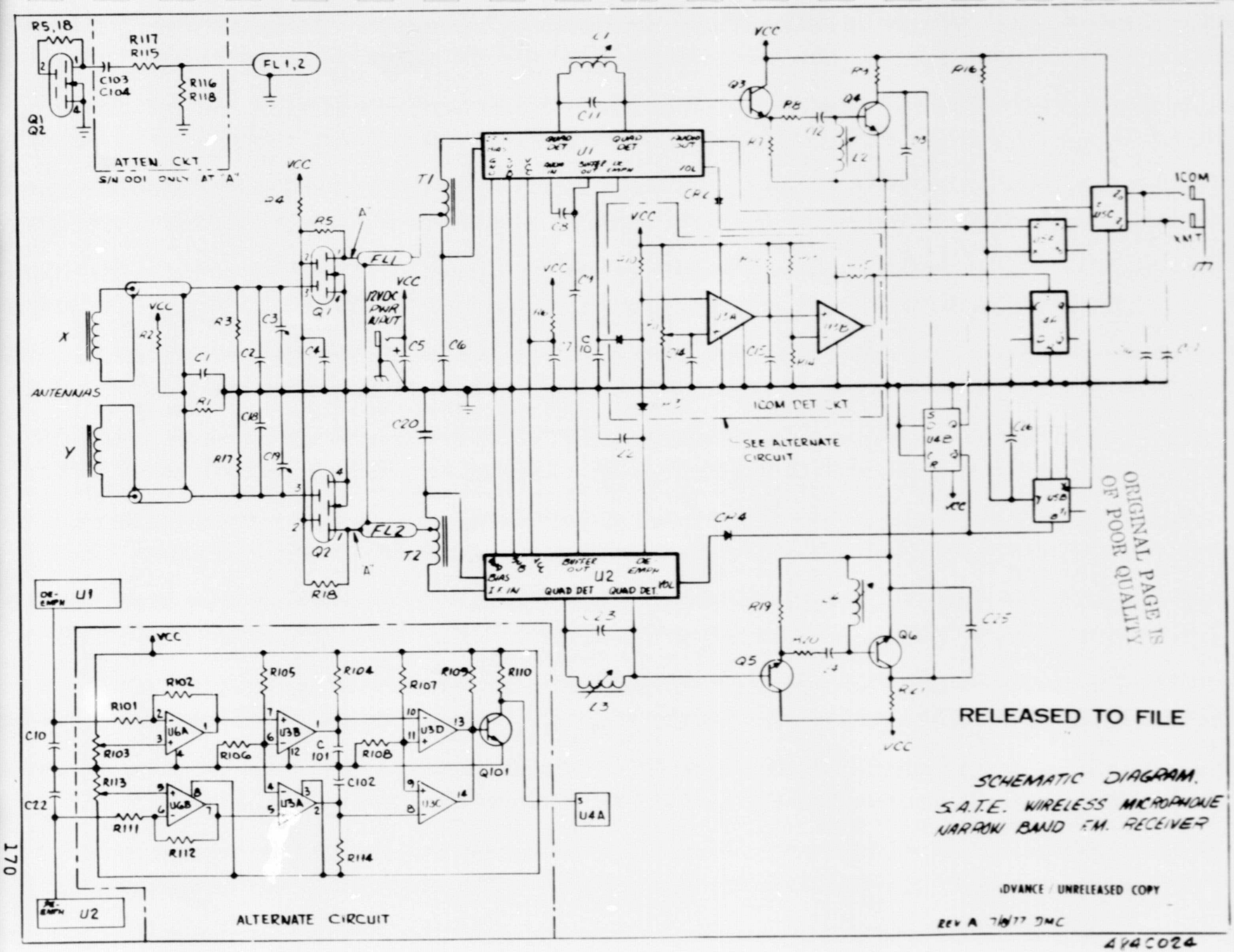
RELEASED TO FILE
SCHEMATIC DIAGRAM.
S.A.T.E. WIRELESS MICROPHONE
NARROW BAND F.M. RECEIVER
ADVANCE / UNRELEASED COPY
REV A 7/6/77 DMC
4A4C024
ATTEN CKT
S/N 001 ONLY AT "A"
ICOM DET CKT
SEE ALTERNATE CIRCUIT
ALTERNATE CIRCUIT
ANTENNAS
12VDC PWR INPUT
ICOM
XMT
ORIGINAL PAGE IS
OF POOR QUALITY

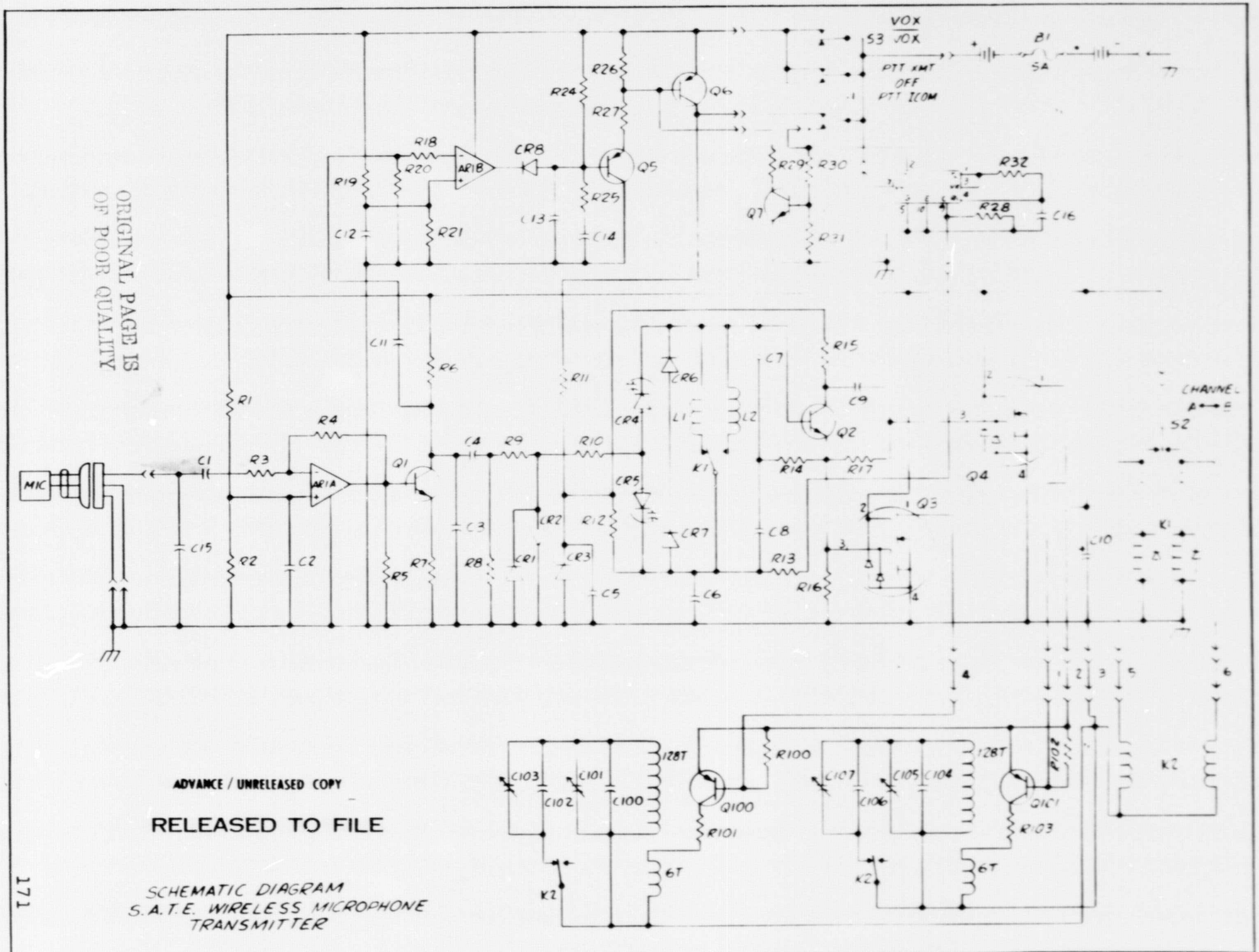

ADVANCE / UNRELEASED COPY

RELEASED TO FILE

SCHEMATIC DIAGRAM
S.A.T.E. WIRELESS MICROPHONE
TRANSMITTER

484C023

Telephonics CORPORATION

WIRELESS MICROPHONE COMMUNICATION SYSTEM

REPORT NO. WMCS–001

APPENDIX D

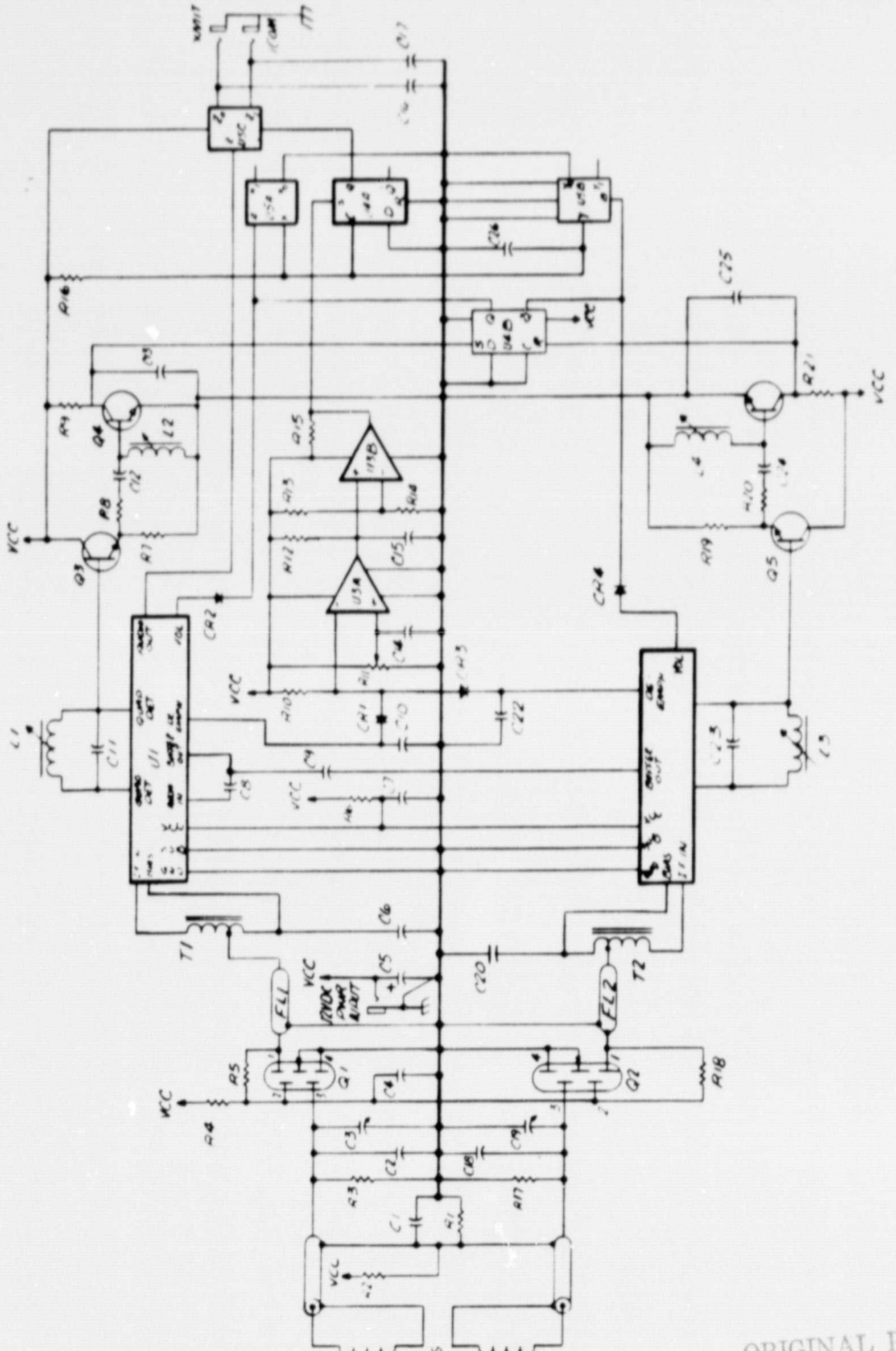

SCHEMATIC DIAGRAM.
S.A.T.E. WIRELESS MICROPHONE
NARROW BAND F.M. RECEIVER

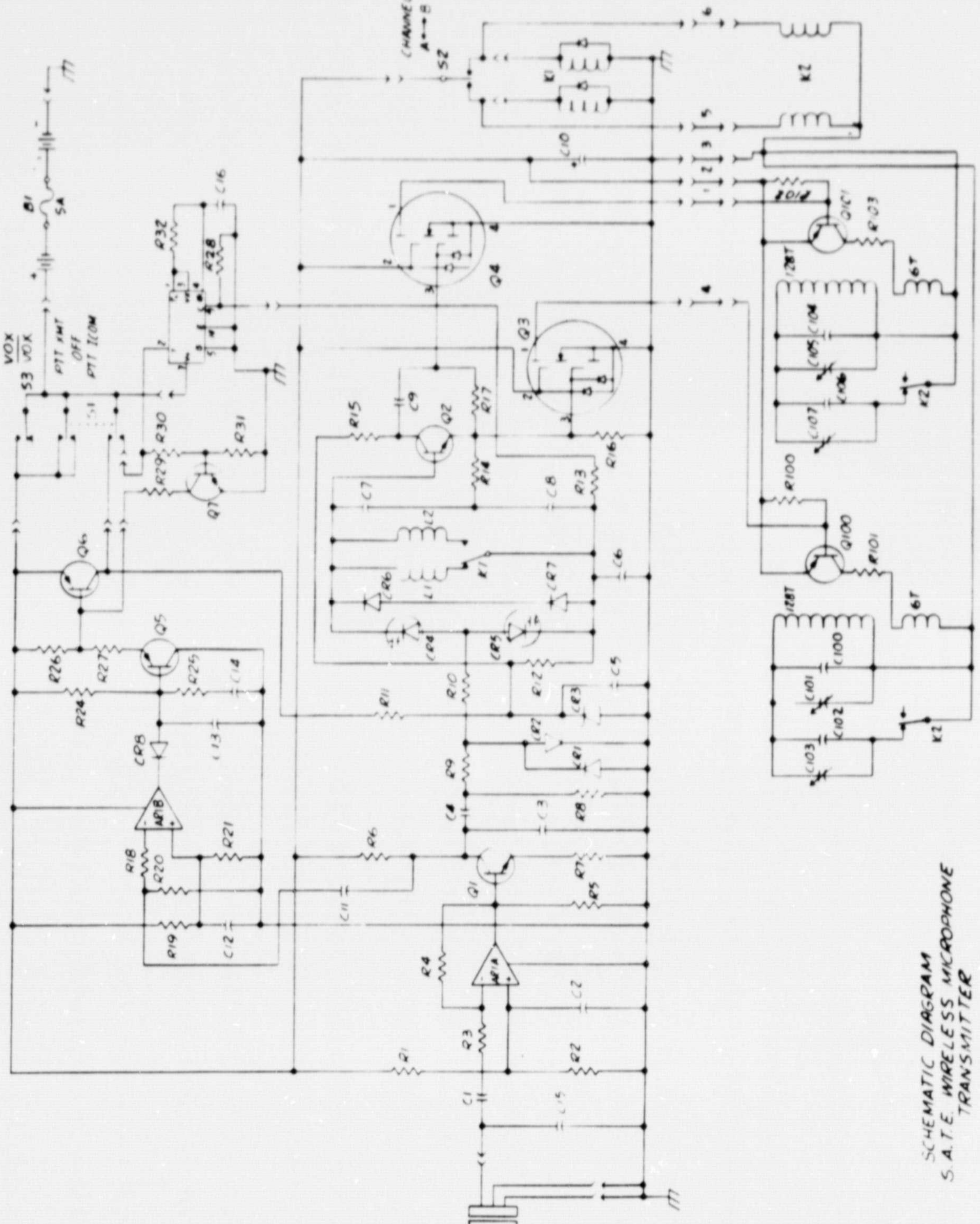

SCHEMATIC DIAGRAM
S.A.T.E. WIRELESS MICROPHONE
TRANSMITTER

ORIGINAL PAGE IS
OF POOR QUALITY

Telephonics CORPORATION

WIRELESS MICROPHONE COMMUNICATION SYSTEM

REPORT NO. WMCS–001

APPENDIX E

FINAL TECHNICAL REPORT

EVALUATION OF LIGHTWEIGHT HEADSETS FOR SPACE SHUTTLE APPLICATION

CONTRACT # NAS-9-14824

DATA ITEM - MA-129T

OCTOBER, 1976

TELEPHONICS CORPORATION
770 PARK AVE.
HUNTINGTON, NEW YORK

Telephonics

A DIVISION OF INSTRUMENT SYSTEMS CORPORATION

TABLE OF CONTENTS

IV. Appendices

A. Sample Letter to Respective Suppliers

B. List of Manufacturers Solicited

C. Subject Audiograms

D. Microphone Measuring System

E. Earphone Measuring System

F. Raw Data

ABSTRACT

The objectives of this study were to obtain contemporary lightweight headsets currently being manufactured and evaluate them for:

- Intelligibility
- Frequency Response
- Sensitivity
- Distortion
- Noise Isolation
- Acoustic Quality
- Weight
- Wearer Comfort

Thirty two letters, a sample of which is in Appendix A, were sent to manufacturers (See Appendix B) of commercial and military headsets. Five of the manufacturers responded affirmatively with a total of eight headsets for evaluation.

Each headset was rank ordered for the categories where statistically significant numbers were obtained. Subjective comments were good, fair, or poor when applied to human factors critiques.

I. Pictoral Description of Headsets

Manufacturer: Avid
Model #: LT-730
Microphone: Dynamic, first order Gradient
Earphone: Circumaural, dynamic

Manufacturer: Telex
Model # : 5x5
Microphone: Electret, First Order Gradient
Earphone: Ear Insert, Magnetic

Manufacturer: Sennheiser
Model #: HMD 110
Microphone: Dynamic, super cardioid
Earphone: Circumaural, dynamic

Manufacturer: Telex
Model #: TAH-29
Earphone: Supraaural, dynamic

Manufacturer: Roanwell
Model #: 125610
Microphone: Magnetic, first order gradient
Earphone: Magnetic, Circumaural

ORIGINAL PAGE IS
OF POOR QUALITY

Manufacturer: Telex
Model #: A610
Earphone: Circumaural, magnetic

Manufacturer: Sennheiser
Model #: HMD 414
Microphone: Dynamic, super cardiod
Earphone: Supraaural, dynamic

Manufacturer: Unex
Model #: HS-2A
Earphone: Single ear insert, magnetic
Microphone: Electret, First order gradient

II. Description of Test Methods

ORIGINAL PAGE IS OF POOR QUALITY

[illegible]

A. Earphones

The method of measurement presented herein was the PB (phonetically balanced) monosyllabic word tests. The subjects listened in a quiet and in a noisy environment.

o General

Five subjects were used in the testing. The listeners were seated in a semi reverberant room isolated from the talker. The talker used a B&K ½" condenser microphone with a foam breath shield. The talker held the breath shield to his or her lips and simultaneously viewed a VU meter to insure uniform talker sensitivity for the duration of the testing. The listeners were allowed to adjust the volume level for each test until a comfortable level was achieved.

Each headset had 5 listening tests in quiet and 5 listening tests in 90 dB of white noise.

Actual measurements in the listening room were as listed in Table A.

TABLE A

S.L.M. SETTING		QUIET AMBIENT (DB)	NOISE AMBIENT (DB)
A Weighting		36	91
C Weighting		63	91
31.5	(HZ) OCTAVE BAND CENTER FREQUENCIES	65	63
63		52	57
125		47	67
250		37	81
500		32	85
1000		22	84
2000		22	85
4000		22	86
8000		22	76
16000		24	65

° Screening of Subject

The subjects were selected on the basis of an audiometric examination. (Audiograms are in Appendix C). The tests were performed by a certified audiometrist. The hearing loss of the selected subjects did not average more than 10dB.

The talkers and listeners had no speech defects or strong accents. The subjects were used no more than 1 hour each day to prevent inattentiveness and biased results which can accompany lengthy psychophysical testing.

° Training of Subjects

The subjects were trained by reading PB word lists to each other in quiet, face to face communication, without the use of headsets. These procedures were repeated until 96% or better scores were universally achieved.

The subjects were then trained using a B&K consenser microphone and a Koss ESP-9 electrostatic headset until the same scoring efficiency was achieved.

B. Microphones

The method of measurement used the same subjects and ambient as was used for the earphone testing.

The talker was seated in the semi reverberant room while the listener was isolated in another room. The listener used a pair of Koss ESP-9 electrostatic earphones and was allowed to adjust the level until comfortable.

The talkers positioned the microphones ¼ inch from their lips and were presented with sidetone to the headset. Five tests were taken in quiet and in 90 dB of white noise.

2. Frequency Response/Sensitivity

A. Microphone

A constant SPL of 94dB was used to excite the microphone under test. A B&K system illustrated in Appendix D was used to sweep the frequency and to record the microphone output. The sensitivity was recorded as E/P.

The microphones were measured under open circuit condition. The sensitivity in dB re $1V/N/m^2$ and the E.O.L. rating are given on the response curves. The E.O.L. rating will give the sensitivity data in terms of power to allow comparison of the microphones with different impedances.

E.O.L. = 20 log E -10 log R + 24
(Effective Output Level)

where E = open circuit microphone output in volts when SPL is 10 dynes /cm^2 or 1 Newton/m^2 or 1 Pascal or 94dB SPL.

R = microphone impedance in ohms.

B. Earphone

A constant source of 1 milliwatt was fed to the earphone under test. A General Radio system illustrated in Appendix E was used to sweep the frequency and to record the earphones output.

A flat plate coupler using a B&K ½ inch microphone was used to couple the headset to the recording microphone. The earphone response curves shown in the DATA SECTION are not to be construed to represent how the ear senses the earphone output. There is, at present, no coupler that can claim recognition as a true "artificial ear" although some do approximate subjective data at the lower frequencies. The curves are taken so that an A/B type comparison can be made between earphones as to their general efficiency and frequency response.

3. Distortion

Distortion measurements were made at 300, 1000, and 3000 HZ using the test setup described above with the addition of a Hewlett Packard model 333 distortion analyzer. The SPL was held at 100 dB at the microphone and from the earphone for the distortion measurements.

4. Impedance

The impedance of the microphone was measured using the 6dB down method, i.e., the open circuit voltage was measured for an input SPL of 94 dB. The microphone output was then loaded with a precision variable resistor. The microphone impedance was taken as the reading of the variable resistor indicated when the initial microphone voltage measured was attenuated 6.0 dB.

The earphone impedance was measured using the dual voltmeter method. The current in the circuit below was measured using a precision 1 ohm resistor. The earphone impedance was then read directly on meter #2.

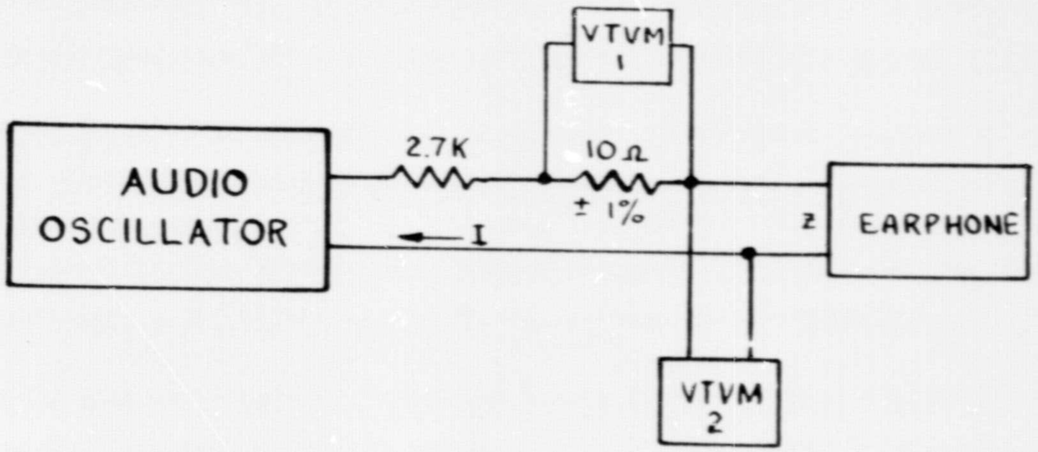

$$I = \frac{V_1}{10}$$

$$\frac{V_2}{I}$$

EARPHONE IMPEDANCE MEASUREMENT

III. Data Section

A. Rank Order of Earphones for Intelligibility/ Noise Isolation. (The best intelligibility in noise condition is deemed the best noise isolation and is not to be construed as noise attentuation of the headset.)

		% INTELLIGIBILITY			
		QUIET ($\bar{X}$)	σ	NOISE ($\bar{X}$)	σ
1.	TAH-29	96.8%	3.03%	92.[illegible]%	3.76%
2.	125610	96	2.8	76.5	23.5
3.	HMD110	94	7.1	70.4	18.5
4.	5 x 5	95.6	4.6	60	21.5
5.	LT-730	96.5	1.0	51	25.4
6.	HS-2A	95.2	3.6	50	11.0
7.	HMD414	97.6	2.6	44.8	12.9
8.	A610	92	3.2	15.6	9.3

The statistical significance of the various measurements is shown in Appendix F together with the Raw Data.

B. Rank Order of Microphones for Intelligibility/ Noise Isolation

		% INTELLIGIBILITY			
		QUIET ($\bar{X}$)	σ	NOISE ($\bar{X}$)	σ
1.	HMD110	98.4%	1.67%	95.2%	2.68%
2.	5 x 5	98.0	2.45	94.0	3.16
3.	HMD414	98.8	1.8	87.2	9.9
4.	125610	97.6	2.2	82.4	16
5.	HS-2A	95.0	2.2	81.0	4.5
6.	LT-730	98.8	1.1	74.8	11

C. Microphone Frequency Response and Sensitivity Figures.

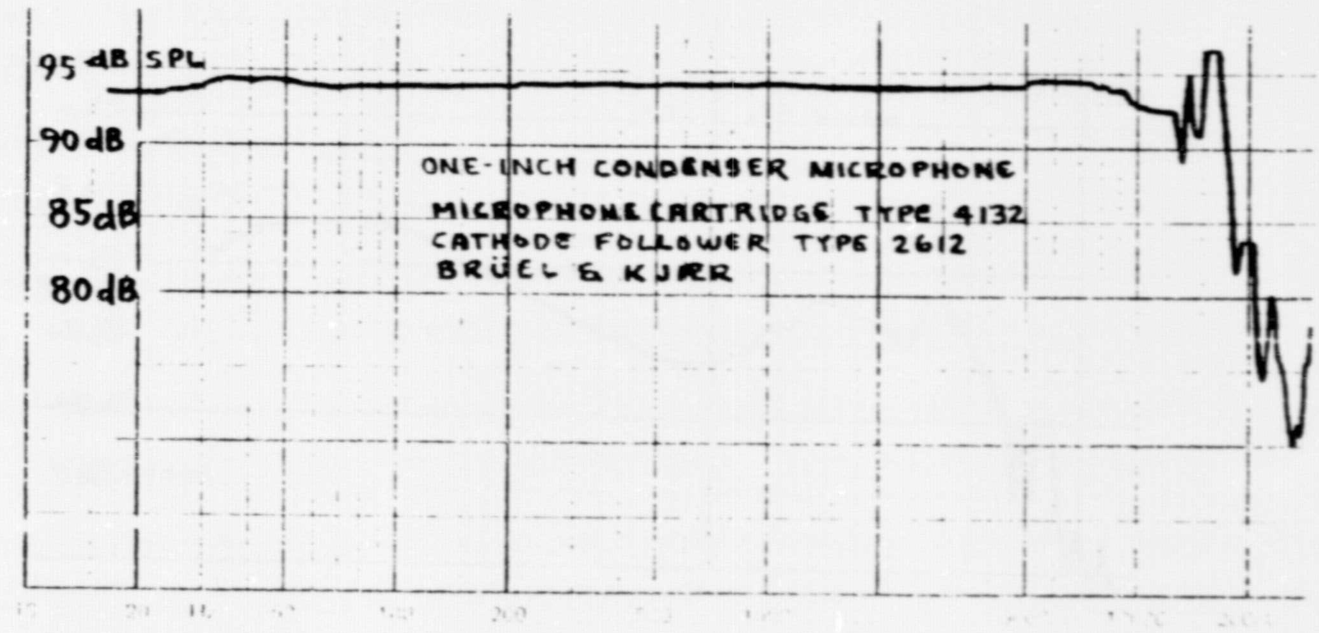

MICROPHONE CALIBRATION AND MEASURING SYSTEM RESPONSE

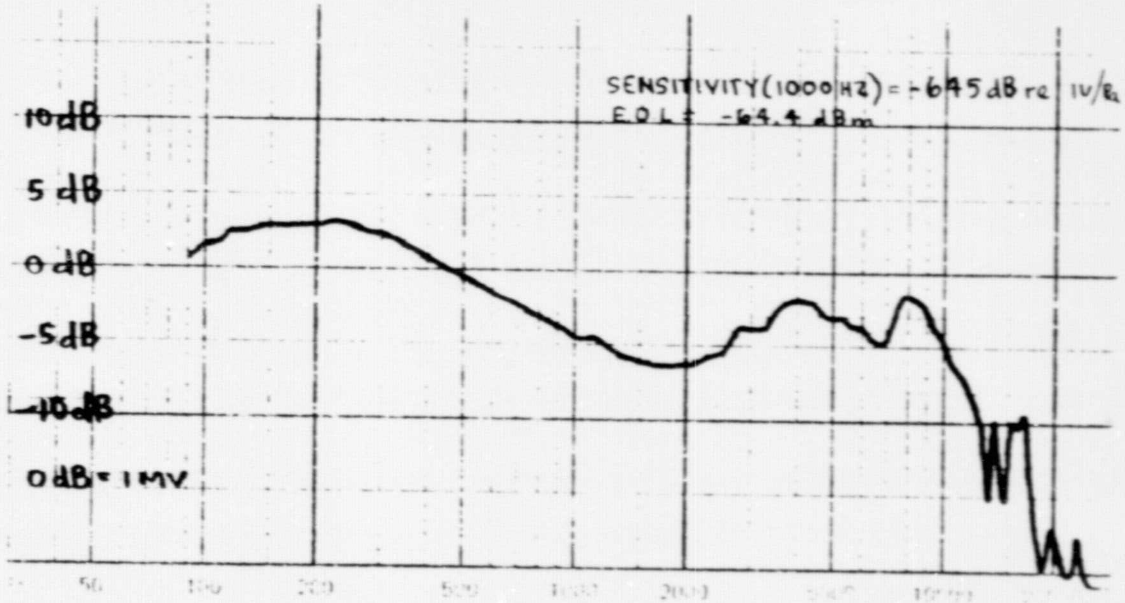

1. HMD110 MICROPHONE

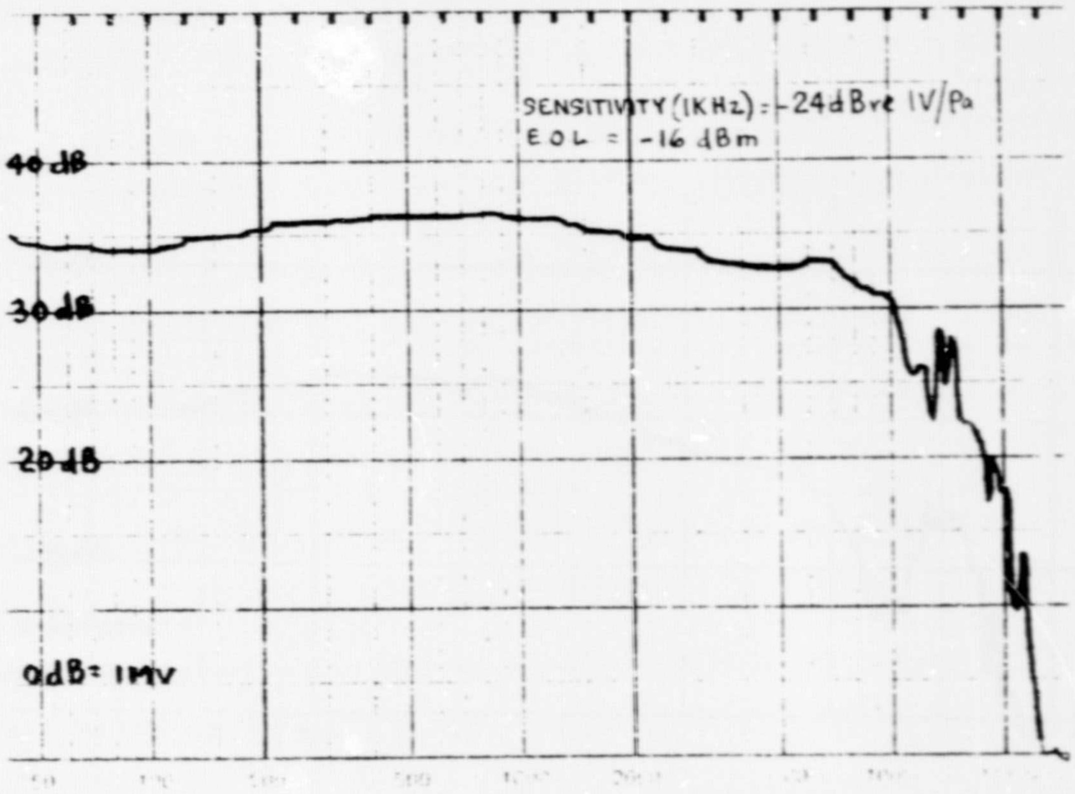

2. 5x5 MICROPHONE (AMPLIFIER IS ASSOCIATED WITH MICROPHONE

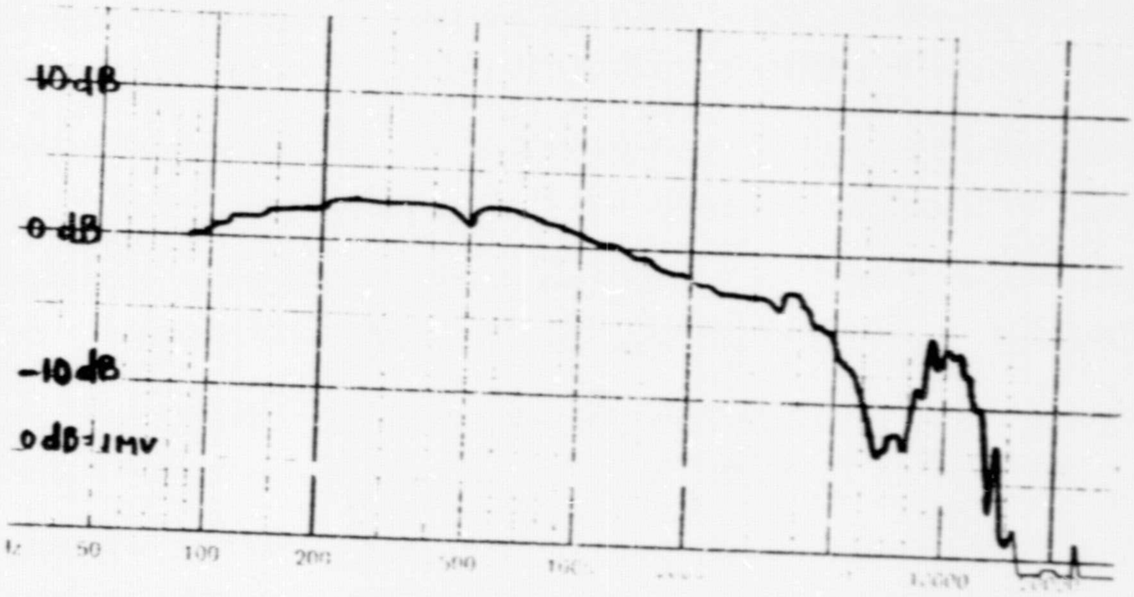

3a. HMD414 (SIDE FIRE)

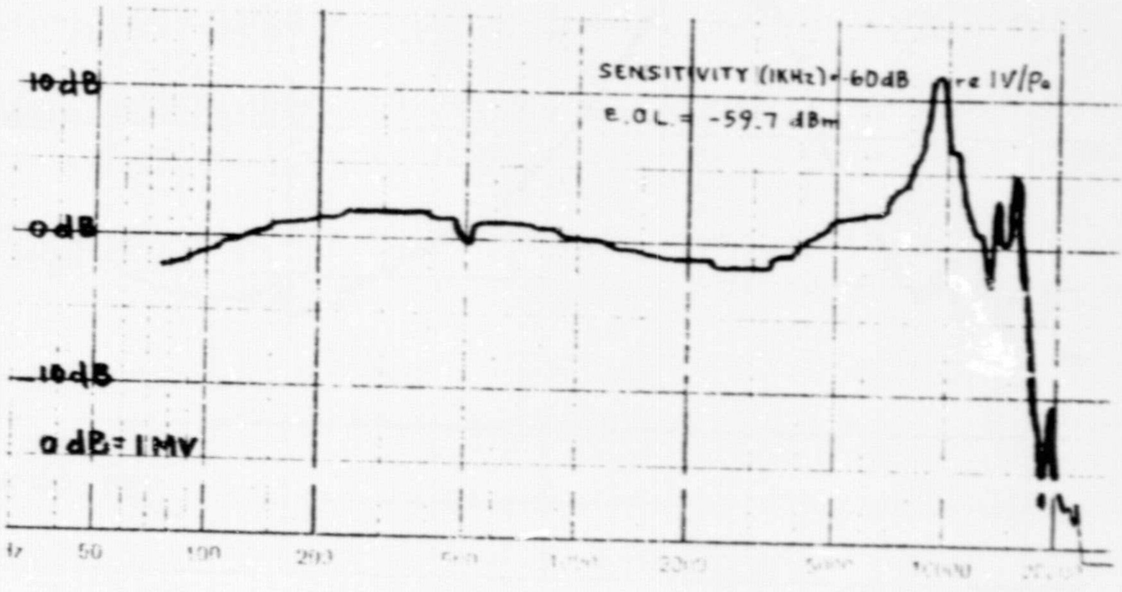

3. HMD414 MICROPHONE (END FIRE)

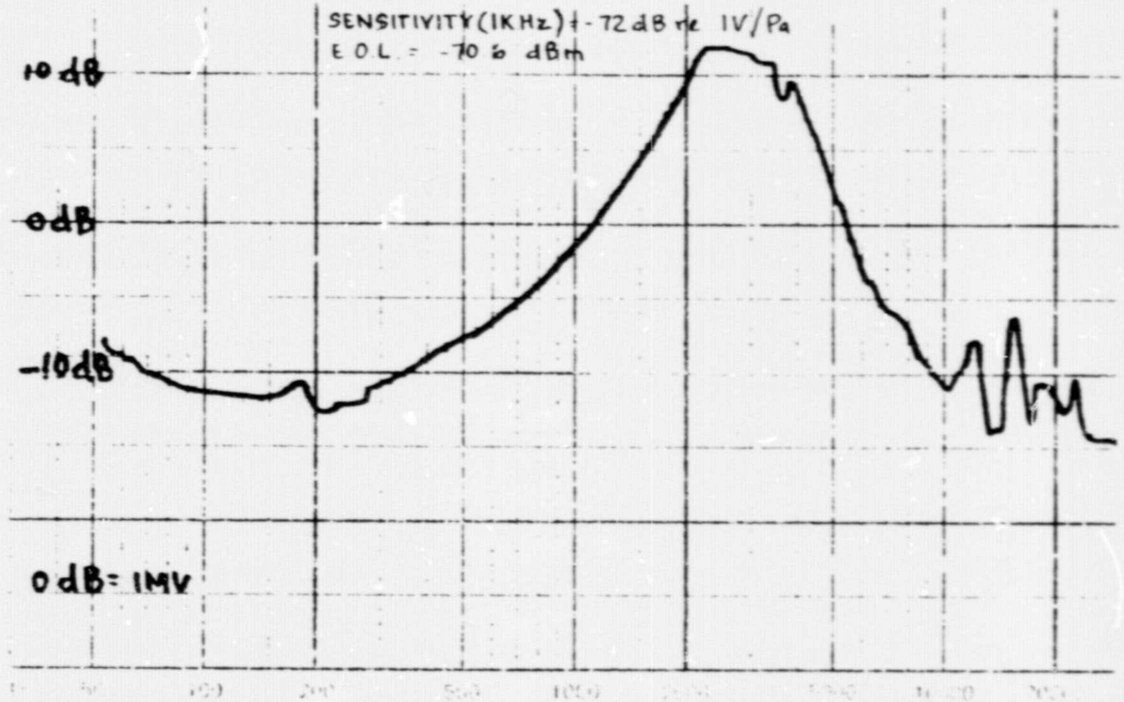

C-3

4. 125610 MICROPHONE

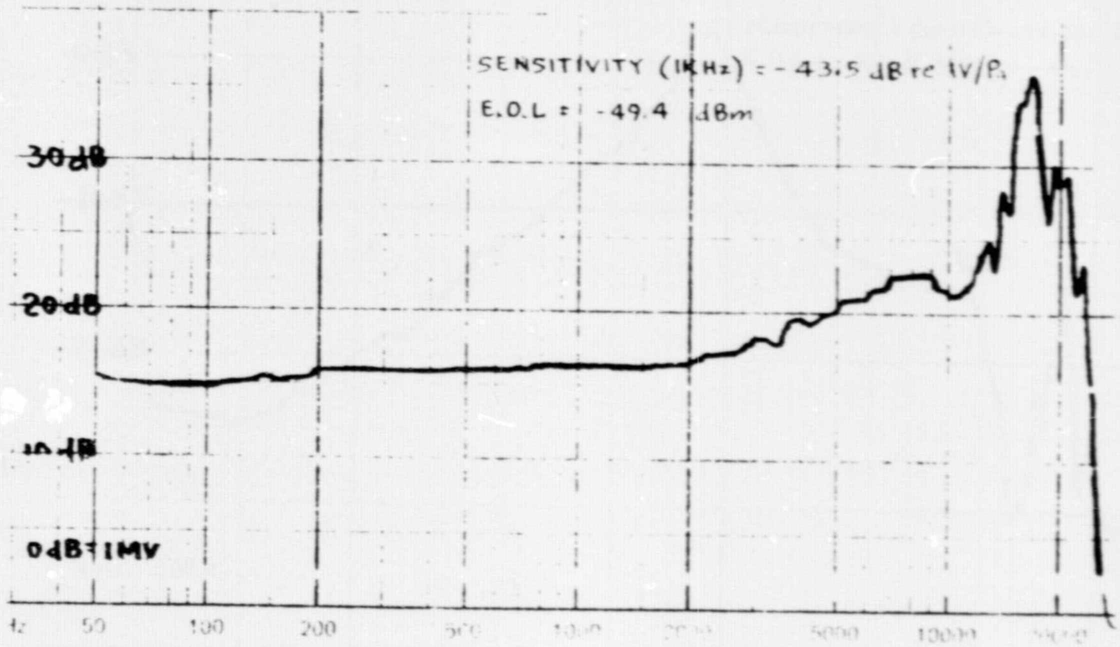

5. HS-2A MICROPHONE (1.5 VOLTS APPLIED TO AMPLIFIER)

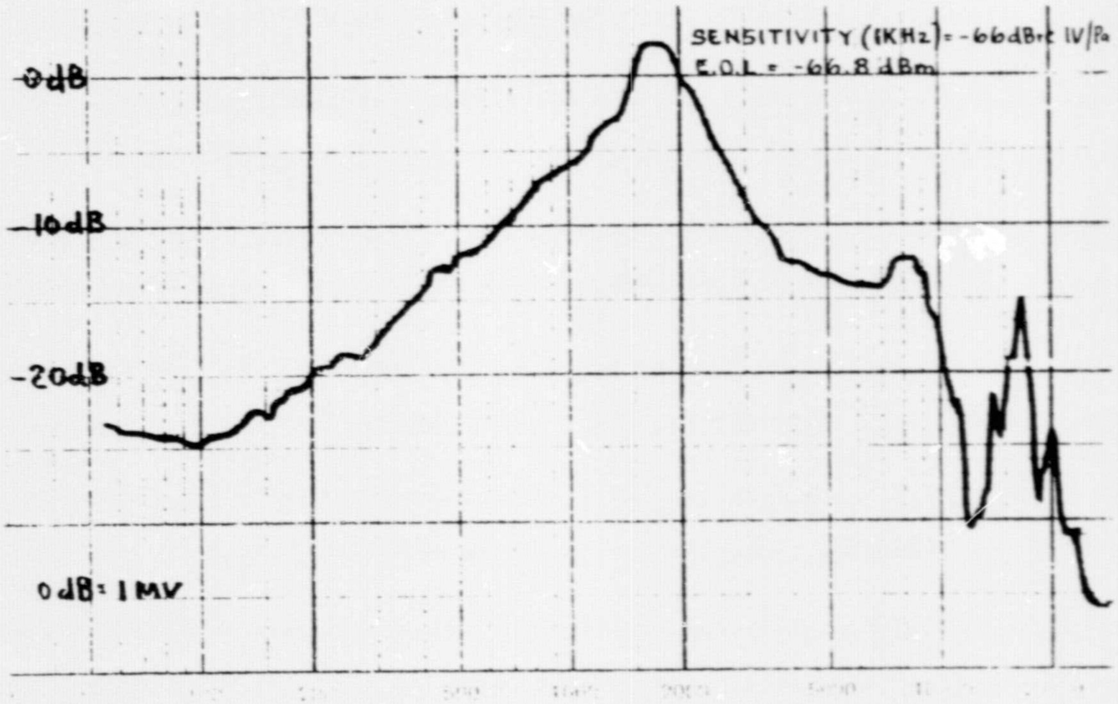

6. LT-730 MICROPHONE

D. Earphone Frequency Response and Sensitivity

ORIGINAL PAGE IS
OF POOR QUALITY

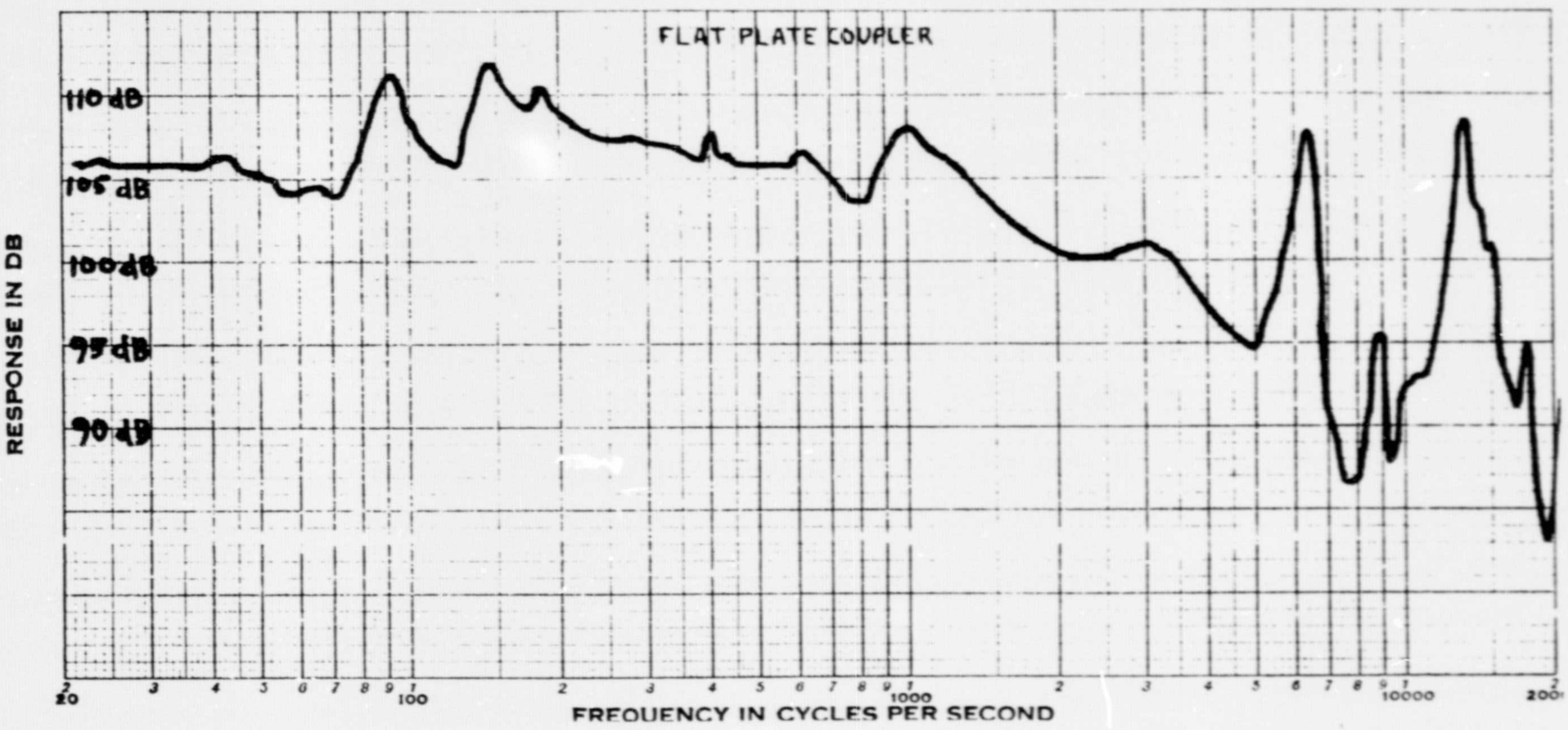

1a. TAH-29 EARPHONE (LEFT)

Telephonics
A DIVISION OF INSTRUMENT SYSTEMS CORPORATION

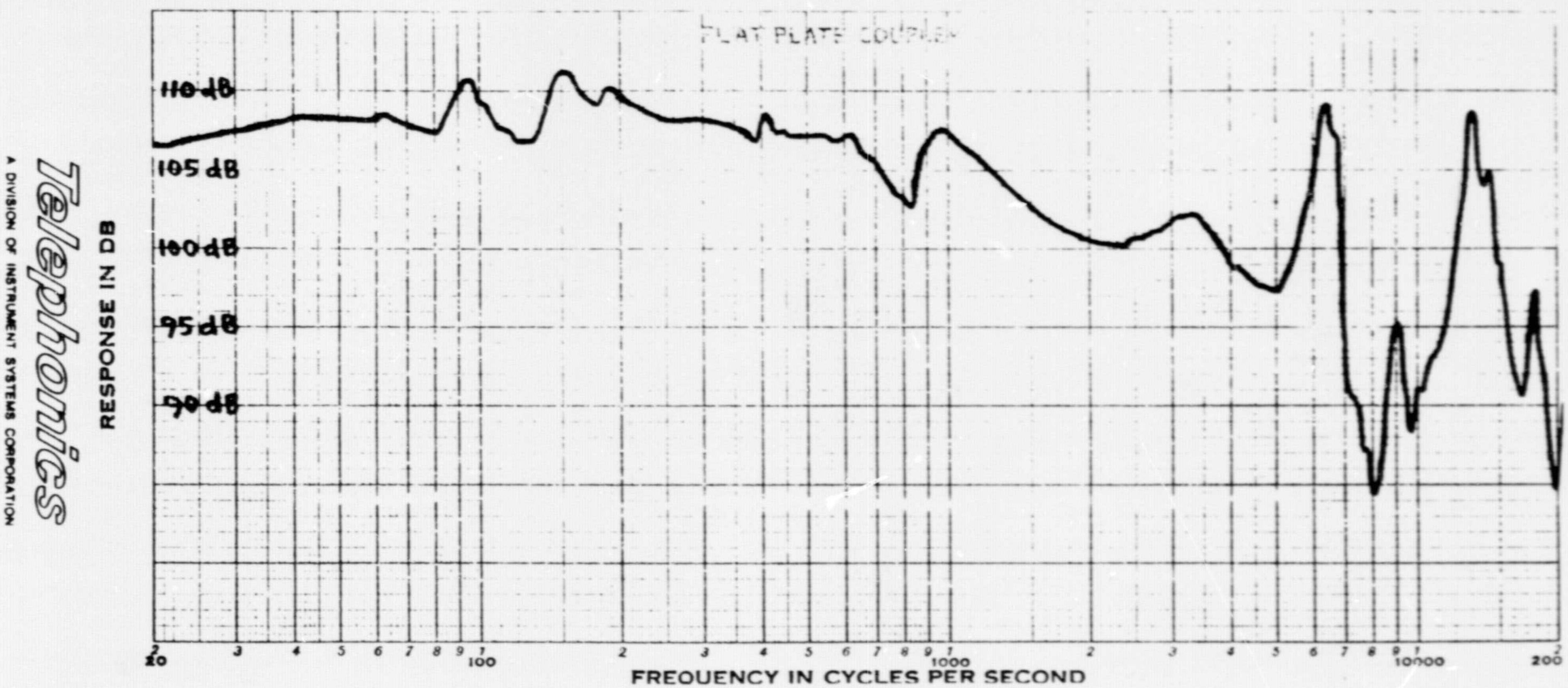
FLAT PLATE COUPLER
110 dB
105 dB
100 dB
95 dB
90 dB
RESPONSE IN DB
20
100
1000
10000
200
FREQUENCY IN CYCLES PER SECOND
Telephonics
A DIVISION OF INSTRUMENT SYSTEMS CORPORATION

1b. RIGHT

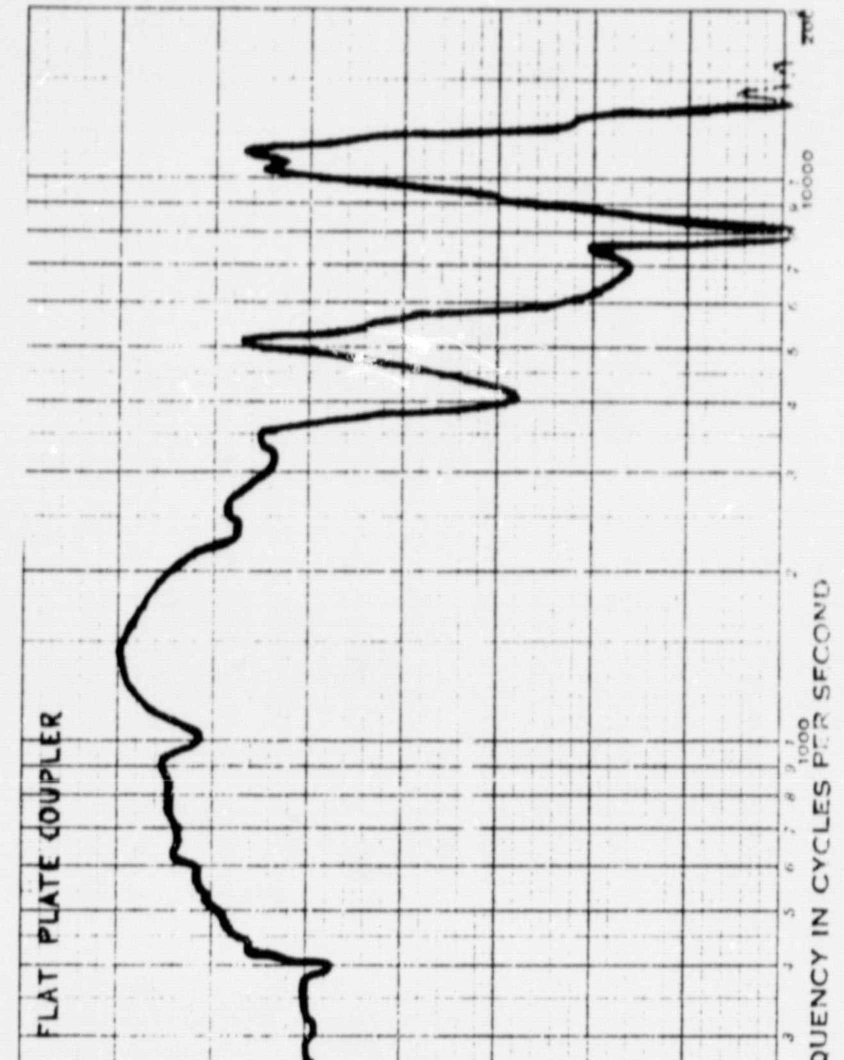
FLAT PLATE COUPLER
FREQUENCY IN CYCLES PER SECOND
RESPONSE IN DB
110 dB
105 dB
100 dB
95 dB
90 dB
100
1000
10000

2a. RIGHT

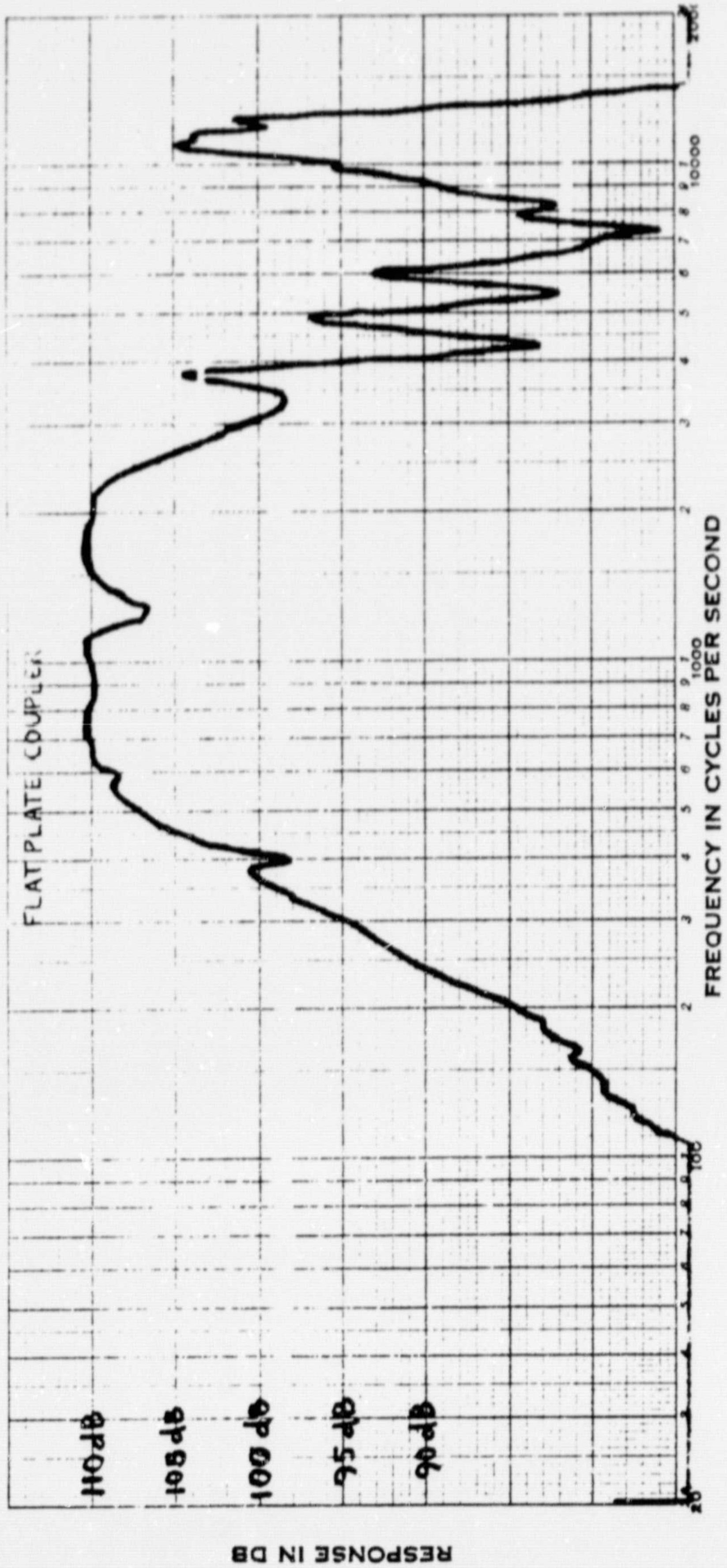

7b. 125610 EARPHONE (LEFT)

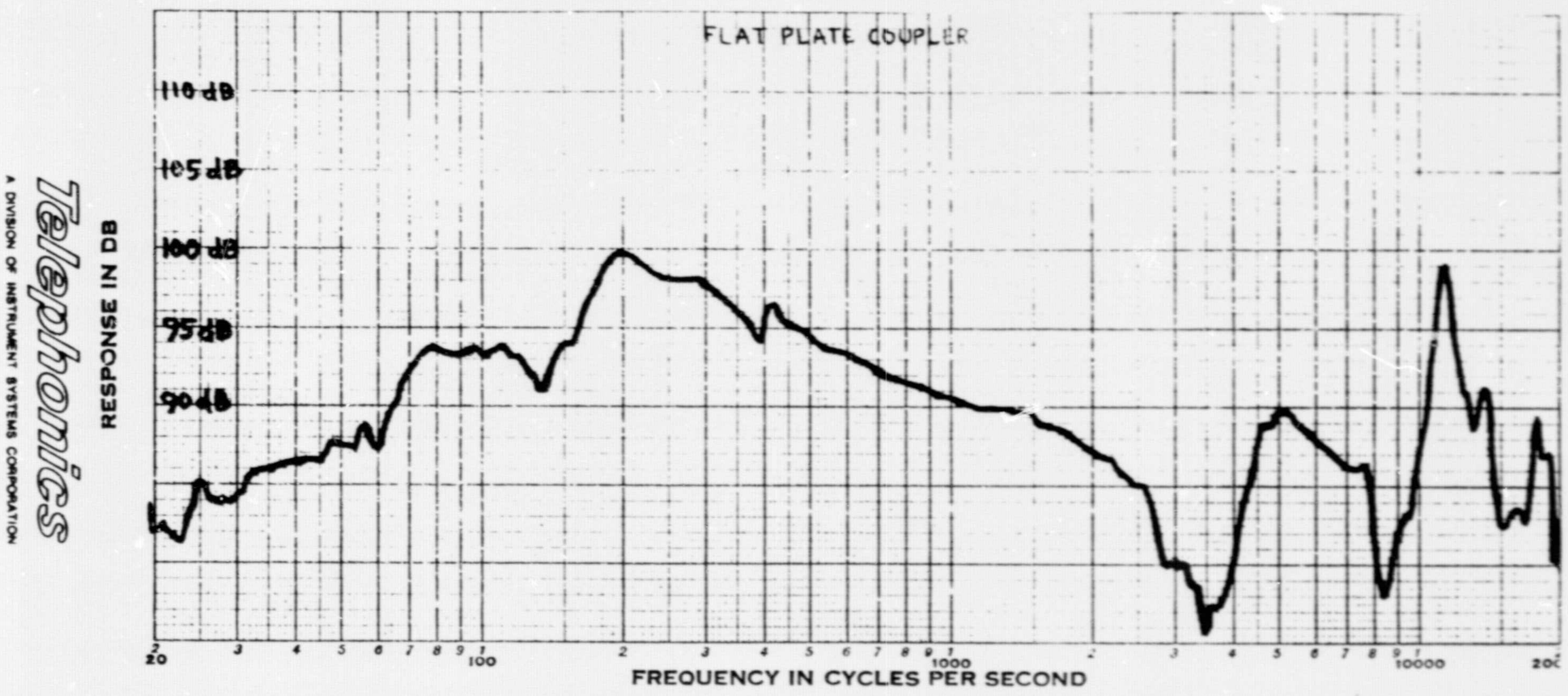

3a. HMD110 EARPHONE (LEFT)

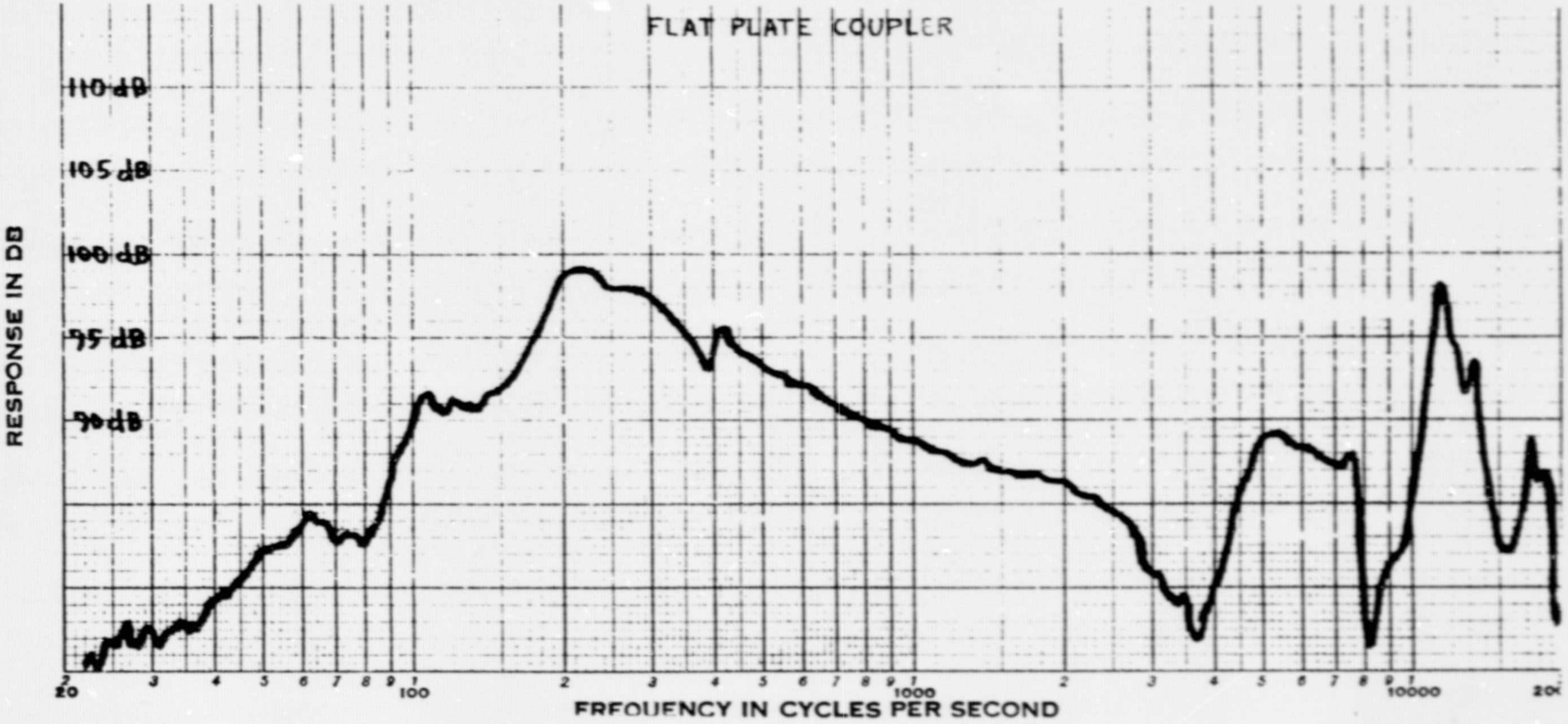

Telephonics
A DIVISION OF INSTRUMENT SYSTEMS CORPORATION

3b. RIGHT

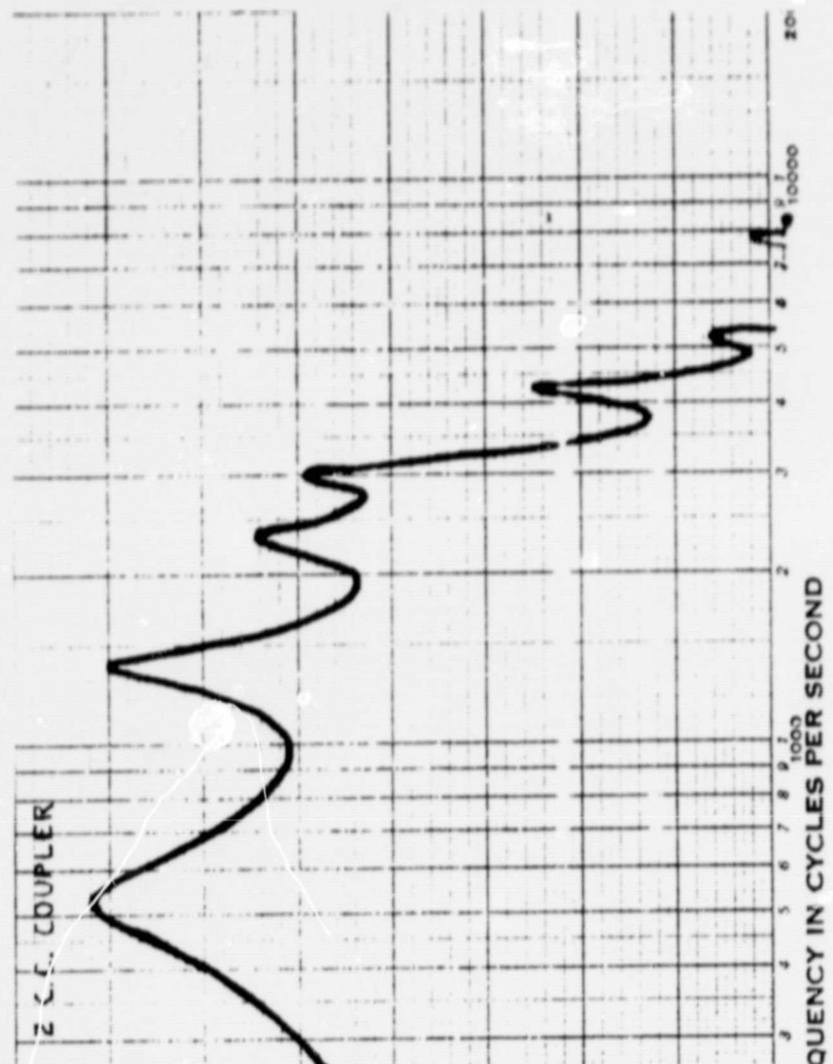

4a. 5x5 EARPHONE (LEFT)

Telephonics

A DIVISION OF INSTRUMENT SYSTEMS CORPORATION

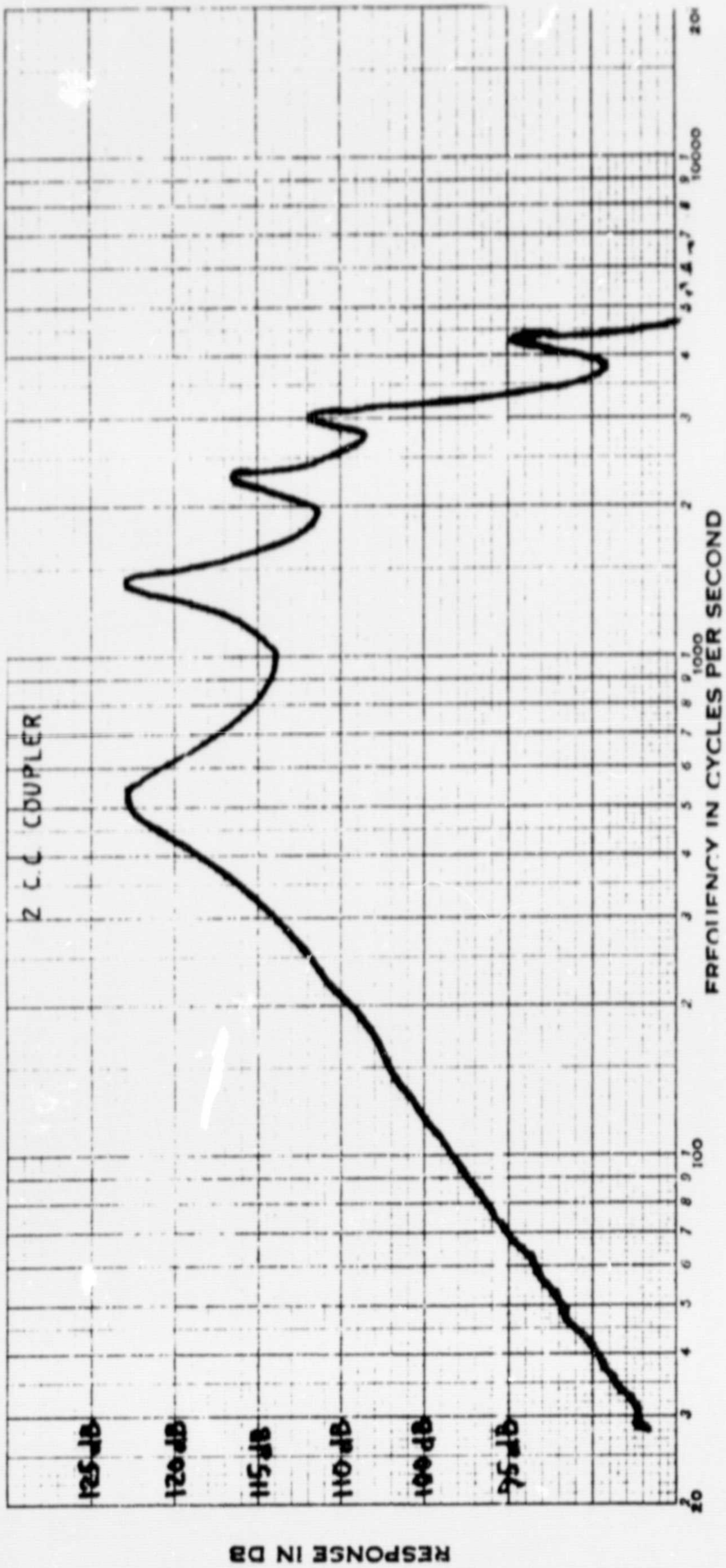

4b. RIGHT

Telephonics

A DIVISION OF INSTRUMENT SYSTEMS CORPORATION

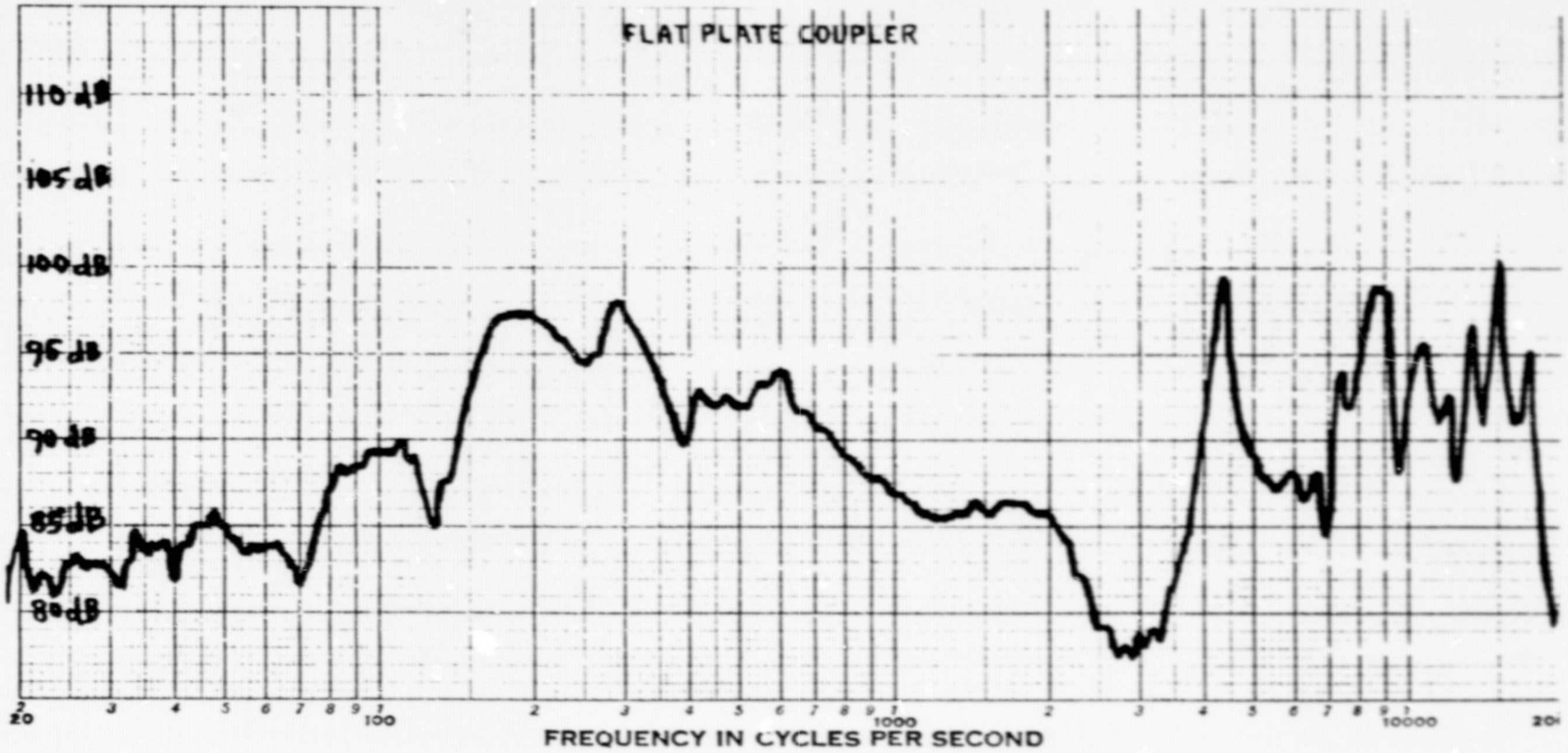

Telephonics
A DIVISION OF INSTRUMENT SYSTEMS CORPORATION

5a. LT-730 EARPHONE (LEFT)

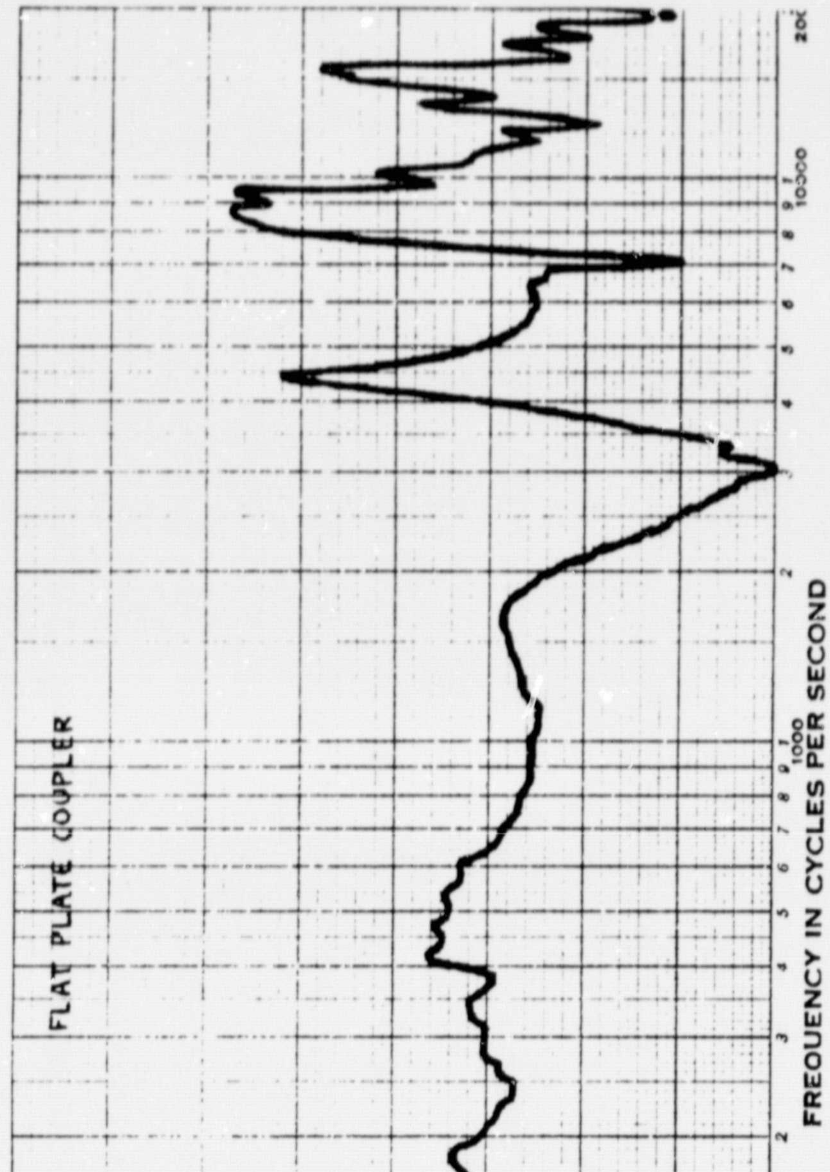

5b. RIGHT

Telephonics

A DIVISION OF INSTRUMENT SYSTEMS CORPORATION

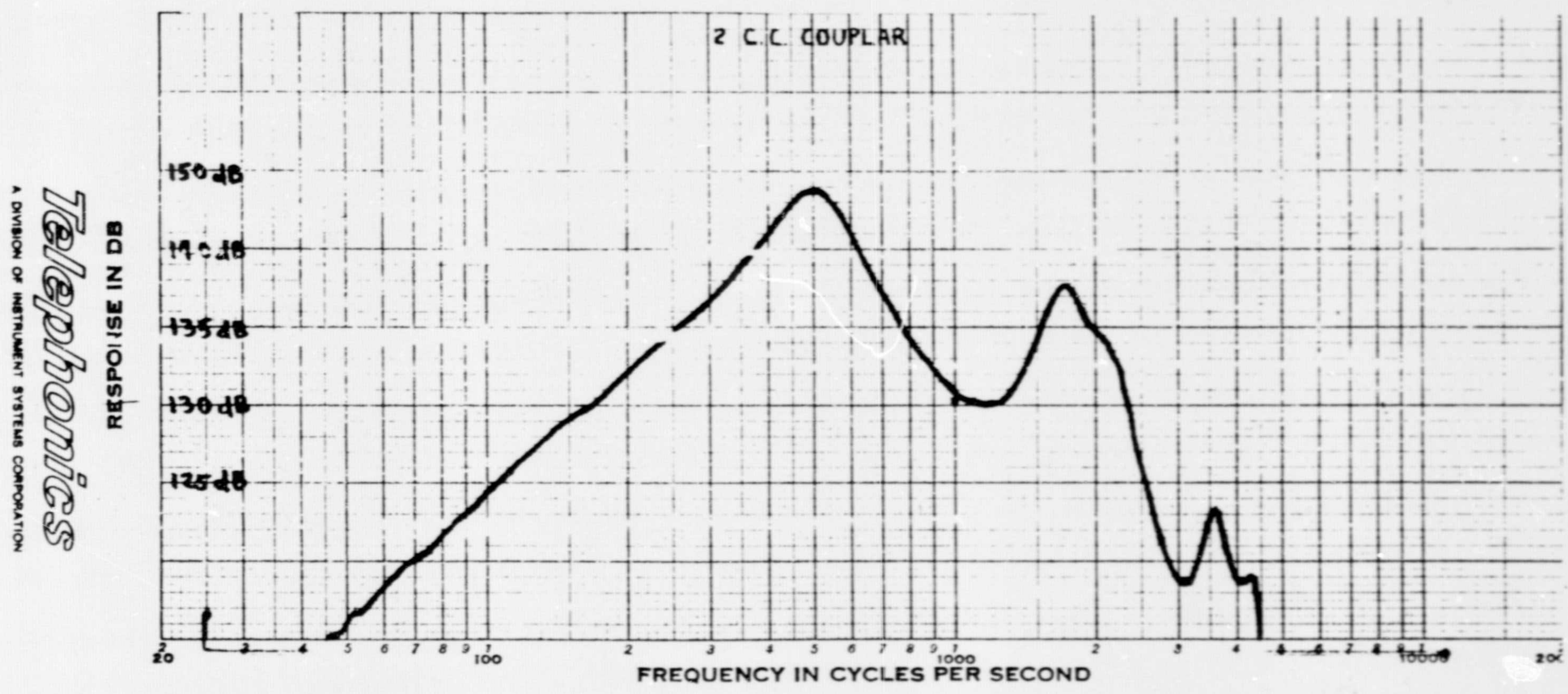

6. HS-2A EARPHONE (SINGLE EAR ONLY)

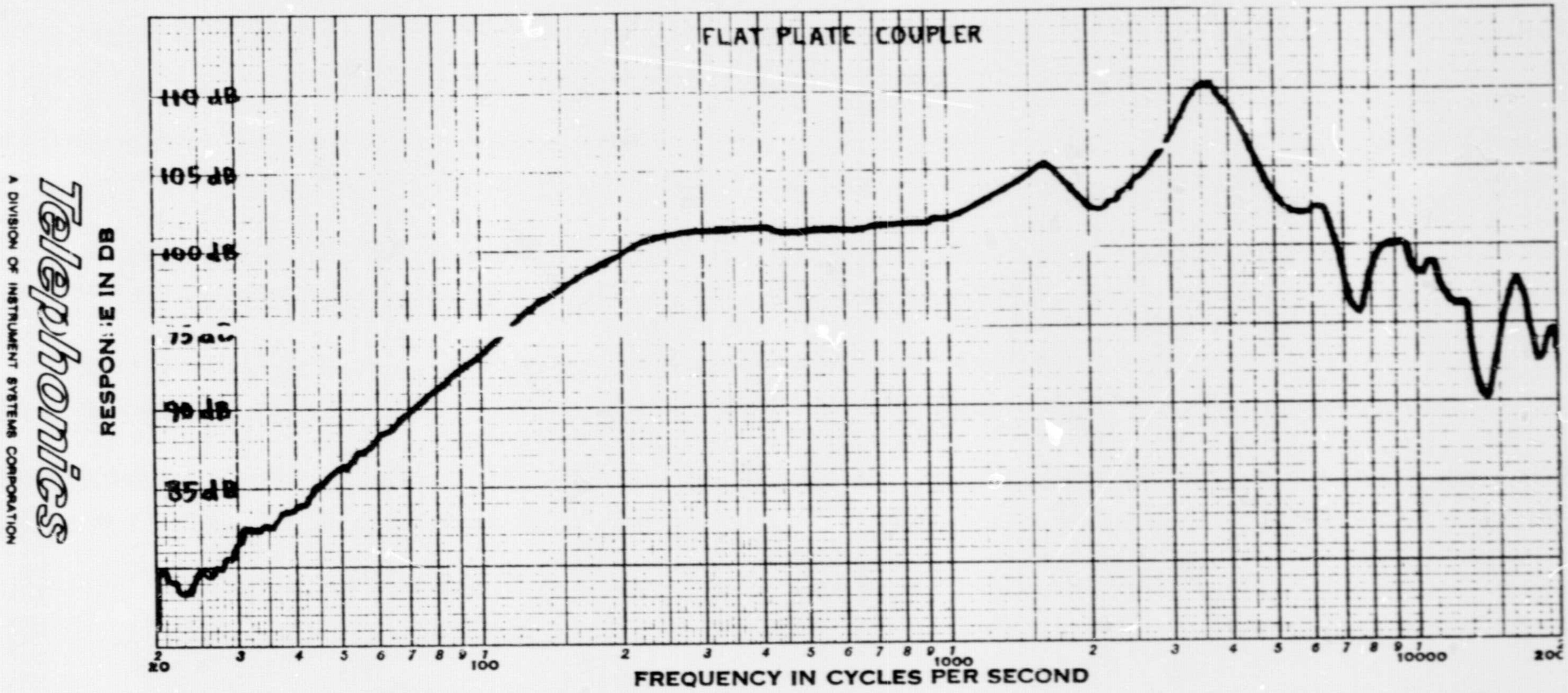

7a. HMD414 EARPHONE (LEFT)

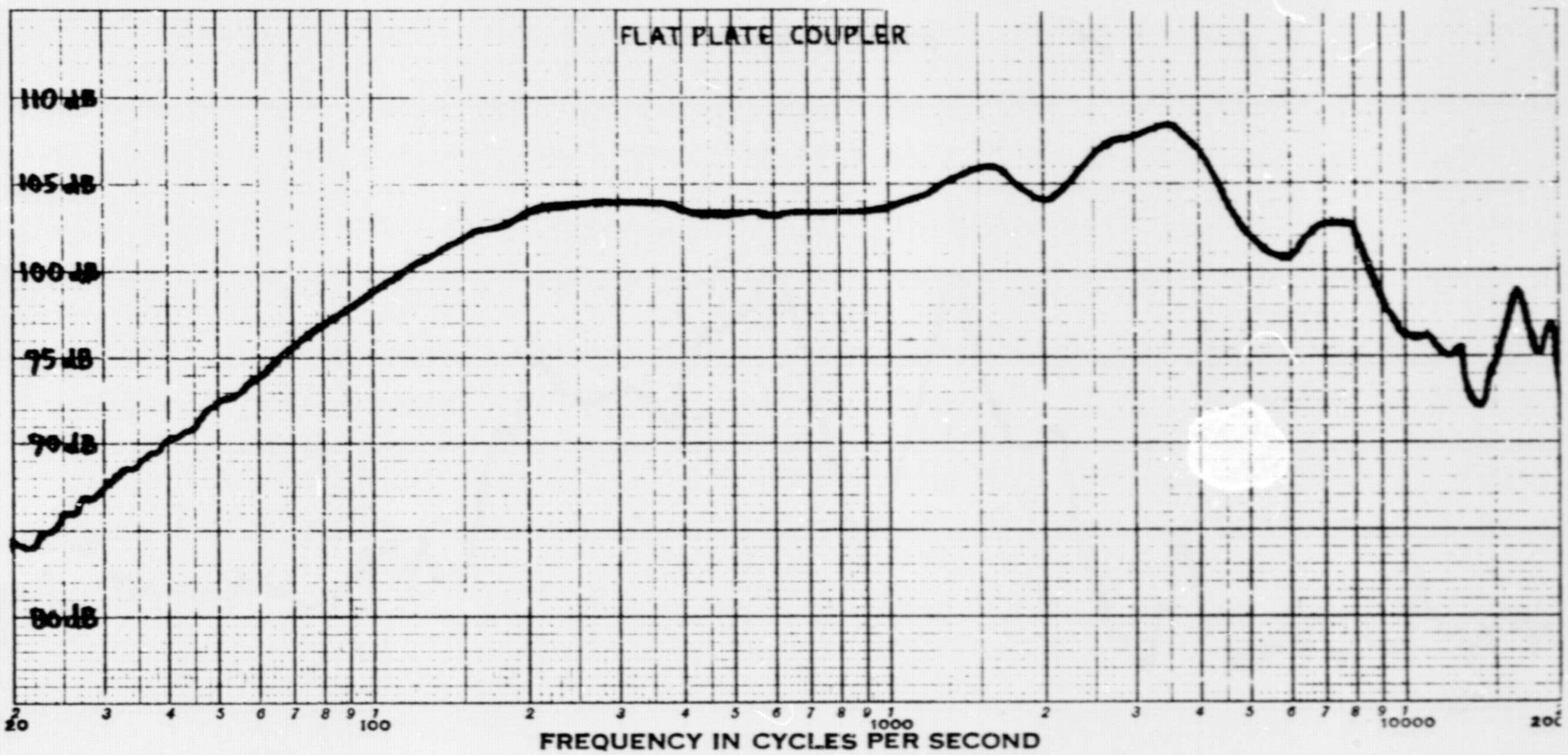

Telephonics
A DIVISION OF INSTRUMENT SYSTEMS CORPORATION

7b. RIGHT

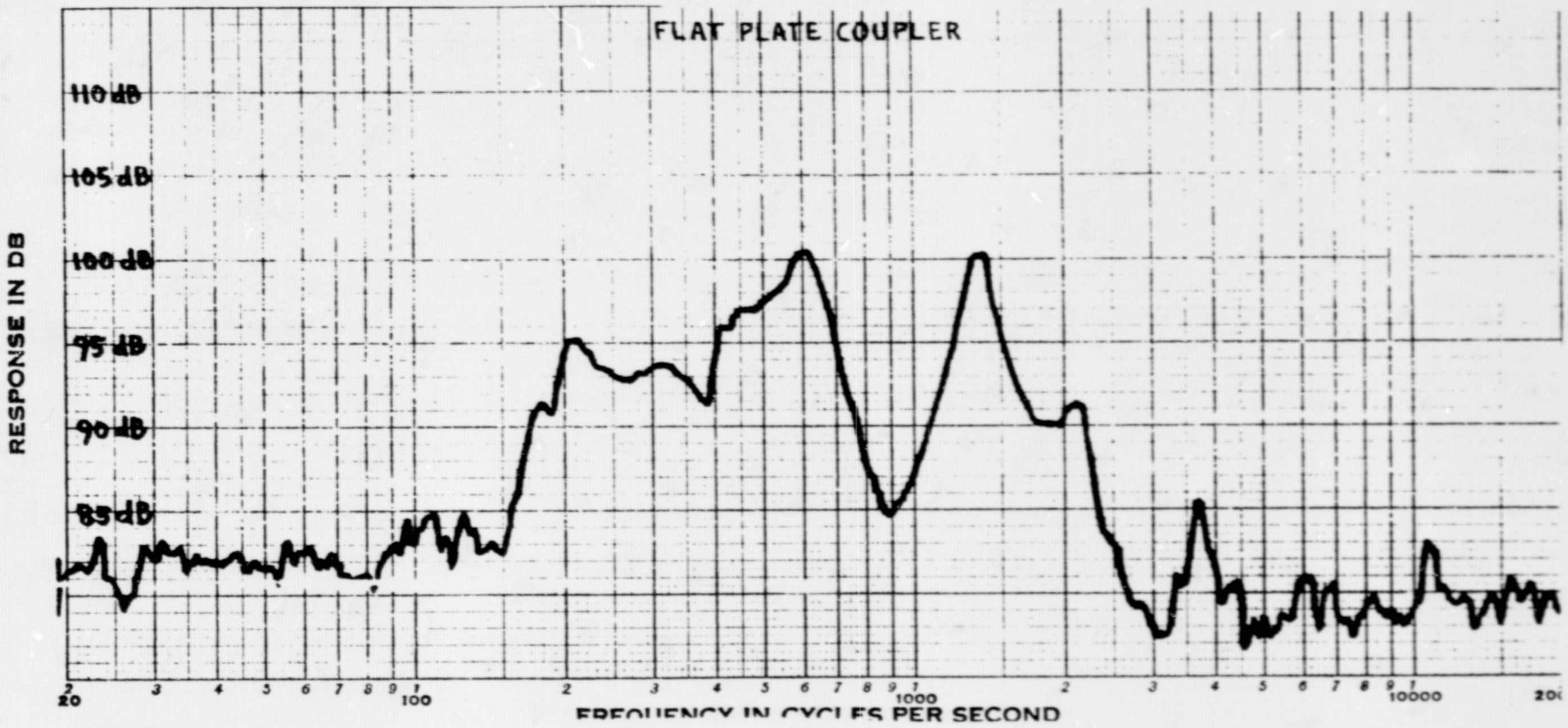

Telephonics
A DIVISION OF INSTRUMENT SYSTEMS CORPORATION

8a. A610 EARPHONE (LEFT)

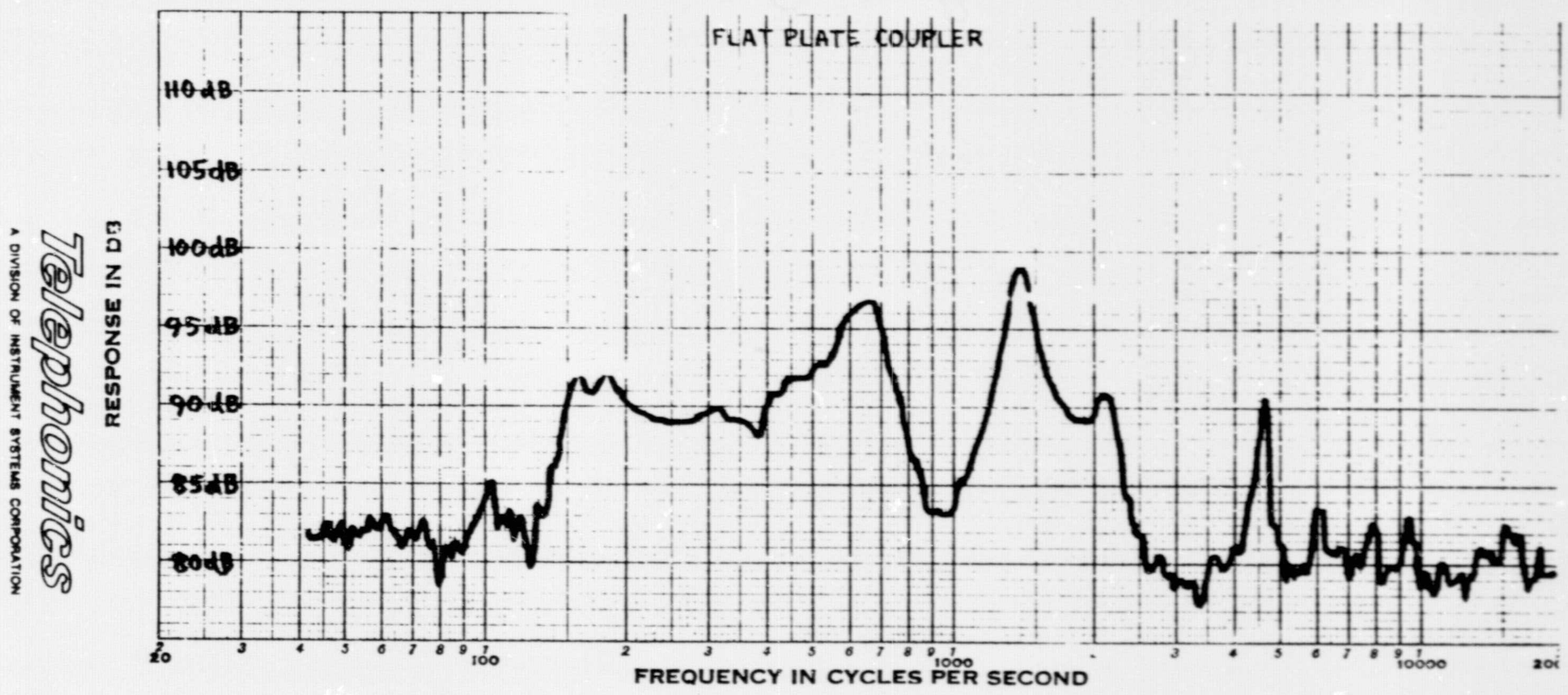
FLAT PLATE COUPLER
110dB
105dB
100dB
95dB
90dB
85dB
80dB
RESPONSE IN DB
20
100
1000
10000
FREQUENCY IN CYCLES PER SECOND
Telephonics
A DIVISION OF INSTRUMENT SYSTEMS CORPORATION

8b. RIGHT

E. Impedance

HEADSET		MICROPHONE (OHMS)	EARPHONE (SINGLE)
1.	HMD110	245	200
2.	HMD414	235	2500
3.	HS-2A	1000	740
4.	5x5	40 (from decoupling circuit)	980
5.	A610	No Mic	270
6.	TAH-29	No Mic	320
7.	LTV-730	300	270
8.	125610	190	280

F. Headset Weight (Lightest to Heaviest)

1.	HS-2A	33 grams	±10%
2.	5x5	210 grams	
3.	A610	240 grams	
4.	HMD414	330 grams	
5.	125610	345 grams	
6.	TAH-29	360 grams	
7.	LT-730	430 grams	
8.	HMD110	436 grams	

G. Distortion

The microphones and earphones measured less than .5% distortion at the 100 dB SPL level. Since the noise figure of the B&K microphone is 46 dB SPL equivalent, the lowest distortion measurement possible is .2% for the earphones. The Artifical voice of B&K is rated at "less than 1%. It was determined that the distortion levels of all microphones and earphones were satisfactory. More stringent measurements were deemed beyond the scope of this report.

I. Wearer Comfort

The subjective comments concerning wearer comfort were taken after the headset had been worn in the test for intelligibility.

	SUBJECT 1	2	3	4	5	AVG
TAH-29	G	F	G	F	G	G-
HMD110	P	G	F	F	F	F
HMD414	P	G	G	P	F	F
LTV-730	G	G	G	G	G	G
125610	F	G	G	F	F	F+
A610	F	G	F	F	F	F
HS-2A	P	G	G	F	F	F+
5x5	P	P	P	P	P	P

P = POOR
F = FAIR
G = GOOD

APPENDICES

Telephonics

770 PARK AVENUE, HUNTINGTON, NEW YORK 11743
(516) 549-6000 / TWX 510-226-6983 / Cable: INSSYSTHTGN

ORIGINAL PAGE IS
OF POOR QUALITY

March [illegible], 19[illegible]

Gentlemen:

Telephonics has recently been awarded a Government contract to develop and manufacture a state-of-the-art audio communication system for the Space Shuttle program.

One aspect of this effort will be to evaluate a light weight headset (consisting of noise cancelling microphone and earphones) currently available for parameters which will include intelligibility, frequency response, sensitivity, distortion, noise isolation, acoustic quality, reliability, weight, wearer comfort, maintainability, and environmental stamina.

The test conditions have not been formally defined at this time, however, all headsts will be tested under identical conditions using ANSI or military test procedures. It is noted that Telephonics does not have a headset which will be part of this evaluation program.

If you feel that you have a headset(s) suitable for the Space Shuttle program, we would appreciate receiving a technical description, together with price and delivery quotation for an evluation unit at your earliest convenience.

Sincerely,

TELEPHONICS, A Division of
Instrument Systems Corporation

Ed Joscelyn
Audio Products Engineering Manager

ISC A DIVISION OF INSTRUMENT SYSTEMS CORPORATION

APPENDIX B

LIST OF MANUFACTURERS SOLICITED

Adec Inc.
David Clark
Sennheiser
J. Ray Morris
Tibbetts Industries
Bolt Beranek & Newman
Dyna Magnetics Devices
Allen Tel Products
Altec Corp, Altec Div.
Applied Magnetics Corp.
Astatic Corp.
Astrocom Electronics Inc.
Audiosears Corp.
Avid Corp.
J.C. Carter Co.
Conrac Corp., Turner Div
Dobbs - Stanford Corp.
Dukane Corp.
Electro Vox Industries
Gulton/Electrovoice Inc.
Knowles Electronics
Koss Corp.
Lear Siegler Inc.
Matsushita, Panasonic
Mura Corp.
Murdock Corp.
Philmore Mfg. Co.
Plantronics Co.
Roanwell Corp.
Rye Industries
Scintrex Inc.
Telex Communications Co.

APPENDIX C

May 24, 1976

TELEPHONICS SCREENING AUDIOMETER

THD-39 with MX41/AR

SPL FOR 60 DB HTL

FREQ.	NORMAL CAL LEVEL (ANSI 1969)	MEASURED LEVEL RED	MEASURED LEVEL BLUE
250 HZ	85.5	8[illegible].0	83.5
500 HZ	71.5	7[illegible].0	69.5
1000	67.0	6[illegible].5	66.5
2000	69.0	6[illegible].0	67.0
3000	70.0	7[illegible].0	69.0
4000	69.5	6[illegible].5	68.5
6000	75.5	7[illegible].0	77.5

Hz	DECIBEL LOSS	
	RIGHT	LEFT
250	20	15
500	25	20
1000	15	15
1500		
2000	5	0
3000	0	0
[illegible]	0	0
6000	10	5
8000		

AUDIOGRAM RESULTS

☐ Hearing Normal
☐ Advised to Consult For Doctor

Class of Impairment ____________

CHECK ONE ☐ ANSI ☐ ISO ☐ ASA

AUDIOGRAM JOE "C"

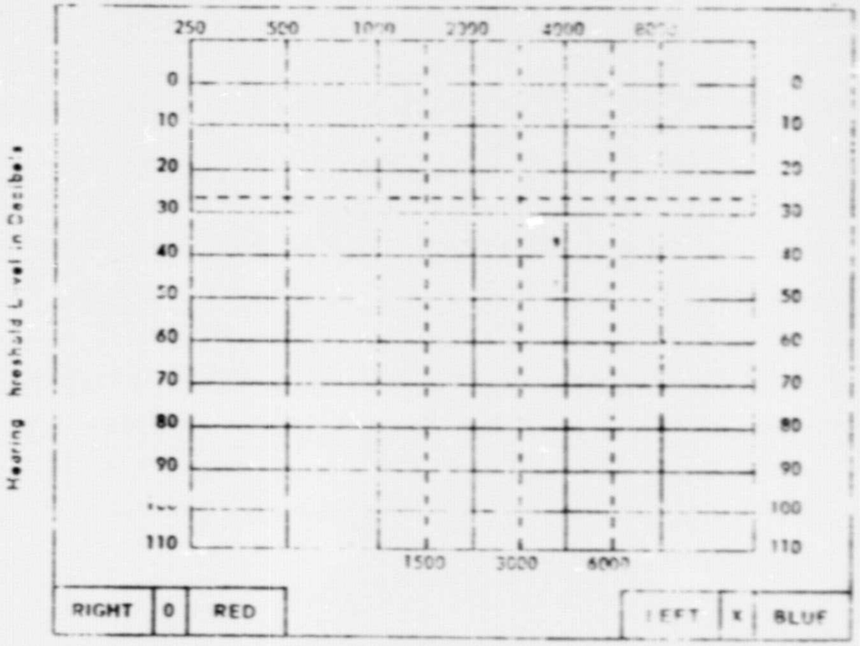

Technician ____________

Station ____________ Audiometer Serial No. ____________

Date ____________ Time ____________

EMPLOYERS INSURANCE OF WAUSAU

Hz	DECIBEL LOSS	
	RIGHT	LEFT
250	15	20
500	[illegible]	[illegible]
1000	10	10
1500		
2000	0	5
3000	0	0
4000	0	10
6000	0	5
8000		

AUDIOGRAM RESULTS

☐ Hearing Normal
☐ Advised to Consult Ear Doctor

Class of Impairment ____________

CHECK ONE: ☐ ANSI
☐ ISO
☐ ASA

PRINTED IN U.S.A.

AUDIOGRAM JUNE "O"

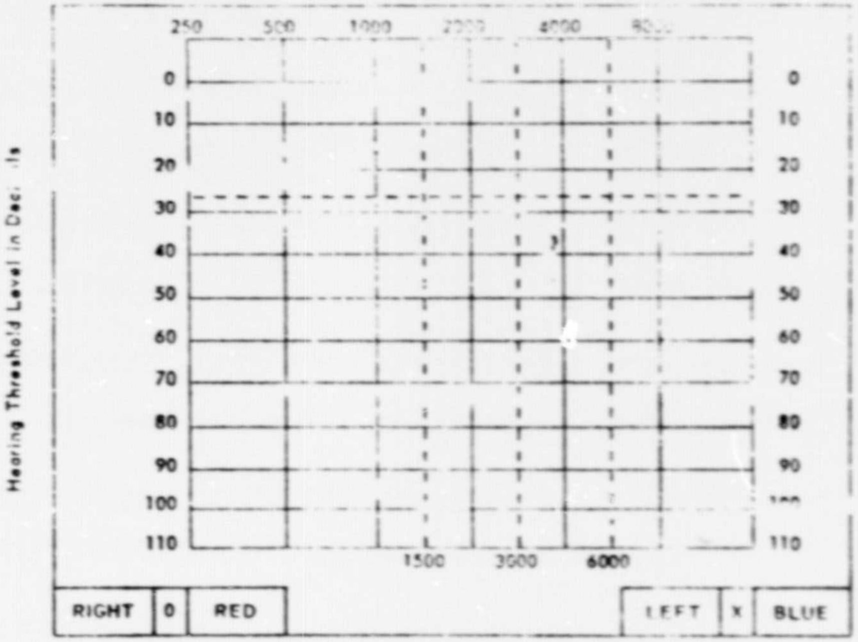

Technician ____________

Station ____________ Audiometer Serial No. ____________

Date ____________ Time ____________

EMPLOYERS INSURANCE OF WAUSAU

Hz	DECIBEL LOSS	
	RIGHT	LEFT
250	20	15
500	15	[illegible]
1000	0	0
1500		
2000	0	0
3000	15	20
4000	10	15
6000	0	10
8000		

AUDIOGRAM RESULTS

[ ] Hearing Normal
[ ] Advised to Consult Ear Doctor

Class of Impairment ______________________

AUDIOGRAM RUSS "G"

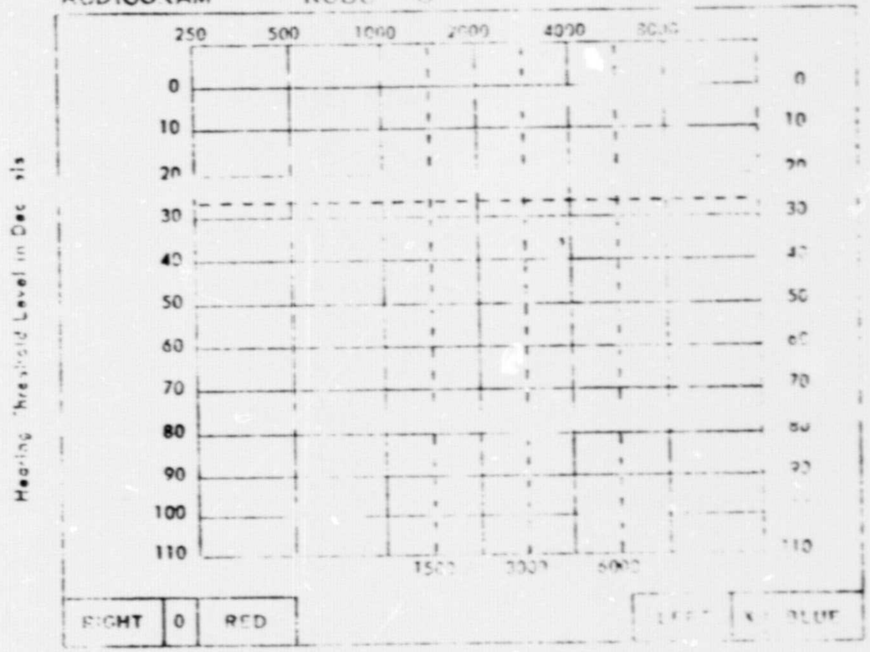

Technician ______________________ Audiometer

Station ______________________

Date ______________________ Time ______

EMPLOYERS INSURANCE OF WAUSAU

Hz	DECIBEL LOSS	
	RIGHT	LEFT
250	15	15
500	15	15
1000	0	0
1500		
2000	0	0
3000	15	20
4000	10	15
6000	0	10
8000		

AUDIOGRAM RESULTS

☐ Hearing Normal

☐ Advised to Consult Ear Doctor

Class of Impairment ____________

CHECK ONE: ☐ ANSI ☐ ISO ☐ ASA

PRINTED IN U.S.A.

AUDIOGRAM CATHY "D"

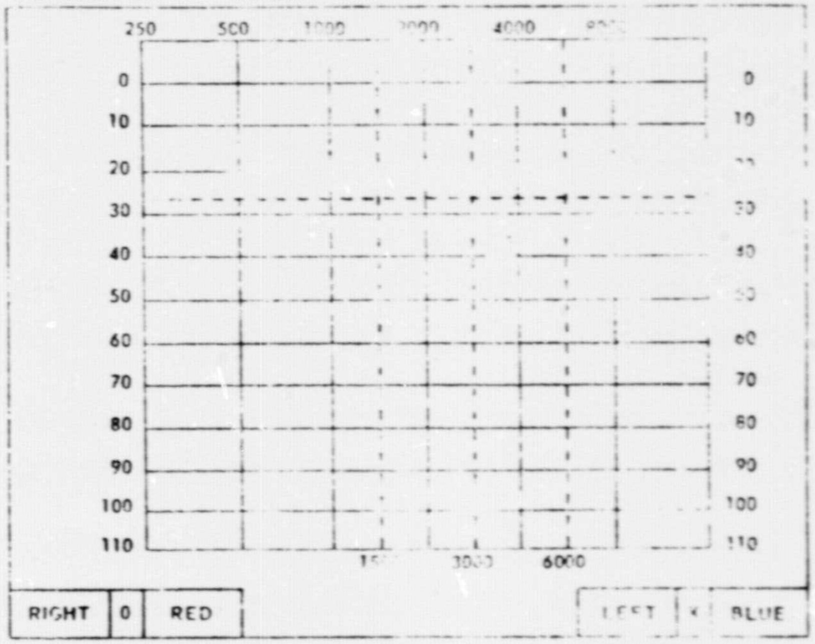

Technician ____________

Station ____________ Audiometer Serial No. ____________

Date ____________ Time ____________

EMPLOYERS INSURANCE OF WAUSAU

Hz	DECIBEL LOSS	
	RIGHT	LEFT
250	10	15
500	10	15
1000	5	10
1500		
2000	0	5
3000	0	5
[illegible]	0	0
6000	0	20
8000		

AUDIOGRAM RESULTS

☐ Hearing Normal
☐ Advised to Consult Ear Doctor

Class of Impairment ____________

CHECK ONE: ☐ ANSI ☐ ISO ☐ ASA

AUDIOGRAM MARIE "F"

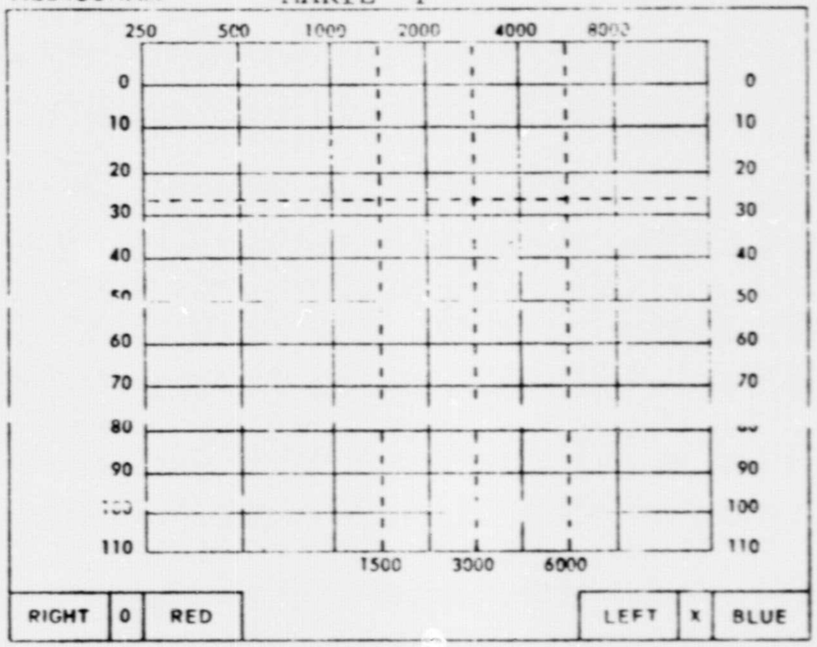

Technician ____________

Station ____________ Audiometer Serial No. ____________

Date ____________ Time ____________

PRINTED IN U.S.A.

EMPLOYERS INSURANCE OF WAUSAU

ORIGINAL PAGE IS
OF POOR QUALITY

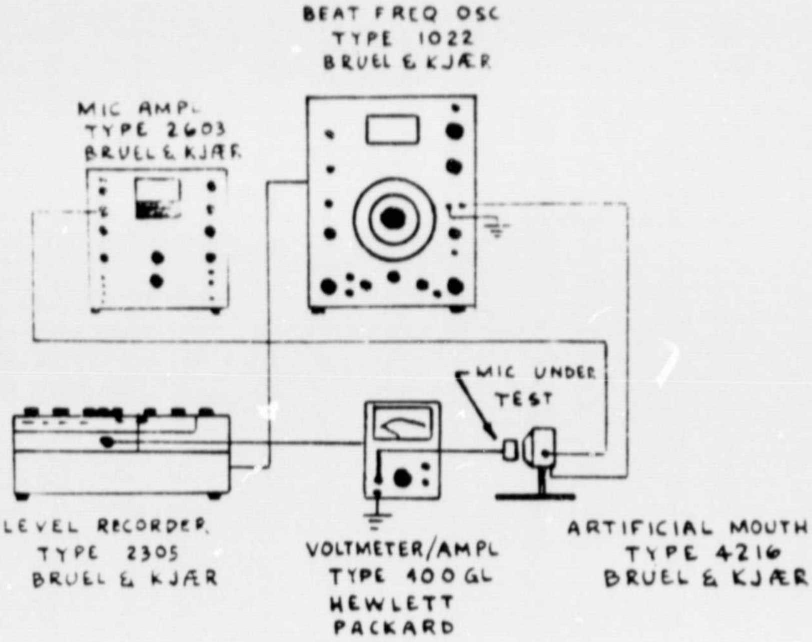

MICROPHONE TEST APPARATUS

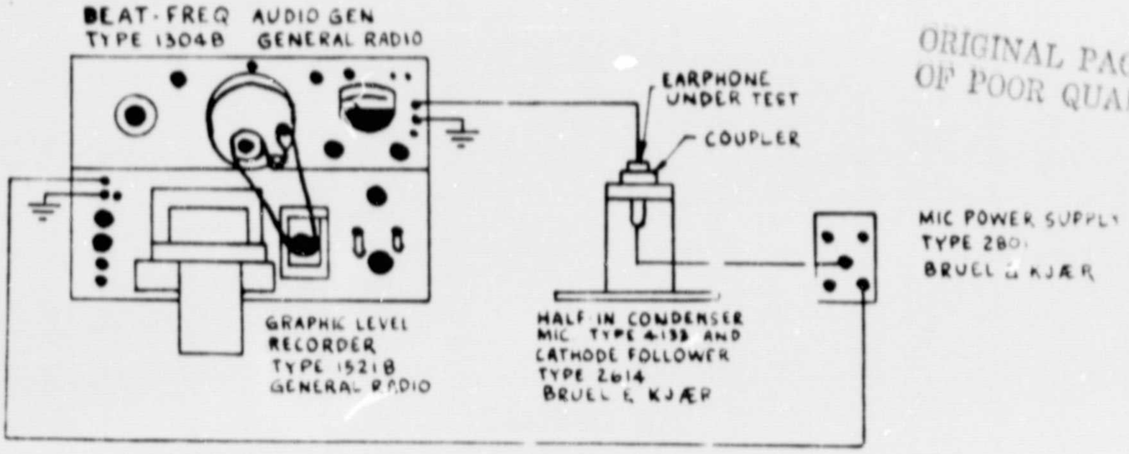

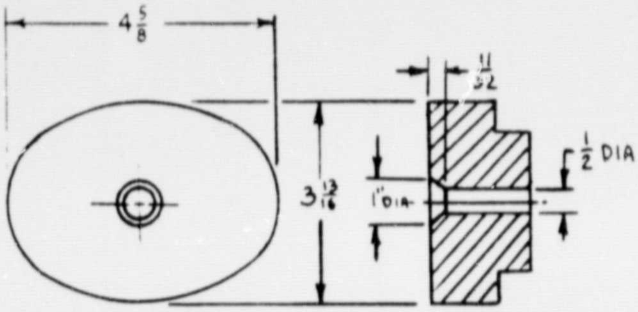

FLAT PLATE COUPLER

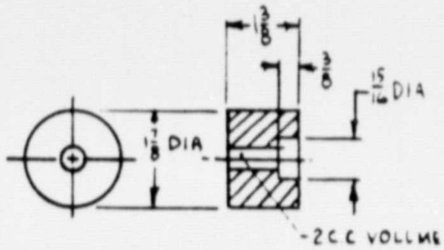

2 C.C COUPLER

EARPHONE TEST APPARATUS

HMD-110 MICROPHONE

QUIET

X	$X-\bar{X}$	$(X-\bar{X})^2$
98	-.4	.16
98	-.4	.16
100	1.6	2.56
96	-2.4	5.76
100	1.6	2.56
492		11.2

$\bar{X}$ = 98.4
V = 2.8
σ = 1.67

NOISE

X	$X-\bar{X}$	$(X-\bar{X})^2$
100	4.8	23.04
94	-1.2	1.44
94	-1.2	1.44
94	-1.2	1.44
94	-1.2	1.44
476		28.8

X = 95.2
V = 7.2
σ = 2.68

5x5
MICROPHONE

QUIET

X	$X-\bar{X}$	$(X-X)^2$
98	0	0
94	-4	16
98	0	0
100	2	4
100	2	4
490		24

$\bar{X} = 98.0$
$V = 6$
$\sigma = 2.45$

NOISE

X	$X-\bar{X}$	$(X-\bar{X})^2$
98	4	16
90	-4	16
92	-2	4
94	0	0
96	2	4
470		40

$X = 94.0$
$V - 10$
$\sigma = 3.16$

LT-730
MICROPHONE

QUIET

X	$X-\bar{X}$	$(X-\bar{X})^2$
98	-.8	.64
100	1.2	1.44
100	1.2	1.44
98	-.8	.64
98	-.8	.64
494		4.8

$\bar{X}$ = 98.8
V = 1.2
σ = 1.095

NOISE

X	$X-\bar{X}$	$(X-\bar{X})^2$
64	10.8	116.64
78	3.2	10.24
64	10.8	116.64
90	15.2	231.04
78	3.2	10.24
374		484.8

$\bar{X}$ = 74.8
V =121.2
σ = 11.0

HMD414
MICROPHONE

QUIET

X	X-$\bar{X}$	$(X-\bar{X})^2$
100	1.2	1.44
100	1.2	1.44
98	-.8	.16
100	1.2	1.44
96	-2.8	7.84
494		12.34

$\bar{X}$ = 98.8
V = 3.08
σ = 1.75

NOISE

X	X-$\bar{X}$	$(X-\bar{X})^2$
90	2.8	7.84
72	-15.2	231.04
98	10.8	116.64
84	- 3.2	10.24
92	4.8	23.04
436		388.8

$\bar{X}$ = 87.2
V = 97.2
σ = 9.85

125610
MICROPHONE

ORIGINAL PAGE IS
OF POOR QUALITY

[illegible]

X	$X-\bar{X}$	$(X-\bar{X})^2$
[illegible]	-1.6	2.56
[illegible]	+[illegible]	5.7[illegible]
[illegible]	-[illegible]	[illegible].5[illegible]
[illegible]	-1.6	[illegible]
[illegible]	+[illegible]	5.[illegible]
[illegible]		1[illegible]

NOISE

X	$X-\bar{X}$	$(X-\bar{X})^2$
94	11.6	134.56
80	-2.4	5.76
56	26.4	696.96
86	3.6	12.96
96	13.6	184.96
41[illegible]		1035.2

$\bar{X}$ = 82.4
V = 258.8
σ = 16

Telephonics
A DIVISION OF INSTRUMENT SYSTEMS CORPORATION

HS-2A
MICROPHONE

QUIET

X	$X-\bar{X}$	$(X-\bar{X})^2$
98	3	9
92	-3	9
96	1	1
94	-1	1
95	0	0
475		20

$\bar{X}$ = 95.0
V = 5
σ = 2.33

NOISE

X	$X-\bar{X}$	$(X-\bar{X})^2$
80	-1	1
82	1	1
74	-7	49
86	5	25
83	2	4
81		80

$\bar{X}$ = 81
V = 20
σ = 4.47

TAH-29
EARPHONE

QUIET

X	$X-\bar{X}$	$(X-\bar{X})^2$
92	-4.8	23.04
96	- .8	.64
98	1.2	1.4[illegible]
98	1.[illegible]	[illegible]
100	[illegible]	[illegible]
484		[illegible]

$\bar{X}$ = 9[illegible].[illegible]
V = 9.[illegible]
σ = [illegible].03

[illegible]

X	$X-\bar{X}$	$(X-\bar{X})^2$
98	5.8	3[illegible].[illegible]
94	1.8	[illegible]
90	-2.2	4.8[illegible]
90	-2.2	[illegible].8[illegible]
89	-3.2	10.2[illegible]
461		56.8

$\bar{X}$ = 92.2
V = 14.2
σ = 3.76

HMD414
EARPHONE

QUIET

X	X-$\bar{X}$	(X-$\bar{X}$)^2
96	1.6	2.56
94	-3.6	12.96
100	2.4	5.76
100	2.4	5.76
98	.4	.16
488		27.2

$\bar{X}$ = 97.6
V = 6.8
σ = 2.6

NOISE

X	X-$\bar{X}$	(X-$\bar{X}$)^2
50	5.2	27.04
40	-4.8	23.04
30	-14.8	219.04
64	19.2	368.64
40	- 4.8	23.04
224		660.8

$\bar{X}$ = 44.8
V = 165.2
σ = 12.85

5x5
EARPHONE

QUIET

X	X-$\bar{X}$	$(X-\bar{X})^2$
98	2.4	5.76
98	-7.6	57.76
96	.4	.16
96	.4	.16
100	4.4	19.36
478		83.2

$\bar{X}$ = 95.6
V = 20.8
σ = 4.56

NOISE

X	X-$\bar{X}$	$(X-\bar{X})^2$
74	+14	196
40	-20	400
54	- 6	36
42	-18	324
90	30	900
300		1856

$\bar{X}$ = 60
V =464
σ = 21.5

UNEX HS-2A
EARPHONE

QUIET

X	X-$\bar{X}$	$(X-\bar{X})^2$
94	-1.2	1.44
90	- 5.2	27.04
96	.8	.64
100	4.8	23.04
96	18	.64
476		52.8

$\bar{X}$ = 95.2
V = 13.2
σ = 3.63

NOISE

X	X-$\bar{X}$	$(X-\bar{X})^2$
48	-2	4
46	-4	16
66	16	256
36	-14	196
54	4	16
250		488

$\bar{X}$ = 50
V = 122
σ = 11.0

125610
EARPHONE

QUIET

X	X-$\bar{X}$	$(X-\bar{X})^2$
98	+2	4
92	-4	16
96	0	0
98	2	4
384		24

$\bar{X}$ = 96
V = 8
σ = 2.83

NOISE

X	X-$\bar{X}$	$(X-\bar{X})^2$
88	-11.5	132.25
82	5.5	30.25
94	17.5	306.25
42	-34.5	1190.25
306		1659.

$\bar{X}$ = 76.5
V = 553
σ = 23.52

HMD110
EARPHONE

QUIET

X	X-$\bar{X}$	$(X-\bar{X})^2$
96	-2	4
94	0	0
100	6	36
98	4	16
82	-12	144
470		200

$\bar{X} = 94$

$V_{or} = \frac{200}{4} = 50$

$\sigma = 7.07$

NOISE

X	X-$\bar{X}$	$(X-\bar{X})^2$
84	13.6	184.96
66	- 4.4	19.36
84	13.6	184.96
78	7.6	57.76
40	·30.4	924.16
352		1371.2

$\bar{X} = 70.4$

$V = 342.8$

$\sigma = 18.5$

A610
EARPHONE

QUIET

X	$X-\bar{X}$	$(X-\bar{X})^2$
92	0	0
88	-4	16
90	-2	4
96	4	16
94	2	4
460		40

$\bar{X}$ = 92
V = 10
σ = 3.16

NOISE

X	$X-\bar{X}$	$(X-\bar{X})^2$
30	14.4	207.36
20	4.4	19.36
10	- 5.6	31.86
8	- 7.6	57.76
10	- 5.6	31.36
78		34.72

$\bar{X}$ = 15.6
V = 86.8
σ = 9.32

Telephonics
A DIVISION OF INSTRUMENT SYSTEMS CORPORATION

LT-730
EARPHONE

QUIET

X	$X-\overline{X}$	$(X-\overline{X})^2$
96	-.5	.25
96	-.5	.25
96	-.5	.25
98	1.5	2.25
-	-	-
386		3

$\overline{X}$ = 96.5
V = 1
σ = 1

NOISE

X	$X-\overline{X}$	$(X-\overline{X})^2$
50	-1	1
48	-3	9
84	33	1089
22	29	841
-	-	-
204		1940

$\overline{X}$ = 51
V = 646.6
σ = 25.42

Statistical Significance

The statistical significance of the intelligibility data is calculated below. The t distribution test was used. The results of the test illustrate that the rank ordering in many cases is justified. The large variance between subjects, however, in other cases showed the data not sampled sufficiently to achieve statistical significance. Samples from perhaps 20-30 tests would be necessary to accomplish this end.

The following example illustrates the calculation techniques used.

Comparison of HMD414 and A610 earphone under no noise conditions.

$\bar{X}_{414} = 97.6$

$\bar{X}_{610} = 92$

Pick 90 as arbitiary origin

Let $\xi = X - 90$ and $C = \bar{X} - 90$

ξ_{414}	ξ^2_{414}
6	36
4	16
10	100
10	100
8	64
	316

$C_{414} = 97.6-90$

$\xi_{[illegible]}$	[illegible]
[illegible]	[illegible]
[illegible]	[illegible]
[illegible]	[illegible]
6	36
4	16
	60

$C_{610} = 92-90$

$$s^2_{414} = \frac{\sum \xi^2_{414} - N_{414}C^2_{414}}{N_{414}-1} = \frac{316 - 5(57.76)}{4} = 6.8$$

$$s^2_{610} = \frac{\sum \xi^2_{610} - N_{610}C^2_{610}}{N_{610}-1} = \frac{60 - 5(4)}{4} = 10.0$$

$$s^2_{\bar{X}_{414}} = \frac{6.8}{5} = 1.36$$

$$s^2_{\bar{X}_{610}} = \frac{10}{5} = 2.00$$

$t_{0.025}\ (n = 4) = 2.776$

Cirtical value $t_{.025} = \pm \frac{1.36\ (2.776) + 2.00\ (2.776)}{1.36 + 2.00} = \pm\ 2.776$

to test difference

$$\frac{\bar{X}_{414} - \bar{X}_{610}}{\sqrt{S^2_{\bar{X}_{414}} + S^2_{\bar{X}_{610}}}} = \frac{97.6 - 92}{\sqrt{1.36 + 2}} = \frac{56}{1.833} = 3.055$$

This does not lie within critical values ± 2.776 and therefore the 414 can be considered statistically significantely better than the A610.

TAH-29 Compared to 125610 Earphone in noise.

$\bar{X}_{29} = 92.2$ Let $\xi = X-90$

Let $C = \bar{X}-90$

$\bar{X}_{125} = 76.5$

$N = 5$		$N = 4$	
ξ_{29}	ξ^2_{29}	ξ_{125}	ξ^2_{125}
8	64	-2	4
4	16	-8	64
0	0	4	16
0	0	-48	2304
-1	1		2378
	81		

$C_{29} = 92.2-90$

$$S^2_{29} = \frac{\Sigma \xi^2_{29} - N_{29}C^2_{29}}{N_{29}-1} = \frac{81 - 5(2.2)^2}{4} = 14.2$$

$$S^2_{125} = \frac{2378 - 4\ (-13.5)^2}{3} = 549.66$$

$$S^2_{\bar{X}_{29}} = \frac{14.2}{5} = 2.84$$

$$S^2_{\bar{X}_{125}} = \frac{549.66}{4} = 137.4$$

Telephonics

A DIVISION OF INSTRUMENT SYSTEMS CORPORATION

$$t_{.025} = \pm \frac{2.84(2.776) + 137.4(3.182)}{2.84 \pm 137.4} = \frac{445.08}{140.24} = \pm 3.17$$

$$\frac{\bar{X} - \bar{X}}{\sqrt{s^2_{\bar{X}} + s^2_{\bar{X}}}} \qquad \frac{92.2 - 76.5}{\sqrt{2.84 + 137.4}} = 1.325$$

Not Statistically Sig

The statistical signficance for noise is indicated in the matrix below:

Headset In
Column below
is statistically
significant when
compared to headset in
Column to the right

	TAH29	125610	HMD110	5x5	LT-730	HS-2A	HMD414	A610
TAH-29	-			/*	/*	/*	/*	/*
125610		-						/*
HMD110			-		*/			/*
5x5				-	*/			/*
LT-730					-			/*
HS-2A						-		/*
HMD414					/		-	
A610								-

*Indicates Statistically Significant

Microphone/Headset

(Not all combinations calculated)

Telephonics CORPORATION

WIRELESS MICROPHONE COMMUNICATION SYSTEM

REPORT NO. WMCS–001

APPENDIX F

1.0 Scope

This report covers the results of performance tests that were conducted on April 4, 5, and 26, 1977 on the wireless microphone for the Space Shuttle Program. These evaluations were performed in a shielded enclosure and in an open laboratory as outlined below:

- The testing in the shielded enclosure measured the operating range of the wireless microphone system at various locations in the enclosure, with various alignments of the transmitter antenna in reference to the receiving antenna, and with the antenna aligned for minimum coupling.

- The testing in the laboratory was to establish the minimum RF level at the band pass filter output for normal system operation.

2.0 Test Location

The tests covered by this report were performed in

a) Copper screen shielded enclosure manufactured by Ace Engineering and Manufacturing Company. The enclosure inside dimensions are 19.5' x 19.5' x 9.5' high.

b) The laboratory area at Telephonics Corporation.

3.0 Test Sample and Test Equipment

3.1 Test Sample

The test sample consisted of one transmitter and one receiver unit. The transmitter unit was powered by a battery pack and the receiver unit by a 60 Hz power supply. The transmitter unit is identified as Prototype Serial #1 and the receiver is Prototype Serial #1 without ICOM function. The receiver was modified by the installation of a transformer at the output of the band pass filter. This four to one auto transformer output was connected to a VTVM that provided for voltage measurements of the RF energy level in each receiver.

3.2 Test Equipment

The test equipment used for the shielded enclosures portion of this evaluation is:

- HP 400D ISC #120177 Cal due 6/10/77

- HP 400 HR ISC #120631 Cal due 6/10/77

The following additional test equipment was employed for the laboratory area:

- HP 654P ISC 120464 Cal due 10/4/77
- HP 400CL ISC 121042 Cal due 8/11/77
- HP 3581C ISC 122105 Cal due 6/10/77
- HP 3593A ISC 120918 Cal due 6/4/77

4.0 Test Procedure

4.1 Shielded Enclosure Tests

A block diagram of the basic test setup is shown on Figure #1 of this report.

The location of the receiver and transmitter within the enclosure is shown on Figures #2 and #3.

The following outlines the procedure used for all measurements:

- RF voltage level was measured at the output of the band pass filters with VTVM.
- Alignment of the receiver transmitter antenna is noted on each data sheet.
- Physical location of transmitter and receiver within the enclosure is shown on Figures #2 and #3 with the applicable figure noted on the individual data sheets.

The data for this evaluation are recorded on Data Sheets 1 through 23.

4.2 Laboratory Area Tests

The purpose of this evaluation was to measure the relationship of the RF level at the band pass filter output to the receiver audio output. A block diagram of the basic test setup is shown on Figure #4.

The following outlines the setup and measurement procedures used for this evaluation.

1. The receiver was modified by removing the antenna and using a loop of wire approximately 2" diameter.

2. The transmitter RF signal was modulated with a 455 Hz signal at an input level of 100 uv.

3. The transmitter and receiver antennas were aligned to provide an RF level at the band pass filter at a predetermined level.

4. The RF level was measured and recorded as was the audio output level.

5. Testing was also performed to measure the loading effect resulting from the transformer that was installed at the band pass filter output.

   The data from this evaluation are tabulated on Data Sheets #23 and #24.

5.0 Results

The following paragraphs outline the results of this evaluation for each test setup.

5.1 Shielded Enclosure

5.1.1 Test Setup per Figure #2 with TX on Line 1

The data for this evaluation are tabulated on Data Sheets 1,4,5,10, and 20. The results are outlined below:

a) Data Sheet #1 indicates that, with this setup, the system had an effective operating range greater than 15 feet. The measured RF level at 15 feet was 50 and 54 dB above one microvolt. The measured system threshold (Data Sheet #24) was 40 dB uv or 10 to 14 dB less than was possible with the test setup used for the shielded enclosure tests. The range increase for 10 dB is equal to a ratio of 1.47 or 22 feet and a ratio of 1.7 or 26 feet for 14 dB.

b) Data Sheets #4,5,10 and 20 are similar to Data Sheet #1, indicating an equivalent range.

These test results, in reference to similar tests that were performed in open areas at Telephonics, indicate that the range was decreased from approximately 30 feet to 24 feet when the system is operated in a metal enclosure.

5.1.2 Test Setup Per Figure #2 with TX on Line 2A - 2B.

The data for this evaluation are tabulated on Data Sheets 2,3,6,9,15,21 22 and 23. The results are outlined below.

a) Data Sheet #2 indicates that, with this setup on Line 2A, the system had an effective operating range of greater than 15 feet. The increased range is in the order of 22 feet. Data with the TX on line 2B indicates that the levels are lower when the TX is located in the corner of the enclosure.

b) Data Sheets #3,6,9 and 23 are similar to Data Sheet #2.

c) Data Sheet #15 has the data with the transmitter next to the floor and wall of the enclosure. At a range of 7.2 feet, the RF output level was 8 to 10 dB above threshold for a calculated range of 10.5 feet.

d) Data Sheet #21 has the data with the receiver on the floor 4 feet from the enclosure corner. The transmitter was next to the enclosure floor and wall. These data indicate that the system range was limited for this condition and that the field attenuation did not conform to a distance cube function. The field attenuation is 4th to 5th power of distance. The calculated range for this configuration is 6.5 to 7.5 feet.

e) Data Sheet #22 has the data with the receiver on the floor and the transmitter on the floor 28" from the wall. These data indicate that the system range is between 6.2 and 8.1 ft. Correcting the range, using the data from data Sheet #24, results in a range of 10.6 feet.

5.1.3 Test Setup per Figure #2 with TX on Line 3A and B

The data from this evaluation are tabulated on Data Sheets #7 and #8. This test was performed on a 2 and 3.66 foot spacing. The data does not show a major difference between Line A and Line B.

5.1.4 Test Setup per Figure #3 with TX on Line 1.

The data for this evaluation are tabulated on Data Sheets #11, 13, and 14. The results are outlined below:

a) Data sheets #11 and #14 indicate that the system effective operating range is 4 to 6 feet. Correcting the range using the data from Data Sheet #24 results in an effective range of 7.7 feet using the data from Data Sheet #11.

b) Data Sheet #13 indicates that the range is increased when the transmitter is moved away from the enclosure wall and floor. The effective range is 8 feet and 11.7 feet with correction.

5.1.5 Test Setup poer Figure #3 with TX on Line 2.

The data for this evaluation are tabulated on Data Sheet #12. The results indicate that the system effective range is between 6 and 8 feet. The effective range is 10.6 feet with correction.

5.1.6 Test Setup per Figure #3 with TX on Line 3

The data for this evaluation are tabulated on Data Sheet #16 and #17 and outlined below:

a) Data Sheet #16 indicates that the system effective operating range is approximately 10 feet. The effective range is 15.25 feet with correction.

b) Data sheet #17 indicates that the system effective operating range is 10 feet. The effective range is 16.5 feet with correction.

The above indicates a small improvement due to spacing the TX away from the floor.

5.1.7 Test Setup per Figure #3 with TX on Line 4.

The data for this evaluation are tabulated on Data Sheets #18 and #19 and outlined below:

a) Data Sheet #18 indicates that the system effective operating range is approximately 10 feet. The effective range is 17 feet when corrected.

b) Data Sheet #19 indicates that the system effective operating range is increased to 12 feet when the Tx is moved away from the floor. The effective range is 17 feet when corrected.

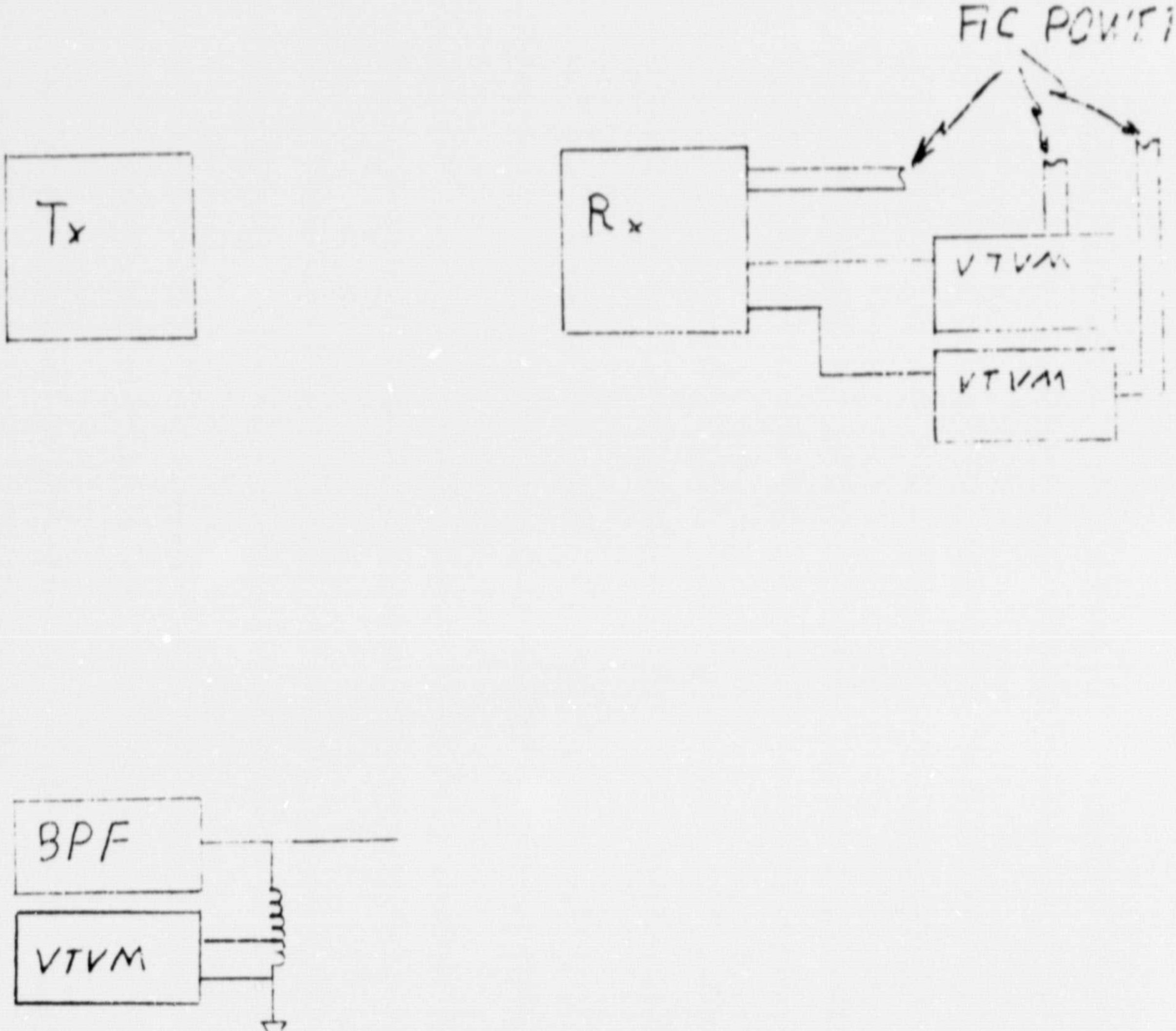

FIG # 1

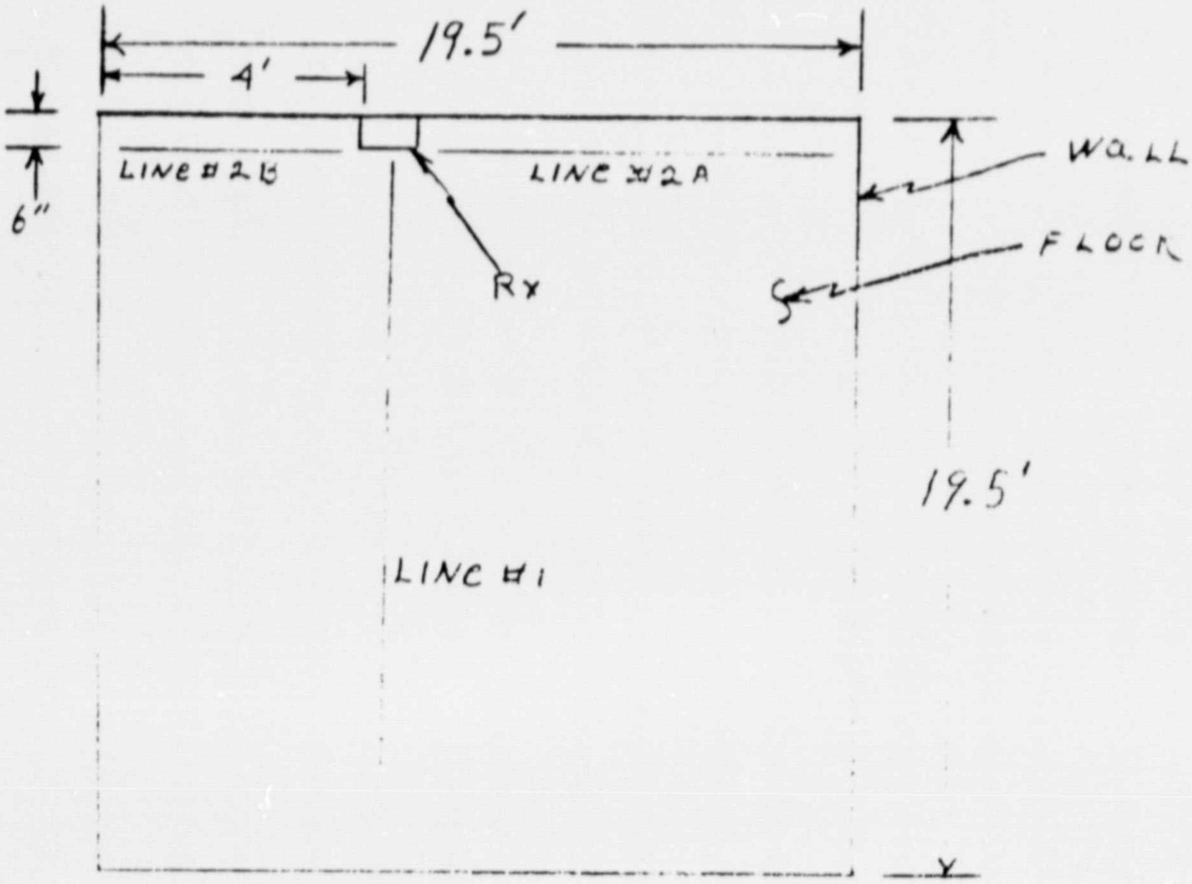
19.5'
4'
6"
LINE #2B
LINE #2A
RX
WALL
FLOOR
19.5'
LINE #1

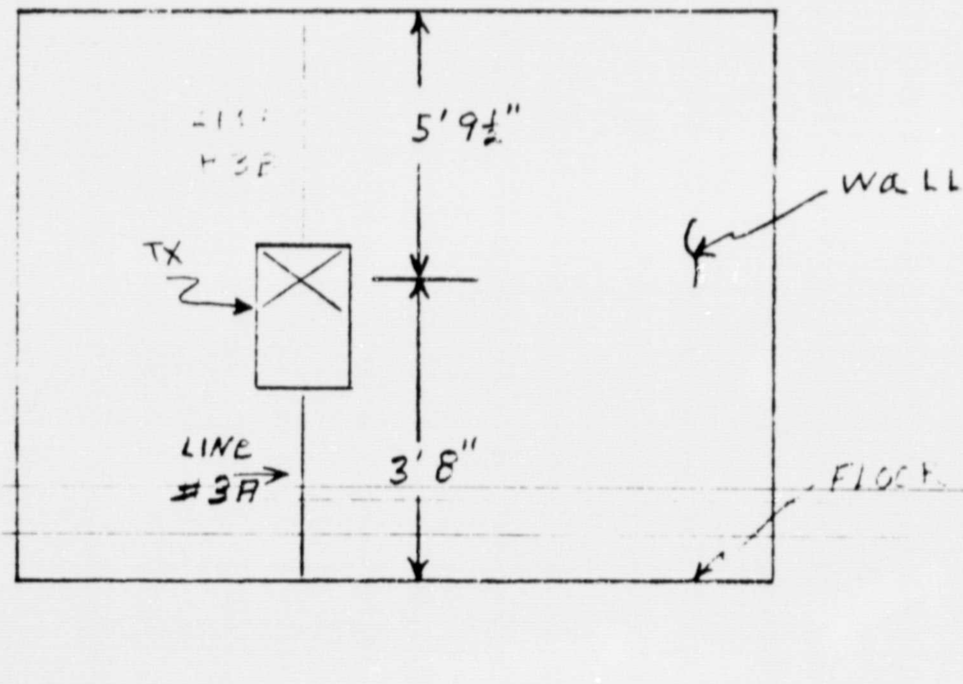
5' 9½"
TX
WALL
LINE
#3A
3' 8"

FIG #2

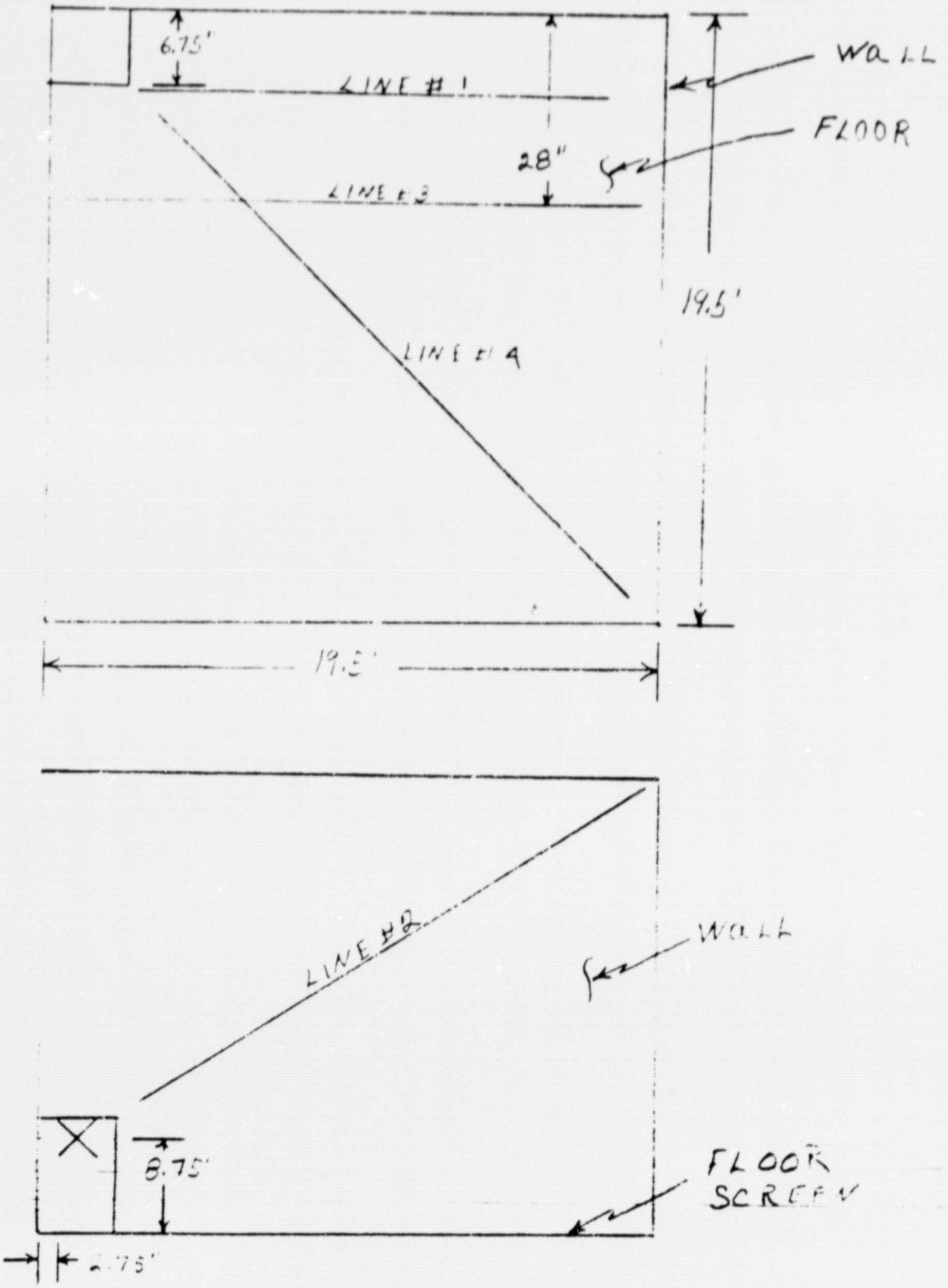
6.75'
LINE #1
WALL
FLOOR
28"
LINE #3
19.5'
LINE #4
19.5'
LINE #2
WALL
8.75'
FLOOR
SCREEN
2.75'

FIG #3

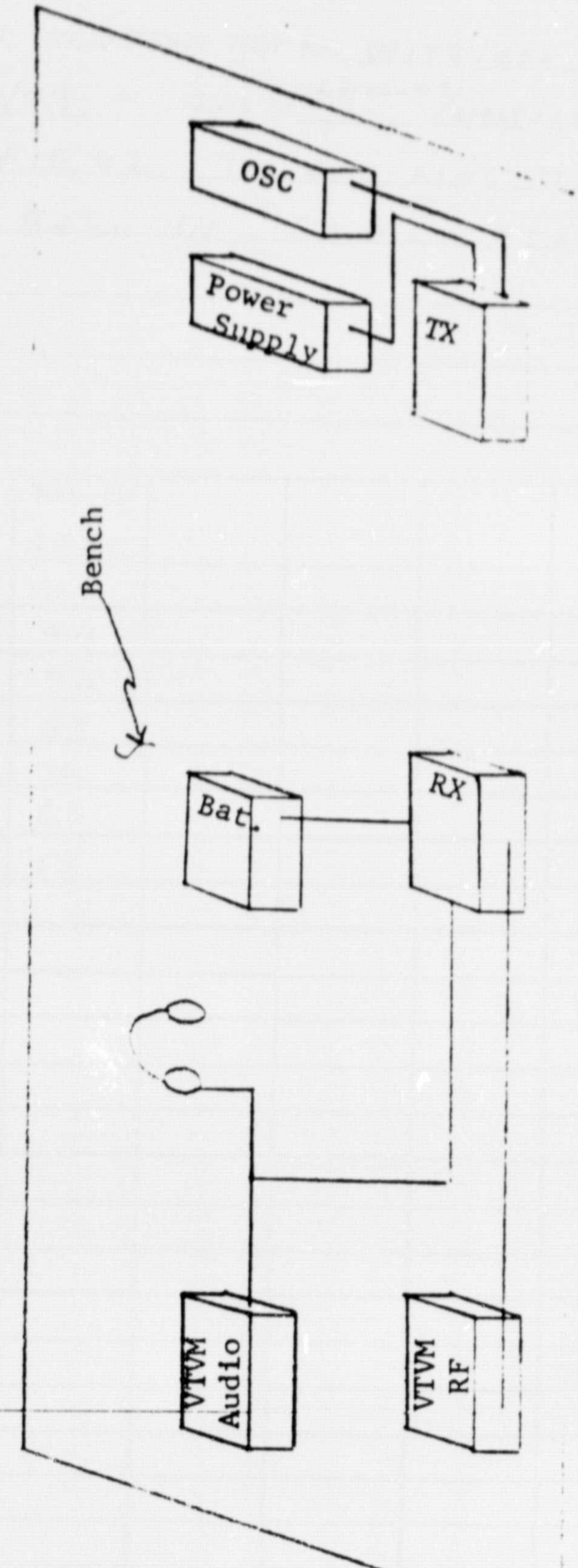

Figure #4

ELECTROMAGNETIC INTERFERENCE TEST NO. Wireless Mic.

TEST DATE 4/4/77 TEST BY LAMONT/WALTERS DATA SHEET 1

TEST SETUP FIG. #2 TX ON LINE #1 TX and RX ANT. IN same plane and aligned

TEST SAMPLE MOD.

TX-TO-RX FT	Rec. A dBμV	Rec. B dBμV
1	106	107
2	94	99
3	82	90
4	72	83
6	63	72
10	54	60
15	50	54

ELECTROMAGNETIC INTERFERENCE TEST NO. Wire less mic

TEST DATE 4/4/77 TEST BY Walters/Lamont DATA SHEET 2

TEST SETUP FIG. #2 TX on Line 2A-2B TX and Rx antenna in same plane and aligned

TEST SAMPLE MOD.

TX-TO-RX. FT	RX.A dBuV	RX.B dBuV					Note
1	106	107					LINE 2A
2	101	102					
3	90	95					
4	77	87					
6	63	72					
10	54	59					
15	48	50					
14	42	56					LINE 2A
2	101	102					LINE 2B
4	71	82					LINE 2B

ELECTROMAGNETIC INTERFERENCE TEST NO. wire less mic

TEST DATE 4/4/77 TEST BY Lamont/walters DATA SHEET 3

TEST SETUP FIG. 02 TX on line 2A TX aligned For. min.

TEST SAMPLE MOD.

TX-TO-RX FT.	RX. A dBμV	RX. B dBμV
2	90	102
2	87	102
2	98	100
2	97	101
2	99	101
4	68	68
4	76	85
6	68	73
6	65	71
10	55	57
10	52	59

ELECTROMAGNETIC INTERFERENCE TEST NO. Wire less Mic

TEST DATE 4/4/77 TEST BY Walters/ Lamont DATA SHEET 4

TEST SETUP FIG. #2 TX ON line #1 TX-RX ANT IN same plane. TX aligned for max.

TEST SAMPLE MOD.

TX-TO-RX Ft	RX. A	RX. B					
2	97	83					
2	91	95					
4	75	66					
4	70	78					
6	65	61					
6	62	69					
10	56	54					
10	53	59					
15	< 48	52					
15	49	< 46					

ELECTROMAGNETIC INTERFERENCE TEST NO. Wire less Mic.

TEST DATE 1/4/77 TEST BY Lamont/ Walters DATA SHEET 5

TEST SETUP FIG #2 line #1 Rx-Tx ant. Planes 90°

TEST SAMPLE MOD.

TX-TO-RX FT	RX, A dBuV	RX. B dBuV					
2	67	98					
2	97	89					
4	61	80					
4	72	71					
6	63	62					
6	56	70					
10	51	60					
10	55	57					
15	49	52					
15	55	46					

ELECTROMAGNETIC INTERFERENCE TEST NO. Wire less Mic

TEST DATE 4/5/77 TEST BY Lamont/Walters DATA SHEET 6

TEST SETUP FIG. #2 LINE 2A-B Rx-Tx ANT PLANES 90°

TEST SAMPLE MOD.

Rx-To-Tx FT.	Rx. A dBμV	Rx. B dBμA					NOTE
2	110	93					LINE 2A
2	88	100					↑
4	80	72					
4	68	82					
6	66	59					
6	59	69					
10	55	48					
10	52	58					
15	48	48					↓
15	*	*					LINE 2A
2	100	90					LINE 2B
2	87	101					↑
4	76	87					
4	52	87					
4	79	46					↓
4	83	80					LINE 2B
*	Level	below	Noise				

ELECTROMAGNETIC INTERFERENCE TEST NO. wireless Mic

TEST DATE 4/5/77 TEST BY Lamont/Walters DATA SHEET 7

TEST SETUP FIG. #2 Tx ON LINE 3A ANTENNA IN SAME PLANE AND ALIGNED

TEST SAMPLE MOD.

Rx-To-Tx Ft	Rx. A, dBμV	Rx. B dBμV					
2	97	95					
3.66	81	87					
ANT.	Same	Plane	Aligned	For max			
2	100	85					
2	97	108					
3.66	83	87					
3.66	80	77					
ANT.	Plane	90°					
2	87	93					
2	92	75					
3.66	83	87					
3.66	78	79					
3.66	75	83					

ELECTROMAGNETIC INTERFERENCE TEST NO. wire Less Mic

TEST DATE 9/5/77 TEST BY Lomont / Wolters DAIA SHEET 8

TEST SETUP FIG #2 TX ON LINE 3B

TEST SAMPLE MOD.

RX-TO-TX FT	Rx A. dBuV	Rx. B dBuV					
3.66	83	81	ANT same plane				
3.66	74	82	90° between ANT				
3.66	81	86	90° between ANT TX on Line 3A.				

ELECTROMAGNETIC INTERFERENCE TEST NO. Wire less Mic

TEST DATE 4/5/77 TEST BY Lamont/ Walters DATA SHEET 9

TEST SETUP FIG. #2 TX ON LINE Z A TX Aligned For min.

TEST SAMPLE MOD.

Rx-To-Tx FT	Rx. A dBuV	Rx. B dBuV					
2	51	91					
2	97	<48					
4	75	<48					
4	<48	86					
6	<48	71					
6	63	<48					
10	<48	57					
10	54	<48					

ELECTROMAGNETIC INTERFERENCE TEST NO. Wire Less Mic

TEST DATE 4/5/77 TEST BY Lamont Walters DATA SHEET 10

TEST SETUP TX ON Line 1 OF FIG #2

ANT ALIGNED FOR min.

TEST SAMPLE NO.

RX-TO-TX Ft	RX.A. dBuV	RX.B. dBuV					
2-	97	92					
2	86	<48					
4	<48	77					
4	65	<48					
6	<48	69					
6	59	<48					
10	<48	60					
10	52	<48					
13	<48	55					
13	48	<48					

ELECTROMAGNETIC INTERFERENCE TEST NO. Wire Less Mic

TEST DATE 4/5/77 TEST BY Lamont/Walters DATA SHEET 11

TEST SETUP FIG. #3 Line #1 ANT. Aligned For MIN. Tx Same Hi AS P.C. Next To wall

TEST SAMPLE N...

RX-TO-TX FT	RX-A dBμV	RX-B dBμV				
2	< 48	82				
2	100	< 48				
4	< 48	56				
4	69	< 48				
6	< 48	< 48				
6	< 48	< 48				

ELECTROMAGNETIC INTERFERENCE TEST NO. Wire Less Mic

TEST DATE 4/5/77 TEST BY Lamont/Walters DATA SHEET 12

TEST SETUP Fig. #3 TX on Line 2 TX ANT Aligned for Min.

TEST SAMPLE MOD.

Rx-to-Tx FT	Rx A dBuV	Rx B dBuV					
2	< 48	93					
2	93	< 48					
4	< 48	67					
4	67	< 48					
6	< 48	56					
6	55	< 48					
8	< 48	< 48					
8	< 48	< 48					

ELECTROMAGNETIC INTERFERENCE TEST NO. wire less mic

TEST DATE 4/5/77 TEST BY Lamont/ Wolters DATA SHEET 14

TEST SETUP FIG #3 TX ON LINE #1 EXCEPT TX ANT NEXT TO FLOOR AND WALL

TEST SAMPLE MOD.

RX-TO-TX FT	RX-A. dBuV	RX-B. dBuV					
2	<48	84					
2	92	<48					
4	<48	59					
4	60	<48					
6	<48	<48					
6	<48	<48					

ELECTROMAGNETIC INTERFERENCE TEST NO. WIRE LOSS MIC

TEST DATE 4/5/77 TEST BY LAMONT/WALTERS DATA SHEET 13

TEST SETUP FIG. #3 TX ON LINE #1 ANT. ALIGNED FOR MIN. TX SAME DISTANCE FROM FLOOR AND WALL AS RX.

TEST SAMPLE MOD.

RX-TO-TX FT	RX-A. dBNV	RX.B. dBNV				
2	<48	95				
2	99	<48				
4	<48	66				
4	67	<48				
6	<48	54				
6	55	<48				
8	<48	<48				
8	50	<48				

ELECTROMAGNETIC INTERFERENCE TEST NO. wire less mic.

TEST DATE 4/5/77 TEST BY Lamont Walters DATA SHEET 15

TEST SETUP Fig #2 TX on line 2A-2B next to floor and wall

TEST SAMPLE MOD.

RX-TO-TX FT	RX-A dBuV	RX-B dBuV					NOTE
4	<48	77					LINE 2A ↑
4	68	<48					
4.5	<48	75					
4.5	64	<48					
5.6	<48	62					
5.6	68	<48					
7.2	<48	50					↓
7.2	40	<48					LINE 2A
5.4	<48	66					LINE 2B
5.4	64	<48					LINE 2B

ELECTROMAGNETIC INTERFERENCE TEST NO. Wire Less Mic

TEST DATE 4/15/77 TEST BY Lamont/Walters DATA SHEET 16

TEST SETUP Fig #3 TX on Line 3, Next to Floor

TEST SAMPLE MOD.

RX-TO-TX FT	RX-A. dBuV	RX-B. dBuV					
0	<50	100					
0	93	<48					
2	<50	91					
2	92	<48					
4	<50	70					
4	70	<48					
6	<50	58					
6	57	<48					
8	<50	<48					
8	55	<48					
10	<50	<48					
10	51	<48					

ELECTROMAGNETIC INTERFERENCE TEST NO. With Less Mic

TEST DATE 4/5/77 TEST BY Lamont / Walters DATA SHEET 17

TEST SETUP Figure #3 TX on Line 3 8.75" above floor

TEST SAMPLE MOD.

RX-TO-TX FT	RX A dBuv	RX B dBuv					
0	48	98					
0	95	<48					
2	<48	90					
2	93	<48					
4	<48	70					
4	71	<48					
6	<48	58					
6	59	<48					
8	<48	50					
8	55	<48					
10	<48	<48					
10	53	<48					

ELECTROMAGNETIC INTERFERENCE TEST NO. Wire Less Mic

TEST DATE 4/5/77 TEST BY Lomont/ Walters DATA SHEET 18

TEST SETUP FIG #3 TX ON LINE 4 ON FLOOR.

TEST SAMPLE MOD.

RX-TO-TX FT.	RX. A. dBuV	RX. B. dBuV
2	<48	97
2	95	<48
4	<48	78
4	69	<48
6	<48	66
6	59	<48
8	<48	59
8	54	<48
10	<48	54
10	51	<48
12	<48	49
12	*	*

* Below Voltmeter Noise

ELECTROMAGNETIC INTERFERENCE TEST NO. Wire Less Mic

TEST DATE 4/5/77 TEST BY Lamont/Walters DATA SHEET 19

TEST SETUP FIG #3 TX on Line 4 6" off Floor

TEST SAMPLE MOD.

RX-TO-TX FT.	RX-A. dBNV	RX-B. dBNV				
2	<48	98				
2	99	<48				
4	<48	80				
4	69	<48				
6	<48	67				
6	58	<48				
8	<48	38				
8	54	<48				
10	<48	53				
10	52	<48				
12	<48	49				
12	*	*				
	* Below	Volt	meter	Noise		

ELECTROMAGNETIC INTERFERENCE TEST NO. Wire Less Mic

TEST DATE 4/5/77 TEST BY Lamont/Wolters DATA SHEET 20

TEST SETUP Fig #2 Rec. 7 FT from corner

Tx on Line #1

TEST SAMPLE MOD. ______

Rx-to-Tx Ft	Rx-A dBuV	Rx-B dBuV					
2	48	93					
2	91	<48					
4	<48	79					
4	71	<48					
6	<48	70					
6	63	<48					
8	<48	63					
8	58	<48					
10	<48	59					
10	55	<48					
12	<48	55					
12	52	<48					
14	<48	53					
14	49	<48					

ELECTROMAGNETIC INTERFERENCE TEST NO. Wire less Mic

TEST DATE 4/5/77 TEST BY (Lamont) Walters DATA SHEET 21

TEST SETUP Fig #2 Rec on Floor

Tx on Line 2A Next to Floor

and Wall

TEST SAMPLE MOD.

Rx-To-TV FT	Rx-A dBNV	Rx-B dBNV					
2	<48	84					
2	97	<48					
4	<48	58					
4	60	<48					
6	<48	<48					
6	<48	<48					

ELECTROMAGNETIC INTERFERENCE TEST NO. Wire Less Mic

TEST DATE 4/5/77 TEST BY Lomont/Walters DATA SHEET 22

TEST SETUP Fig H2 Rec on Floor

TX on Line 2A Next to Floor

28" From wall

TEST SAMPLE MOD.

RX-TO-TX FT	RX-A. dBuV	RX-B. dBuV					
2.33	<48	90					
2.33	101	<48					
3	<48	83					
3	87	<48					
4.3	<48	62					
4.3	60	<48					
6.2	<48	54					
6.2	53	<48					
8.1	<48	<48					
8.1	<48	<48					

ELECTROMAGNETIC INTERFERENCE TEST NO. wire less mic

TEST DATE 4/5/77 TEST BY lamont/ walters 23

TEST SETUP Fig 2 TX on line 2A next to wall

TEST SAMPLE NO.

ORIGINAL PAGE IS OF POOR QUALITY

RX-TO-TX FT	RX-A. dBuV	RX-B. dBuV					
2	<48	99					
2	95	<48					
4	<48	81					
4	71	<48					
6	<48	67					
6	62	<48					
8	<48	59					
8	57	<48					
10	<48	55					
10	53	<48					
12	<48	50					
12	50	<48					

ELECTROMAGNETIC INTERFERENCE TEST NO. Wire Less Mic

TEST DATE 1/26/77 TEST BY Walters DATA SHEET 24

TEST SETUP Fig #4.

TEST SAMPLE NO.

RX-A. RF dBμV	RX-A. Audio dBμV			RX-B. RF dBμV	RX-B. Audio dBμV		
38	OFF			40	88 *		
40	102 *			46	101 *		
46	105			50	101		
50	104			52	100		
52	104			54	101		
54	104			56	101		
56	104			57	101		
57	105			58	101		
58	105			59	101		
59	105			60	101		
60	105			64	102		
64	105			66	102		
66	105			70	102		
70	105			72	102		
74	105			74	102		
76	105			76	103		
77	105			77	103		
80	105						
86	105						
90	105						
92	104						
94	104						
96	104						
			* Rx	output	squeal		